UNIVERSITI TEKNOLOGI MARA

THE EFFECT OF SURFACE POROSITY ON PERFORMANCE OF THE NICKEL-TITANIUM IMPLANT IN POSTERIOR MANDIBLE

NOR WATI @ NUR ATIKAH BT. MUSTAFA

PhD

June 2026

UNIVERSITI TEKNOLOGI MARA

THE EFFECT OF SURFACE POROSITY ON PERFORMANCE OF THE NICKEL-TITANIUM IMPLANT IN POSTERIOR MANDIBLE

NOR WATI @ NUR ATIKAH BT. MUSTAFA

Thesis submitted in fulfilment
of the requirements for the degree of
Doctor of Philosophy
(Dentistry)

Faculty of Dentistry

June 2026

CONFIRMATION BY PANEL OF EXAMINERS

I certify that a Panel of Examiners has met on 25th February 2026 to conduct the final examination of Nor Wati @ Nur Atikah Bt. Mustafa on her Doctor of Philosophy thesis entitled "The Effect of Surface Porosity on Performance of the Nickel-Titanium Implant in Posterior Mandible" in accordance with Universiti Teknologi MARA Act 1976 (Akta173). The Panel of Examiners recommends that the student be awarded the relevant degree. The Panel of Examiners was as follows:

Siti Mariam Abdul Ghani, PhD
Associate Professor
Faculty of Dentistry
Universiti Teknologi MARA
(Chairman)

Nurul Aida Ngah, PhD
Faculty of Dentistry
Universiti Teknologi MARA
(Internal Examiner)

Chai Wen Lin, PhD
Professor
Faculty of Dentistry
Universiti Malaya
(External Examiner)

PROFESSOR DR HJH ZURAEDA IBRAHIM
Dean
Institute of Postgraduates Studies
Universiti Teknologi MARA
Date: 24 June 2026

AUTHOR'S DECLARATION

I declare that the work in this thesis was carried out in accordance with the regulations of Universiti Teknologi MARA. It is original and is the result of my own work, unless otherwise indicated or acknowledged as referenced work. This thesis has not been submitted to any other academic institution or non-academic institution for any degree or qualification.

I hereby acknowledge that I have been supplied with the Academic Rules and Regulations for Postgraduate Studies at Universiti Teknologi MARA, which regulate the conduct of my study and research.

Name of Student	:	Nor Wati @ Nur Atikah Bt. Mustafa
Student ID. No.	:	2020833964
Programme	:	Doctor of Philosophy (Dentistry) – DS950
Faculty	:	Dentistry
Thesis Title	:	The Effect of Surface Porosity on Performance of the Nickel-Titanium Implant in Posterior Mandible
Signature of Student	:	
Date	:	June 2026

ABSTRACT

Background: Porous nickel–titanium (NiTi) alloys have emerged as promising biomaterials for dental and orthopedic use owing to their shape-memory effect, mechanical compatibility with bone, and intrinsic bioactivity. Although preclinical studies have confirmed their cytocompatibility and osteogenic potential, clinical validation in humans remains limited. Objective: This study aimed to evaluate the short-term clinical performance, peri-implant tissue response, and biological compatibility of NiTiDent Tuah, a porous NiTi dental implant, and to compare its outcomes with a commercially established titanium implant system (AnyRidge®). Materials and Methods: Thirty participants were recruited and randomly assigned to two groups (AnyRidge®, n = 18; NiTiDent Tuah, n = 12). Clinical parameters assessed included implant stability quotient (ISQ), peri-implant inflammation, bleeding on probing (BOP), probing depth (PD), and crestal bone level (CBL) across six follow-up intervals. Patient satisfaction (PSQ) and oral health-related quality of life (OHRQoL) were evaluated using the S-OHIP-14. Histopathological and energy-dispersive X-ray (EDX) analyses were performed on failed implants, while *in vitro* studies using human mesenchymal stem cells (hMSCs) assessed cell viability, alkaline phosphatase (ALP) activity, calcium deposition, and bone matrix formation. Results: AnyRidge® implants maintained high and progressively increasing ISQ values (mean 52.18 ± 13.63; $p = 0.01$). Peri-implant tissues were predominantly healthy (88.9%) with mild inflammation in 11.1%. Although CBL decreased from baseline to 22 weeks, bone height remained above the abutment–implant interface, with partial recovery noted by week 36. Patient satisfaction was high (mean PSQ = 6.01 ± 1.54), and OHRQoL improved significantly post-treatment ($p < 0.001$). NiTiDent Tuah demonstrated a significant reduction in ISQ values after 20 weeks (7.33 ± 11.67; $p < 0.001$). Histopathology revealed chronic peri-implantitis with foreign-body giant cell reactions, while EDX detected metallic contaminants (Al, Si, Mn, Fe, Cr) from degraded surgical drills. *In vitro*, NiTiDent Tuah supported strong hMSC adhesion, proliferation, osteogenic differentiation, elevated ALP activity, calcium deposition, and mature bone matrix formation after 28 days. Conclusion: Early clinical failures of NiTiDent Tuah implants were procedural, caused by drill wear and debris contamination rather than intrinsic material deficiencies. Porous NiTi exhibits strong bioactivity, osteoconductivity, and safety, reinforcing its promise as a next-generation implant material pending refinement of system-specific surgical instrumentation.

ACKNOWLEDGEMENT

بِسْمِ اللهِ الرَّحْمٰنِ الرَّحِيْمِ

“In the name of Allah, the Most Gracious and the Most Merciful”.

All praise and gratitude are due to Almighty Allah for His boundless blessings, guidance, and strength throughout the journey of completing this research and thesis. Without His mercy and will, none of this would have been possible.

I would like to express my deepest appreciation to my husband, Jais Bin Ismail, for his unwavering love, patience, and steadfast support, which have been invaluable during the most challenging moments of this journey. Your encouragement and understanding have been a source of great motivation for me. I extend my heartfelt gratitude to my parents, children, and siblings; your tremendous support has been deeply appreciated.

Sincere gratitude to my supervisor, Professor Dr Rohana Binti Ahmad, Associate Professor Dr Nur Hafizah Binti Kamar Affendi and Associate Professor Dr Eshamsul Bin Sulaiman, whose invaluable guidance, expertise, and constructive feedback have been instrumental in shaping this work. Their mentorship and continuous encouragement have inspired me to strive for excellence.

Special thanks are also due to Dr. Muhammad Asif Bin Ahmad Khushaini and Nitium Technology Sdn. Bhd., who believed in my potential and entrusted me with direct involvement in this research. Your trust and support have made this study a meaningful endeavour. My deepest appreciation also goes to Professor Dr. Muhammad Hussein Bin Ismail for his contribution to the development of the porous NiTi implant.

I am grateful to the research team for their collaboration, dedication, and joint efforts, which have greatly contributed to the project's progress and success. Collaborating with such dedicated individuals has been a truly enriching experience. I would also like to express my sincere appreciation to the patients whose trust and enthusiastic participation in this study have been greatly valued.

To all supporting members and friends, thank you for your constant encouragement, moral support, and understanding throughout this academic journey. Each of you has played a vital role in helping me achieve this milestone.

Finally, to everyone who has contributed, whether directly or indirectly, to the completion of this thesis, thank you. This achievement is as much yours as it is mine.

TABLE OF CONTENTS

LIST OF TABLES

LIST OF FIGURES

LIST OF SYMBOLS

Symbols

µm	Micro Metre
Af	Austenite Finish Temperature
Al	Aluminium
Cu	Copper
Fe	Ferum
Ga	Gallium
GPa	Gigapascal
kHz	Kilohertz
Md	Detwinned Martensite
mm/s	Millimetre per Second
Mn	Manganese
mN/m	Milli Newton Metre
Mo	Molybdenum
MPa	Megapascal
Ms	Martensite Start Temperature
Mt	Twinned Martensite
Nb	Niobium
Ncm	Newton centimetre
Ni	Nickel
nm	Nanometre
Sn	Tin
Ta	Tantalum
Ti	Titanium

V	Vanadium
Zr	Zirconium
θ	Contact Angle

LIST OF ABBREVIATIONS

Abbreviations

AISI 316L	Austenitic Stainless Steel Alloy
ALP	Alkaline Phosphatase
AM	Additive Manufacturing
AR	AnyRidge® Dental Implant
ARS	Alizarin Red Staining
BAFO	Bone Area Fraction Occupied
BIC	Bone-Implant Contact
BOP	Bleeding on Probing
CADCAM	Computer-Aided Design and Computer-Aided Manufacturing
CBCT	Cone-beam Computed Tomography
CBL	Crestal Bone Loss
CE	Conformité Européenne or European Conformity
COVID-19	Coronavirus Disease 2019
CP	Chemical Passivation
CS	Conventional Sintering
DAC	Dual Asymmetric Centrifuge
DM	Diabetes Mellitus
EBM	Electron Beam Melting
EDS	Energy Dispersive X-Ray Spectroscopy
EP	Electropolished Polished
FBGCs	Foreign Body Giant Cells
FBR	Foreign Body Reactions
FDA	U.S Food and Drug Administration

H&E	Hematoxylin and Eosin
HIP	Hot Isostatic Pressing
HMDS	Hexamethyldisilazane
hMSCs	Human Mesenchymal Stem Cells
ISO	International Organisation for Standardisation
JE	Junctional Epithelium
KM	Keratinised Mucosa
LENS	Laser Engineered Net Shaping
LENS	Laser Engineered Net Shaping
MBL	Marginal Bone Loss
MCO	Movement Control Order
MDA	Medical Device Authority
MIM	Metal Injection Moulding
mNiTi	machined-surface NiTi
MP	Mechanically Polished
MRONJ	Medication-Related Osteonecrosis Of The Jaw
MWS	Microwave Sintering
NiTi	Nickel-Titanium
NT	NiTiDent Tuah Porous NiTi Dental Implant
OE	Oral Epithelium
OHIP	Oral Health Impact Profile
OHRQoL	Oral Health-Related Quality of Life
OI	Osseointegration
OM	Osteogenic Medium
PD	Probing Depth
PDL	Periodontal Ligament
PE	Pseudoelasticity

PI	Peri-Implantitis
PIE	Peri-Implant Epithelium
PIIDs	Peri-Implant Infectious Diseases
PIM	Peri-Implant Mucositis
PISE	Peri-Implant Sulcus Epithelium
PISF	Peri-implant Sulcular Fluid
PIT	Peri-Implant Tissue
PM	Powder Metallurgy
PM	Platform-Matched
pNiTi	Porous Nickel-Titanium
PS	Primary stability / Platform-Matched Abutment Connection
PSQ	Patient Satisfaction Questionnaire
SEM	Scanning Electron Microscope
SHS	Self-Propagating High Temperature Synthesis
SLM	Selective Laser Melting
SLS	Selective Laser Sintering
SMA	Shape Memory Effect
SPS	Spark Plasma Sintering
SS	Secondary Stability
SSRI	Selective Serotonin Reuptake Inhibitors
TEM	Transmission Electron Microscope
VAR	Vacuum Arc Remelting
VIM	Vacuum Induction Melting

LIST OF NOMENCLATURES

Nomenclatures

$(PO_4)^{3-}$	Phosphate Ion
3Y-TZB	Yttria-Stabilised Zirconia
AP-1	Activator Protein-1
BMP	Bone Morphogenetic Protein
Ca^{2+}	Calcium Ion
CLRs	C-Type Lectin Receptors
Co-Cr	Cobalt-Chromium
COO^-	Carboxyl Group
CP-Ti	Commercially Pure Titanium
ECM	Extracellular Matrix
H_2SO_4	Sulphuric Acid
H_3PO_4	Phosphoric Acid
HA	Hydroxyapatite
HF	Hydrogen Fluoride
HNO_3	Nitric Acid
IL	Interleukin
IRF	Interferon Regulatory Factor
ISQ	Implant Stability Quotient
IT	Insertion Torque
M	Macrophages
M1	Pro-inflammatory Macrophages
M2	Anti-inflammatory Macrophages
mRNA	Messenger Ribonucleic Acid

NF-κB Factor	Nuclear Factor Kappa B
NiTi	Nickel-titanium
Nitinol	Nickel-titanium and 'nol' Naval Ordnance Laboratory'
NLRs	NOD-like Receptors
OPG	Osteoprotegerin / Orthopantomogram
PDGF	Platelet-derived Growth Factors
PEEK	Polyetheretherketone
PEG	Polyethene Glycol
PMMA	Polymethyl Methacrylate
PPC	PEG-polypropylene Carbonate
NaCl	Sodium Chloride
PRRs	Pattern Recognition Receptors
RANK	Receptor Activator of Nuclear Factor-κB
RANKL	RANK Ligand
RFA	Resonance Frequency Analysis
RLRs	RIG-I-like Receptors
RUNX	Runt-related Protein
TiO_2	Titanium Dioxide
TLRs	Toll-like Receptors
TNF	Tumour Necrotic Factor
VEGF	Vascular Endothelial Growth Factor
ZrO_2	Zirconia
α-Ti alloy	Alpha-titanium Alloys
α-β-Ti	Alpha-beta-titanium Alloy
β-type Ti	Beta-titanium Alloys

CHAPTER 1
INTRODUCTION

1.1 Research Background

As life expectancy continues to grow, the demand for implant treatments is projected to increase exponentially. Implants have emerged as the most dependable and efficient option for oral rehabilitation, catering to aesthetic, functional, and psychological demands, due to successful osseointegration (Boven et al., 2015; Adell, 1981).Furthermore, implants significantly minimise complications that are commonly associated with fixed (Pjetursson et al., 2007) and removable partial prostheses (Tsujioka et al., 2024).

Dental implant technology has advanced significantly following extensive research conducted both *in vitro* and *in vivo*. Today, internationally recognised dental implant companies, including Straumann Group, Nobel Biocare, Dentsply Sirona, Zimmer, and BioHorizons, have a long history of implant manufacturing. Straumann®, for instance, was founded in 1954 by Reinhard Straumann in Waldenburg, Switzerland. It initially focused on bone implants for fracture stabilisation and, by the 1980s, had expanded its global operations. Over time, Straumann® has continued to refine and develop its designs and systems, introducing its first titanium hollow-cylinder dental implants in 1974 and the soft-tissue Morse taper design in 1986. The company also launched SLA® in 1997 and the SLActive® surface in 2005. Their most recent offering, a fully tapered implant design with various dimensions and heights, was developed in 2021 to meet current market demands. What makes Straumann Group unique is its holistic approach to implant systems, which includes surgical technique guidance, prosthetic components, and a range of tissue regeneration systems (https://www.straumann.com/group/my/en/home/about/our-history.html)

Several factors influence the success of dental implant treatment, and these can vary greatly depending on the specific placement site. For example, implants placed in posterior regions, such as the maxillary area, often encounter challenges, including reduced bone quality and volume and higher functional demands. Furthermore, certain medical conditions, including diabetes mellitus and osteoporosis, as well as lifestyle

habits like smoking and parafunctional activities (such as bruxism), can affect the feasibility of implant placement (Albrektsson et al., 2017).

To improve implant survival rates, especially in complex clinical cases, researchers are actively exploring innovative strategies. One focus point is on designing the implants themselves. By refining macro-, micro-, and even nanoscale designs, it is possible to increase the surface area in contact with bone, thereby promoting faster osseointegration and enhancing overall treatment outcomes. This constructive approach holds promise for enhancing the effectiveness of dental implants across diverse patient groups.

Titanium remains the primary material used for dental implants. It has been classified as conventional pure Ti (Cp-Ti), α-Ti alloy grades II–IV, α-β-Ti alloy (Ti6Al4V), and β-type Ti alloy. Among these, Ti6Al4V has become the most common due to its high biocompatibility, wear resistance, and corrosion resistance. However, its high Young's modulus (110 GPa) compared to cortical and cancellous bone (10- 30 GPa) causes stress shielding, which can lead to bone resorption, implant loosening, or fracture (Brizuela et al., 2019; Brunski, 1999; Niinomi & Nakai, 2011). β-type titanium, such as Ti35Nb4Sn, demonstrates a lower elastic modulus (80 GPa), but it is still under investigation *in vitro* and *in vivo* (Niinomi & Nakai, 2011). The use of low elastic modulus coatings is also being explored to reduce the overall modulus; however, this involves complex manufacturing processes and poses challenges related to the interfacial weakness of multiple materials (Vishwakarma et al., 2023)

Nickel-titanium (NiTi) implant material has been studied since the 1960s as a potential intraoral biomaterial due to its unique elastic properties and shape memory. Its first application in dentistry was as orthodontic wires introduced in 1980, with interest in its potential as an implant material emerging in the mid-1990s (Jani et al., 2014). NiTi possesses not only inherent superelasticity and shape memory but also low elastic moduli that are closest to those of bone, which helps prevent issues arising from mismatched implant stiffness and the supporting bone. However, its complex manufacturing processes have historically limited its use.

The implant surface area can be increased by creating surface irregularities through grit blasting, acid etching, surface coating, and biofunctionalisation (Smeets et al., 2016). Nonetheless, the surface irregularities that are most effective in accelerating biological responses and establishing both peri-implant soft and hard tissue integration remain unclear due to a lack of long-term, evidence-based data. Furthermore, surface

treatment may raise the overall manufacturing costs of implants, and some coatings might detach over time, potentially leading to peri-implantitis (Hashim & Cionca, 2020). Meanwhile, nano-roughness has demonstrated positive effects in preclinical and animal studies at the molecular level, although clinical evidence remains limited.

The porous structure has been shown to expedite osseointegration and is suitable for use in clinically compromised situations (Wally et al., 2015). The pore size, shape, and interconnectivity have been identified as promoting bone ingrowth and contributing to osseoincorporation. Nonetheless, the manufacturing process of porous implants is complex and costly, rendering their usage unpopular and limited to highly compromised situations (Bencharit et al., 2013). Recently, the manufacturing issues of porous implants have been overcome through economical metal injection moulding techniques using nickel-titanium (NiTi) implant material (Ismail et al., 2012). This new porous NiTi dental implant, also known as Nitinol, with a nearly 1:1 nickel-to-titanium powder ratio, has undergone a series of physical and mechanical tests. *In vitro* and animal models showed that this new material is biocompatible and comparable to the Ti6Al4V (Mustafa et al., 2023; Mustafa et al., 2024). Furthermore, an animal study with rabbits revealed bone ingrowth (osseoincorporation) into this porous NiTi dental implant surface, as well as higher bone-to-implant contact than a dense surface conventional implant, as shown in Figure 1.

This innovative porous NiTi dental implant was developed by Nitium Technology Sdn. Bhd., a recent start-up that has the full support and recognition of the Malaysian government as a high-potential dental manufacturer in Malaysia. It meets strict regulatory standards and guidelines for medical device development, including comprehensive biocompatibility testing (ISO 10993), preclinical testing (ISO 14801), as shown in Table 1 and successful osseointegration with evidence of bone ingrowth in Figure 1. Moreover, this porous NiTi implant has received approval for clinical investigation from the CE, FDA, and MDA, with an approval identification document (ID) number of IU-20210201-13. Utilising metal injection moulding (MIM) enables low manufacturing costs and high-volume production. Making affordable implant therapies accessible to Malaysians fosters a new wave in dental rehabilitation. To thoroughly evaluate its safety and efficacy, a clinical trial is the next step in its development. Accordingly, a study to assess its safety and compare it to a conventional, dense (non-porous) commercial dental implant will be conducted. However, the development of the implant system coincided with the Movement Control Order (MCO)

during the COVID-19 pandemic. As a result, while the implants were successfully produced, the drill system had to be outsourced due to time and financial constraints. This limitation affected the scope and outcomes of the clinical trials.

Table 1.1
Biocompatibility, Physical and Mechanical Testing of NiTiDent Tuah Porous NiTi Dental Implant (Khushaini & Ahmad, 2021)

Name of the study	**Laboratory / Facility**	**Standards/compliances**	**Conclusion**
In-vitro Cytotoxicity Study of Porous Nickel Titanium by Elution Method	Bioneeds India private Limited, Karnataka, India	OECD GLP ISO 10993-Part 5 ISO 10993-Part 12	Porous Nickel Titanium is considered non-cytotoxic to the subconfluent monolayer of L-929 mouse fibroblast cells.
Acute Systemic Toxicity Study of Porous Nickel Titanium in Swiss Albino Mice	Bioneeds India private Limited, Karnataka, India	OECD GLP ISO 10993 — Part 11 ISO 10993 - Part 2 AAALAC-accredited facility	Porous Nickel Titanium did not reveal any systemic toxicity under the experimental conditions employed.
Bacterial Reverse Mutation Test of Porous Nickel Titanium Using *Salmonella Typhimurium* and *Escherichia Coli* Tester Strains	Bioneeds India private Limited, Karnataka, India	OECD GLP ISO 10993 - Part 3 ISO 10993 - Part 33: ISO 10993 - Part 12	Porous Nickel Titanium was found to be "non-mutagenic" under the laboratory conditions tested.
Intracutaneous Reactivity Test of Porous Nickel Titanium in New Zealand White Rabbits	Bioneeds India private Limited, Karnataka, India	OECD GLP ISO 10993- Part 10 ISO 10993 - Part 12 ISO 10993 - Part 2 AAALAC-accredited facility	Porous Nickel Titanium was considered "Non-irritant" under the experimental conditions employed.
In Vitro Micronucleus Assay	Makmal Bioserasi, UKM Bangi, Malaysia	OECD GLP ISO/IEC 17025 OECD 487 ISO 10993 - Part 3	The *Porous Nickel Titanium Dental Implant* is considered non-clastogenic under the condition of this study.

Name of the study	Laboratory / Facility	Standards/compliances	Conclusion
		ISO 10993 - Part 12 ISO 21427– Part 2	
Cytotoxicity: MTT Assay	Makmal Bioserasi, UKM Bangi, Malaysia	OECD GLP ISO/IEC 17025 ISO 10993 - Part 5 ISO 10993 - Part 12 ISO 10993 - Part 1:	*Porous Nickel Titanium Dental Implant* demonstrated a non-cytotoxicity effect under the condition of this study.
Test for local effect after implantation in Femur of *Oryctolagus cuniculis* using International Standard Method ISO 10993 -Part 6	Preclinical Translational Unit Animal Research Complex, Advanced Medical & Dental Institute (IPPT), USM Bertam, Malaysia Veterinary Laboratory Services Unit (VLSU), Faculty of Veterinary Medicine, UPM Serdang, Malaysia	OECD GLP MS ISO/IEC 17025 MS ISO 9001 ISO 10993— Part 6 ISO 10993 - Part 1	Clinically healthy rabbits were selected for implantation of the test item (Tuah NitiDent *Porous Nickel Titanium dental implant*) and control Titanium Gr5 (6Al-4V). Both implants are biologically compatible with the host. However, the test item is deemed to be more superior compared to the control item.
Physical and Mechanical Testings of NiTi Dent Tuah Porous NiTi			
In vitro corrosion assessment of Porous Nickel Titanium (NiTi**)**	Faculty of Mechanical Engineering, UMP Pekan, Malaysia	ASTM F2129	*In vitro* corrosion assessment was performed on three different samples of *Porous NiTi Dental Implant*. And the average value of the potential breakdown was determined to be at 677 mV. No pitting or corrosion related defects were observed in the microscopic examination.
Fatigue testing of Porous Nickel Titanium (NiTi) Dental Implant System	Strength of Materials Laboratory, Faculty of Engineering, Universiti Putra Malaysia	MS ISO/IEC 17025 ISO 14801	In the static loading, maximum load at the rupture for 3.5mm diameter Porous Nickel Titanium (NiTi) Dental Implant is 596.27 N which is adequate for intended application of

Name of the study	Laboratory / Facility	Standards/compliances	Conclusion
			the implant diameter. In dynamic fatigue, the system survived 2,000,000 cycles criteria of the test with dynamic load of 47% of established maximum static load.
Compression Testing of Metallic Materials at Room Temperature	Jabatan Kejuruteraan Mekanik, Fakulti Kejuruteraan, Universiti Malaya, 50603, Kuala Lumpur, Malaysia	ASTM E9	The maximum compressive load of Porous Nickel Titanium is between 5kN (5000N) to 7kN (7000N).
Rockwell Hardness of Metallic Materials	Jabatan Kejuruteraan Mekanik, Fakulti Kejuruteraan, Universiti Malaya, 50603, Kuala Lumpur, Malaysia	ASTM E18	The average value of Rockwell hardness obtained from conducted on the 9.

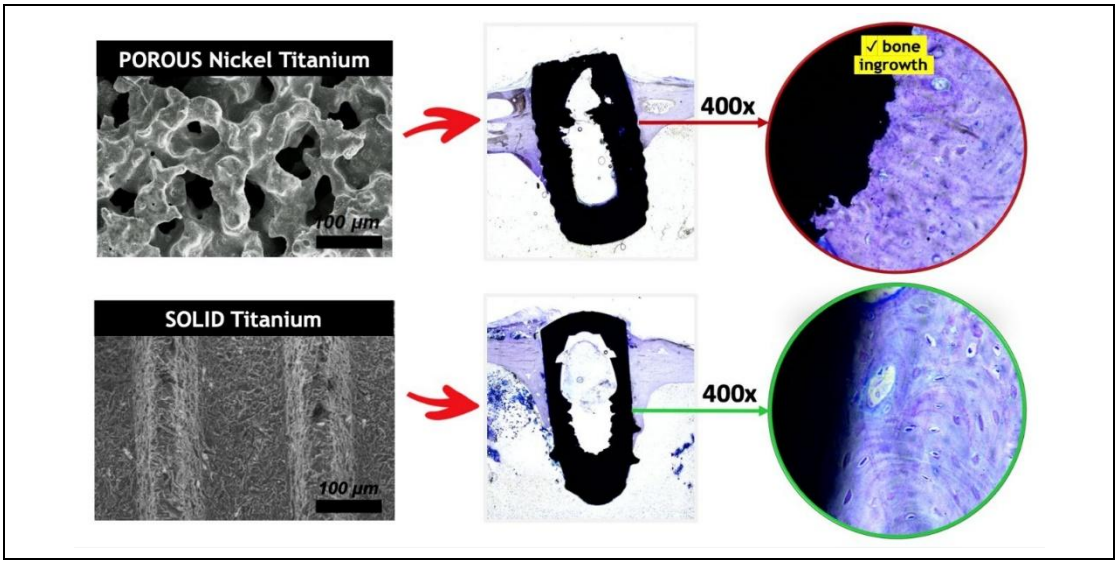

Figure 1.1 A Comparison of Bone Ingrowth Surrounding Implants Placed in the Proximal Tibia of a Rabbit between Porous NiTi and Solid-Dense Straumann Implants.

Note: High bone ingrowth and excellent bone-implant contact in porous NiTi are evident. (Rahimi, 2023)

1.2 Problem Statement

Implant treatment relies heavily on successful bone integration. Titanium and titanium alloys are currently the most commonly used implant materials, demonstrating high long-term survival rates in healthy individuals. Implant surface characteristics and morphologies positively influence the behaviour of local tissue during healing and remodelling. The large surface area created by increasing implant surface roughness expedites osseointegration, but this surface treatment increases the cost of dental implants. Meanwhile, surface coating may detach, leading to periimplantitis. Porous dental implants have been shown to foster bone growth without requiring additional surface treatment. The porous implant is recommended for use in areas with low bone quality, such as the posterior maxilla. However, the complex and costly manufacturing process of porous implants has limited their widespread adoption. Nickel–titanium (NiTi) alloys have attracted interest as potential biomaterials for dental implants due to their superelasticity, shape-memory properties, and lower elastic modulus than titanium alloys, which confers stress shielding benefits. Recently, a promising Malaysian government-supported start-up has successfully fabricated a porous NiTi dental implant using a more cost-effective metal injection moulding technique. This innovative, affordable technology has the potential for mass production, which could significantly benefit populations in Malaysia and other developing countries requiring oral rehabilitation (Padhye et al., 2019). The development of this implant design would enhance biological integration, especially in patients with poor bone quality or compromised systemic conditions that reduce bone density, such as ageing, osteoporosis, metabolic bone disorders, and systemic diseases that can hinder bone healing and affect implant stability (Lemos et al., 2023; Radi et al., 2018; Shibli et al., 2025). This would ultimately enhance their quality of life. Preclinical *in vitro* and *in vivo* animal studies have been conducted in full compliance with all relevant regulatory requirements, as previously outlined. The implant is now ready for human clinical trials to assess its safety and clinical performance, which is the primary objective of this PhD study. If the clinical trials prove successful, further optimisation of the system will be undertaken. This will include developing various implant designs and sizes, as well as prosthetic supra-structure components, paving the way for local market introduction.

This PhD project initially aimed to conduct a clinical trial comparing the outcomes of a newly developed porous NiTi implant system with those of a commercial

implant. The project was planned to span three years, from October 2020 to September 2023. However, unforeseen circumstances necessitated significant adjustments to the study's timeline and scope. The implementation of the Movement Control Order (MCO) due to the COVID-19 pandemic caused a one-year delay in the clinical trial. Manufacturing of the implant system was disrupted, as production had to be halted. Once the implant fixtures were finally completed, the clinical trial could commence in February 2022. However, due to financial and time constraints, mainly because the government reallocated resources to combat the pandemic, the implant drills could not be manufactured locally. As a result, it was decided to source the drills from a company in Pakistan, which could supply the necessary components quickly and at a lower cost.

In July 2022, the clinical trial faced another major challenge. A series of osseointegration failures was observed among participants using the porous NiTi implants. This prompted the suspension of the trial to investigate the underlying causes of these failures. A series of laboratory investigations was conducted, including analyses of peri-implant tissues, implant surfaces, surgical drills, nickel ion release, and *in vitro* osteogenic potential. These investigations were completed in October 2024.

The challenges encountered during this project necessitated a shift in its direction. While the initial focus was on the clinical trial and its outcomes, unforeseen delays and complications redirected attention towards understanding the factors contributing to implant failures. These findings have provided valuable insights into the performance of the porous NiTi implant system and will guide its future development and optimisation.

As a result, this thesis will be structured into two distinct parts: Part A and Part B.

i. Part A focuses on the clinical trial, which spanned two years and three months.
ii. Part B covers the laboratory investigations, which were conducted over an additional year.

To ensure clarity and prevent confusion, the hypothesis, research questions and objectives will be presented separately for each section of the thesis.

1.3 Part A – Clinical Trial

1.3.1 Hypothesis

i. The hypothesis was set to no difference in the clinical and biological performance of two types of dental implants (NiTiDent Tuah Porous NiTi implant and Megagen Anyridge Implant) based on the implant stability, peri-implant soft tissue conditions, crestal bone loss and survival.

1.3.2 Research Questions

i. How does a porous NiTi dental implant influence implant stability compared to a conventional dense-surface dental implant in restoring a single tooth gap in the posterior mandible?
ii. Does the porous NiTi dental implant system influence peri-implant soft tissue and crestal bone level in the posterior mandible compared to the control dense dental implant?
iii. How do the oral health-related outcomes and patient satisfaction of patients receiving porous NiTi dental implants compare to those receiving dense dental implants?

1.3.3 Aims of Study

This study aimed to evaluate the safety, clinical, and biological performance of a porous NiTi dental implant (NiTiDent Tuah, Nitium Technology Sdn. Bhd, Malaysia), including the survival rate, implant stability, peri-implant tissues, and crestal bone level of porous NiTi dental implant (NiTiDent Tuah, Nitium Technology Sdn. Bhd, Malaysia), in restoring single-tooth gaps in the posterior mandible, in comparison to a dense surface non-porous dental implant. Additionally, the biological response of peri-implant tissues and the physical characteristics of porous NiTi implants and tools associated with the system would be further investigated through supplementary laboratory analyses, if necessary.

1.3.4 Specific Research Objectives

i. To assess the implant stability quotient of porous NiTi implants compared to the control group using Resonance Frequency Analysis at the time of implant placement, 16 weeks, 26 weeks, and 52 weeks after implant placement.
ii. To assess the condition of the peri-implant soft tissues of the porous NiTi implant compared to the control group by measuring probing depth, bleeding on probing, suppuration, and dehiscence at 16 weeks, 26 weeks, and 52 weeks after implant placement.
iii. To evaluate the crestal bone level associated with porous NiTi implant compared to the control group through serial periapical radiography at the time of implant placement, 16 weeks, 26 weeks, and 52 weeks after implantation.
iv. To compare patients' satisfaction and oral health-related quality of life between the NiTi implant group and the control group for single missing molar replacement.

1.4 Part B – Laboratory Studies

1.4.1 Hypothesis

i. Peri-implant tissues, implant and tools associated with porous nickel–titanium (NiTi) implant systems do not exhibit any specific biological and physical features through laboratory assessments.

1.4.2 Research Questions

i. What biological characteristics are present in peri-implant tissues associated with porous NiTi implants?
ii. What is the physical appearance of the implant and tools associated with the porous NiTi implant system?

1.4.3 Research Objectives

i. To characterise peri-implant tissue responses through laboratory analyses
ii. To evaluate the porous NiTi implant and its related tools used in this porous NiTi implant system.

1.5 Significance of the Study

This PhD study investigated porous NiTi dental implants (NiTiDent Tuah, Nitium Technology Sdn. Bhd., Malaysia) for single-tooth replacement in the posterior mandible. The aim was to compare their survival, stability, peri-implant tissue health, and crestal bone loss with dense, non-porous implants. Porous NiTi was expected to enhance osseointegration without additional surface treatment, offering potential benefits in low-bone-quality sites.

The study, however, faced significant challenges. In addition to delays caused by the COVID-19 pandemic and financial constraints, a critical factor in implant failure was the use of outsourced drills, whose limitations were not evident prior to clinical application. These drills compromised osseointegration during clinical trials, necessitating a shift to laboratory-based investigations.

The significance of this study lies in its dual contributions: clinically, by documenting survival and stability outcomes of porous versus dense implants; and scientifically, by examining peri-implant tissue responses, implant surface properties, and the osteogenic potential of human mesenchymal stem cells. Together, these findings highlight both limitations and future directions for improving porous implant design and instrumentation.

1.6 Scope of Study

This study assessed the safety and clinical performance of a novel porous NiTi dental implant (NiTiDent Tuah, Nitium Technology Sdn. Bhd., Malaysia) in restoring single-tooth gaps in the posterior mandible, concentrating on survival rates, implant stability, peri-implant tissue health, and crestal bone loss. Initially, a clinical trial was conducted to compare the porous implant with a dense, non-porous implant.

Following osseointegration failures observed during the trial, the study expanded to include laboratory investigations. These focused on identifying factors that contribute to implant failure, including peri-implant tissue responses, implant surface characteristics, nickel ion release, and the osteogenic potential of human mesenchymal stem cells.

The scope covers both clinical and laboratory aspects, offering insights into the performance and limitations of porous NiTi implants and guiding future improvements in implant design and application.

1.7 Conclusion

This study examines a porous NiTi dental implant produced via metal injection moulding, with the aim of improving implant performance and clinical outcomes. The research investigates factors leading to implant failures, such as biocompatibility, material degradation, and their effects on osseointegration. By identifying and understanding these factors, the study seeks to enhance implant success rates through detailed analysis and future innovations.

The following chapter offers a detailed review of the literature, analysing implant materials and their surface modifications, including porous surfaces, with a particular focus on nickel-titanium alloys in medical applications. It also discusses the stages of osseointegration, the influence of microdesign on implant surfaces, and the clinical parameters essential for measuring successful osseointegration. This review will then lead to an exploration of potential factors contributing to the failure of porous NiTi implants, establishing the foundation for the experimental research in this study.

In the following sections, we will provide detailed descriptions of each chapter, carefully outlining the methodology employed, the results achieved, and the subsequent discussion to address possible questions that may have influenced the outcome. This discussion will conclude with an outline of the study's limitations and offer insightful recommendations for future research efforts.

CHAPTER 2
LITERATURE REVIEW

2.1 Chapter Outline

This literature review examines both previous and recent studies, emphasising the importance of implant treatment in oral rehabilitation, supported by evidence-based data on implant success and survival rates. The review also briefly discusses the materials used for implants, with a particular focus on nickel-titanium (NiTi or nitinol) and the development of the porous NiTi dental implant, which is the primary material tested in this study. Additionally, this review covers the fundamental principles of osseointegration and explores how implant properties, especially surface characteristics like pore-associated surfaces, influence biological behaviour, supported by in vitro, animal, and human research. Furthermore, clinical assessments such as implant stability, crestal bone levels, and peri-implant conditions serve as predictive parameters to evaluate implant performance in humans. Finally, it examines early implant failure, potential contributing factors, the pathophysiology, particularly mechanisms of foreign body reactions, and clinical presentation.

2.2 Burden of Tooth Loss: Functional, Psychological and Esthetic Implications

As life expectancy continues to rise, tooth loss is emerging as a critical age-related issue that demands urgent attention in oral health management. In the US, the prevalence of edentulism among adults shows a clear upward trend as age increases: it rises from 1.2% in the 35–49 age group to 5.9% for those aged 50–64 years, further increasing to 11.4% at 65–74 years, and reaching 19.7% in individuals 75 years and older (Centers for Disease Control and Prevention, 2024). In Malaysia, the statistics reflect a similar concern. Only 34.3% of individuals aged 60 years or older reported having at least 20 functional teeth (Ministry of Health Malaysia, 2022).

The consequences of tooth loss are profound, adversely affecting oral health and overall quality of life, with the severity of this impact directly correlated to the number and position of the missing teeth (Emami et al., 2013). The effects of these losses can

vary dramatically based on patients' sociodemographic factors and perceptions, ranging from negligible to severe impairment (Bernabe et al., 2020; Emami et al., 2013).

2.3 The Emergence and Evolution of Dental Implants

The evolution of dental implants marks a remarkable journey that spans thousands of years, showcasing significant progress from basic methods to advanced modern practices. Early evidence of dental implants dates back to ancient civilisations such as the Mayans and Egyptians, who used materials like jade, gold, ivory, and shells to replace missing teeth (Stević et al., 2021; Ionescu et al., 2022). While these early efforts laid the foundation for dental restoration, they often lacked the functionality and stability found in contemporary implants.

A pivotal moment in the history of dental implants came in the mid-20th century, driven by advances in materials science and surgical methods (Abraham, 2014; Harris, 2014). In the 1950s, Swedish orthopaedic surgeon Per-Ingvar Brånemark made a breakthrough discovery: titanium's capacity to bond effectively with bone through a process called osseointegration (Brånemark et al., 1969). This finding laid the groundwork for modern dental implantology, leading to the development of the first successful titanium dental implants, which provided durable solutions for tooth loss (Adell et al., 1981; Albrektsson et al., 1981). The success of the Brånemark implant system in the 1980s offered new insights into prosthodontic management of the edentulous jaw (Adell et al., 1981). Prior to the 1980s, the implant was believed to be anchored by fibrous tissue known as "pseudo-periodontium," which resembled the periodontal ligament and could affect the medium-term survival (Brånemark et al., 1983). Healing with this tissue results in decreased resistance to mechanical, chemical, and bacterial invasion (Adell et al., 1981).

The advancements persisted throughout the 1980s and 1990s, characterised by notable improvements in implant design and materials (Calazans Neto et al., 2024; Nicholous, 2020; Osman & Swain, 2015). During this period, a range of implant types emerged, including endosseous implants, which are placed directly into the jawbone and became increasingly popular. Additionally, the introduction of guided-surgery techniques significantly enhanced the precision and predictability of implant placement, leading to better patient outcomes.

Today, dental implants are recognised as a reliable option for oral rehabilitation, addressing aesthetic, functional, and psychological needs (Adler et al., 2019; Boven et al., 2015). The success of dental implants depends not only on patient factors and surgical techniques but also on the selection of implant materials (Albrektsson et al., 1981; Brånemark et al., 1969a). Looking ahead, the field of dental implants continues to evolve through ongoing research and technological progress. Advances in materials and surface enhancement aim to speed up healing and integration with surrounding tissues, ensuring the continued success of dental implants.

2.4 Implant Success and Survival Rates

A dental implant functions as an abutment that supports a prosthesis in the mouth. Although implant therapy was introduced over 50 years ago, the criteria for success remain unclear (Adler et al., 2019; Papaspyridakos et al., 2012). Survival refers to an implant that remains in the mouth regardless of biological or technical issues (Adler et al., 2019). From the 1980s to 2000, various criteria were proposed, focusing on the absence of persistent subjective complaints (such as pain, sensation of a foreign body, or dysesthesia), the absence of recurrent peri-implant infection with pus, the absence of detectable implant mobility, and the absence of radiolucency around the implant (Buser et al., 1990). Furthermore, technical, aesthetic, and patient satisfaction factors have been proposed for a comprehensive assessment of the implant (Adler et al., 2019; Papaspyridakos et al., 2012).

The emergence of modern implant surfaces has significantly increased the 10-year implant survival rate (89% to 97%) (Adler et al., 2019; Franchis et al., 2021; Pjetursson et al., 2012). Despite its high predictability, systemic or local conditions such as diabetes mellitus, osteoporosis, post-radiation therapy, smoking, or periodontitis are among the factors that could reduce its success rate (Albrektsson et al., 2012; Chrcanovic et al., 2014; Chrcanovic et al., 2015; Qian et al., 2012; Samara et al., 2024). A summary of implant survival and success rates is presented in Table 2.1.

Table 2.1
Success and Survival Rates of Dental Implants

Study Design	General Information	Specific Finding	Risk factor	References
A systematic review of clinical trials of single implants with different placement and loading protocols in different locations	45 publications (13 RCTs, 21 prospective, 11 retrospective studies. Location: anterior maxilla (35 studies, 1391 implants), Posterior maxilla (19 studies, 567 implants), anterior mandible (3 studies, 42 implants, posterior mandible (13 studies, 447 implants), Implant type: rough surface	**Survival rate** Anterior maxilla: 97.5 – 99.6 % (30 failures: 12 – early failures, 14 – late failures, 4 - unknown Posterior maxilla: 85.7 – 100 % (6 failures: 10 – early failures, 14- late failures, 2 – unknown) Anterior mandible: 98.5 – 100 % (1 early failure) Posterior mandible: 95.0 – 100 % (6 - early failures, 10 - late failures) Treatment protocol based on location Anterior maxilla: Type 1c and 4A Posterior maxilla: Type 1c - Posterior mandible: type 4c		Zhou et al., 2021
A retrospective, longitudinal observational cohort study from July 1995 to April 2019 (22 years) of 4247 dental implant patients in the Calgary, Alberta region. Assess the long-term clinical performance, including: - implant failure - marginal bone level around implants.	**Follow-up**: 22.2 years (mean = 4.5 ± 4.2). 56.4% female, **Mean age:** 53.8 ± 13.5 years. **Total implant:** 10,871 (mean of 2.56 implants/patient: range 1 -17 implants); 57.3% in maxilla. I**mplant location:** 25.2% posterior mandibular, 19.9% maxillary incisor, 17.2% maxillary premolar. **Implant type**: 55.2% Straumann tissue	3.3% (n = 140) of patients experienced a combined total of 178 implant failures. The cumulative survival rate at: **Implant level** - 3 years - 98.9%, - 5 years - 98.5%, - 10 years - 96.8%, - 15 years - 94.0%	**Risk for implant failure**. - Multiple implant/patient (HR:5.85) - Shorter implant length (HR: 3.53) - Immediate loading (HR:1.14) risk disappears after 10 years of loading - Implant + GBR (HR: 1.85)	French et al., 2021

Study Design	General Information	Specific Finding	Risk factor	References
	level standard implant with SLA surface. **Implant diameter/length:** 4.8/10, 4.1/10, and 4.1/12; narrow diameter in the incisor, wider in the molar areas. **Restoration:** 34.5% single crown, 47.9% multiple splinted/bridge, 7% removable prosthesis	**Patient level** - 3 years - 97.4%, - 5 years - 96.7%, - 10 years - 92.5%, - 15 years - 86% Bone level: - Baseline - 0.09 ± 0.28 mm 8–10 years - 0.49 ± 0.74 mm. Peri-implant mucositis incidences at the implant level - 2–3 years - 9.4%, - 4–5 years - 9.3%, - 6–7 years -12.1%, - 8–10 years -11.9% Peri-implantitis incidence: - 2–3 years - 2%, - 4–5 years - 2.6%, - 6–7 years - 3.2%, - 8–10 years - 7.1%	- Heavy cigarette smoking (HR: 2.02) - Diabetes mellitus (HR: 2.17) HR: Hazard Ratio	
Longitudinal, retrospective study of patients (n = 376) treated with dental implants (n = 1095) between 1999 and 2005 at a specialist clinic in Stockholm, Sweden. Evaluate the long-term (9-15 years):	**Mean follow-up:** 11 years (9 – 15). **Mean age:** 54 years (20–81), female: 55 %, smoker: 19 %, former smoker: 31 %, history of generalised periodontitis stage III–IV: 44%, history of treated severe periodontitis stage III- IV: 26%, self-reported cardiovascular: 28% and diabetes mellitus: 7%.	**The cumulative implant survival rate** - at 10 years - 89.7% - up to 15 years - 82.6% - with restricted peri-implantitis and/or medium/major technical complications -71.9%	**Implant loss in** - history of treated severe periodontitis Stage III-IV (P = .008) - implant surgery complications (P = .010). was a significant risk indicator	Adler et al 2019

Study Design	General Information	Specific Finding	Risk factor	References
- survival rate - complication rates identify the risk indicators of these complications at patient and implant levels.	**Implant system:** Astra Tech implants (Dentsply, IH AB, Mölndal, Sweden)- 99.7% of cases, Nobel Biocare implants (Nobel Biocare Zurich, Switzerland) - 65% of cases and Straumann implant system (Straumann, Basel, Switzerland) - 0.3% of cases.	**Cumulative success rate** - 10 years, without biological or technical complications - 50.0% - up to 15 years -20% **Complication prevalence at the patient level** - biological - 52% - technical - 32% 65% of patients experienced at least one complication (n=763 complications)	**Peri-implantitis** - smoking (P = .006). The frequency of biological and technical complications did not differ significantly between implant systems based on the number of implants or prosthetic units.	
- Systematic review and meta-analysis	Implant in smoker, n=19836 In non-smoker:, n=60464 Risk factor: Chronic smoker	• Implant failure in smokers: 123% • Implant failure rate: 6.35% (RR=2.23 times higher than non- smoker (3.18%). • Incidence of post-op infection in smokers: RR=2.01 times that of non-smokers. • Marginal bone loss in smokers, $p < 0.00001$ **Failure in different implant surfaces:** • Turned implant: RR=2.17, $p<0.0001$,		Chrcanovic et al.,2015

Study Design	General Information	Specific Finding	Risk factor	References
		• Acid-etched surface; RR=2.07, p = 0.09, • Sandblasted & acid-etched: RR=2.92, p = 0.0005, - Sandblasted and fluoride-modified surface: RR=4.18, p < 0.0001		
A systematic review of prospective and retrospective cohort studies and case series on FDPs between 1994 and 2010 (32 studies). Assess - 5- and 10-year survival of implant-supported fixed dental prostheses (FDPs) the incidence of biological and technical complications.	No of studies included: 32 No of patients reported: over 2100 patients. **Age:** between 15 and 87 years. **Implant system used:** Astra® Tech dental implants (Astra®Tech AB, Molndal, Sweden), Bioceram® sapphire dental implants (Kyocera America, Inc., San Diego, CA, USA), Brånemark® implant system (Nobel Biocare AB, Goteborg, Sweden), Camlog® dental implants (Camlog Biotechnologies, Basel, Switzerland), Frialit-2® dental implants (Friadent, Mannheim, Germany), IMZ® dental implants (Friadent), ITI® dental implant system (Straumann AG, Waldenburg, Switzerland), Minimatic® implants (Minimatic Implants Technology, Boca Raton, FL, USA), and Zimmer® dental	**Implant survival:** Mean follow-up 5 years (5.0 – 7.1 years) (20 studies) - Total implant: 4266 - Implant lost: 216; 47% (102/216) early failure, 53% late failure (114/216) - Estimated survival rate: 95.6% - Estimated failure rate 0.89 per 100 implant years - Machined (13 studies) vs rough surface (7 studies) annual failure rate: 1.03 and 0.57, survival rate: 95% and 97.2%, respectively (p<0.0001) Mean follow-up around 10 years (7 studies) - Total implant: 873 - Implant lost: 62 - Estimated survival: 93.1%		Pjetursson et al 2012

Study Design	General Information	Specific Finding	Risk factor	References
	implants (Zimmer Dental Incorporation, Carlsbad, CA, USA). **Total FDP**: 1881 supported by approximately 5200 implants (mean number implant supporting FDPs: 2.75), **Restorative material used** in 18 studies: 66% metal ceramic, 32%: gold-acrylic, 2% all ceramic. **Retention used** (in 17 studies): 81% screw-retained, 19% cement-retained	- Estimated failure rate 0.72 per 100 implant years **FDP survival** Mean follow-up around 5 years - Total FDPs: 1723 - FDP lost: 83 - Estimated survival rate: 95.4 % (93.1-96.9) - Veneer material used (15 studies, n=1127): metal-ceramic (96.5%) vs gold-acrylic (89.3%), p<0.001 Mean follow-up around 10 years - Total FDPs: 243 - FDP lost: 41 - Estimated survival rate: 80.1% - Survival of veneer material used: metal-ceramic (1 study: 93.9%) vs gold-acrylic (3 studies: 77.4%), p<0.0001 **Success rate** Mean follow-up (5 years): - 66.4% of the patients free of any complications after 5 years. The most frequent complications fractures of the veneering material		

Study Design	General Information	Specific Finding	Risk factor	References
		(13.5%), peri-implantitis and soft tissue complications (8.5%), loss of access hole restoration (5.4%), abutment or screw loosening (5.3%), and loss of retention of cemented FDPs (4.7%).		
Prospective study on ITI dental implant system (7 years)	Patients (n=250), Implants (n=759): ISC, n=137, CFP, n=42 FPI, n=137, ITP, n=13 FCP,n=5, O, n=37	**Survival rate:** • ISC: 95.6%, • CFP:94.4% • FPI:96.1%, • FCP: 100% • I-TP::90.6% • O: 95.7%, Success rate • ISC: 75.6% • CFP:63.3% • FPI: 73.8% • FCP:63.8% • TP: 70.6% • O: 78.6% **Prosthetic complications:** Decementation, abutment- framework screw loosening, retention anchor failure, fractured prosthesis, **Other finding**		Romeo et al.,2004

Study Design	General Information	Specific Finding	Risk factor	References
		- Both maxillae and mandible showed similar survival and success - Overdenture (OD) supported by two implants were comparable to 3 or more implants		
10-years prospective study	Patient, n = 53, Implant, n = 112 - Hx of periodontitis:8 patients, implant,n=21. - Without hx of periodontitis: 45 patients, implant n=91	**Survival rate** • Hx of periodontitis- 90.5 % • Without hx of periodontitis- 96.5 % **Success rate set at PD 5mm, BOP, annual bone loss <0.2 mm** • Hx of periodontitis:52.4% • Without hx of periodontitis:79.1%	**Risk of peri-implantitis:** • Patients with hx of periodontitis: 28.6%, • Without hx of periodontitis: 5.8% **Failure rate**: • Patients with hx of periodontitis- 9.5%, • Without hx of periodontitis- 3.5%. Implants placed in previously periodontally compromised patients demonstrated statistically significantly lower success rates than implants placed in patients having lost their teeth due to reasons other than periodontitis $p < 0.025$	Karoussiss et al.,2003
3-years prospective study	Total patient n=663, implant n=2 887.	**Survival rate** • non-DM: 93.2% (6.8% failures)		Morris et al.,2000

Study Design	General Information	Specific Finding	Risk factor	References
	- Implant placed in non-DM: 2632, - implant placed in DM patient: 255	• with DM:92.2% (7.8% failures). **Other findings** • ↑implant failure in DM patient, p = 0.02 The use of chlorhexidine rinses following implant placement resulted in a greater improvement in Type 2 (9.1 %), the use of preoperative antibiotics improved survival by 4.5 % in non-DM patients and 10.5% in DM patients. The use of HA-coated implants improved survival by 13.2 % in DM.		

2.5 Implant Materials in Modern Dentistry

Dental implants have become a viable option for replacing missing teeth, offering significant improvements in both function and aesthetics (Adler et al., 2020). Alongside patient-related factors and surgical technique, the success of a dental implant also heavily depends on the choice of implant material (Albrektsson et al., 1981; Brånemark et al., 1969).

The oral environment presents unique challenges for dental implants. Unlike orthopaedic implants, which are placed in a contained, closed setting, dental implants are exposed not only to masticatory forces but also to fluctuating pH levels influenced by diet, interactions among normal oral flora in the presence of biofilm, and oral hygiene products. Additionally, dental implants must support complex biological processes essential for bone integration and soft tissue healing. Therefore, the materials used must meet mechanical, chemical, and biological requirements to withstand occlusal forces, resist corrosion, and integrate effectively with surrounding tissues. Poor material performance, for example, overly rigid materials, may cause stress shielding. At the same time, those prone to corrosion may release toxic ions that trigger inflammation, leading to early implant failure, foreign-body reactions, and peri-implant bone loss.

The introduction of the Brånemark oral implant in the 1960s marked a significant advancement in dentistry, offering a reliable option for replacing missing teeth, a fact that gained further recognition in 1981 (Adell, 1981). Initially, implants were mainly fixed to the bone using cement; however, this method faced challenges due to the exothermic effect of the material, leading to failure (Albrektsson et al., 1981). Early research also believed that only ceramic materials could achieve successful bone-implant integration, as exposing metals to host tissue often led to the formation of fibrous tissue, which weakened the bond between the implant and the bone (Albrektsson et al., 1981).

Historically, precious metals such as gold, silver, and platinum were commonly used; however, their high costs and limitations, including poor mechanical properties, inconsistent biological compatibility, and manufacturing challenges, have led to their replacement by more affordable metals with superior qualities (Calazans Neto et al., 2024). To find better options, vitallium, tantalum, cobalt-chromium (Co-Cr) alloys and stainless-steel base metals are also being explored in bone implantation, as in

orthopaedics (Albrektsson & Wennerberg, 2019; Albrektsson, 1981). Co-Cr alloys are valued for their strength and resistance to wear and corrosion, but cobalt can sometimes release harmful ions, potentially causing inflammatory reactions in some patients (Karimi & Alfantazi, 2014). Meanwhile, stainless steel, particularly AISI 316L, offers a less expensive alternative; however, it can corrode locally and erode in extreme physiological environments, releasing toxic metal ions (Kurgan & Varol, 2010), the drawback of implant material as presented in Figure 2.1.

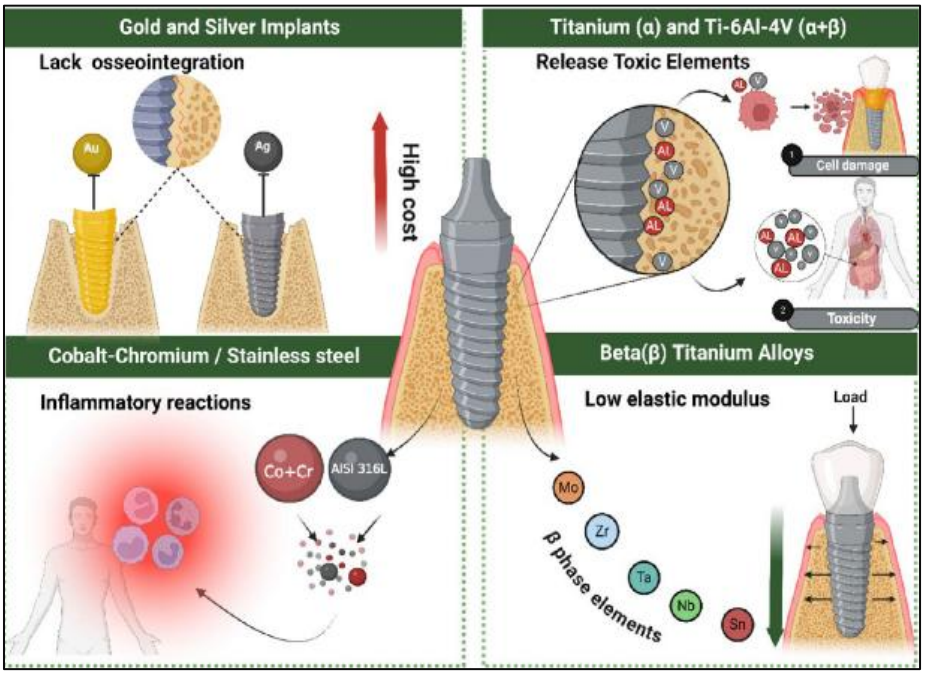

Figure 2.1 Materials Used in Dental Implants and Their Drawbacks

Notes: Gold and silver lack osseointegration and are costly. Cobalt-chromium and stainless steel (AISI 316L) trigger inflammatory reactions. Titanium (α) and Ti-6Al-4V release toxic elements, such as aluminium (Al) and vanadium (V), damaging cells and causing systemic toxicity. β-Ti alloys (Mo, Zr, Nb, Ta, Sn) have a lower modulus, better load distribution, and potentially improved osseointegration (Calazans Neto et al., 2024).

An ideal implant material should possess biocompatibility, acceptable toughness and strength, and resistance to corrosion, wear, and fracture. Among these, titanium (Ti) and its alloys have emerged as the gold standard due to their superior ability to achieve stable bone integration (Albrektsson & Wenneberg, 2019; Adell et al., 1981; Brånemark et al., 1969; Berglundh et al., 2003; Lang et al., 2011). The ability to form a stable TiO_2 oxide layer leads to excellent corrosion resistance and

biocompatibility, which significantly influence the acceptance of Ti and its alloys for osseointegration (Albrektsson & Wennerberg, 2019).

Titanium alloys, particularly Ti-6Al-4V (Grade V), are widely utilised in load-bearing applications due to their exceptional strength and fatigue resistance. However, concerns about the release of aluminium (Al) and vanadium (V) ions have prompted the development of alternative alloys, such as Ti-6Al-7Nb, Ti-5Al-2.5Fe, and β-Ti alloys (containing Nb, Ta, Zr, and Mo). These alloys offer a lower elastic modulus, closer to that of bone, which enhances load transfer and reduces stress shielding (Calazans Neto et al., 2024: Niinomi & Nakai, 2011). For example, a notable innovation, Roxolid® (Ti-Zr alloy), combines high strength with excellent osseointegration, making it a suitable choice for narrow-diameter implants (Berner et al., 2009). This could be particularly useful in high-load areas with insufficient bone width.

Zirconia (ZrO_2) implants have emerged as metal-free alternatives, particularly valued in esthetic zones where titanium's greyish hue may compromise appearance. Particularly in individuals with a thin gingival biotype and/or gingival recession (Thoma et al., 2014). Yttria-stabilised zirconia (3Y-TZP) demonstrates adequate fracture strength and osseointegration comparable to Ti (Andreiotelli & Kohal, 2009; Gahlert et al., 2010). Clinical studies report cumulative survival rates of around 95% at 10 years, though with higher fracture risk than titanium (Mohseni et al., 2024). Limitations include brittleness and a high elastic modulus (210 GPa), which leads to stress concentration in the bone, as well as susceptibility to low-temperature degradation (Chevalier, 2006). While zirconia offers superior aesthetics and low plaque affinity, its long-term reliability in high-load areas remains to be evaluated.

Recently, polymeric biomaterials such as polyetheretherketone (PEEK) have been explored. PEEK's elastic modulus (~3.6 GPa) closely matches bone, potentially reducing stress shielding. It is chemically stable, radiolucent, and biocompatible (Kurtz & Devine, 2007). However, unmodified PEEK is bioinert, hydrophobic, and prone to fibrous encapsulation rather than osseointegration (Koch et al., 2009). Surface modifications (plasma treatment, coating with bioactive ceramics) improve the bone response, but clinical data remain insufficient for routine use. Currently, PEEK is more suitable as a framework or abutment material than as a root-form implant. The classification framework of dental implant materials, based on their chemistry, divides

them into three main categories: metals, ceramics, and polymers, as shown in Figure 2.2.

i. METALS

Material	Common Name/ Abbreviation
Titanium	**cpTi**
Ti alloy	Ti-6Al-4V extra low interstitial (ELI) Ti-6Al-4V Ti-6Al-7Nb Ti-5Al-2.5 Fe Ti-15 Zr-4Nb-2 Ta-0.2Pd Ti-29Nb-13Ta-4.6Zr Roxolid (83%-87%Ti-13%-17% Zr
Stainless Steel	SS,316LSS
Cobalt Chromium Alloy	Vitallium, Co-Cr-Mo
Gold Alloy	Au Alloys
Tantalum	Ta

II. CERAMICS

Material	Common Name/ Abbreviation
Alumina	Al2O3, polycrystalline alumina or single-crystal sapphire
Hydroxyapatite	HA, Ca10(PO4)10, (OH)2
Beta-Tricalcium phosphate	β-TCP, Ca3(PO4)2
Carbon	C vitreous, low-temperature isotropic (LTI), ultra-low-temperature isotropic (ULTI)
Carbon-Siliconi Bioglass Zirconia Zirconia-toughened alumina	C-Si SiO2/CaO/Na2O/P2O5 ZrO2 ZTA

III. POLYMER

Material	Common Name/ Abbreviation
Polymethylmethacrylate	PMMA
Polytetrafluoroethylene	PTFE
Polyethylene	PE
Polysulfone	PSF
Polyurethane	PU
Polyether ether ketone	PEEK

Figure 2.2 The Dental Implant Material Classification (Nicholson, 2020).

2.5.1 Nickel-Titanium (NiTi) as An Endosseous Implant Material

Due to the remarkable shape memory effect (SME) and superelasticity, shape memory alloys (SMAs) are becoming increasingly popular in various applications. SMA is an advanced smart material capable of converting thermal energy into mechanical work and exhibiting unique mechanical properties. Among various SMAs, such as NiTi, Cu-Zn-Al, Co-Ni-Al, Cu-Al-Ni, Ni-Mn-Ga, and Ti-Cu, NiTi exhibits excellent shape memory features, including high shape recovery, recovery stress, and superelastic strain (Elahinia et al., 2012; Zhang et al., 2021).

Nickel-titanium alloy is also known as NiTi or Nitinol. The name Nitinol derives from nickel, titanium, and 'nol'. Nol is an abbreviation for Naval Ordnance Laboratory, where it was first discovered by Buehler and Frederick Wang in 1962 (Jani, 2014). The initial biomedical applications began in the 1960s; however, concerns about nickel ion leaching and manufacturing challenges delayed its use. Nonetheless, exploration of its potential continued until around the 1980s to the 1990s, when many researchers observed positive bone-implant contact in bone-fixation plates in animal models. Since then, the increasing use of Nitinol in medical engineering has marked a significant advancement in modern medical practices. This trend is mainly driven by a growing

preference for non-invasive treatments, alongside improvements in Nitinol manufacturing processes.

Nitinol, an alloy of nickel and titanium, is known for its unique properties, including the shape memory effect (SMA) and pseudoelasticity (PE), along with notable yield strength and high ductility. These features, combined with wear resistance, non-magnetic qualities, corrosion resistance, and biocompatibility, make Nitinol an ideal material for a diverse range of applications. Beyond its medical uses, Nitinol is utilised in aerospace for its lightweight, durable properties and in manufacturing for components such as couplings and fasteners. It is also used in electrical safety devices, microelectromechanical systems, and sports equipment, where its strength and flexibility improve performance. Additionally, the navy depends on Nitinol's resilience in challenging environments (Jani, 2014).

In the medical field, the versatility of Nitinol (NiTi) is especially evident. Specifically, its hysteretic behaviour, the connection between damping properties and material wettability with biological tissues, and its dependable performance within the body under cyclic conditions allow the use of NiTi-based alloys in various medical applications to address complex issues. Through body heat or external heat sources, the SMA and PE can be activated, a phenomenon not typically observed in conventional alloys (Es Souni et al., 2005). Notably, NiTi-based implants are used in traumatology, the treatment of urological and gynaecological conditions, vascular surgery, as components in orthodontic devices, and in ophthalmology. For example, in orthopaedic bone implants, they aid skeletal movement. Similarly, in cardiopulmonary procedures such as stent placement, their ability to expand and contract efficiently meets bodily requirements as they approach blood vessels and the heart. NiTi also plays a significant role in non-invasive surgery, improving procedural efficiency by enabling access through small incisions. In endodontics, its superelastic properties and ability to return to its original shape allow files to be used in complex root canal systems without breaking. Similarly, in orthodontics, nitinol's unique features, including its superelastic properties, facilitate efficient tooth movement. An example of NiTi's application in the medical field is shown in Figure 2.3 and summarised in Table 2.1.

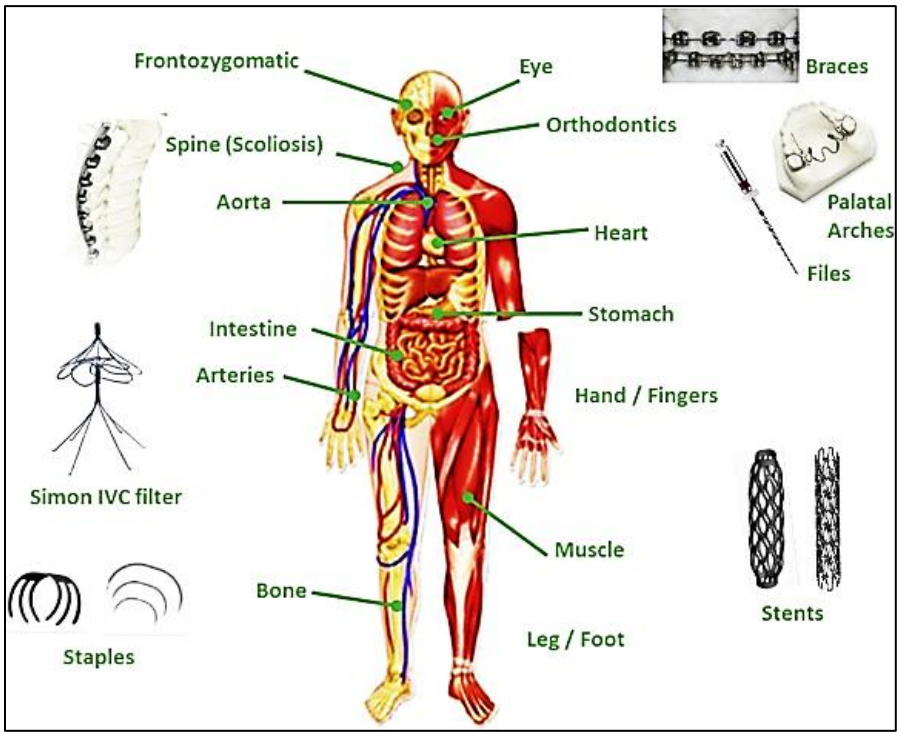

Figure 2.3 Application of NiTi in the Medical Field (Jani et al., 2014)

Table 2.2
Example of Clinical Applications of NiTi as a Biomedical Device

Field	Application	References
Orthopaedic therapy	Scoliosis treatment	Chan et al., 2018; Cheung et al., 2018
	Staples, intramedullary nails, intramedullary implant	Payo-Ollero et al., 2019; Safranski et al., 2020; Wu et al., 2019
	Lumbar interbody implant	Abduljabbar et al., 2017
Endovascular therapy	Stent	Elhamdy et al., 2017; Barras & Myers, 2000; Lammer et al., 2011; Rocha-Singh et al., 2012
ENT	Stapes prosthesis	Roosli et al., 2011; Révész et al., 2016
Genitourinary therapy	C-shape nitinol prosthesis	Vjaters et al., 2020
Pulmonary therapy	Endobronchiol coil	Zoumot et al., 2015
Orthodontic therapy	Self-ligation of fixed appliances	Gölz et al., 2016

2.5.1.1 Mechanical Properties Advantages of NiTi for Endosseous Applications

What makes nearly equiatomic NiTi unique is its shape memory effect (SME) and pseudoelastic (PE) properties. These two features are inherent to a thermomechanical martensitic-austenitic phase transformation, which is uncommon in other shape-memory alloys (Duering et al., 2017). NiTi exhibits two distinct phases: austenite (a high-temperature phase) and martensite (a low-temperature phase) (Zhang et al., 2021). Changes in its crystal structure depend on the transformation temperature or applied stress, especially the martensite start temperature (Ms) and the austenite finish temperature (Af). The transition between these phases occurs through lattice distortion rather than atomic diffusion, a process known as a martensitic transformation. There are two types of martensite arrangements: twinned martensite (Mt), which includes self-accommodated variants, and detwinned martensite (Md), comprising detwinned or reoriented variants (Zhang et al., 2021). The SMA follows the path from A to B and C, as shown in Figure 2.7. When low-temperature Mt is loaded, deformation causes Mt to reorient, resulting in detwinning of the martensite, Md (along the path A to B). Upon removing the load from Md, the deformed shape persists (B to C). This Md remains in a detwinned structure until the SMA is heated above Af; to revert Md to austenite, where the shape is fully restored (C to D), as shown in Figure 2.4. This phenomenon is called the shape memory effect (SME).

Meanwhile, NiTi's superelastic behaviour is evident during loading and unloading above Af (austenite finish temperature). Initially, NiTi exists in an austenitic state at point O. When stress is applied, it transforms from austenite to martensite along the path from O to E. During unloading, it reverts to austenite (E to O).

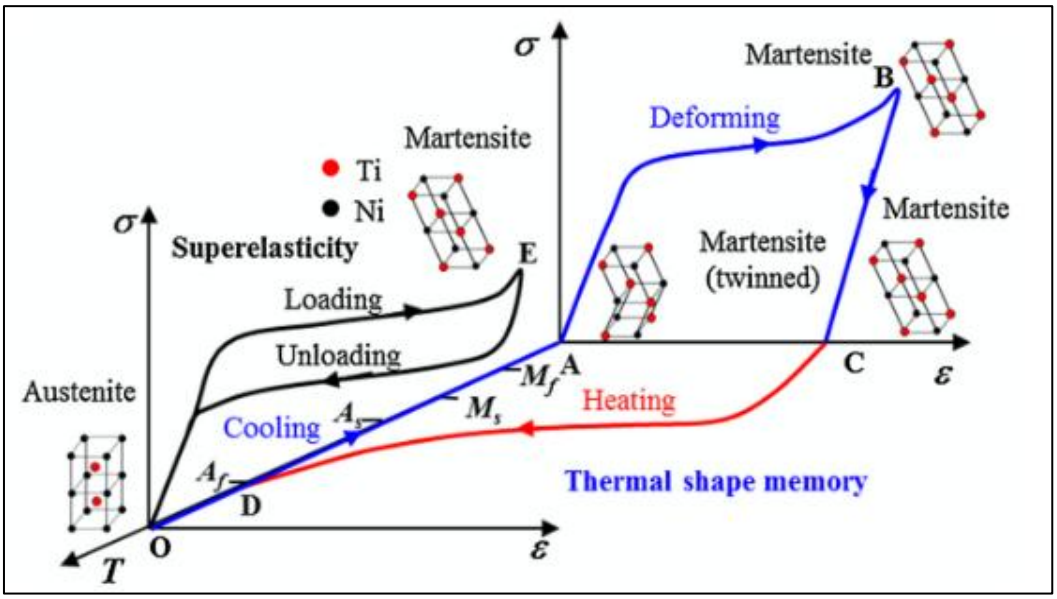

Figure 2.4 Diagram of Stress-Strain of NiTi System.

Notes: T is Temperature, σ is stress, ε is strain; Af is austenite finish temperature, As is austenite start temperature, Ms is martensite start temperature, Mf is martensite finish temperature (Guo et al., 2013).

As shown in Figure 2.5, these stress–strain diagrams further illustrate the advantages of NiTi as an implant material. This diagram compares how three different materials deform: bone, nickel-titanium (NiTi), and stainless steel. The bone exhibits a significant amount of recoverable strain, exceeding 1%, and shows hysteresis during both loading and unloading cycles. NiTi exhibits similar features, with a remarkable ability to sustain high load-bearing capacity, even under loads as high as 11%. From certain deformations, recoverable deformation returns 9-10% of its strain after unloading. For stainless steel, the recoverable strain is relatively low, typically less than 0.5%. Furthermore, NiTi can tolerate cyclic strain amplitudes between 4% and 12%, exceeding the capacity of other alloys, which are limited to 1% or less. Unlike common metallic implants, which typically endure only around 0.1%, NiTi exhibits this capability. (Amerinatanzi et al., 2016; Mahtabi et al., 2015). The similar deformation patterns and mechanical hysteresis of NiTi and bone highlight the biomimetic nature of NiTi shape memory alloy (SMA) implants during loading and unloading cycles within the body (Basinddhi et al., 2008). These properties improve the biomechanical compatibility of the implants. NiTi's unique shape memory and superelastic characteristics allow it to bend and revert to its original shape effectively over multiple fatigue cycles and repetitive loading and unloading, making it suitable for implants in areas subject to high loads (Bansiddhi et al., 2008). While other titanium and cobalt

alloys can also endure cyclic loading, their atomic bonds tend to weaken over time, leading to plastic deformation or fracture (Bansiddhi et al., 2008).

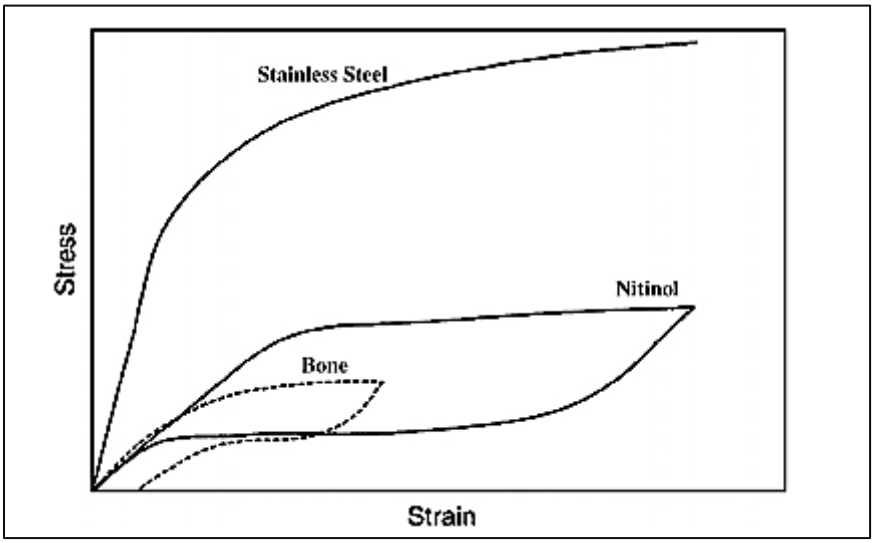

Figure 2.5 Schematic Diagram of Stress-Strain Curves for Stainless Steel, NiTi and Bone (Shabalovskaya et al., 2008).

Aside from the properties noted earlier and other features such as high compressive strength, shock absorption, ductility, acceptable corrosion rates, and excellent biocompatibility (Mustafa et al., 2023; Wang et al., 2020), NiTi's Young's modulus of elasticity, which ranges from 30 to 70 GPa, is a significant advantage for biomedical applications, especially in orthopaedic and dental implants. This modulus is considerably lower than that of common biomedical alloys such as titanium, cobalt-based alloys, and stainless steel, and it closely matches the elastic properties of human bone. Cancellous bone features a Young's modulus of less than 3 GPa, whereas cortical bone ranges from approximately 12 to 20 GPa (Safranski et al., 2020). Such compatibility diminishes stress shielding, a condition where implants with a much higher Young's modulus bear most of the load, leading to reduced mechanical stimulation and bone resorption, ultimately causing implant loosening and failure (Zhang et al., 2021). Using implant materials with similar elastic properties fosters balanced stress distribution and supports bone remodelling (Safranski et al., 2020). In the end, NiTi demonstrates potential as an alternative to traditional implants or fixation plates in orthopaedic and maxillofacial surgery, which are often vulnerable to failure under high loads (Amerinatanzi et al., 2016; Mahtabi et al., 2015; Safranski et al., 2020).

Table 2.9 compares the mechanical properties of natural human bone with various biomedical metals.

While NiTi's Young's modulus significantly exceeds that of traditional materials, further research aimed at reducing its stiffness could enhance its compatibility with natural bone, thereby improving implant integration and durability. One approach is to utilise porous NiTi, whose mechanical properties can be customised by adjusting porosity, pore size, shape, and distribution to more closely replicate natural bone (Elahinina et al., 2012). In addition to decreasing elasticity and density, pores increase permeability for biological processes during healing, thereby promoting bone ingrowth (Rhalmi et al., 1999). The porous surface allows body fluids to infiltrate the voids, encouraging new bone formation. Over time, bone ingrowth into the pores increases due to the material's cellular, bone-like structure (Abduljabbar et al., 2017), thereby eliminating the need for bone grafting (Wally et al., 2015). Its porosity may also facilitate capillary fluid movement and tissue ingrowth (Assad et al., 2003; Assad et al., 2004), and enhance tissue-implant contact and stability (Kapanen et al., 2001). Studies have demonstrated active bone metabolism within interconnected pores and perpendicular to soft tissue fibres, in contrast to the parallel orientation observed in non-porous implants (Assad et al., 2003). This structure promotes faster bone growth than conventional dense Ti6Al4V.

Although larger pores enhance biological integration, they compromise mechanical strength, thereby increasing the risk of implant failure in load-bearing areas, such as long bones and jaws. The ideal pore size to balance these effects remains debated, with some studies suggesting that a pore size of approximately 200–300 μm is suitable for achieving this balance (Zhang et al., 2021). The impact of different pore sizes on the mechanical properties of biomaterials is also summarised in Table 2.3. The detailed biological effects of pore size and shape, interconnectivity, and porosity are further discussed in section 2.7.3

Table 2.3
Mechanical Properties of Biomedical Metallic Materials and Natural Human Bone

Material	**Yield strength (MPa)**	**Elastic modulus (GPa)**	**Reference**
Stainless steel	760	~190	Torres et al., 2016
Co-based alloy	-	~210	Simske et al., 1997
CP-Ti	240–550	100	Geetha et al., 2009
Ti-6Al-4V	950	112	Wang et al., 2018
Ti-35Nb-7Zr-5Ta	596	55	Simske et al., 1997
Cortical bone	188–222	15–35	Wang et al., 2020
Trabecular bone	2–70	0.01–3	Li et al.,2015
Dense NiTi	1050	48	Wang et al., 2018
Metallic porous material mechanical properties			
Material with porosity (vol% %)	Compressive strength (MPa)	Elastic Modulus (GPa)	Reference
Bone (5-90%)	-	0.1-30	Mediaswanti et al., 2014
NiTi (49%)	273.45 ± 9.25	8.71 ± 0.24	Nakaş et al., 2011
NiTi (58%)	174.75 ± 10.75	5.87 ± 0.31	
NiTi (64%)	93.27 ± 5.30	2.93 ± 0.03	
Ti (78%)	-	5.3	Mediaswanti et al., 2014
Ti6Ta4Sn (75%)	-	4.6	
Ti NbSn (30–60 %)	-	10.8–33.2	
Ti10 Nb10Zr (59%)	-	5.6	
TiZr (70%)	-	15.3	
Ti15Mo5 Zr3Al (26%)	-	20	
Ta (75–85%)	-	2.5–3.9	

2.5.1.2 Manufacturing of Porous NiTi

Creating porous structures is a well-recognised approach to reducing Young's modulus, which has spurred substantial research into effective manufacturing methods to achieve optimal results (Elahina et al., 2012; Zhang et al., 2021). Traditional

techniques like casting, often employed to produce NiTi, face significant challenges in efficiently and cost-effectively fabricating complex porous designs. The casting process generally requires high-temperature melting, which can introduce impurities such as carbon and oxygen. These impurities may impair the functional and mechanical integrity of NiTi (Elahinia et al., 2018). Additionally, employing casting techniques to machine these super-ductile alloys introduces further complexity (Elahinia et al., 2012; Ismail et al., 2012) and results in excessive tool wear (Elahinia et al., 2012), as illustrated in Figure 2.6. Due to this sensitivity, traditional NiTi components are usually limited to simple shapes such as wires, plates, strips, and tubes.

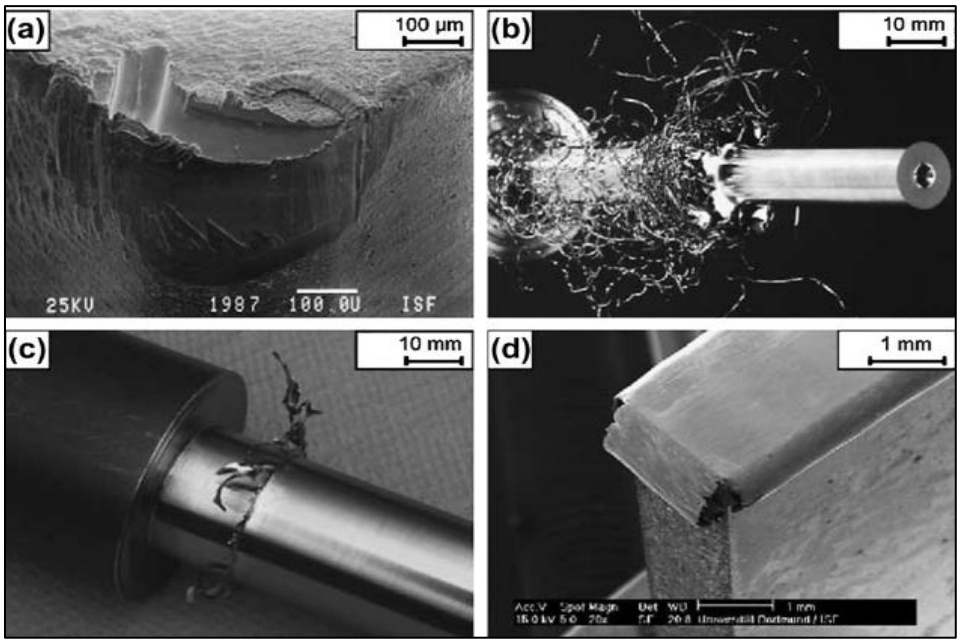

Figure 2.6 Major Drawbacks in Machining NiTi Shape-Memory Alloys

Note: (a) High Tool Wear; (b) Undesirable Chip Formation; (c) Formation of Burrs After Turning (d) and Grinding (Elahina et al., 2012).

Furthermore, the melting point of NiTi is 1310°C, which complicates the production of both monolithic and dense Nitinol structures (Bansiddhi et al., 2008; Lojen et al., 2020). In comparison, titanium has a higher melting point of 1670°C, but NiTi's high viscosity and tendency to oxidise at elevated temperatures further impede its casting and manufacturing processes (Lojen et al., 2020).

Manufacturing NiTi presents challenges due to its distinctive properties, including its sensitivity to stoichiometry, complex thermal and mechanical processing requirements, and resistance to deformation, all of which complicate production. For

instance, a slight change of just 0.1 atomic % in nickel content can lead to a substantial shift in transformation temperatures of nearly 10°C (Es Souni et al., 2005; Zhang et al., 2021). This emphasises the importance of accurately controlling the chemical composition.

Preventing impurities such as oxygen, nitrogen, and carbon is essential because they can react with intermetallic phases to form precipitates like TiC and $Ni_4Ti_3O_x$.

These impurities can significantly affect transformation temperatures, hysteresis behaviour, and key properties including strength, ductility, corrosion resistance, and biocompatibility (Ismail et al., 2012; Ismail et al., 2016; Sharma et al., 2018; Zhang et al., 2021). The presence of 1.0 at. % oxygen significantly influences the martensite transformation temperatures, reducing them by 92.6 K and increasing the brittleness of the parent phase (Bram et al., 2002).

As depicted in the binary phase diagram (Figure 2.7), in addition to the primary NiTi phase, stable phases such as $NiTi_2$ and Ni_3Ti are present within this composition range. Although these phases do not demonstrate shape memory behaviour, their formation alters the composition of the remaining NiTi matrix, thereby affecting the transformation temperature. At lower temperatures, nickel solubility diminishes, leading to the precipitation of finely dispersed metastable Ni_4Ti_3 phase (Sharma et al., 2018). Annealing at 300°C or 600°C causes this metastable phase to coarsen and eventually transform into the stable Ni_3Ti phase (Sahrma et al., 2018; Zhang et al., 2021). The finely dispersed Ni_4Ti_3 precipitates are particularly significant due to their strong influence on material properties and the austenite/martensite transformation.

These manufacturing constraints limit the broader adoption of NiTi in advanced applications and emphasise the need for innovative techniques to fully realise its potential. Improvements in manufacturing methods and materials could help resolve these issues, enabling more efficient production of porous structures and reducing waste, thereby improving outcomes in titanium and NiTi implant manufacturing. Various techniques for NiTi fabrication, some of which are regarded as superior to others, are thoroughly examined. It is also suggested that, to overcome the manufacturing challenges of complex structures, powder metallurgy (PM) and additive manufacturing (AM) are currently the most suitable solutions (Ismail et al., 2012; Zhang et al., 2021). A classification of NiTi manufacturing methods is provided in Figure 2.8.

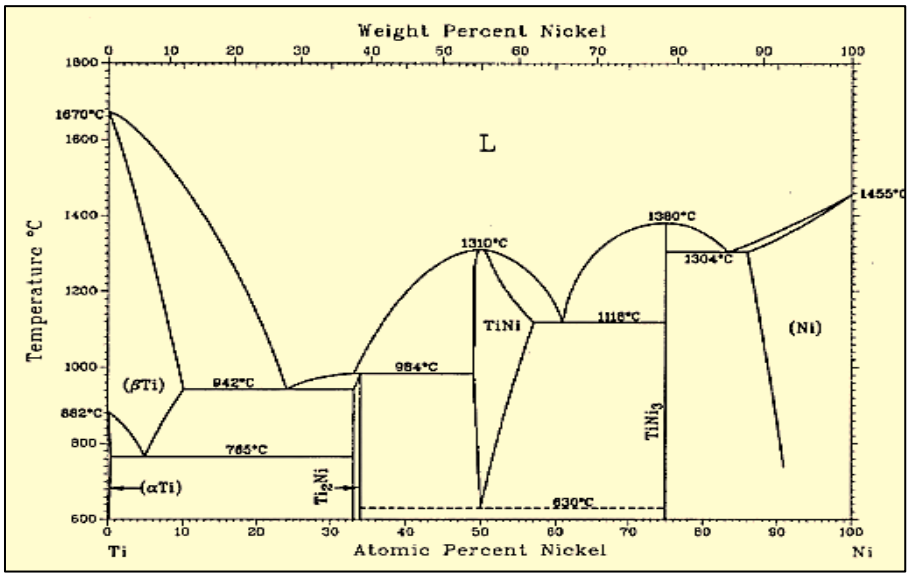

Figure 2.7 Diagram of the Binary Phase of the NiTi System. (Murray, 1990)

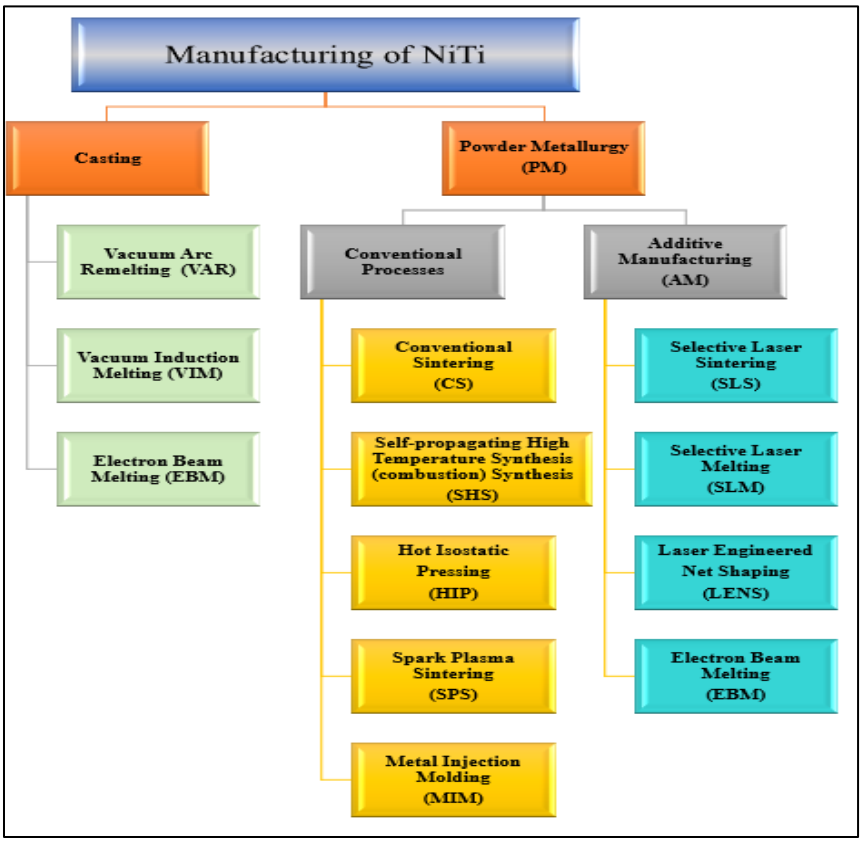

Figure 2.8 The Overview of NiTi Fabrication Process

2.5.1.3 Powder Metallurgy Production of Porous NiTi

The traditional method of producing shape memory alloys (SMAs) involves processes such as arc or induction melting, followed by hot working to achieve the

desired properties and then machining to their final specifications. However, cast metals may exhibit segregation, and during subsequent high-temperature processing, rapid grain growth can occur, negatively affecting their fatigue properties (Bram et al., 2002). This is because arc melting requires multiple remelting cycles to ensure a uniform composition, whereas induction melting can encounter issues such as crucible contamination and oxygen exposure.

A highly effective method for producing Nickel-Titanium (NiTi) alloys is through powder metallurgy (PM). This process involves carefully mixing nickel and titanium powders in nearly equal proportions, followed by heating to form the alloy (Elahinia et al., 2012). The main advantage of powder metallurgy for NiTi alloys is its ability to create highly alloyed compositions with a consistent microstructure. This uniformity and homogeneity result in isotropic mechanical and physical properties, which are crucial for applications requiring reliable, predictable performance and significantly enhance machinability (Ismail et al., 2016). Additionally, compared to traditional ingot metallurgy, the rapid solidification during powder production and consolidation in powder metallurgy significantly reduces property variability (Ismail et al., 2016).

Over the past thirty years, extensive research has focused on the PM processing of NiTi alloys, recognising it as a promising method for creating porous, near-net-shape components (Ismail et al., 2012, 2016; Mustafa et al., 2018). Despite advancements in PM techniques, several challenges remain, especially in practical applications. One key issue is the high presence of brittle oxides, particularly $Ti_4Ni_2O_x$, in sintered alloys. The levels of these oxides tend to be considerably higher than those in melt-cast alloys, which could affect the performance and durability of the final products (Zhang et al., 2021). Addressing these challenges is essential for further improving the reliability and efficiency of PM processes in producing NiTi components.

In the manufacturing of NiTi alloys, two primary powder metallurgy methods are used: sintering raw metal powders and sintering alloyed powders. The first method involves mixing, pressing, and sintering pure metal powders, which can cause some inconsistencies in the alloy's composition. Conversely, the second method utilises prealloyed powders, resulting in a more uniform sintered alloy. This uniformity ensures that the resulting alloy exhibits excellent properties, comparable to those of vacuum-melted alloys. A significant advantage of powder metallurgy is that it bypasses melting

processes that can cause compositional errors, enabling precise control over transformation temperatures.

The fabrication of PM-NiTi presents both opportunities and challenges, particularly regarding impurity levels. These impurities can include intermetallic phases that considerably influence the material's mechanical properties. Achieving high-quality results remains challenging, especially when using elemental mixtures of nickel and titanium. This challenge arises from the differing diffusivity rates of titanium and nickel, as well as the capillary effects induced by liquid eutectics such as Ti_2Ni and Ni_3Ti. Moreover, the highly exothermic reactions involved in the formation of the NiTi compound further complicate the sintering process.

Secondary phases often form because they are thermodynamically more stable than the NiTi matrix. Common inclusions in these materials include carbides, such as titanium carbide (TiC), intermetallic oxides such as $Ti_4Ni_2O_x$, and other phases, including $NiTi_2$, Ni_3Ti, and Ni_4Ti_3. While Ni_4Ti_3 precipitates can sometimes offer specific benefits, it is crucial to recognise that the presence of carbides and oxides may pose challenges, particularly with respect to corrosion resistance, biocompatibility, and transformation temperature. Therefore, employing PM technology to manufacture porous NiTi structures involves a range of considerations and limitations that deserve our attention.

To address these complexities, powder-based methods are generally divided into two main categories: 1. traditional powder metallurgy techniques, which encompass various compaction and sintering processes, and 2. innovative additive manufacturing methods that leverage recent advances in 3D printing. These categories illustrate the ongoing development and exploration of PM techniques to optimise the production of NiTi components. Several successful PM methods for manufacturing NiTi include Self-Propagating High Temperature Synthesis (SHS) (Li et al., 2000), Hot Isostatic Pressing (HIP) (Bertheville et al., 2004), and Spark Plasma Sintering (SPS) (Zhao et al., 2005). Other approaches involve Metal Injection Moulding (MIM) (Ismail et al., 2012), pressure cold pressing followed by sintering, and conventional sintering (CS) (Elahinia et al., 2012). Additionally, spark plasma sintering (SPS) and microwave sintering (MWS) are used in NiTi fabrication (Xu et al., 2015). A summary of the benefits and disadvantages of NiTi manufacturing methods is provided in Table 2.4.

Table 2.4
Mechanism, Advantages and Disadvantages of Manufacturing Method

Manufacturing Method		Mechanism	Advantages	Disadvantages	References
Casting	Vacuum Induction Melting (VIM), Vacuum Arc Remelting (VAR)	- Casting molten metal into moulds - Solidifying at relatively slow cooling rates (e.g., 0.1 °C/s) - Converting to the final product form through thermomechanical processing - Using an inert gas working atmosphere to minimise contamination during melting	- Low cost - Easily handled	- The alloy has poor compositional homogeneity, with excess titanium or nickel. - Carbides and oxygen-rich phases reduce titanium, lowering phase transition temperatures and weakening mechanical properties. - Melting can create defects in the structure. - Achieving precise shapes and good surface quality often requires additional machining, which is difficult for nickel-titanium (NiTi) due to its ductility and tool wear. - Methods like laser cutting and water jet cutting have limitations in producing complex shapes - Rapid grain growth resulting from subsequent high-temperature working, which leads to poor fatigue properties. - Ni-rich/Ti-rich segregates, oxide, C inclusions, carbon content in final products ranges from 0.04% to 0.06%	Elahina et al., 2012; Kubášová et al., 2024; Sharma et al., 2018
	Electron beam melting (EBM)	- Melting performed in a water-cooled copper crucible and under a high vacuum (pressure less than 10^{-2} Pa)	- Minimise carbon and oxygen contamination	- High vacuum operation and heating temperature complicate control of chemical composition.	Elahina et al., 2012

Manufacturing Method		Mechanism	Advantages	Disadvantages	References
			- Carbon content in final products is very low and ranges from 0.007% to 0.016%	- Element evaporation alters martensitic transformation temperatures, especially on the nickel-rich side of the phase diagram. - Insufficient composition homogeneity in the ingot due to unidirectional solidification from the bottom. - Despite these issues, the method is used for preparing NiTi SMAs without precise control of transformation temperature.	
Powder Metallurgy	Conventional Sintering (CS)	- Elemental Ni and Ti powders is prepared and sintered at near melting temperatures to yield in binary NiTi from diffusion of Ni and Ti elements.	- Low cost, - Good dimensional precision, - High production rate, - Availability of wide variety of materials - Elimination of the need for secondary machining operations	- Products contain large amount of pores (as high as %40), - No reasonable control on pore size and amounts, - Creation of secondary phases is probable - Presence of residual porosity, size and shape limitations, - Long heating time	Elahinia et al., 2012
	Self-propagating High-temperature Synthesis (SHS)	- A thermal explosion occurs at one end and propagates through the specimen. - requires preheating of the sample to achieve self-sustained combustion	- Low energy requirement, - Relative simplicity of the process and equipment, - Higher purity of the products - Low cost	- Inhomogeneous reaction - Homogeneity is dependent on the uniformity of temperature - brittle due to presence of intermetallic phases of Ti_2Ni, Ni_3Ti, and Ni_4Ti_3 - Products contain large size and amount of porosities - (as high as %65)	Bansiddhi et al., 2008; Elahinia et al., 2012; Li et al., 2000;

Manufacturing Method	Mechanism	Advantages	Disadvantages	References
			- Contain precipitates due to the short forming time and high heating rates, incomplete reactions between elemental powder particles,	
Hot Isostatic Pressing (HIP)	- Pressure enhanced sintering technique - The mixture of elemental powder particles is encapsulated in an evacuated gas-tight welded canister - Undergoes simultaneous isostatic pressure and elevated temperature. - Argon gas can be used as an inert environment without the need for the airtight chamber. - HIP can be used to compress and trap Ar gas bubbles in between the elemental powders. - Subsequent high-pressure diffusion stage leads to Ar-filled pores. Sintering the product at reduced pressures causes the gas to expand and bring about near-spherical pores in the final product.	- Dense products with no pores and good mechanical - properties possible [69,75], good control on pore size - [69], low sintering temperature [75], nearly complete - reaction while taking low process time [69,1], able to - produce large size and/or complex shape products, - high efficient in materials use [68]	- Expensive equipment, slow processing - NiTi2 /Ni3Ti precipitates in the matrix cannot be avoided - Trapped gases, inclusions - Inert gas may cause porosities up to %40	Elahinia et al., 2012
Spark Plasma Sintering (SPS)	- Also known as Pulsed Electric Current Sintering (PECS) - Used prealloyed powders, loaded and pressed in a graphite die. - A strong pulsed current introduces high energy to the compact, causes a joint formation in the	- Fast sintering compared to sintering processes such as CS, HIP, or SHS - Fine microstructure a very short period of time due to the spark discharge	- Expensive, equipment-intensive - Surface oxides, residual carbon - Simple shapes	Elahinia et al., 2012; Sharma et al., 2018

Manufacturing Method		Mechanism	Advantages	Disadvantages	References
		particles at relatively low temperatures and in -	- Low sintering temperature and short processing time - Uniform sintering, - Ease of operation		
	Metal Injection Molding (MIM)	Four major steps: - Feedstock fabrication, - Injection moulding, - Debinding, and - Sintering	- Complex shapes, - Geometrical precision - Minimal machining - Massive production - Cost-effective	- Products with residual pores, - High sintering temperature (large amount of impurity phases - Costly tooling	Elahinia et al., 2012; Ismail et al., 2012; Ismail et al., 2016; Sharma et al., 2018; Li et al., 2000
Additive Manufacturing	Selective Laser Sintering (SLS)	- Uses a high power laser to fuse small powder particles of materials into a mass which has a desired 3-dimentional (3D) shape. - Pre-heating treatment is necessary to minimise the laser powder requirements and also to prevent warping during thermal expansion and shrinkage (curling). - Avoid warping and oxidation, by controlled cool-down cycle of build from working temperature to ambient temperature	- Low melting point - Powders act as a binder, - Capability of having versatile design for porous products	- Materials must be in powders, - Weak surface finish (powdery surface), - Post-processing is required (to increase product density and improve mechanical properties)	Elahinia et al., 2012; Zhang et al., 2021
	Selective Laser Melting (SLM)	- High-powered laser beam (usually a yttrium fiber laser) to create 3D metal parts by fusing fine metallic powders together. - The use of lasers with wavelengths better tuned to the	- No distinct binder and melt phase - No need to time consuming and costly furnace post-processes, infiltration or post-sintering, manufacturing fully dense samples	- Not suited for well controlled composite materials - Small scan velocity (long build time), - Low surface quality of products, - High amount of residual	Elahinia et al., 2012; Zhang et al., 2021

Manufacturing Method	Mechanism	Advantages	Disadvantages	References
	absorptivity of metal powders is one enabling feature of SLM of metals. - Nd:YAG laser results in a much better absorptivity for metal powders instead of the CO_2	- high materials efficiency	- Stress (delamination-distortion) - High energy level needs for laser power (costly), - Difficulty of unbounded powder removal from porous internal architecture	
Laser Engineered Net Shaping (LENS)	- Use LENS machine, - Heat from a laser beam forms a small melt-pool. - Simultaneously, metallic powder is injected into the molten pool, building up a feature.	- Low processing time, - Low cost for modules and dies - Good mechanical properties	- High energy level needs for laser power (costly), - materials must be in powder	Elahinia et al., 2012
Electron Beam Melting (EBM)	- Melting metal powders layer by layer using an electron beam. - The entire process takes place at temperatures around 1000 °C and - in a high vacuum at 10^{-4} mbar in the chamber and 10^{-6} mbar in the electron beam producing gun.	- Fast scan speed - Easily controlled electron beam - Low processing time - Lower energy cost (compared to laser) - Vacuum chamber assures stress-relieved and impurity-free parts - High energy of the electron beam results in dense parts with low porosity and good mechanical properties - Precisely controlled process eliminates expensive secondary processing such as machining, forging, swaging, or forming	- Only for producing metallic product, - Poor surface finish, - Low dimensional accuracy, - Costly (vacuum costs) - Repel between powder particles - Incoming negatively charged electrons themselves leads to the sudden spreading of the powder and also require a more diffuse beam	Elahinia et al., 2012

2.5.1.4 Porous NiTi Implant Fabrication Via Metal Injection Moulding

Among various methods for producing nickel-titanium (NiTi) alloys, powder metallurgy (PM) stands out as a particularly effective and cost-efficient approach for creating near-net-shape components compared to traditional methods (Bram et al., 2002; Elainia et al., 2012; Sabahi et al., 2020). Furthermore, metal injection moulding (MIM) has been successfully employed to produce both porous and dense NiTi alloys (Whitney et al., 2009). Demonstrating remarkable versatility, MIM enables the fabrication of complex shapes, high geometric accuracy, and detailed designs while maintaining excellent mechanical properties and offering low costs for large production volumes (Bram et al., 2002; Ismail et al., 2012). The process begins with less expensive metal powders, enabling faster, more cost-effective production than conventional machining (Elahinia et al., 2012; Ismail et al., 2012).

The significant potential of metal injection moulding (MIM) to produce complex shapes at cost-effective prices becomes particularly clear when used with advanced materials, such as NiTi alloy. However, it is crucial to address the primary challenge of maintaining low impurity levels, particularly for oxygen and carbon. This issue is not just a technical matter; the alloy's purity directly influences its mechanical properties and overall performance.

The MIM process involves four main stages (Figure 2.9): blending to create a uniform powder-binder feedstock, injection moulding to form the component, debinding to eliminate the binder, and sintering to fuse the powder particles. These stages are interconnected; issues at one stage can negatively affect the entire process. Highly porous NiTi can be produced through metal injection moulding (MIM) of elemental powders, which are subsequently alloyed by the heat generated during their interaction (Ismail et al., 2012). However, this method has shown considerable dimensional variation, indicating inconsistencies in the process (Ismail et al., 2012). This highlights the importance of achieving a homogeneous mixture and maintaining consistent processing at each step. Additionally, specific time, temperature, and other parameters for each stage are crucial to optimise the injection moulding process, providing a baseline for the Ti-MIM process (Bram et al., 2002).

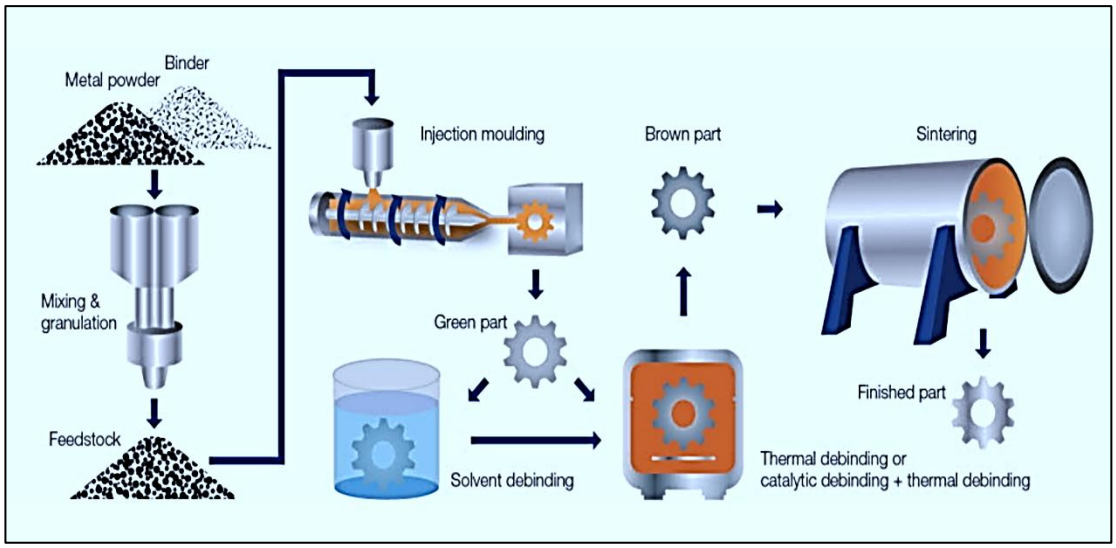

Figure 2.9 A Schematic Diagram of the Metal Injection Moulding (MIM) Process for Producing Net-Shape NiTi.

Source: https://www.hoganas.com/en/powder-technologies/metal-injection-molding/mim-process/

One factor to consider is the preparation of the feedstock. Achieving a smooth and well-mixed combination of NiTi powder and binder is essential for the successful execution of the feedstock injection process (Ismail et al., 2016). Several efficient methods for mixing the feedstock, including batch mixers, continuous mixers, and Dual Asymmetric Centrifuge (DAC) Speed Mixers, have been identified (Maso'od et al., 2018). Among these, the DAC Speed Mixer is considered particularly notable. It minimises handling, quickly produces a uniform mixture, and significantly reduces the risk of contamination in the feedstock (Ismail, 2012).

Furthermore, contamination can occur during the MIM process, but a major challenge in manufacturing NiTi components is effectively controlling impurities from binder systems, which typically include waxes and polymers (Bram et al., 2002). It is essential to develop a suitable binder system for shaping NiTi alloys via MIM while minimising contamination levels (Ismail et al., 2013). This binder assists the process during mixing and injection moulding. However, during debinding, when the binder decomposes, existing pore channels formed before sintering can become contaminated with carbon and oxygen from the binder components. These contaminants may react with titanium during this phase, potentially affecting the shape memory properties and increasing brittleness (Ismail et al., 2016).

The design of the binder system and the associated debinding techniques are vital for the success of MIM and for managing impurities (Neto et al., 2022). Various binder systems have been used, including wax-based and polymeric materials (Bram et al., 2002), as well as a water-soluble binder composed of polyethene glycol (PEG), which is environmentally friendly due to its high water solubility and non-toxicity (Abdullah et al., 2016). The PEG-based binder includes PEG-polymethyl methacrylate (PMMA) (PEG/PMMA) (Ismail et al., 2013), PEG-polypropylene carbonate (PPC), PEG/PPC (Hayat et al., 2017), and a mixture of PEG/PPC with stearic acid and polyvinyl acetate (Abdullah et al., 2016). Other binders consist of palm stearin (Maso'od et al., 2018) and agar-based binders (Chen et al., 2013). Researchers often prefer this water-soluble binder system because of its environmental friendliness and its ability to be removed at low temperatures (Hayat et al., 2017). Some studies have examined the use of pre-alloyed NiTi powder combined with NaCl as a removable space holder. This method produces a well-defined structure with minimal impurities and exhibits pseudoelastic behaviour (Köhl et al., 2009). However, pre-alloyed atomised NiTi powders can be quite expensive (McNeese et al., 2000). To ensure high-quality, reliable components, careful control and supervision throughout the entire process are essential.

Research on creating porous NiTi through MIM has advanced considerably, particularly by a team at Germany's Jülich Research Centre. They used NaCl as a spacer, effectively reproducing the desired pore structure (Abdullah et al., 2016). This innovative approach yielded impressive results, with porosity between 50-70% and pore sizes ranging from 100 to 500 μm. The pore structures exhibited excellent shape memory properties, underscoring strong potential for practical applications.

In 2012, notable progress was made with the successful fabrication of porous NiTi from a mixture of elemental Ni and Ti powders, followed by transient liquid-phase (TLP) sintering. The chosen binder system, PEG/PMMA, produced open pore structures averaging 100-120 μm in size and achieving 39-45% porosity (Ismail et al., 2012). The pore-formation process is clearly illustrated in Figure 2.10, and the final product is shown in Figure 2.11. Furthermore, in 2013, Ismail et al. experimented with an agar-based binder, resulting in approximately 40% porosity, with pores smaller than 20 μm (Chen et al., 2013). These advancements establish a strong foundation for future innovations in porous NiTi materials.

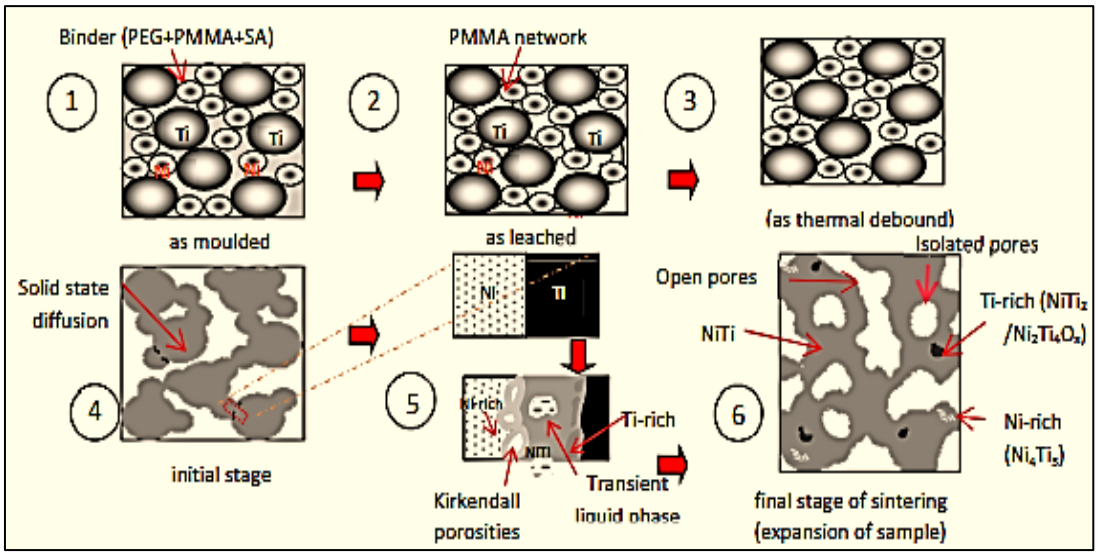

Figure 2.10 Schematic Diagram of the Pore Formation Mechanism (Abdullah et al., 2016).

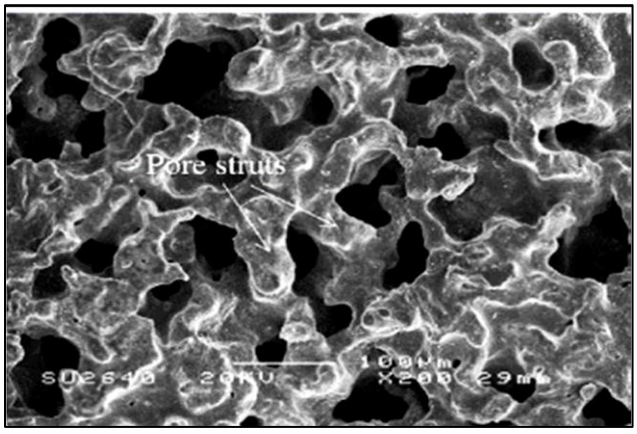

Figure 2.11 Scanning Electron Microscopy (SEM) Image of Porous and Its Interconnected Channels of NiTi Implant Biomaterial Fabricated Through Metal Injection Moulding Technique (Ismail et al.,2012).

2.5.1.5 Concerns of NiTi Implant for Oral Rehabilitation

Biocompatibility is essential to ensure that the selected material is biologically acceptable and non-toxic to living tissues. The dissolution of chemical constituents may lead to anything from local irritation to systemic toxicological effects, and even carcinogenic or mutagenic responses (Shabalovskaya, 1996).

Nickel (Ni) is recognised as an essential trace metal, with the European Food Safety Authority 2020 advising a tolerable daily intake of 2.8 micrograms per kilogram of body weight to 13 micrograms per kilogram of body weight (https://www.efsa.europa.eu/en/topics/topic/metals-contaminants-food#). This metal

naturally occurs in various alloys and can be found in environmental sources such as air, water, and certain foods, especially chocolate, nuts, peas, and grains. The human body can absorb Ni through inhalation, skin contact, or oral ingestion. Biologically, Ni acts as a cofactor in vital metabolic processes, including protein synthesis and the metabolism of sulphur-containing amino acids (Es Souni et al., 2005). Although Ni is necessary, excessive intake beyond recommended levels may cause a range of adverse health effects, from acute to chronic conditions.

NiTi is an intermetallic compound characterised by a well-ordered crystal lattice, exhibiting strong atomic bonding with both covalent and metallic features (Shabalovskaya, 1996). This robust metallic bonding helps stabilise Ni ions within the material, making it difficult for them to escape (Es Souni et al., 2005). Research has shown that the NiTi alloy offers excellent corrosion resistance, comparable to that of titanium and the titanium alloy Ti-6Al-4V (Wever et al., 1997; Figueira et al., 2009).

Similar to other titanium alloys, NiTi can form a protective outer layer mainly made of TiO_2. This layer effectively reduces the leaching of Ni ions, as observed in Ti6Al4V (Abduljabbar et al., 2017; Clarke et al., 2006; Morgan, 2004; Tian et al., 2011). Additionally, the TiO_2 layer promotes the formation of a calcium-phosphate layer during *in vitro* testing and when the implant interacts with the biological environment (Wever et al., 1997). Both the TiO_2 and calcium-phosphate layers are considered crucial for preventing free ions from diffusing into surrounding tissues (Clarke et al., 2006; Tian et al., 2011; Wever et al., 1997).

In potentiostatic and potentiodynamic tests, the NiTi surface demonstrates excellent durability, with no breakdown up to 1300 mV (Shabalovskaya et al., 2008). However, the pitting potential, which is the point at which ion leaching begins, can occur at lower potentials between 150 and 300 mV under open-circuit conditions or in the presence of scratches (Aziz-Kerrzo et al., 2001; Shabalovskaya et al., 2008). Scratches may facilitate nickel-ion diffusion to nearby structures, potentially increasing diffusion by up to 100-fold (Tian et al., 2011). Significantly, a surface film primarily composed of TiO_2 forms through repassivation even at potentials as low as -150 mV, including in acidic environments (Asserghine et al., 2019).

Numerous researchers have studied the importance of implant surface stability, particularly highlighting the role of the TiO2 layer thickness (Shabalovskaya, 1996). By accurately adjusting the Ni ion concentration at the outermost surface layer, it is

possible to reduce the pitting potential of nitinol, with promising implications for material performance (Clarke et al., 2006).

The techniques used in casting, polishing, and surface treatment are crucial for shaping the outer surface layer of NiTi (Milošev & Kapun, 2012). Proper oxidation at suitable temperatures can produce a fully stabilised TiO_2 layer with an ideal thickness of around 130 nm. This process can effectively lock Ni ions within the metallic lattice, resulting in an oxide surface free of Ni traces (Tian et al., 2011). Among various surface treatments, electropolished surfaces (EP) have demonstrated better stability and corrosion resistance compared to other methods, such as electropolished followed by chemical passivation (CP) and mechanically polished (MP) surfaces, the latter of which showed increased material loss due to higher corrosion rates (Cissie et al., 2001). This enhanced performance may be due to a uniform surface topography that promotes a thicker oxidised layer than a more uneven surface structure (Shabalovskaya et al., 2008).

Although coated surfaces increase thickness and offer benefits, they often fail to preserve nitinol's superelastic properties, leading to early cracking even at low strain levels (<1%) (Shabalovskaya et al., 2008). This emphasises the need for further research to balance surface treatments with nitinol's desired mechanical properties.

Changes in pH as low as 3, especially under oxygen-deficient conditions, can trigger the release of nickel (Ni) ions into the environment (Clarke et al., 2006). In the oral cavity, such conditions may arise from interactions among the organic and inorganic components of blood and interstitial fluid, or from activities associated with oral biofilms and diet. Inflammation and ischaemia can create a locally acidic, oxygen-poor environment, which may weaken surface layers and lead to the release of Ni ions into neighbouring structures (Figueira et al., 2009; Sodor et al., 2015). It has been observed that at pH 3, disruption of the oxide layer facilitates this release.

Despite this, the healing process through repassivation can naturally reduce the effects of leached Ni ions. Both *in vitro* and *in vivo* studies show that Ni ions are released in amounts ranging from less than 0.01 to 9.0 µg/g; however, this release is generally considered negligible, as it stays below the dietary intake, which ranges between 100-300 µg/day (Cempel & Nikel, 2006; Gopikrishnan et al., 2015; Mudjari et al., 2019). This emphasises the importance of monitoring pH and oxygen levels to minimise the release of Ni ions and promote oral health.

Animal studies showed that nitinol is biocompatible with living tissues, as illustrated in Table 2.5. In short-term analyses, no signs of adverse tissue reactions or metal traces were found in local, adjacent, or distant tissues, including the liver, spleen, brain, and kidneys (Castleman et al., 1976). NiTi has proven to be safe, demonstrating excellent biocompatibility, gene compatibility, and cytocompatibility, along with good tissue adhesion after implantation and increased fixation over time (Abduljabbar et al., 2017; Assad et al., 1999; Assad et al., 2003; Mustafa et al., 2023; Rhalmi et al., 1999). Immunity testing for sensitivity and allergic reactions in animal studies also confirmed the material's safety, as no acute symptoms like convulsions or biological reactions were observed *in vivo* (Assad et al., 2002; Mustafa et al., 2023).

Further analysis of local mechanical stress suggests that, in clinical use, NiTi alloy self-ligating devices may not cause significant corrosion or nickel release, as salivary nickel ion levels remained below the average dietary intake (Gölz et al., 2016). Nickel ion concentration was highest immediately after wire and bracket placement, then returned to baseline after two weeks of exposure. Several clinical applications of nitinol have been documented (Table 2.6), with outcomes comparable to those of other biomaterials.

Table 2.5
In-Vitro and *In-Vivo* Studies on Ni Ion Diffusion

Study Design	Medium	Material	Methodology	Finding	Reference
Longitudinal study aim of this study was to analyse the N= 15 patients (9 females, 6 males, aged: 16-28 years old)e) of gcf nickel and chromium levels with the increase of hair nickel and chromium levels.	levels of nickel and chromium in GCF and hair of orthodontic patients	- 0.018inch slot pre-adjusted Roth prescription stainless steel brackets (Protect, China) on all teeth except the molars, - Stainless steel orthodontic bands (Protect, China), and NiTi wires (Nitinol; Ormco Corporation, California, USA).	Atomic Absorption Spectroscopy	GCF significant (paired t-test, *P*=0.000 1. Nickel level: baseline: 3.39 µg/g 4 months: 9.00µg/g; 2. Chromium level: baseline: 1.88 µg/g 4 months: 6.85 µg/g. Hair significant (paired t-test, *P*=0.000) 1. Nickel level: baseline:0.14 µg/g, 4 months: 0.42µg/g; 2. Chromium level: baseline: 0.09 µg/g 4 months: 0.11 µg/g. No significant correlation between the increase in ion level in GCF and that in hair.	Mudjari et al., 2019
In-vitro study	0.1M NaCl solution at pH=7 and 3	Mechanically polished 55Ti45Ni (4000 grit silicon carbide paper and polished with alumina silica)	Electrochemical impedance spectroscopy (EIS), scanning electrochemical microscopy (SECM) and atomic absorption spectroscopy (AAS).	Acidic environment influences passive oxide film resistance from 36.04 kΩ.cm2 to 28.24 kΩ.cm2. Dissolution and repassivation of the surface layer occurred in acidic solution.	Asserghine et al., 2019

Study Design	Medium	Material	Methodology	Finding	Reference
Animal study (nitinol stent implantation with various surface polishing on iliac artery of minipig) – 6 months evaluation		4. Surface polishing preparation: 1. Machined surface, MS 2. Air Furnace, AF 3. Salt Pot, SP 4. Oxidised tube, OT	Necropsy assessment, clinical chemistry, haematology, Artery Ni & histopathology analyses	Throughout 180 days - Liver and kidney function were not different from baseline values White blood cell, red blood cell, and platelet counts were similar to baseline stents with nonoptimized surface finishing (AF & OT) had significantly greater nickel levels in the surrounding artery compared to polished stents.	Nagaraja et al., 2018
Prospective clinical study N= 30 (age between 10-13)	Unstimulated saliva	self-ligating brackets (SmartClipTM), molar bands, and nickel–titanium (NiTi) archwire	Spectrometer (SCIEX ELAN 5000; Perkin Elmer, Wellesley, MA, USA).	Ni ion level at: T0: 21.85 µg/l T1: 85.34 µg /l T2: 19.19 µg /l T4: 57.74 µg /l T5: 13.73 µg /l T6: 19.83µg /l Return to the baseline level and even lower at 4-week	Gölz et al., 2016

Study Design	Medium	Material	Methodology	Finding	Reference
In vitro laboratory study (duration: 28 days)	Artificial stimulated saliva	1. Stainless steel (SS): Preform arch wires, Ortho-Organizers, Inc, Sanmarcos, California 2. NiTi: Nitinol XL, 3M Unitek, Monrovia, California 3. TMA: TMA, ormco corporation, Glendora, California copper NiTi (C-NiTi): Copper NiTi, Ormco Corporation. lendora, California	Inductively coupled plasma spectroscopy	Leaching out of 3 Nickel, Chromium & Iron from SS, NiTi & C-NiTi. • SS archwire: Nickel - 0.006 ppm, Cr - 0.011 ppm, and iron -0.289 ppm • NiTi archwire: Ni - 0.002 ppm • C-NiTi wire: Ni- 0.004 ppm and Cr - 0.003 ppm	Gopikrishnan et al., 2015
In vitro study	Normal human dermal fibroblasts cells (NHDF) at 3 and 6 days	Negative control: no metal exposure Positive control: opper amalgam Tested: Gr. A-NiTi coil springs, Gr. B- metallic brackets, and Gr. C-orthodontic stainless steel archwires.	Microscopic analysis	Varying intensity of cellular changes without a cytotoxic character around metal brackets. Different preferential tropism between the coils of NiTi coil spring. There is a decrease in cell density at six days for the stainless steel archwires. An increase in cell density was observed in the archwire areas where bending was practised.	Sodor et al., 2015

Study Design	Medium	Material	Methodology	Finding	Reference
An animal study of nine adult mongrel female clinically healthy dogs aged Between 2 and 3-year-old (between 24-32 kg weight)		Ni and Ti with 50.5 at.% fabricated using SHS (self-propagating high temperature synthesis) technique, cold pressed at different pressures (50, 75, and 100 MPa) The porosity in the The synthesised products were in the range of 50.7–59.7 vol. %.	Histomorphometry	Good tissue reaction between the bone tissue and the implant. Newly formed bone observed mainly at 6/months of porous NiTi implant made with 100MPa repair.	Tosun et al., 2013
Animal study	Guinea pigs, rabbit and mice after 30- and 54-hours, followed by day-6,	immunity testing for sensitivity and allergic potential	classical skin sensitisation assay (Buehler patch test, in guinea pigs), intracutaneous test (rabbit), and the systemic injection test(mice)	**The Buehler patch test in guinea pigs:** No significant change in skin reactions such as erythema or swelling was observed between the induction and at 30 and 54 hours, on days 6, 14, and 30. **Intracutaneous irritation test**: No irritation or sensitisation reactions were observed in saline-extracted PTN samples. Slight irritation (PTN samples extracted in cottonseed oil) and similar control **Injected with porous titanium–nickel extracts**: No toxic symptoms at 4, 24, 48, and 72 h after treatment.	Assad et al., 2008 .

Study Design	Medium	Material	Methodology	Finding	Reference
Animal study	12 months -sheep model (Implantation of tested material at two non-contiguous lumbar sites and evaluated at 3, 6, and 12 months post-surgery	Porous titanium-nickel (PTN) compared to TiAlV	scanning electron microscopy (SEM) combined with backscattered electron analysis (BSE) and inductively coupled plasma–mass spectrometry (ICP-MS).	Nickel ions in adjacent and remote tissues were low, <1μg/g. Blood nickel levels were observed to be within acceptable levels at all post-instrumentation times. No sign of surface corrosion macroscopically and through SEM.	Assad et al., 2003
In-vitro study		Control: Ti cp and Ti6Al4V Tested: Ti45Ni	Anodic polarisation and electrochemical impedance measurements	Pitting potential of Ti45Ni at 200-540 mV (Average 380mV) in normal saline. There is more pitting potential with H2O2 solution exceeding 800mV. Repassivation potential with and without surface modification was similar, as low as -150mV.	Aziz-Kerrzo et al., 2001
In vitro study	Human peripheral blood lymphocytes	equiatomic nickel-titanium, 316L stainless steel rods, commercially pure titanium and commercially pure nickel	Electron microscopy Immunogold counting and image analysis	Both pure titanium and nickel-titanium specimens showed a relative *in vitro* biocompatibility.	Assad et al., 1999
Animal study	Rabbit (3, 6 and 12 weeks evaluations)	5. Porous NiTi	Histology	All implants held firmly by the back muscle and bone. An adherent of the tissue to the implant increases in strength with time. Fibroblasts have also been seen penetrating implant pores, indicating short-term positive cytocompatibility of NiTi to the cell tissue, *in vivo*. -	Rhalmi et al., 1999

Study Design	Medium	Material	Methodology	Finding	Reference
In vitro laboratory study	Hank solution at 37 °C	Control: stainless steel and Ti6Al4V Tested: NiTi alloy	X-ray electron spectroscopy (XPS) and scanning electron microscopy (SEM)	**Before immersion**, a passive TiO2(mainly) film on the NiTi alloy with minimal amounts of nickel in the outermost surface layers. **After immersion**, a calcium-phosphate layer was observed. Initial release rate of Ni ion: 14.5×10^{-7} μg/cm2/s. Not detected at 10 days.	Wever et al., 1997
Animal study implantation of bony plates of the beagle		-	Radiology, Histology Neutron activation analysis	No adverse tissue formation of local, adjacent tissues, including liver, spleen, brain and kidney, indicated positive reaction of tissue radiologically and histologically. At the same time, neutron activation analyses of those tissues reported no metal traces present in nitinol. In contrast, cobalt-chromium trace metal is seen adjacent to the bone.	Castleman et al., 1976

Table 2.6
Clinical Applications of NiTi Biomaterial

Study method/ clinical application	Findings	Author
Nitinol sleeve on the implant abutment	With 5000 cycles of compressive loading, the retention of nitinol sleeves showed no change after 6 months of clinical use.	Linsley et al. (2020)
Nitinol sleeve on the implant abutment	Good peri-implant tissue health, positive patient responses, and offer screw-less and cement-less restoration to facilitate easy retrieval and reinsertion.	Shah et al., 2020
1-year clinical efficacy of orthopaedic implant (intramedullary fusion implant for correction of claw toe and hammertoe deformities),	Average follow-up was 2.4 years (range 1-5.7), arthrodesis rate was 98% with no wound infection, implant mobilisation, chronic pain or revision surgery. 2% (1/50) were reported with non-union without symptoms.	Payo-Ollero et al., 2019
Retrospective study of the primary patency rate of a completely occluded femoropopliteal lesion using a self-expandable nitinol stent	There were 81.4%, 77.7% and 74.4% mean patency rates following 1, 2 and 3 years respectively. The primary endpoints achieved were comparable to those of open bypass surgery. The outcome showed that this stent is safe for long-term use, with higher primary patency compared with first-generation peripheral stents, which had a higher 1-year restenosis rate (>60%). Clinical restenosis did occur and is suggested to be associated with patient pre-operative surgery condition (TASC II type D), male, DM and smoking. Surprisingly, the material also showed a reduced implant fracture rate (15.3%) after 3 years compared with published stents, which ranged from 8-37%.	Elmahdy et al., 2017
NiTi alloy self-ligating wire in orthodontic case	NiTi may not be sufficient to corrode and release a significant amount of nickel in the saliva. The median salivary Ni2+ was below the average dietary intake.	Gölz et al. (2016)

2.5.1.6 NiTiDent Tuah Porous NiTi Dental Implant

It is important to note that NiTi's high melting point (1310°C) limits its manufacturing primarily to powder metallurgy techniques, which can be technically demanding, especially when producing interconnected open porosity with the desired average pore surface area. Additionally, using incomplete elemental powder methods

and having a heterogeneous surface structure may pose a risk of Ni release. This could result in allergic reactions or other complications, such as cytotoxicity or genotoxicity, raising significant health concerns.

The development of a NiTiDent Tuah porous dental implant (NT) employs the MIM technique, addressing this issue through established methodologies (Ismail et al., 2012; Ismail et al., 2013; Mustafa et al., 2023). This process involves several stages, including injection moulding, solvent and thermal debinding, and sintering, all carried out at Nitium Technology's ISO 13485:2016-certified facility in Selangor, Malaysia.

The feedstock for this pNiTi implant consists of a mixture of nickel (Ni) and titanium (Ti) powders, accounting for 67.5% of the total volume, with the remainder composed of polymer binders. To achieve the desired pseudoelastic properties, a specific nickel/titanium ratio of 56 wt% Ni/44 wt% Ti is used. The binders involved in the process include three components: a water-soluble binder that facilitates smooth feedstock flow during MIM, a backbone binder that provides rigidity to the shaped parts, and a surfactant that prevents powder agglomeration. The formation of porosity in the final product results from interactions among the molecular chains of these binders, particularly during the thermal debinding phase, when the backbone binder is removed.

During sintering, particle densification and bonding form a highly interconnected porous structure with average pore diameters of about 50 μm and porosities ranging from 25% to 30%. Scanning electron microscopy (SEM) images illustrate the development of the implant at various processing stages, as shown in Figure 2.12. This innovative, porous, near-equiatomic NiTi (56-44 wt%) alloy features a well-homogenised composition, a tapered fixture design, and distinctive threaded features, including a knife edge at the apex and a square shape along the middle and coronal third. It offers the potential to significantly enhance biological performance in both cortical and trabecular bone regions, contributing to a future with less reliance on additional surface coatings.

The development of the ‘NiTiDent Tuah Porous NiTi Dental Implant’ was carried out using a risk-based approach, in accordance with ISO 14971:2019, and its manufacturing is certified under ISO 13485:2016. It complies with the following regulatory requirements: Medical Device Authority (MDA/GD/0007, MDA/GD/008, MDA/GL/MD01), European Commission, CE (MDR 2017/745), and Food and Drug Administration (FDA, US) (Title 21 CFR 807, Title 21 CFR 801). Preclinical testing of

its physical, mechanical, and biocompatibility properties is presented in Tables 2.7 and 2.8 and Figures 2.12 and 2.13.

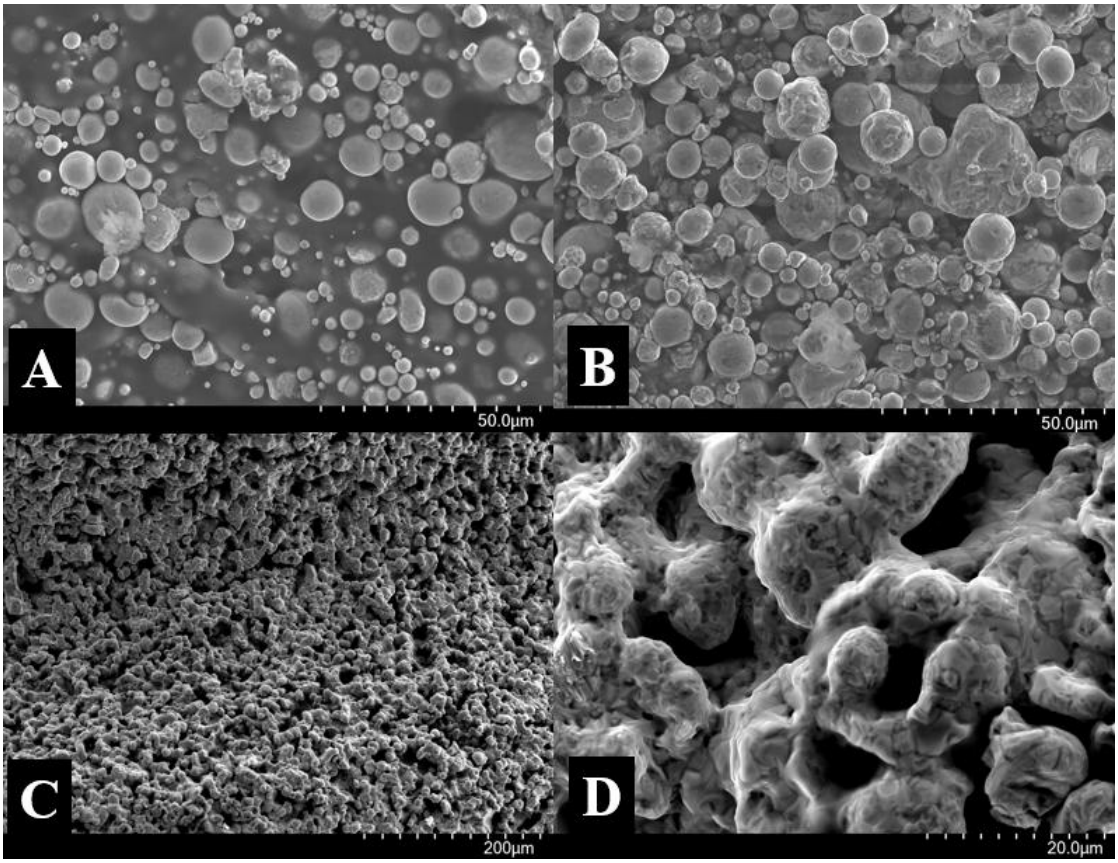

Figure 2.12 SEM Images of NiTiDent Tuah Porous NiTi Microstructural Changes during Processing.

Notes: (A) As-moulded samples show binders filling the interstitial spaces within the powder network; (B) as-leached: fine channels form between powder particles following the solvent de-binding process; (C) as-sintered at 200 µm magnification; and (D) as-sintered at 20 µm magnification, illustrating the pore structure and their interconnectivity (Mustafa et al., 2023).

Table 2.7
Biocompatibility Tests of NiTiDent Tuah Porous NiTi Dental Implant

Name of study	Findings	Conclusion	References
In Vitro Cytotoxicity Study of Porous Nickel Titanium by Elution Method	An elution test comparing the cytotoxic effect of this porous Niti implant with negative (High-Density Polyethene) and positive (Polyurethane) controls. There was no cell lysis, no reduction in cell growth, and no reactivity, indicating that the implant is non-toxic to mouse fibroblasts. In contrast, the positive control showed evidence of the complete or near destruction of the cell layer and severe reactivity.	Porous NiTi implant is considered non-cytotoxic to the mouse fibroblast cells.	Mustafa et al., 2023 (Appendix 1)
Bacterial Reverse Mutation Test of Porous Nickel Titanium Using *Salmonella Typhimurium* and *Escherichia Coli* Tester Strains	Under the Bacterial Reverse Mutation Test, both polar and non-polar compounds from 60% up to 100% extractable porous NiTi were tested with and without metabolic activation. Based on the results obtained, both polar and non-polar porous niti extracts were non-mutagenic.	Porous Nickel Titanium was found to be "non-mutagenic" under the laboratory conditions tested.	
Intracutaneous Reactivity Test of Porous Nickel Titanium in New Zealand White Rabbits	0.2 ml of NiTi extract injected intracutaneously at 5 skin sites in the New Zealand White rabbit demonstrated no skin irritation during the 72-hour observation period. A similar finding reported using the Micronuclei Assay and MTT Assay indicated	Porous Nickel Titanium was considered "non-irritant" under the experimental conditions employed.	
In Vitro Micronucleus Assay and Cytotoxicity: MTT Assay	Both polar and non-polar extracts of this material were non-clastogenic and non-cytotoxic.	Porous nickel-titanium dental implant demonstrated a non-clastogenic and non-cytotoxic effect under the conditions of this study.	
Acute Systemic Toxicity Study of Porous Nickel Titanium in Swiss Albino Mice	Acute systemic toxicity effects were observed in 20 female Swiss Albino mice. They were randomly assigned to receive 5ml/kg of polar and non-polar NiTi, injected via intravenous or intraperitoneal routes. The observation was conducted at 30 to 40 min, 1 hr, 2 hrs and 4 hrs on day 1 postoperatively, followed by days 2, 3 and 4. No acute systemic toxicity was revealed under these experimental conditions.	Porous Nickel Titanium did not reveal any systemic toxicity under the experimental conditions employed.	
Test for local effect after implantation in the Femur of *Oryctolagus cuniculus* using the International Standard Method ISO 10993 - Part 6	Clinically healthy rabbits were selected for implantation of the test item (Tuah NitiDent *Porous Nickel Titanium dental implant*) and control Titanium Gr5 (6Al-4V).	Both implants are biologically compatible with the host. However, the test item is deemed to be superior to the control item.	Mustafa et al., 2024 (Figure 2.13 & 2.14, Appendix 2)

Table 2.8
Preclinical Testings of NiTiDent Tuah Porous NiTi Dental Implant

Name of study	Findings	Conclusion
In vitro corrosion assessment of Porous Nickel Titanium (NiTi)	A corrosion test was also conducted to identify the dissolution of Ni ions into the milieu. With open-circuit and cyclic polarisation, no Ni-ion leaching was observed, indicating high pitting and crevice corrosion resistance, and this finding was consistent with the microscopic examination (absence of surface defects).	No pitting or corrosion-related defects were observed in the microscopic examination.
Fatigue Testing of Porous Nickel Titanium (NiTi) Dental Implant System	With a 3.5 mm diameter, this Tuah NiTiDent Implant under static compression demonstrated an average load at the yield point up to 529.4 N, and a maximum load at rupture for a 3.5mm diameter Porous Nickel Titanium (NiTi) Dental Implant is 596.27 N. With a peak load of 250 N applied under a dynamic fatigue test, this implant was able to withstand up to 2,000,000 cycles, which will be useful to accommodate the force applied by incisors to premolars	High static and dynamic fatigue resistance, which is adequate for the intended application of the implant diameter. In dynamic fatigue testing, the system met the 2,000,000-cycle criterion at a dynamic load of 47% of the established maximum static load.

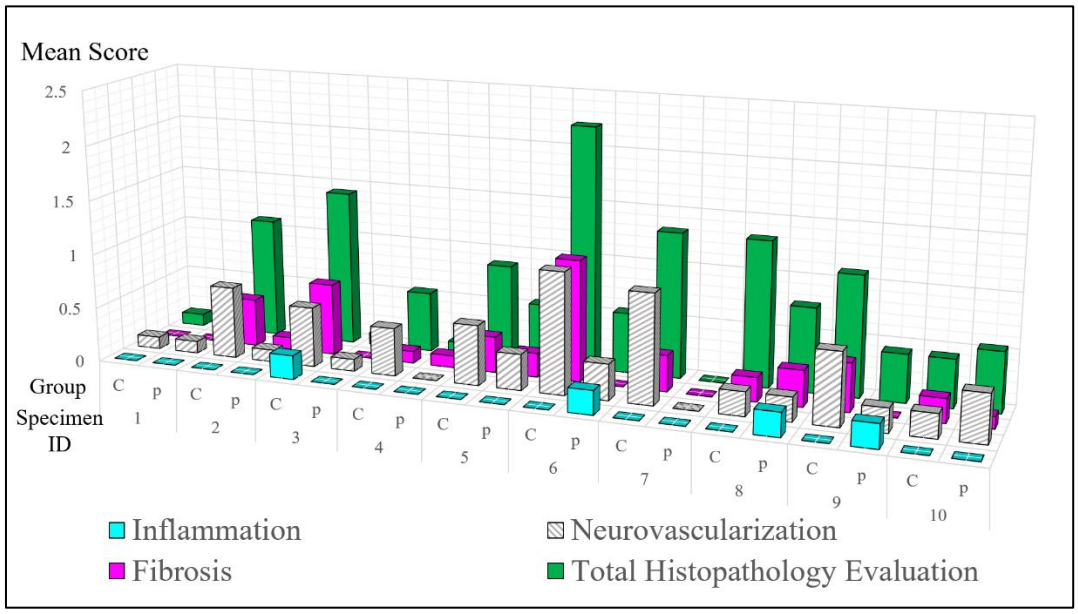

Figure 2.13 Comparative Biological Responses of Subjects, Evaluated Based on the Histopathology of Bone Tissue Specimens Surrounding Control and Porous NiTi Implants After 13 Weeks of Implantation.

Note: 'C' indicates the control implant, and 'P' indicates the porous NiTi (Mustafa et al., 2024) (Appendix 2).

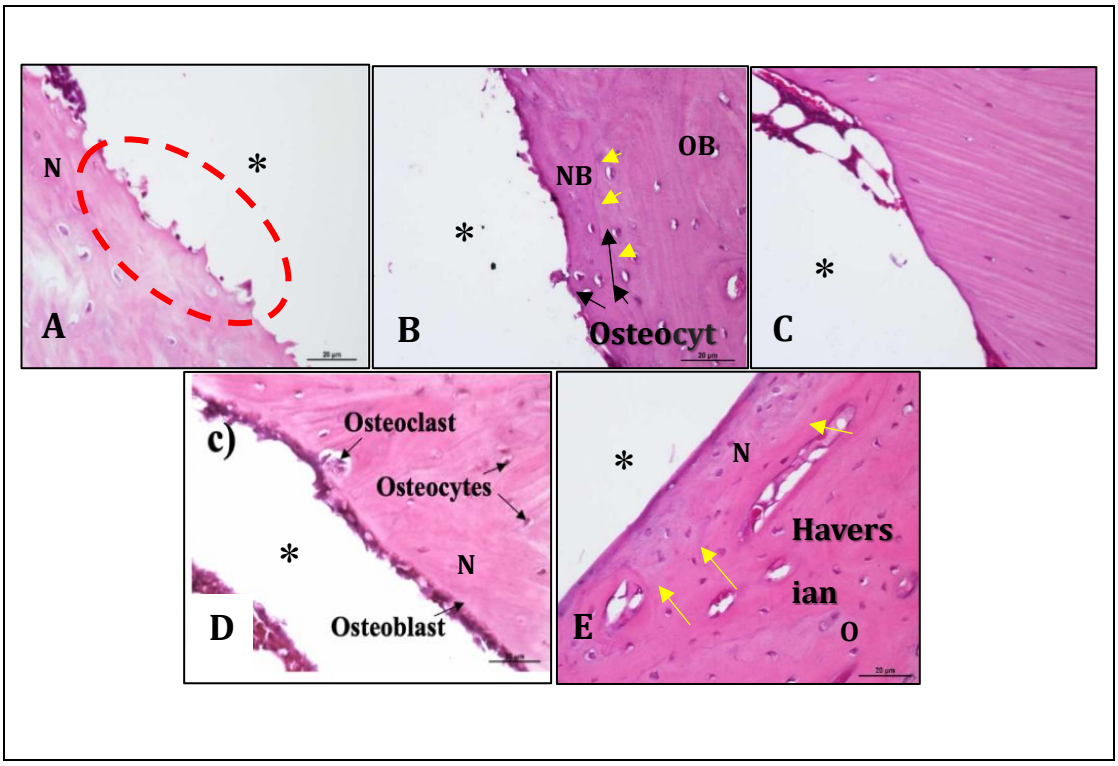

Figure 2.14 Light Micrograph of the (A−C) Porous NiTi and (D, E) Control Bone-implant Interface at 13 Weeks Post-surgery (Haematoxylin and Eosin (H&E) Stain; Original Magnification of 400×).

Notes: (A, red circle) indicates irregular bony formation projected into space formerly occupied by the porous NiTi implant. (B, E) The yellow arrow denotes the basophilic line, showing new bone apposition onto the original bone. The asterisk (*) marks the space previously occupied by the implant; NB: new bone and OB: original bone. (A, B, D, E) The bone tissue runs parallel to the long axis of the implant; (C) the bone tissue is shown in the implant cross-section. Copyright 2022 NITIUM/AMDI (Mustafa et al., 2024).

2.6 Bone Response to Dental Implant

Before the 1980s, the concept of healing in bony implantation involved soft-tissue intervention between the implant and bone, whether cement-retained or cementless (Adell et al., 1981; T. Albrektsson & B. Albrektsson, 1987). Direct contact between bone and implant was first observed in animal models under light microscopy in 1962. Unfortunately, due to limitations in tissue destruction and handling at the time, these findings had limited significance (T. Albrektsson & B. Albrektsson, 1987). Osseointegration was first defined in 1977 as a direct structural and functional connection between living bone and a loaded implant surface, specifically describing direct bone-to-implant contact under light microscopy, following the successful clinical

outcome of an oral implant in a Swedish man (Albrektsson et al., 2017). From a biomechanical perspective, bone-to-implant contact refers to the connection that resists tensile and shear forces. This term is further defined as the process of securely fixing an artificial material to the bone while ensuring it remains asymptomatic under functional loading. A new paradigm has emerged that views this process as an immune-driven phenomenon in which interfacial bone forms to prevent adjacent tissue from contacting the implant material (Albrektsson & Wenneberg, 2019; T. Albrektsson & B. Albrektsson, 1987).

Osseointegration is a dynamic process involving the gradual integration of a dental implant with the surrounding jawbone, requiring a delicate balance between bone resorption and formation in the early stages following implant placement. This balance ultimately results in a stable connection between the implant and the bone tissue. As the process progresses, it is maintained through ongoing remodelling and adaptation to the transferred load, ensuring the long-term success of the dental implant.

2.6.1 Osseointegration – A Physical Connection Between the Host System and the Dental Implantation

The healing process following implant placement shows the body's natural ability to recover and restore balance, reflecting the resilience seen in bone injuries or fractures. It involves cell-to-cell communication across four stages: haemostasis, inflammation, proliferation, and remodelling. This active biological response is directly controlled by mediators secreted through paracrine and autocrine mechanisms (Raines et al., 2019). While similar pathways may operate during normal bone healing and healing with biomaterials, notable differences exist at cellular and molecular levels (Shah et al., 2019). The presence of an implant affects the host response, depending on its physicochemical properties, stability within the bone, and thermal effects during drilling, which can cause osteocyte injury or death extending roughly 100–500 μm into the parent bone (Eriksson & Albrektsson, 1984; Cimini et al., 2024; Shah et al., 2018). The process of intramembranous ossification around a dental implant involves contact, distance, and de novo osteogenesis, all of which are essential for successful integration into the osseous bed (Berglundh et al., 2003; Davies, 2003). These terms were first described by Osbon & Newesley in 1980 (Davies, 1988). In contact osteogenesis, bone forms from the implant surface through physicochemical interactions that leverage the

implant's inherent osteoconductive potential, recruiting osteogenic cells that migrate to the surface and produce bone matrix (de novo bone formation) (Albrektsson & Wenneberg, 2001; Davies, 1988; Davies, 2003). In distance osteogenesis, new bone develops from the existing bone towards the implant. Additionally, woven bone forms within the healing chamber, a space between the implant and the parent bone that contains autogenous bone fragments or debris (Berglundh et al., 2003; Rossi et al., 2014). This bone-implant interface is a heterogeneous zone comprising unmineralized, partially mineralised, and mineralised areas. At the meso-, micro-, and nano-levels, mineralised collagen fibrils create the foundational structure, along with non-collagenous macromolecules such as osteopontin, bone sialoprotein, and osteocalcin (Alexander & Ricci, 2017; Shah et al., 2019). The success of interfacial bone formation on the implant depends on factors including biocompatibility, design, surface properties, condition of the surgical bed, surgical technique, micromovement, loading, and patient-specific factors like systemic illness and bone quality (Albrektsson & Wenneberg, 2019; Bosshardt et al., 2011; Eriksson & Albrektsson, 1984; Mavrogenis et al., 2009; Shah et al., 2018; Shah et al., 2019; T. Albrektsson & B. Albrektsson, 1987).

2.6.2 Healing Phases of Implantation

The healing process around dental implants follows a series of overlapping biological phases that ultimately establish a direct and functional bone–implant interface. Immediately after implant placement, the haemostasis phase begins with the formation of a blood clot or haematoma within the wound chamber (Terheyden et al., 2011). Activated platelets release cytokines and growth factors, while the fibrin network provides the initial scaffold for cell migration. Concurrently, proteins such as fibronectin and vitronectin adsorb onto the implant surface, preparing the environment for subsequent cellular adhesion (Schell et al., 2017; Terheyden et al., 2011).

This is followed by the inflammatory phase, which begins within minutes and predominates during the first few days (Terheyden et al., 2012; Davies, 2003). Vascular changes increase permeability, enabling the recruitment of neutrophils and macrophages (Davies, 2003; Kumar et al., 2022). These cells clear surgical debris and potential contaminants through phagocytosis while releasing signalling molecules that orchestrate the repair process. The resolution of inflammation and the release of pro-

angiogenic mediators by macrophages facilitate the transition into the proliferative stage (Andersson, 2008; Bosshardt et al., 2011; Mavrogens et al., 2009).

During the proliferative phase, beginning around day three, granulation tissue forms and is characterised by fibroblast activity, extracellular matrix deposition, and angiogenesis (Berglundh et al., 2003; Bosshardt et al., 2016; Lang et al., 2011). Endothelial cells and fibroblasts, stimulated by vascular endothelial growth factor (VEGF) and other growth factors, establish a new vascular network that restores oxygen supply to the site (Behr et al., 2012; Terheyden et al., 2011). Osteoprogenitor cells migrate to the implant surface, differentiate into osteoblasts, and begin depositing woven bone through both contact and distant osteogenesis (Berglundh et al., 2003; Bosshardt et al., 2011; Terheyden et al., 2011). Within 10–14 days, the provisional matrix is largely replaced by a three-dimensional network of immature bone, providing early biological stability (Berglundh et al., 2003; Bosshardt et al., 2011).

Finally, the remodelling phase ensures the maturation of this new tissue. Woven bone is gradually replaced by lamellar bone under the balanced actions of osteoclasts and osteoblasts, regulated through the RANK/RANKL/OPG system (Boyce & Xing, 2008; Terheyden et al., 2011). This stage continues for months to years, aligning bone architecture with functional loading conditions as described by Wolff's law (Mavrogenis et al., 2009). The outcome is a stable, load-bearing interface where lamellar bone provides long-term structural support and osseointegration is fully established. The summary of healing phases following implantation is presented in Table 2.9 and illustrated in Figure 2.15.

Table 2.9
Healing Phases of Osseointegration

Phase	**Time Frame**	**Key Events**	**Dominant Cells**
Haemostasis	Seconds - Hours	Blood clot/ haematoma forms; fibrin network stabilises; growth factor released by activated platelet and protein adsorption on implant surface	Platelet, erythrocytes
Inflammatory	Hours - Days	Vasodilation, neutrophil & macrophage recruitment (phagocytosis of debris, foreign material & initiation of healing)	Neutrophils, macrophages

Phase	Time Frame	Key Events	Dominant Cells
Proliferative	3 – 14 Days	Granulation tissue formation: angiogenesis (VEGF, FGF), ECM deposition, osteoprogenitor → osteoblast→ woven bone deposition	Endothelial cell, fibroblast, osteoblast
Remodelling	Weeks – Months/Years	Replacement of woven bone with lamellar bone (balanced between resorption & deposition), adaptation to mechanical load	Osteoblast, osteoclast

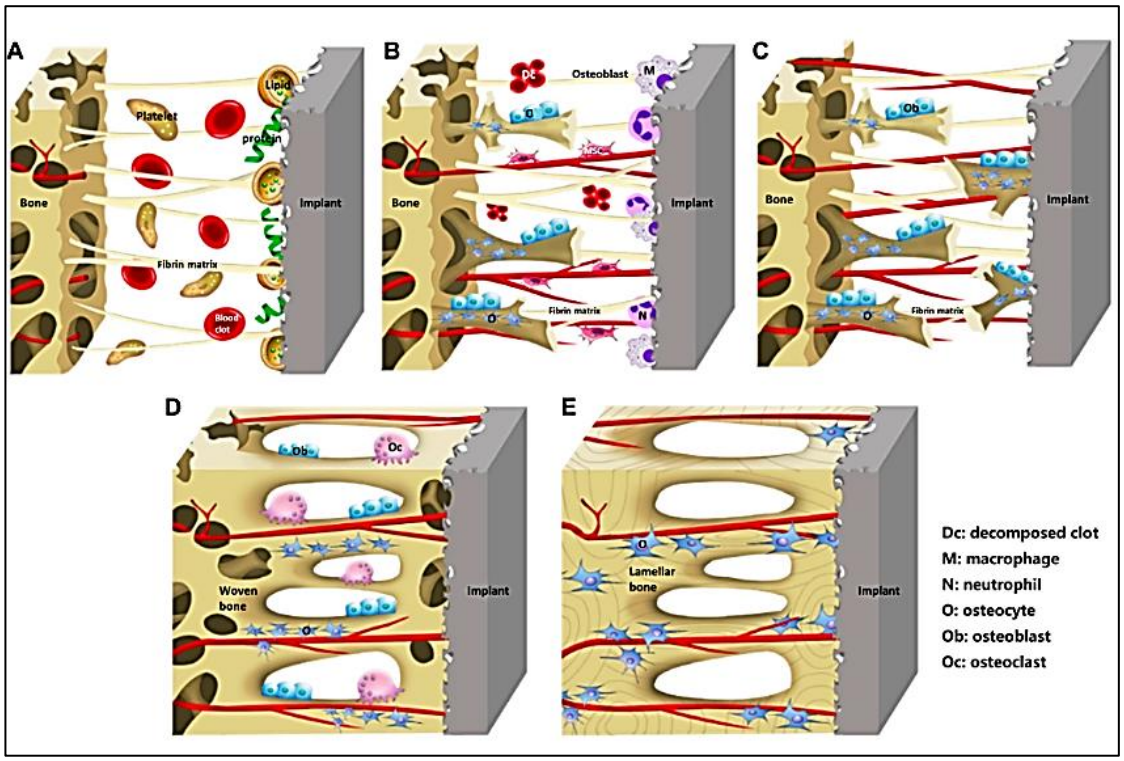

Figure 2.15 Schematic Diagram of the Process of Implant Osseointegration.

Notes: (A) Formation of Blood Clot and Fibrin Matrix. (B) Formation of Woven Bone. (C) Distance osteogenesis and contact osteogenesis. (D) Newborn woven bones fill up the gap. (E) Woven bone matures into lamellar bone (Liu et al., 2020).

2.7 Implant Factors Affecting Biological Responses

The primary factor in wound healing around endosseous implants is the properties of the biomaterial itself. Biocompatibility is essential, as it determines how effectively the host tissue integrates with the implant, ideally establishing direct bone-implant contact without fibrous tissue formation or rejection. However, regarding Ti and its alloy, mRNA-related inflammation observations have demonstrated a shift in

cytokine profiles, with increased levels of the anti-inflammatory cytokine IL-10, decreased levels of pro-inflammatory cytokines (IL-1, IL-6, IL-8, and TNF), and a reduction in chemokine ligand 2 associated with apoptosis and cell death after seven days in human mesenchymal cell assays conducted on various titanium alloy surfaces (Raines et al., 2019). This indicates that titanium implants, with proven success and survival rates of up to 25 years, are well accepted biologically and widely used in orthopaedics and dentistry (Albrektsson & Wennerberg, 2019).

Proper integration of dental implants with the surrounding bone is essential for the longevity and function of implant-supported prostheses. A key biological process during healing is the ability of cells to adhere, proliferate, differentiate, and function at the interface between host tissue and the implant (Boyan, 2004; Berglundh, 2003). These biological responses are mainly influenced by three primary factors: mechanical properties, physicochemical characteristics, and surface topography (Albrektsson & Wenneberg, 2004).

The mechanical and physicochemical properties are crucial for the performance of the implant. Elastic modulus, yield strength, and fatigue resistance are essential for the durability of dental implants. An effective implant material must balance mechanical strength with biological compatibility to ensure optimal load distribution and promote osseointegration (Elias et al., 2008; Geetha et al., 2009). Highly elastic-modulus materials, such as dense titanium, can cause stress shielding, interfere with bone remodelling, and increase the risk of crestal bone loss (Brunski, 1999). Fracture resistance and fatigue behaviour are also critical, especially for small-diameter implants or in high-load regions such as the posterior mandible (Wang et al., 2020). Furthermore, factors such as low corrosion resistance, especially in physiological extracellular fluids containing sodium and chloride ions, as well as under low-pH and low-oxygen conditions during the early biological response after implantation, can affect the host's reaction. Complications like tribiocorrosion, where mechanical friction between the surgical drill or implant and bone causes surface degradation with the possibility of excessive heat generation during drilling, causing necrosis and death of osteocytes, and ongoing injury at the surgical site due to micromotion, can lead to adverse tissue reactions (Alexander & Ricci, 2017; Bosshardt et al., 2016; Mavrogenis et al., 2009). The details on the effects of mechanical properties are in Table 2.10.

Manufacturing methods and surface treatments significantly influence the surface finish and physicochemical properties of implants, including surface chemistry,

energy, wettability, topography, and roughness. For example, anodising an implant can increase its surface roughness, alter the crystalline structure of the oxide layer, and introduce ions to the surface (Sul et al., 2002). Conversely, machined implants typically have free ions on their surfaces, showing lower titanium and higher carbon levels than those achieved with treatments such as sandblasting, acid etching, or plasma spraying (Morra et al., 2003). These surface characteristics are crucial in determining how nearby cells and blood components, including immune cells, respond, thereby influencing differentiation, proliferation, and the expression of transcription factors required for bone matrix formation and osseointegration (Grassi et al., 2006). Research has shown that surface features such as energy and wettability (Sartoreto et al., 2015) and topography (Gittens et al., 2013; Hotchkiss et al., 2018; Navarrete et al., 2015) significantly influence gene expression (Hotchkiss et al., 2018; Olivares Navarrete et al., 2015; Sartoretto et al., 2015 Terheyden et al., 2011), protein adsorption (Shah et al., 2018), apatite formation (Xia et al., 2011), and the differentiation of osteoblastic cell lineages during early stages of osseointegration (Palmquist et al., 2010; Schwartz, 1999). The early models of Brånemark dental implants had smooth surfaces, which, although they demonstrated clinical success, required longer healing times for osseointegration. With optimised surface properties, healing times are reduced, and the restoration process is accelerated following implantation (Albrektsson & Wennerberg, 2019; Wang et al., 2020).

Table 2.10
Mechanical Properties and Their Effects

Property	**Definition**	**Effect on Implant Performance**
Elastic Modulus	The resistance of a material to elastic deformation. Titanium: ~110 GPa; cortical bone: ~10–30 GPa	Mismatch may lead to stress shielding and bone resorption (Brunski, 1999; Li et al., 2020). Lower modulus materials reduce this effect.
Yield Strength	The stress at which a material begins to deform plastically	Ensures the implant does not deform under occlusal loading (Geetha et al., 2009).
Fatigue Resistance	Withstand cyclic loading without failure.	Key for long-term survival, particularly under repetitive mastication (Wang et al., 2020).
Hardness	Resistance to surface indentation	Higher hardness improves wear resistance. This is especially needed at the abutment interface (Elias et al., 2008).

Property	Definition	Effect on Implant Performance
	Corrosion resistance	Prevents degradation and ion release (e.g., Ni, Al, V), reducing the risk of peri-implantitis and hypersensitivity reactions.
Tensile Strength	Maximum stress before fracture	Prevents catastrophic failure under extreme conditions (Sidambe, 2014).
Fracture Toughness	Resistance to crack propagation	Prevents implant fracture under multiaxial stress (Wang et al., 2020).

2.7.1 Physicochemical Characteristics

The physicochemical properties of dental implants include surface energy, wettability, surface topography, and roughness, all of which influence interactions between the implant and surrounding biological tissues by affecting the adhesion and differentiation of osteoblastic and other related cells (Albrektsson & Wenneberg, 2018; T. Albrektsson & B. Albrektsson, 1987).

Wettability, defined by the ability of a liquid to maintain contact with a solid surface, plays a crucial role in protein adsorption and cell adhesion. A surface that promotes good wettability can facilitate the formation of a biological film and enhance the initial stages of healing by encouraging the adherence of osteoblasts and other crucial molecules (Gitten et al., 2014; Sartoretto et al., 2015)

Meanwhile, surface energy, which relates to the interfacial forces between the implant and surrounding tissues, also plays a crucial role in the biological response. Materials with high surface energy may attract proteins more effectively, promoting better cellular activities and thereby enhancing the overall integration of the implant with the bone (Gitten et al., 2013).

Surface topography refers to the microscopic and macroscopic features of an implant's surface, which can significantly influence how tissues respond to it. Rough surfaces are particularly beneficial as they enhance mechanical interlocking with bone, resulting in improved stability and a reduced risk of implant failure. This roughness can be engineered to optimise bone-to-implant contact, which is essential for effective osseointegration (Albrektsson & Wenneberg, 2018).

These physicochemical properties of dental implants are essential to their function and effectiveness. By altering these properties, manufacturers aim to enhance

osseointegration, accelerate healing, and prolong the lifespan of dental implants in clinical practice (Gitten et al., 2013; Gitten et al., 2014; Sartoretto et al., 2015).

2.7.1.1 Role of Physicochemical Properties in Influencing Initial Osseointegration

Regarding Ti and its alloys, rapid oxidation of titanium both *in vitro* and *in vivo* offers an advantage for this material. It provides biocompatibility through a passivating effect, influencing resistance to corrosion and wear, and preventing direct contact between the implant and the bone (Furqan et al., 2020). The oxide layer may consist of TiO, TiO_2, Ti_2O_3, and Ti_3O_4 (Albrektsson, 1981) at thicknesses ranging from 3 to 7 nm on machined surfaces. Depending on surface polishing and finishing methods such as electropolishing or anodic oxidation, it can reach several hundred nanometres (Wälivaara et al., 1994). This layer may be amorphous, crystalline, or a mixture of both (Lindahl et al., 2010; Palmquist, 2010; Wälivaara et al., 1994; Xia et al., 2011). Samples retrieved from humans show a two- to threefold increase in layer thickness, indicating ongoing electrochemical interactions in the bone-implant environment (Puleo & Nanci, 1999). Especially when crystalline, the oxide layer is highly hydroxylated. Once a biomaterial is implanted, water absorption and dissociation lead to the formation of OH groups (Ti-OH, TiO^{-}, and $TiOH^{2+}$) (Barberi & Spriano, 2021). These OH groups can be deprotonated or protonated, affecting the electrical potential around the Ti surfaces. This affects the surface charges and can induce the spontaneous formation of hydroxyapatite (HA) (Barberi & Spriano, 2021; Xia et al., 2011). In vitro, Ca^{2+} and $(PO_4)^{3-}$ ions are more readily adsorbed onto the 001 and 100 crystallographic planes of single-crystal rutile than onto the 110 planes of the oxide layer (Lindahl et al., 2010). Nonetheless, when examining protein activity on implant surfaces, it is essential to note that human serum albumin and fibrin exhibit significant adsorption onto Ti surfaces, regardless of the specific TiO_2 structures present. This interaction holds promise for therapeutic applications, as these proteins can activate the intrinsic coagulation pathway *in vitro* (Walivaara et al., 1994). OH groups are believed to attract protein adsorption through electrostatic interactions between OH-2 and the carboxyl group (COO-), or via hydrogen bonding followed by proton transfer (Cámara et al., 2010).

Research indicates that high-energy surfaces tend to promote adsorption more effectively, suggesting that oral implants with higher surface energy could achieve superior osseointegration compared to those with lower energy (Albrektsson &

Wennerberg, 2004). A prevalent method for measuring surface energy is through contact angle measurement, which helps determine a surface's hydrophobicity or hydrophilicity, effectively indicating its wettability. Surfaces with a wetting tension exceeding 30 mN/m are classified as hydrophobic, whereas those below this threshold are considered hydrophilic (Gittens et al., 2013).

The dimensions of a dental implant play a critical role in its biogenesis, as variations in contact angle can enhance its interaction with biological substances and cells (Gittens et al., 2013). Hydrophilic surfaces, typically characterised by a water contact angle between 40° and 70°, are particularly conducive to biological interactions with human body fluids and cells (Wang et al., 2020). For optimal protein adsorption, a water contact angle of approximately 65° has been reported (Xu & Siedlecki, 2007).

Implants exhibiting high hydrophilicity and uneven surface textures are recognised as excellent candidates for successful osseointegration (Albrektsson & Wenneberg, 2019). These hydrophilic surfaces are favoured over hydrophobic ones due to their enhanced affinity for cells and biological substances. Increased surface energy not only boosts protein adsorption and cell attachment but also facilitates early healing by improving fibrin anchoring and platelet aggregation (Rupp et al., 2006). Additionally, hydrophilic surfaces promote protein binding and osteoblast proliferation, thereby enhancing blood clot formation and stability, both of which are essential for effective wound healing (Schwarz et al., 2009). Research indicates that hydrophilic implants, such as SLActive, exhibit faster bone-to-implant contact in animal studies (Schwarz et al., 2009). These surfaces facilitate protein adsorption and osteoblast adhesion, thereby promoting osseointegration (Rupp et al., 2018).

Moreover, the chemical composition of the implant significantly influences its surface energy and wettability, both of which are vital for initial protein adsorption and cellular adhesion (Anselme et al., 2000; Anselme, 2000). Chemically treated titanium surfaces not only enhance hydrophilicity and surface free energy but also reduce hydrocarbon contamination (Elias et al., 2008; Rupp et al., 2006).

Nevertheless, it is essential to note that proteins possess unique structures that enable them to adsorb onto both hydrophilic and hydrophobic surfaces. Hydrophobic materials predominantly attract proteins through hydrophobic interactions, whereas on hydrophilic surfaces, electrostatic forces and van der Waals forces primarily facilitate adsorption. Once adsorbed, proteins can diffuse, alter their shape, and reorient themselves due to the Vroman effect, which is critical for subsequent cell attachment.

For instance, bone morphogenetic protein (BMP) plays a key role in recruiting osteoprogenitor cells, which are essential for osteogenesis (Sartoretto et al., 2015). Although proteins typically prefer hydrophobic surfaces, hydrophilic surfaces elicit a significant host response in both *in vitro* and *in vivo* settings, thereby promoting bone integration (Bosshardt et al., 2011; Donos et al., 2011; Lang et al., 2011; Raines et al., 2019). Charge distribution on hydrophilic substrates creates interactions that can either attract or repel surrounding extracellular proteins (Barberi & Sapreno, 2021).

In a comparative study, Sartoretto et al. (2015) analysed the impact of chemical and wettability properties on bone-implant contact (BIC) and bone area fraction occupied (BAFO) using an implant with uniform surface roughness in a rabbit model. The study revealed rapid increases in BIC and BAFO on hydrophilic surfaces at 14 days, matching the results observed on hydrophobic implants only at 28 days. By 28 days post-implantation, the BIC and BAFO in the hydrophilic group were 1.5 times higher than those in the hydrophobic group. Additionally, hydrophilic surface implants showed promise in enhancing bone healing in animal models with osteoporosis (Siqueira et al., 2020). The study suggested that these implants may be beneficial even in compromised bone conditions, as both healthy and osteoporotic mice exhibited an upregulation of osteogenic gene expression. Evidence of gene expression related to bone mineralisation and ossification was observed as early as 7 days post-implantation on hydrophilic surfaces (Donos et al., 2011). This was corroborated by histological evaluations, which demonstrated a significant increase in BIC over the 14 to 28-day interval post-implantation in human studies (Lang et al., 2011).

2.7.2 Implant Topography and Surface Roughness

Surface topography refers to the degree of roughness and the orientation of irregularities on an implant's surface (Ogle, 2015). For over a decade, the implant surface has evolved from macro to micro and even nano scales. These textures are often quantified using parameters such as Ra (arithmetic mean roughness) and Sa (surface area). Macroscopic changes, such as body shape and the threaded geometry of implants, directly affect the biomechanical response of local structures. Any functional forces generated, such as compressive, shear, or tensile strains, can enhance bone density or weaken the surrounding bone (Abuhussein et al., 2010; Albrektsson et al., 2001). Micrometre-scale surface irregularities, on the other hand, influence biological

behaviour, accelerate the osseointegration process (Buser et al., 1991), and promote mechanical interlocking between the surrounding bone and the implant structure (Almassri et al., 2020). While nanometre-scale roughness influences protein adsorption and osteoblastic cell adhesion, ultimately affecting osseointegration (Karazisis, 2016; Smeets, 2016). Surface roughness is categorised as shown in Table 2.11 (Albrektsson & Wennerberg, 2004).

Table 2.11
Classification of Surface Roughness

Surface roughness category	**Range of surface roughness (Sa)**	**Clinical usage**
Smooth implant	0.0-0.4 μm	Solely on abutment. Too smooth for osseointegration.
Minimally rough	0.5 to 1.0 μm	Turned Brånemark, Osseotite, most implants used before 1995.
Moderately roughened	1.0 and 2.0 μm	Almost all modern implants, such as the Astra Tech, TiOblast TM and OsseoSpeed TM surfaces, Nobel TiUnite, Straumann SLA and Dentsply Cellplus designs Stronger bone response.
Rough surface	> 2.0 μm	Plasma-sprayed, HA-coated Ti is among today's implants.

Note: Sourced from Albrektsson and Wennerberg, 2004.

Various techniques are employed to create surface irregularities on implants, which can improve their interaction with surrounding tissues. Concave texturing is achieved through methods such as chemical or electrochemical etching, as well as mechanical techniques like sandblasting, shot peening, and laser peening. Conversely, convex textured surfaces are usually formed by depositing particles onto the implant surface, often via plasma spraying. Several surface treatments are available to generate specific topographies, as shown in Table 2.12.

Table 2.12
Classification of Surface Treatment for Dental Implants

Physical (and Subtractive) Surface Treatment	Chemical (and Additive) Surface Treatment	Biological/Biomimetic Surface Treatment
• Machined surface Abrasive/sandblasting with grit media • Laser etching • Nanoparticle compaction, Porous tantalum, trabecular metal	• Acid etching • Alkaline treatment Anodization of the surface • Peroxidation • Fluoride treatment • Vacuum treatment Plasma coatings and surface treatments	• Bioactive coatings • Attachment of peptides • Attachment of antibiotics • Attachment of growth factors • Attachment of bone remodelling agents

Note: Sourced from Ting et al., 2017

Choosing the right surface roughness is essential because it enhances interfacial adhesion and decreases the risk of ionic leakage and peri-implantitis (Wang et al., 2020). A roughness level between 1 and 10 μm is considered optimal for improving the locking of mineralised bone with implant surfaces (Albrektsson & Wenneberg, 2004). This level of roughness significantly boosts both bone-to-implant contact and resistance to torque removal. Ideally, the surface should feature hemispherical pits approximately 1.5 μm deep and 4 μm in diameter (Albrektsson & Wenneberg, 2004). However, debate continues about the precise degree of surface roughness required for effective bone cell attachment (Wang et al., 2020).

Surface treatment involving acid etching, followed by sandblasting with alumina, plasma spraying with titanium oxide, and hydroxyapatite coating, effectively creates surface irregularities (Buser et al., 1991; Buser et al., 2016; Albrektsson & Wenneberg, 2019). By removing or reorganising the outermost surface of the implant, features such as pits, grooves, or protrusions are formed. These modifications increase surface area and alter wettability, thereby enhancing biological haemostatic activity. Successful surface treatments have been demonstrated in both *in vitro* and *in vivo* studies; however, coating materials can dissolve over time, potentially causing adverse biological effects on surrounding tissues, such as peri-implantitis (Hashim & Cionca, 2020; Wally et al., 2015). Additionally, hydroxyapatite coatings have failed to improve osseointegration and have been associated with marginal bone loss (Albrektsson & Wenneberg, 2019).

By the mid-1990s, studies increasingly indicated that implants with a surface roughness of roughly 1.5 μm (Sa) promoted a stronger bone response than smoother

turned surfaces or rougher plasma-sprayed surfaces. However, it is important to note that higher interfacial bone levels observed in animal studies do not always lead to better clinical outcomes. While surface roughening can improve osseointegration, it may also raise the risk of complications such as peri-implantitis and ionic leakage (Albrektsson & Wennerberg, 2004). Some clinical data suggest that very rough plasma-sprayed implants (bone-implant contact (BIC) and bone area fraction occupied (BAFO) > 2.0 μm) could be associated with a higher risk of peri-implantitis (Becker et al., 2000). Nevertheless, moderately rough surfaces, like those on the Tioblast screw from Astra Tech, have shown stable bone levels over five years with no significant increase in peri-implantitis rates (Norton, 2004; Palmer et al., 2000). The potential for increased ionic leakage on rough surfaces might stem from greater tissue-implant contact; however, the actual risk remains uncertain, and mild roughening appears to cause minimal leakage (Albrektsson & Wennerberg, 2004).

There is substantial interest in nanostructures, particularly their potential effects on surface roughness and bone response. It remains unclear whether nanoscale irregularities influence how bone interacts with implants. Changes in implant roughness at the micrometre level may also cause alterations at the nanometre scale, making it difficult to separate the effects of nanometre-sized surface features on bone response. Extensive research has examined their influence on osseointegration and the overall success of dental implants, including the role of nanoscales. As a result, nano-textures provide multiple bonding sites for cell integration, promoting more efficient and faster osseointegration (Kandavalli et al, 2021; Wennerberg et al., 2009). However, clinical evidence of nano-roughness remains limited, with the most favourable results reported in an animal study (Almas et al., 2019).

One study found that macrophage cell lines respond to microgrooves at the nanometre scale, while another study observed no significant effect on cell adhesion across different nanotopographies (Elias & Meirelles, 2010). This highlights the need for more *in vitro* and *in vivo* data to assess the importance of nanostructures in this context. For clinical purposes, however, it is generally more relevant to describe an oral implant's surface characteristics in terms of its micrometre-sized irregularities (Wenneberg & Albrektsson, 2004).

Biochemical methods for surface modifications, such as incorporating bone morphogenetic protein-2 (rhBMP-2) and fluoride, offer a promising approach to enhance osseointegration; however, their current effects appear somewhat limited. The

main aim of these biochemical modifications is to effectively immobilise proteins, enzymes, or peptides on biomaterials, thereby triggering specific cellular and tissue responses. By focusing on improving the tissue-implant interface, this method seeks to incorporate bioactive molecules directly at that vital boundary. Such progress could notably improve the interaction between implant materials and surrounding tissues, ultimately resulting in better healing and higher implant success (Albrektsson & Wenneberg, 2004). It is crucial to recognise that different implants available on the market vary in titanium composition and surface modification techniques, as detailed in Table 2.13. These differences can substantially influence the effectiveness of the implants and their integration with adjacent bone tissue.

Table 2.13
Surface Treatment and Dental Implants

Method	Surface	Material & Method	Implant Systems
Physical (and subtractive) surface treatment	Machined	Smooth surface as a result of manufacturing	Branemark, Astra Tech
	Sand blasted	Using abrasive particles, e.g alumina or titanium dioxide, to create a porous layer	Biohorizons Tapered (blasted with resorbable blasted media), Astra Tech Tioblast (blasted with titanium oxide), Zimmer Dental MTX SwissPlus (blasted with hydroxylapatite), inclusive tapered implants
	Shot-peening, laser-peening	- Shot-peening (similar to sandblasting but more controlled) - cold working process; the surface is bombarded with small spherical particles to create small indentations or dimples on the implant surface. - Laser peening - striking the metal with high-intensity pulses of laser light beam, produces a deep and regular honeycomb pattern with small pores (Ogle, 2019).	Bra˚nemark BioHelix, Biohorizon Laserlok
	Nanoparticle compaction		Nil
	Porous tantalum trabecular metal		Zimmer Trabecular Metal
Chemical (and additive) surface treatment	Acid etched	Generated by hydrochloric, sulfuric or nitric acids	Biomet 3i OsseoTite
	Chemical reaction with surface elements		Nil
	Anodization	Thickens the oxide layer on Ti between 600 – 1000 nm by action of strong acids (HF, H_3PO, HNO_3, H_2SO_4) are utilised for galvanostatic-anodization of Ti surface at high current density (200A/m 2) or potential (100 V) (Sue et al., 2001; Marenzi et al., 2019).	Nobel biocare TiUnite

Method	Surface	Material & Method	Implant Systems
	Peroxidation		Nil
	Fluoride modified		Astra Tech OsseoSpeed
	Vacuum treatment		Nil
	Plasma coating	Ti or hydroxyapatite (HA) particles sprayed to form a rough, bioactive coating	Dentsply Frialit, Adin Touareg CloseFit, Adin Touareg-OS, Straumann ITI titanium plasma-sprayed (TPS), Hiossen HS II, Hiossen HG II/ III,
Biological/biomimetic surface treatment	Bioactive coating/HA		Zimmer Screw Vent, Zimmer Dental MP-1
	Attachment of peptides, Attachment of enzymes, Attachment of BMP		Nil
Combination of surface treatment	Sandblasted and acid etched		Straumann SLA Active, Dentsply Ankylos Plus, Camlog Promote, Adin Touareg-S, Adin Swell, Adin One, Hiossen ET III SA, DentiumUSA SuperLine, DentiumUSA Implantium, DentiumUSA SimpleLine II
	Sandblasted, acid etched, and chemically modified		Biomet 3i NanoTite, Astra Tech OsseoSpeed

Notes: Sourced from Ting et al., 2017.

2.7.3 Surface Topography and Biological Interaction

Macro design, such as threads, facilitates mechanical anchorage and provides primary stability during early implant placement. The presence of a wound or healing chamber between the implant body and the surrounding bone, as well as between the threads, expedites the formation of a hematoma or blood clot. The clot serves as a vital source of osteoimmunology-related cells and proteins, which play a crucial role in bone healing (Schell et al., 2017). Micro (1 to 10 μm) and nano (1 to 100 nm) scale surface irregularities significantly increase surface area, affecting biological behaviour and accelerating osseointegration (Buser et al., 2016). In turn, this promotes mechanical interlocking with the surrounding bone (Almas et al., 2019).

Initial blood clot formation was slowest on a smooth surface (Li et al., 2023) and healed with a fibroblast-like character by releasing a fibrous connective matrix rich in type 1 collagen (Schwartz et al., 1999). An *in vitro* osteoblast model using different osteoblast cell lineages (committed osteoblasts (MG63), multipotent osteoprogenitors from fetal rat calvaria (FRC), secretory osteoblasts (OCT-1), and osteocytes (MLO-Y4)) showed that each cell type responds differently to varying surface roughness levels. Their morphology changes significantly from a flat, thin monolayer on a smooth surface to a relatively cuboidal shape with cytoplasmic extensions that span the spaces between surface peaks and between cells on moderately rough surfaces (Schwartz et al., 1999). Conversely, the roughest surface exhibited mixed behaviour among these cells. Morphological changes increased in both MG63 and FRC, whereas fewer OCT-1 and MLO-Y4 cells were observed, primarily located in the depressions. This study indicates that moderately rough surfaces influence cell behaviour, thereby enhancing osseointegration. Moreover, smooth implant surfaces tend to favour distance osteogenesis. In contrast, rougher surfaces allow for both distance and contact osteogenesis, making them more effective in promoting peri-implant bone growth than smoother ones (Mavrogenis et al., 2009). An example of dental implants with various surface topographies and their significant findings is presented in Table 2.14.

Table 2.14
Example of Dental Implants Surface Topography

Surface Topography	Surface Treatment	Example	Method	Animal study	Human study
Micro-roughness	Sandblasted and acid-etched (Sa:1.3µm)	SLA (Straumann Holding AG, Basel, Switzerland)	Macroroughness: 0.25-0.5 mm large grit sandblasting at 5 bar followed by acid etching (HCl/H_2SO_4) at high temperature (Fischer & Stenberg, 2012).	- BIC at 3 and 6 weeks: 50-60% superior in large grit (HCl/H2SO4 and HA coated-implant compared to other surface roughness (30-40%: Ti plasma-sprayed, 20-25% electropolished. However, HA-coated showed signs of resorption (Buser et al., 1991). - ↑ removal torque in SLA compared to machined-acid etched surface (Li et al.,2002)	- 12-year follow-up of partial dentate and total edentulous (303 implants): cumulative survival rate: 96.1%, MBL: 1.18±0.64mm. Periimplantitis rate: 13% (Velasco-Ortega et al.,2025) - 5-year success rate: 97.4%, cumulative survival rate: 99.3% (Cochran et al., 2007)
	Grit-blasted, acid-etched, and neutralised (mean Ra:3.19 µm)	FRIADENT plus surface (DENTSPLY Implants, Mannheim, Germany)	Large grit-blasted (354-500 µm) (hydrophobic surface), then acid etching (HCl, H_2SO_4, hydrofluoric, oxalic acid) and finalised by a proprietary neutralising technique produced macro with micropores (2-5 µm) with hydrophilic surface $\theta = 0°$ (Rupp et al., 2006)	- No significant difference in BIC after 6 and 12 weeks in the beagle dog model with Brånemark MK III (Nobel Biocare Holding AG, Zürich, Switzerland), Osseotite (BIOMET 3i, Palm Beach Gardens, FL, USA), XiVE (DENTSPLY Implants, Mannheim, Germany), and Compress implants (IGfZ eG, Diez, Germany). (Streckbein et al., 2014). - Successful OI (↑BIC) in immediate loading in minipig compared to unloaded implant (Neugebauer et al.,2006)	- 1-year prospective study Success rate: 99.6% (Degidi et al., 2006)

Surface Topography	Surface Treatment	Example	Method	Animal study	Human study
Nano roughness	Discrete crystalline deposition, DCD (nanoscale: 20-100nm)	Nano Tite (BIOMET 3i, Palm Beach Gardens, FL, USA)	Calcium phosphate (CaP, size: 20 -100 nm) deposited on dual acid etched by sol-gel process (DCD) (Bonfante et al., 2013)	- Similar pattern of healing as in other modified implant surfaces (Favero et al., 2016)	- The 1-year survival rate of the immediate loading protocol: 99.4%, mean marginal bone loss 1.01 mm (non-randomised and no controlled study) (Östman et al., 2013)
	Anodic Oxidation: a combination of both micro and nano surfaces	TiUnite (Nobel Biocare Holding AG, Zurich, Switzerland)	Electrochemical modification using anodic oxidation. ↑ TiO_2 layer from 17-200 nm to 600-1000 nm produced microstructure with pore sizes (13-2.0 mm^2),~20% porosity, moderate Sa = 1 µm, known as Ti porous oxide (TPO) (Sul et al., 2002)	- After 6- and 12-week implant placement, ↑BIC was compared to the machined Ti implant in a rabbit model (Zechner et al., 2003). - 74% BIC after 16 weeks of implantation in the type IV monkey bone model (Rocci et al., 2013)	- ↑ BIC in histology after 3- and 6-month implantation in the mandible and maxilla. (Ivanoff et al., 2003) - 5-month survival rate: 100% as compared to the turned surface (96.4%) (Quirynen & Van Assche, 2012)
	Titanium oxide blasted and acid-etched	OsseoSpeed implant (DENTSPLY Implants, Mannheim, Germany)	microscale roughness by Titanium oxide blasting and the nano roughness by etching with hydrofluoric acid (Coelho et al., 2015). The manufacturing effect causes fluoride to accumulate on the surface, hypothesised to promote the host-to-implant reaction in early osseointegration (Coelho et al., 2008).	- ↑ reverse torque, shear strength and BIC after 1- and 3-month implantation compared to unmodified surface (Ellingson et al., 2004). - Similar OI outcomes between OsseoSpeed and TiUnite implants (Choi et al., 2012)	- 5-year prospective evaluation: irrespective of immediate or delayed loading protocols; survival rate: 97 %, mean marginal loss: 0.1 mm (Raes et al., 2013)

2.7.4 Porous Surface in Dental Implants

Porous surface design represents a significant advancement in dental implantology, improving biological integration and mimicking the natural structure of bone. It has garnered significant attention due to its ability to enhance osseointegration, strengthen mechanical interlocking, and reduce stress shielding. Porous implants replicate trabecular bone architecture and promote bone ingrowth, resulting in a more secure implant fixation (Mour et al., 2010).

The unique design of porous implants is crucial for improving their physical and biological performance. Specifically, by reducing their elastic modulus to closely match that of cortical bone, which typically ranges from 10 to 30 GPa, effective alignment reduces stress shielding. This, in turn, allows for better load distribution and more even force distribution, minimising bone resorption around the implant (Liu et al., 2022). However, the mechanical strength of these implants depends heavily on the size, shape, and distribution of their pores, with an optimal range of 100 to 600 μm most effective in promoting robust bone ingrowth without compromising structural integrity (llister, 2005).

Acting as scaffolds for bone regeneration, the porous structure of these implants significantly increases the contact surface area, accelerating osseointegration, in which bone tissue seamlessly bonds with the implant. Studies have shown that such porous implants have a markedly higher bone-implant contact (BIC) compared to their dense-surfaced counterparts. The interconnected channels within the structure not only support bone growth but also promote neovascularisation, a vital process for nutrient delivery and new bone formation (Assad, 2004).

The features of porous surfaces greatly affect the host immune response. They frequently encourage M2 macrophage polarisation, which aids the healing process. However, a potential drawback is that these surfaces may also provoke a foreign body reaction (FBR), especially when metallic debris is present (Anderson et al., 2008; Gittens et al., 2013). For instance, porous-surfaced implants such as Trabecular Metal from Zimmer Biomet have demonstrated impressive outcomes, including early stability, enhanced bone ingrowth, and high long-term survival rates (Edelmann et al., 2019). These implants are especially beneficial for patients with poor bone quality, offering renewed hope for successful recovery and improved function (Edelmann et al., 2019).

2.7.4.1 The Importance of Pore Size, Shape and Porosity in Porous Dental Implants

Pore size, shape, and interconnectivity are vital for enhancing cell migration, supporting neovascularisation for nutrient transport, and improving bone integration with the implant surface, thereby increasing implant stability. Identifying the optimal pore size and shape remains an ongoing research focus. Most studies suggest pore sizes ranging from 100 μm to 400 μm for effective osteointegration (Tsuchiya et al., 2008; Zaharin et al., 2018). A minimum pore size of 100 μm is generally beneficial for mineralised bone formation and the migration of key osteogenic cells, such as osteoblasts (20-50 μm) and osteocytes (5-20 μm) (Sundelacruz & Kaplan, 2009). Evidence indicates that pores between 300 and 600 μm effectively promote osteoblast movement, vascular invasion, and bone ingrowth. Pores between 200 and 350 μm are especially suitable for capillary formation (Karageorgiou & Kaplan, 2005). Conversely, smaller pores, particularly those ranging from 10 to 75 μm, may promote fibrous tissue growth due to limited cell penetration (Karageorgiou & Kaplan, 2005).

In vivo studies on rabbits analysing various pore sizes (300, 600, and 900 μm) with a fixed porosity of 65% demonstrated that a pore size of 600 μm achieved significantly better fixation. Bone growth on implants with a 300 μm pore size was comparatively lower (Taniguchi et al., 2016). Additionally, implants with a 500-μm pore size promoted better bone formation in the cancellous bone bed of the rabbit femoral condyle than those with a 200-μm pore size (Kühne et al., 1994).

When the pores exceed 300 μm, a uniform stress distribution occurs, which may positively influence the biological behaviour of the surrounding bone (Li et al., 2020; Mangano et al., 2019). In contrast, smaller pores create concentrated stress and may diminish bone stimulation (Li et al., 2020; Mangano et al., 2019). Unfortunately, increasing the pore size further beyond 700 μm can weaken mechanical strength and reduce the surface area available for osseointegration (Taniguchi et al., 2016). In this case, although larger pore sizes promote osteoconductive and vascular infiltration, they can lower Young's modulus and yield strength. At the same time, they may also decrease the stiffness and strength of implants (Ran et al., 2018).

Designing optimal pore geometry remains difficult, as controlling pore shape during traditional manufacturing is challenging (Sun et al., 2025). Nevertheless, additive manufacturing enables the creation of porous implants with complex, predefined pore structures (Sun et al., 2025). This development is significant because

pore shape greatly influences cell behaviour (Fu et al., 2009), and optimising it can enhance permeability and encourage bone tissue growth (Jeong & Hollister, 2010).

Chang et al. studied the tissue response of porous HA implants with different pore shapes: cylindrical, sponge, and cross. They found that cylindrical pores provided the best osteoconductivity (Chang et al., 2000). Similarly, Fu et al. (2009) discovered that scaffolds with a cellular microstructure more effectively supported cell proliferation and function than lamellar structures (Fu et al., 2009). Despite these advancements, the search for the ideal pore geometry continues, driven by the desire to understand how pore shape influences cell behaviour fully.

2.7.4.2 Pore size

The Haversian system is a crucial structural component supporting long bones, with pore sizes ranging from 50 to 250 μm. For effective bone formation within these pores, the pore size must be larger than that of the Haversian systems. Osteoblasts are generally 20 μm long, while capillaries have diameters of 10–15 μm (Oers, 2010). Additionally, the size of interconnected pores significantly influences cell and blood vessel migration (Wu et al., 2012). Typically, to enable smooth passage for cells and vessels, pores should be larger than 35 μm. Connecting pores smaller than this cannot accommodate capillaries and osteoblasts simultaneously due to spatial constraints during migration and vascular development (Karageorgiou & Kaplan, 2005). Furthermore, a porous structure with pores between 50 and 300 μm and good connectivity has been shown to support bone tissue formation (Zheng et al., 2019).

Previous research indicates that the ideal pore size of hydroxyapatite ranges between 150 and 500 μm (Chang et al., 2000). Interestingly, even without bearing weight, porous titanium implants with pore sizes of 50–125 μm support effective bone ingrowth (Ylä-Soininmäki et al., 2013). Pore size is crucial for osteogenesis, as Biffi et al. (2020) observed in hydroxyapatite scaffolds with small (90–120 μm) and large (350 μm) pores; cartilage forms first in smaller pores, whilst larger pores promote blood vessel formation, enhancing oxygen and nutrient supply to aid bone growth, as presented in Figure 2.4.

A pore size of 200 μm is ideal for early osseointegration, while 300 μm promotes lamellar bone formation (Kapat et al., 2017; Götz et al., 2004). Smaller pores may limit cell and blood flow due to reduced permeability, whereas larger pores (>300 μm)

enhance nutrient and oxygen flow, thereby supporting vascularisation (Karageorgiou & Kaplan, 2005). Employing a graded porous structure with varied pore sizes can synergistically boost osteogenesis, as shown in Figure 2.16. Taniguchi et al. (2016) investigated the effects of pore size in SLM-fabricated porous titanium implants in rabbits, creating three types with 65% porosity and average pore sizes of 309, 632, and 956 μm, and observed that vascularisation increases with pores exceeding 400 μm but not linearly, with larger pores favouring angiogenesis.

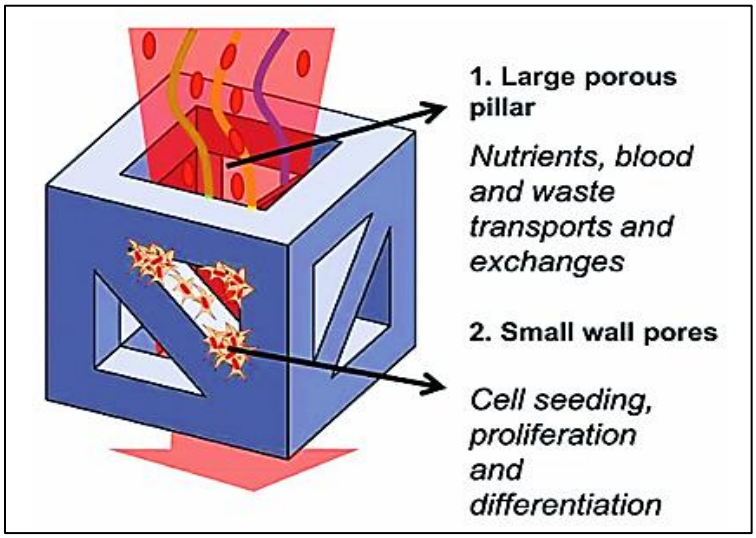

Figure 2.16 Schematic Diagram of the Biological Functional Unit Cell with Different Pore Sizes. (Wang et al., 2020)

Conversely, a higher average curvature, which inversely correlates with pore size, promotes tissue expansion *in vitro* (Knychala et al., 2013). Smaller pores may positively influence osteogenesis through curvature effects (Bai et al., 2020). These findings suggest that 300 μm implants may pose greater challenges to blood vessel growth than 600 and 900 μm implants. Additionally, although 900 has larger pores, its osteogenesis performance is lower, possibly due to decreased curvature (Taniguchi et al., 2016).

2.7.4.3 Pore Shape

Mechanically, whether as rectangles or spheres, pore shapes exhibited similar Young's modulus, with rectangular pores at 1.38 GPa and spherical pores at 1.98 GPa (Abidi et al., 2015). Nonetheless, spherical pores exhibited the highest compressive

strength, reaching 107 MPa, whereas rectangular pores reached 68 MPa. The spherical shape enhances strength by reducing stress concentration, as the sharp edges of rectangular pores can induce cracks during deformation.

Biologically, pore size affects how cells sense their environment, influencing their behaviour (Taniguchi et al., 2016; Wang et al 2020). Triangular scaffolds with 500 μm pores showed a significant increase in ALP activity, indicating that triangular pores may promote cell growth and differentiation. Smaller triangular pores with sharp angles aid cell attachment and support differentiation (Van Bael et al., 2012). Conversely, circular pores can help prevent pore blockage. Combining different pore shapes to utilise their respective benefits could be a promising design strategy in the future (Van Bael et al., 2012).

2.7.4.4 Porosity

Porosity, defined as the percentage of void space within a solid, is a vital morphological characteristic that influences material behaviour. The type of bone ingrowth primarily depends on pore size and porosity; larger pores are beneficial because they promote direct bone formation by enhancing blood vessel development and oxygen delivery, whereas smaller pores may lead to complications such as osteochondrosis (Zhang et al., 2021). It is essential to consider the mechanical properties and degradation rates of materials, as these factors determine the ideal limits for pore size and porosity.

When designing scaffolds, it is crucial to strike a balance between high porosity and mechanical performance. For example, scaffolds made from biomaterials with high degradation rates should not exceed 90% porosity to preserve their mechanical and structural integrity over time. Conversely, scaffolds made from biomaterials with lower degradation rates and enhanced mechanical strength can have greater porosity.

Research conducted by Zheng et al (2019) provides valuable insights into the relationship between porosity and mechanical properties in porous titanium implants (designated A30, A40, and A50, representing the volume fractions of NaCl used). This study demonstrates that as the NaCl volume fraction increases from 30% to 50%, the mechanical properties, including compressive and yield strengths, decrease. Notably, the A30 sample exhibits better mechanical properties, while the A50 sample, with a yield strength of approximately 59.8 MPa, falls below that of cortical bone but is similar

to human trabecular bone. Additionally, the elastic modulus of the A50 sample is significantly lower than that of cortical bone, aligning more closely with the properties of human trabecular bone (Zhang et al., 2021).

2.7.4.5 Interconnectivity

Previous research has shown that porous implants require interconnected pores to support vascular tissue, which is essential for ongoing mineralised bone growth (Wu et al., 2012). Connectivity between pores is vital for bone ingrowth, and well-connected pores can improve both bone growth and cell differentiation (Wu et al., 2012). Different levels of porosity elicit varied biological responses; for example, implants with 30% porosity (A30) exhibit less bone ingrowth than those with 40% (A40) and 50% (A50) porosity (Zheng et al., 2019). This difference mainly stems from variations in blood vessel formation, which is crucial for bone development. Importantly, substantial blood vessel formation occurs in pores larger than 400 μm (Zhang et al., 2021).

Regarding angiogenesis, A40 and A50 implants perform better than A30, emphasising that optimal pore size and interconnectivity are vital for the growth of both bone and vascular tissue. Adequate blood supply is essential for enhancing bone integration with porous implants (Taniguchi et al., 2016). In addition to nutrient delivery, capillaries facilitate the migration and differentiation of bone cells by transporting functional factors (Wang et al., 2020).

2.7.4.6 Porous Surface and Biological Effect

As discussed earlier, one approach to addressing surface preparation challenges and potentially reducing implant material density is to employ a porous structure. Bone is a unique tissue with a complex three-dimensional architecture, comprising a dense cortical layer and a spongy, trabeculated medullary cavity. The development of porous implants with a hierarchical structure that mimics bone is a significant advance in the field of osseointegration and has attracted attention since the 1970s (Young & Keller, 1984). Such implants have demonstrated considerable potential in facilitating integration with surrounding tissues. The porous surface of an implant offers numerous benefits. Firstly, it increases the surface area, enabling more cellular activity around it. Additionally, the porous structure provides an optimal surface for bone cells to attach,

thereby promoting sufficient bone formation. The interconnected pores facilitate capillary action, allowing fluid transport into the pore structures, which is essential for bone ingrowth and maintenance. This could herald a brighter future for patients requiring such implants. Since the 1990s, porous surfaces have been utilised to combat marginal bone loss resulting from excessive stress around the crestal bone. Studies have shown that porous architecture promotes strong bone ingrowth when evaluated via histology and radiography (Assad et al., 2003; Assad et al., 2004). Moreover, implant stability can be significantly enhanced by a porous surface topography, in which bone formation is also observed perpendicular to the implant's long axis. In contrast, dense metallic biomaterials tend to form bone parallel to their surfaces, which can pose challenges (Assad et al., 2004).

When it comes to porous implant design, several crucial factors must be considered, including pore shape, size, porosity distribution, interconnectivity, and the base metal used to fabricate the porous implant. These characteristics play a vital role in determining the implant's mechanical and biological properties (Wally et al., 2015). Although there is no consensus on the ideal pore size for promoting bone growth, researchers have proposed various ranges, including a minimum of 100 μm for mineralisation and osteoprogenitor cell migration (Sundelacruz & Kaplan, 2009), between 200 and 500 μm (Wen et al., 2001), and 500 to 1500 μm (Otsuki et al., 2006). Some researchers suggest that a minimum size of 150 μm is essential for osteoid formation (Bobyn et al., 1980), whereas larger sizes, approximately 300 μm and above, are necessary to retain both osteoid and vascular structures (Karageorgiou & Kaplan, 2005). An increase in porosity and pore size enhances biological interactions, such as vascularisation and perfusion (Karageorgiou & Kaplan, 2005), leading to improved cellular growth and spreading, as well as a reduction in Young's modulus and yield strength, thereby mitigating stress-shielding effects. However, it can also negatively impact mechanical strength and decrease corrosion resistance (Ran et al., 2018). Meanwhile, pore interconnectivity plays a critical role in facilitating fluid transport for cells and proteins, as well as nutrient exchange, which is vital for OI. Therefore, well-connected pores allow adequate circulation, whereas closed cell channels hinder tissue integration and long-term fixation. A summary of the bone healing pattern on porous endosseous implants is presented in Table 2.15.

Table 2.15
Bone Ingrowth into the Porous Structure of Implant: Animal and Human Studies

Material Description	Experiments	References
Porous Ti trabecular cylindrical scaffold, 20 mm long x 5 mm diameter (powder metallurgy technique), 53 % interconnected porosity, average pore size 210 µm, interconnectivity – 57 µm	**Rabbit model** Percentage of bone inside the implant after placement 3-month – 49.3 %, 6-month – 75.6 %, 12-month – 81.3 % Bone regeneration exhibits a similar pattern for both cortical and marrow, and is superior to control (spontaneous healing). Complete bone regeneration at 6 months in porous trabecular scaffold.	Torez Perez et al., 2021
Cylindrical and root form porous Ti alloy, Ti6Al4V, porous interconnected size = ~550 µm, average strut size ~200 µm, porosity 80 % (AM-SLM Technique), control: dense Ti alloy implant, cylindrical shape	**Rabbit Model:** Push-out test: Porous > control at 2nd, 3rd, 4th and 8th week after implantation **Beagle dog mandible model:** Analysis in 2, 4 and 8 weeks after implantation **Radiographic finding:** increased bone density with time, especially at cortical bone. Bone resorption around the neck region was identified in the control group at 8 weeks. **Histological evaluation:** bone ingrowth completely to the small pore structure and partially in larger sizes. **BIC** was found to be smaller on the pore implant (34.61 ± 6.52 %) than the bulk implant (43.75±5.1 %), but the difference was not significant. **Fluorescence evaluation**: New bone ingrowth was identified at 2nd week.	Liu et al.,2020
Highly porous, tantalum material (TM) (Trabecular Metal™ Material, Zimmer TMT, Parsippany, NJ). Porosity 75 -80 %, interconnected pores size = ~ 440 µm and dodecahedron-shaped cells	**Human model- 1-year study** 105 patients (57 maxillary and 88 mandibular) 28 patients had concomitant health conditions (smoker, hx of periodontitis, cardiac disease, unhealthy habit, bone graft, oral infection). Three implants failed due to local or systemic infection, and four implants failed to integrate. Cumulative implant survival was 95.2% (n = 138/145) with 0.43 ± 0.57 mm of mean marginal bone loss. 7 implants failed (5 maxillary, 2 mandibular)	Schlee et al., 2015

Material Description	Experiments	References
size = ~ 540 µm	Cause of failure: infection (3), failure to integrate with unknown cause (3), failure to integrate d/t habit (1).	
Porous NiTi, PNT, Actipore™, diameter: 11 mm x length: 20 mm, pore size: 230 ± 130 µm, porosity: 65 ± 5%; Biorthex Inc., Montreal, QC, Canada) and titanium intervertebral fusion implants (TiAlV, BAK™, diameter: 11 mm, length: 20 mm, Sulzer Spine-Tech Inc., Minneapolis, MN, USA).	**<u>Sheep model – Intervertebral lumbar region</u>** Bone fusion is superior on porous surfaces. Both materials showed biological fusion at 12 months, Ti6Al4V seemed to take a longer time to obtain intervertebral fusion. Bone resorption and endochondral calcification were observed at the periphery border of control, Ti6Al4V. Bone density lower in PNT but not significant. Soft tissue fibre orientation in porous PNT is perpendicular to the implant surface, subsequently followed by osteoblast migration and proliferation for osteointegration. Parallel orientation of the non-porous implant	Assad et al.,2004
Porous NiTi, PTN, Actipore™, diameter: 11 mm x length: 20 mm, pore size: 230 ± 130 µm, porosity: 65 ± 5%; Biorthex Inc., Montreal, QC, Canada) and titanium intervertebral fusion implants (TiAlV, BAK™, diameter: 11 mm, length: 20 mm, Sulzer Spine-Tech Inc., Minneapolis, MN, USA).	**<u>Sheep model – Intervertebral lumbar region</u>** **Histomorphometri**c evaluation from 3 – 12 months**:** **% of OI from 3 – 12 months:** PTN: 21.4 % – 37.6 %, Ti6Al4V: 22.7 % – 25.4 % **Bone apposition from 3 – 12 months:** PTN 10.9 % - 24.2 %, Ti6Al4V: 1.1 % - 5.1 % **Radiological fusion scores from 3 to 12 months**: PTN: 12.5 – 18.5, Ti6Al4V: 2.0 – 15.0 **Histology evaluation:** ***3-month implantation:*** histologically found active bone metabolism around PTN with woven bone growth within interconnected pores, dense bone matrix filled with capillaries, and intervening bone marrow spaces filled with mesenchymal and pluripotent cells. The bone formation increases with time. ***12-month implantation:*** The remodelling bone takes place where PTN is surrounded by mature cortical and trabecular bone, and cancellous bone shows ingrowth into the porous structures. PTN bone apposition was	Assad et al.,2003

Material Description	Experiments	References
	significantly higher than that of the control. This finding was corroborated with a radiological evaluation, where PTN showed a superior outcome without the need for a bone graft.	
Cylindrical shape core: Ti6Al4V, porous cp Ti, 8 mm length, 5 mm diameter, average pore size 400 µm (300 – 500 µm), 55 % porosity	**<u>Human model - Knee arthroplasty</u>** **Bone ingrowth**: *0 months* – 1- 2 %, *3 months* – 5 - 19 %, *6 months* – 6 - 28 %, *9 months* – 19 – 37 %, *12 months* 13 – 46 %. Significant bone ingrowth from 0 – 6 months, with no difference in 9 & 12 months **Histology:** *0 months*: similar pattern between peri-implant interface and within porous (bone fragment, RBC and bone marrow mixed with bone debris), except porous, ↓ bone debris, and some were empty. *3 months*: interfacial region: new bone along the edge of the parent bone and bone debris/fragment within the porous. Osteoblasts along the epithelioid layer, osteoid with osteoblasts and bone fragments intervening along the surface. *6 months*: bone remodelling, reduced epithelioid osteoblastic lining and osteoid compared to the 3-month evaluation *9 & 12 months*: osteoid with osteoblast rarely seen, fibrous tissue and/or bone marrow seen in porous coating, which is not filled by bone	Hofmann et al., 1997
Sintering porous structure to dense Ti alloy, Porosity: 34 %. Average pore size: 125 µm, root-form	**<u>Monkey model</u>** A significant dense bone ingrowth into a porous structure. 59% and 71% porous surface occupied with bone, 13.6 % and 7.6 % fibrous tissue intervened around the neck region in < 2 years and between 2-5 years after implantation **<u>Human model</u>** Serves as the distal abutment of a 3-unit bridge of mandibular molar opposed to natural maxillary molars. 5 patients had bilateral, 3 patients had unilateral. **Failed:** 1 (bilateral), 3 unilateral, related to surgical technique, healing duration, and patient factor (risk case). **Survived**: 4 patients (bilateral)	Young and Keller 1984

2.8 Evaluating Osteointegration

2.8.1 Implant Stability

When intimate contact with the new bone forms and is established on the implant surface, the implant becomes firmly anchored in its bone bed, with no movement, even under load (Manzano-Moreno et al., 2015). The success of an implant is highly dependent on its stability, which is a critical clinical indicator of osseointegration (Meredith, 1998).

Implant stability varies over time. Primary stability (PS) indicates the initial biometric stability gained through direct mechanical engagement between the implant macrostructure and the prepared bone immediately after placement. It is crucial to ensure the implant is well-seated to allow the healing process to proceed smoothly (Javed et al., 2011). In contrast, secondary stability (SS) refers to established biological osseointegration, as defined by Branemark et al. (1969), in which direct bone apposition occurs on the implant surface.

The mechanism underlying implant-biological integration is similar to the reduction concept in the management of long-bone fractures to achieve biological union. The greater the PS, the lower the likelihood of micromovements that positively contribute to SS, according to Frost's mechanostat concept (Olmedo-Gaya et al., 2023). Without prolonged inflammation, bone loss, biomechanical stress and osteonecrosis, secondary stability would be established. This reflects biological compensation through new bone formation and remodelling at the bone-to-implant interface, resulting in progressive increases in stability. Thus, ensuring optimal primary and secondary stability is key for successful implant outcomes.

Numerous research studies have demonstrated that the mechanical stability of dental implants decreases during the early stages of healing. This biological phenomenon eventually improves as new bone formation and apposition occur slowly along the implant surface and the healing bed (Berglundh et al., 2003; Lang et al., 2011). In the first three weeks following implant placement, active bone resorption along the existing parent bone by osteoclast activity (Berglundh et al., 2003) results in a loss of PS (Barewal et al., 2003). Excessive pressure during implant installation also impacts implant stability, potentially leading to microcracks and compression necrosis, especially during tight-fit implant placement or when the surgical bed is under-prepared

in high-density bone (Antonacci et al., 2023). These transient biological changes are known as the implant stability dip phenomenon (Barewal et al., 2003; Smeet et al., 2016). It is crucial to recognise that the transition from primary to secondary stability carries a significant risk of micromotion, which can cause bone loss, dis-osteointegration, and subsequent implant failure (Olmedo-Gaya et al., 2023; Rodrigo et al., 2010). Limited micromotion within a range of 50-150 μm is acceptable (Alexander & Ricci, 2017; Chrconovic et al., 2015). However, micromovement exceeding this range is considered excessive and harmful (Ottoni et al., 2005), potentially leading to distant osteogenesis (Marković et al., 2011) and fibrous encapsulation (Alexander & Ricci, 2017; Bosshardt et al., 2016; Mavrogenis et al., 2009). Both inadequate PS and excessive micromovements increase the risk of implant failure (Rodrigo et al., 2010).

Primary stability (PS) is a crucial factor that reduces implant movement during healing, significantly supporting the long-term success of dental implants (Atieh et al., 2012). Research has demonstrated a strong link between the primary stability of dental implants and the insertion torque value (ITV) (do Vale Souza et al., 2021; Trisi et al., 2009). Furthermore, the connection between ITV and the implant stability quotient (ISQ) during placement emphasises the importance of achieving optimal conditions for implant success (Baldi et al., 2018).

Although there is no universally accepted classification system for ITV as low, intermediate, or high, many studies suggest that an ITV below 30 Ncm may be regarded as low. At the same time, values above 50 Ncm are classified as high. An intermediate range of 32 to 50 Ncm has been recognised as suitable for single restorations (Lemos et al., 2021; Ottoni et al., 2005), whereas exceeding 20 Ncm is considered a threshold for splinted implants (Darriba et al., 2022). When it comes to loading protocols, ensuring adequate primary stability is particularly important when dental implants are subjected to immediate loading (Lemos et al., 2021; Trisi et al., 2009). A minimum ITV of 35 Ncm for a single crown at an ISQ of 70 or above allows for immediate or early loading; if ITV and ISQ values are lower, a delayed loading approach is advised (Darriba et al., 2022; do Vale Sauza et al., 2021; Trisi et al., 2013).

It is noteworthy that the absence of primary stability, particularly when associated with low ITV, has been linked to a significantly higher risk of early implant failure, up to 14 times that of high-stability scenarios (Carr et al., 2022). However, a commendable survival rate of 97.2% was reported for 213 implants exhibiting instability after a healing period of 2 to 4 months (Rodrigo et al., 2010). A similar study

by Norton (2017) demonstrated 100% survival at low ITV (<20 Ncm) with acceptable marginal bone loss over a 1-year observation period. Clinical studies examining implant survival rates in cases of low primary stability have revealed a wide range, from 56% to 100%, over durations spanning from 6 months to 9 years (Al Samman et al., 2022; Darriba et al., 2022; Lemos et al., 2021). These studies encompass various scenarios, including immediate and delayed placement (Al-Samman et al., 2022), immediate or delayed loading (Darriba et al., 2022; Cobo-Vázquez et al., 2018), single crowns (Koutouzis et al., 2011; Ottoni et al., 2005), bridges (Cesaretti et al., 2016; Daher et al., 2019), full-arch prostheses (Degidi et al., 2011; Schincaglia et al., 2016), different bone qualities such as soft bone (D3, D4 types) and D2 type (Cobo-Vázquez et al., 2018; Lee et al., 2019), and instances involving bone grafting (Lee et al., 2019).

Bone density and quality (Marquezan et al., 2012), surgical drilling protocols applied (Alghamdi et al., 2011), and implant factors such as thread design, implant length, and surface topography (Abuhussein et al., 2010; Darriba et al., 2023; Menini et al., 2020; Vollmer et al., 2022) are vital factors influencing primary stability. It is expected that high bone quality and density, such as in types II and III, based on Lekholm and Zarb, especially in the posterior mandible, result in higher stability values compared to low bone quality (type IV), as seen in the posterior maxilla (Barewal et al., 2003; Olmedo-Gaya et al., 2023), which correlates with its higher survival rate (Zhou et al., 2021). This reflects bone architecture, in which the posterior mandible typically has thicker cortical bone and denser cancellous tissue. Conversely, the posterior maxilla generally has thinner cortical bone and spongy cancellous tissue. Some researchers believe that bone quality influences PS more than macro design, because direct implant-bone contact affects cortical bone, regardless of implant macrostructures such as length and shape (Shayesteh et al., 2013). Regarding the surgical technique used, there is a positive correlation with PS. It is suggested that in soft-type bone, underprepared or bone-condensing osteotome techniques generate better PS than conventional drilling (Insua et al., 2023; Olmedo-Gaya et al., 2023). Lateral and apical condensation in osteotome surgical techniques increases the density of the bone in contact with the implant surface. However, excessive impaction exceeding the bone's compressive strength threshold of 100 MPa can impair microcirculation, negatively affecting angiogenesis and the supply of nutrients, oxygen, and osteocyte viability, as well as necrosis (Cory et al., 2010; Bashutski et al., 2009; Insua et al., 2023; Ueda et al., 1991).

It is crucial to consider various factors that may affect implant stability during the shift from mechanical attachment to a biological response. This prompts the question of whether PS remains a dependable predictor of implant success. Increasing healing time enhances secondary stability, making it a more significant indicator of successful implant outcomes (Andreas Vollmer et al., 2020; Rodrigo et al., 2010). A summary of the implant stability timeline is provided in the following Table 2.16.

Table 2.16
The Chronology of Implant Stability Phenomenon

Time Point	**Stability**	**Event**	**References**
Immediate (Day 0–1)	Primary	Mechanical engagement with bone is affected by bone density, implant design, and insertion torque	Javed et al., 2011; Meredith et al., 1998; Wang et al., 2018
Early Healing (Days 2–14)*	Decreasing primary; initial biological response	Inflammatory response, clot formation, osteoclast-mediated bone resorption at the interface	Barewel et al., 2003; Berglundh et al., 2003; Lang et al., 2011; Terheyden et al., 2012; Wang et al., 2018.
Transition Phase (Weeks 2–4)*	Minimum total stability	Primary stability declines; secondary stability not fully developed; risk of micromotion	Almassri et al., 2020; Barewal et al., 2003; Sennerby & Meredith, 2008; Wang et al., 2018
Osseointegration (Weeks 4–8)	Increasing secondary	New bone formation, mineralisation, and bone-to-implant contact (BIC) increase	Almassri et al., 2020; Berglundh et al. 2003; Buser et al. 2004; Wang et al., 2018
Maturation Phase (>8 Weeks)	Predominantly secondary	Lamellar bone remodelling, mechanical interlocking at the microscopic level	Wang et al., 2018.

Notes: (*) indicates the time point may varies depending on implant surface treatment, loading protocol, host condition (healthy vs compromised, different size animal model and location (Barewel et al., 2003; Wang et al., 2018)

2.8.1.1 Measurement of Implant Stability

Accurate measurement of implant stability can predict the success of dental implants. Several methods have been proposed for assessing implant stability at various clinical stages. The original technique, the percussion test, involves tapping the implant with the handle of a mouth mirror to produce a high-pitched sound. Radiographic evaluation of the clinical bone level surrounding the implant has also been employed; however, both techniques seem unreliable in quantifying implant stability. Conversely, histomorphometric assessment using electron microscopy can evaluate bone-to-implant contact, but this method is more suitable for animal or experimental studies than for humans (Chen et al., 2019). Other techniques, such as pull-out or push-out tests, resistance to reverse torque, and percussion, are invasive and imprecise, potentially damaging the osseous bed and hindering healing, thereby making them clinically impractical (Schliephake et al., 2006). Insertion torque values and other non-invasive quantitative methods, such as the Periotest device (Siemens) and the Osstell instrument, are now widely utilised as alternatives for assessing osseointegration in clinical settings. The insertion torque value ranges from 4 to 42.34 Ncm, depending on location and individual bone density (Marquezan et al., 2011). The insertion torque tends to be higher in dense areas such as the mandible than in the posterior maxilla, which has a thin cortical layer and abundant trabecular bone (Schliephake et al., 2006). Periotest and Osstell technologies aim to achieve optimal accuracy in predicting the timing of loading and implant success (Baldi et al., 2018).

Measuring implant stiffness within the bone using Ostell by identifying the resonance frequency (RFA) is becoming increasingly popular as a non-invasive, reliable, and reproducible method for clinically monitoring long-term implant stability. It measures the stiffness of the implant-to-bone system based on vibration theory. The data collected is automatically processed and displayed as an implant stability quotient (ISQ) ranging from 1 to 100 (kHz). The higher the ISQ value, the greater the implant stiffness within its bone bed, and the more likely there is to be a successful bone-to-implant interface, or vice versa. There is no consensus on what constitutes a normal ISQ value during implant placement; values greater than 65 are generally regarded as acceptable (Baltayan et al., 2016). This complexity increases with immediate-loading protocols, in which the only RFA measurement taken before loading is obtained at the time of implant placement. Therefore, it is crucial to establish a safe ISQ threshold for

planned immediate loading to better predict which implants are at high risk of failure and which are suitable for immediate loading. Clinical studies have suggested different threshold values for immediate loading, with some proposing ISQ values of ≥ 42 and others recommending values above 65 at placement (Meredith et al., 1998; Sennerby & Meredith, 2008).

While the relationship between ISQ and histomorphometric evaluation is complex, both positive (Scarano et al., 2007) and negative correlations have been documented (Abrahamsom et al., 2009; Schliephake et al., 2006). Numerous studies have examined the connection between implant stability quotient (ISQ) values and bone quality. Some have identified a strong correlation between ISQ values and bone quality, according to Lekholm and Zarb's criteria. However, other research indicates a weak association between operator-perceived primary stability and both bone quality and ISQ values. Furthermore, some studies have found no significant association between ISQ values and bone volume density or trabecular connectivity, as assessed by micro-computed tomography.

Interestingly, although RFA measurements have not been proven to correlate with insertion torque, they are closely linked to cortical bone thickness and cutting resistance during implant placement. Implant surface chemistry and finishing, as well as implant diameter, do not appear to influence ISQ values. However, implant length has been shown to enhance primary stability, as longer implants provide a larger bone-implant contact area. Due to inconclusive findings regarding the parameters used to measure implant stability, supplementary tools, such as clinical and radiographic evaluations, are recommended for routine implant assessment to determine clinical success (Chen et al., 2019). These methods can help evaluate the long-term stability and success of dental implants.

2.8.2 Peri-Implant Tissue Condition

Maintaining the health of the peri-implant tissue is essential for the stability and functionality of implants. The peri-implant tissues complex (PIT) comprises the peri-implant mucosa alongside the bone surrounding the osseointegrated implants. The mucosa serves as a structural and immunological interface between the implant and the host, forming a barrier to microbial invasion (Berglundh et al., 2003). The bone provides mechanical support to the implant through a process known as osseointegration.

Similar to natural periodontal tissue, peri-implant tissue can be prone to inflammation and degradation, leading to complications such as peri-implant mucositis and peri-implantitis. Deviations from healthy features signal important indicators of disease development; therefore, understanding the biology of peri-implant tissues is essential for clinical success and the prevention of complications (Mombelli & Lang, 1998). Several factors influence peri-implant health, including surgical techniques, implant and prosthetic design, patient-related risk factors (such as smoking and diabetes), and maintenance care (Pokrowiecki et al., 2017). Despite implants with favourable surface topography that promote osseointegration and soft-tissue adhesion (Albrektsson & Wennerberg, 2004), effective tissue management, including augmentation techniques, ensures sufficient keratinised mucosa and supports the long-term health of peri-implant tissues (Lin et al., 2019). Simultaneously, regular maintenance protocols, including debridement and monitoring of peri-implant tissues, are vital in preventing disease onset and progression (Lin et al., 2019).

2.8.3 Peri-Implant Mucosa

2.8.3.1 Morphogenesis of Peri-Implant Mucosa

The morphogenesis of peri-implant tissues has been extensively studied by Berglundh & Lindhe (1996) using a single-stage implant/abutment placement protocol in a canine model. Two primary biological processes begin with implant insertion and subsequent abutment placement: peri-implant tissue integration and osseointegration (Ríos-Osorio et al., 2025). Both processes occur as part of a foreign-body response, involving a cascade of complex physiological and immunological mechanisms similar to those seen in soft-tissue injuries and bone fractures. Peri-implant tissue integration involves the intricate biological processes underlying the formation and maturation of peri-implant soft tissues surrounding a transmucosal abutment (Pokrowiecki et al., 2017; Ríos-Osorio et al., 2025). This process establishes a direct and functional connection between the intraosseous implant and the oral cavity. Typically, this occurs between 8 and 12 weeks after the installation of the transmucosal abutment (Choe et al., 2024). Meanwhile, osseointegration involves significant dysregulation of the immune-inflammatory response, which subsequently leads to the overexpression of genes

relevant to osteogenesis, angiogenesis, and neurogenesis during the initial phases of healing (Salvi et al., 2015).

Notably, two hours after surgery, a blood coagulum forms in the interstitial space between the implant, the mucosa, and the alveolar process, where numerous granulocytic neutrophils infiltrate the coagulum. Macrophage presence is minimal; however, a dense fibrin mesh enriched with leukocytes forms as the initial peri-implant mucosal seal (Araujo & Lindhe, 2018). As healing progresses, this clot undergoes degradation due to significant leukocyte infiltration, which activates angiogenesis mediated by epithelial, endothelial, and fibroblast cells. This cascade promotes healing and epithelial proliferation, ultimately facilitating the formation of the peri-implant epithelium (PIE) (Araujo & Lindhe, 2018; Choe et al., 2024; Ríos-Osorio et al.,2025). One week after implantation, the initial mucosal seal remains intact. However, the fibrin and leukocyte content diminishes, mainly localised to the marginal area of the soft tissue-implant interface, which is primarily composed of a thick layer of fibroblasts and collagen (Ríos-Osorio et al.,2025). This layer maintains close adherence to the implant surface and is supported by a connective tissue matrix rich in fibroblasts and vascular structures, indicating the formation of peri-implant tissue similar to the junctional epithelium (JE) observed in periodontal tissues.

During the second to third week of the healing process, fibroblast density decreases while collagen and matrix component levels increase; epithelial cells extending from the oral epithelium begin to populate the marginal regions of the connective tissue wound. After approximately four weeks, collagen fibres within the aforementioned wound area are organised into bundles. Between six and twelve weeks, a dense arrangement of fibroblasts accompanies the maturation of the peri-implant tissue, aligned parallel to the implant surface, thereby contributing to the subepithelial peri-implant connective tissue structure. The bone crest is established around 3–4 mm below the soft tissue margin (Araujo & Lindhe, 2018; Choe et al., 2024; Ríos-Osorio et al.,2025).

Even after achieving successful osseointegration, PIT exhibit significant differences compared to periodontal tissues (Pokrowiecki et al., 2017; Sculean et al., 2014). While periodontal tissues develop concurrently with tooth eruption, PIT arise from a healing process following surgical trauma (Sculean et al., 2014). These distinctions in morphogenesis result in specific structural and morphological features of peri-implant tissues, such as the absence of a periodontal ligament (PDL). Histological

examination reveals that the peri-implant epithelium (PIE) is longer than the junctional epithelium (JE), resembling an elongated JE, with the peri-implant connective tissue exhibiting characteristics akin to scar-like connective tissue and reduced vascular supply due to this scar-like nature (Araujo & Lindhe, 2018; Ríos-Osorio et al., 2025). The longer PIE results from the downgrowth of epithelial cells during soft tissue healing compared with connective tissue (Choe et al., 2024). Furthermore, differences exist in both the histological and functional aspects of the PIE and connective tissue, which are essential to the biological seal around dental implants. Consequently, these biological structures have a lower capacity than those formed by periodontal tissues (Atsuta et al., 2016). The detailed anatomy and biological components of periodontal tissue around the tooth and implant are summarised in Figure 2.17.

2.8.3.2 Anatomical Components of Peri-Implant Mucosa

The peri-implant mucosa around dental implants is structurally complex, similar to gingival tissue. It comprises three types of epithelium: the outer layer is oral epithelium (OE), a stratified keratinised layer that interfaces with the external environment. Additionally, two other components extend from the OE and face the abutment, known as the peri-implant sulcus epithelium (PISE) and the peri-implant epithelium (PIE).

PISE, the epithelium facing the abutment, is located coronally and covered by a thin barrier epithelium. The more apical, deeper region consists of non-keratinised tissue known as PIE, which directly contacts the implant surface (Atsuta et al., 2016). PIE is made up of several layers of flattened epithelial cells that lack keratin in their stratum corneum, resembling the JE found in periodontal tissues (Ríos-Osorio et al., 2025). Similar to the tooth-epithelium attachment, which includes hemidesmosomes and a basement membrane linking to enamel or cementum, the attachment to the implant is comparatively weaker, more susceptible to bacterial invasion (Berglundh et al., 1991), and positioned more apically than that of a natural tooth, aligning with the entire JE-tooth.

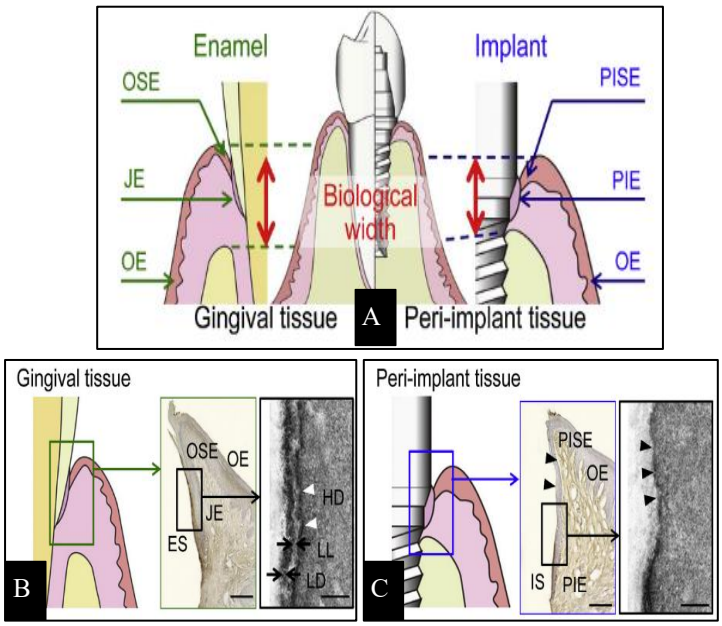

Figure 2.17 Anatomy Comparison of the Periodontal Tissue and Peri-Implant Tissue (PIT).

Notes**:** A Indicates the Soft Tissue Attachment to a Natural Tooth (Left) and an Implant (Right). JE: Junctional Epithelium, OSE: Oral Sulcular Epithelium, OE: Oral Epithelium, PIE: Peri-Implant Epithelium, PISE: Peri-Implant Sulcular Epithelium. These supracrestal complex attachments form a biological width as a functional seal. The most coronal portion of the epithelial-sealing structure is the OSE (tooth) and PISE (implant). The middle portion resides in the PIE, sharing a structure similar to the JE that surrounds a natural tooth (left). B and C: Histological analysis of the periodontal tissue (B) and PIT (C) attachment to the tooth (ES) and implant surface (IS). The samples were stained with anti-rat Laminin-322 (Ln) g2 chain antibody and lightly counterstained with hematoxylin. Black arrows in B: typical feature of a dual layer representing the lamina densa (LD) and lamina lucida (LL). Black arrowheads denote: no evidence of this dual layer in the PIT attachment to the implant surface, white arrowheads indicate hemi-desmosome-like structures present in both B and C (Atsuta et al., 2016)

The apical region of the PIE is recognised as the zone of connective tissue adhesion, which plays a critical role in integrating the implant with the surrounding tissue. This core connective tissue comprises mainly collagen fibres, especially types I and III, and matrix (85%), fibroblasts (3%), and vascularisation (5%) (Araujo & Lindhe, 2018). These form a robust biological seal against microbial invasion around the transmucosal part of the implant (Berglundh et al., 1991).

In natural teeth, this component is primarily composed of type III collagen fibres, arranged in multiple orientations that connect the mucosa to the tooth (dento-gingival), the periosteum (dento-periosteal), the alveolar bone (alveolo-gingival), and

the gingiva (transeptal). In contrast, dental implants lack this essential anatomical feature (Berglundh et al., 1991). These collagen fibres are organised either parallel to the implant surface or in a circular pattern around it. Despite the absence of a periodontal ligament, the blood supply is also relatively compromised. Reduced blood flow, primarily due to the absence of the periodontal ligament (Atsuta et al., 2016), significantly diminishes immune surveillance, shock absorption, and the mechanical stability of the surrounding tissues (Schwarz et al., 2007). The comparison between periodontal connective tissue and peri-implant connective tissue is shown in Table 2.17 and Figure 2.18.

Table 2.17
Differences between Periodontium and Peri-Implant Mucosa

Feature	**Natural Tooth Periodontium**	**Peri-Implant Tissue**
Presence of PDL	Present	Absent
Collagen Fiber Orientation	Gingival fibres complex: Multidirection PDL: Perpendicular (inserting fibers)	Parallel or circular
Vascular Supply	Rich (via PDL and bone)	Limited due to the absence of PDL. Vascular supply from supraperiosteal vessels only)
Proprioception	Present via PDL	Absent
Attachment Mechanism	Hemidesmosomes + Sharpey's fibers	Hemidesmosomes only

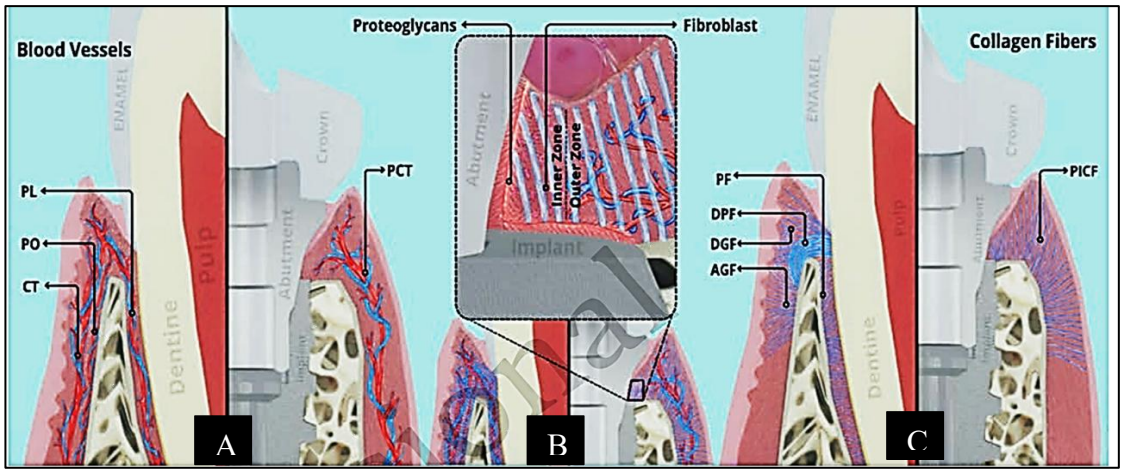

Figure 2.18 Schematic Comparison of Periodontal Connective Tissue (CT) and Peri-Implant Connective Tissue (PCT).

Notes: A: Left: Periodontal tissue receives blood circulation from the periodontal ligament (PL) and periosteum (PO). A: Right: Peri-implant tissue receives vascular supply mainly from its connective tissue. B: Histological features of PCT. Note: PCT is separated from the implant surface by a 20-nm proteoglycan layer. C. Schematic diagram shows multi-directional arrangement of collagen fibres (PF, DPF, DGF, AGF) through periodontal CT (left) and parallel arrangement of peri-implant collagen fibres, PICF, in relation to the abutment surface. PF: Periodontal fibres, DPF: Dento-periosteal fibres, DGF: Dento-gingival fibres, AGF: alveolo-gingival fibres, PICF: Peri-implant collagen fibres. (Ríos-Osorio et al., 2025).

2.8.3.3 Biology of Peri-Implant Tissue

The scar-like characteristics and biology of peri-implant tissues significantly contribute to their susceptibility to peri-implant diseases (Pokrowiecki et al., 2017). The quality of the soft tissue, including factors such as thickness and keratinisation, greatly influences peri-implant health, affecting bone remodelling, mucosal recession, and aesthetic outcomes. Thicker soft tissue (greater than 2 mm) provides better volume stability, reducing the risk of gingival recession and implant exposure and thereby enhancing aesthetic stability (Thoma et al., 2018). This is further supported by clinical trials demonstrating that connective tissue grafts for soft tissue augmentation increase peri-implant soft tissue thickness, thereby promoting long-term stability (Zuhr et al., 2014).

Implants with peri-implant soft tissue thickness less than 2 mm are associated with greater marginal bone loss (MBL) due to inadequate protection against bacterial invasion and mechanical stress (Linkevicius et al., 2010). The morphogenic characteristics of peri-implant tissues, which include the absence of a periodontal

ligament, limited vascular supply, a deeper peri-implant sulcus, inadequate integration of the implant, and weak adhesion of connective tissue to the titanium surface, facilitate the infiltration of highly pathogenic bacteria into the depths of the peri-implant mucosa and the underlying alveolar bone (Atsuta et al., 2016; Pokrowiecki et al., 2017). Keratinised mucosa (KM) plays a debated yet potentially significant role in peri-implant health by enhancing soft-tissue adaptation around dental implants, thereby reducing inflammation and the risk of peri-implant disease (Monje et al., 2019; Ravida et al., 2022; Wennström & Derks, 2012). Research indicates that implants with less than 2 mm of KM are associated with a higher incidence of mucosal inflammation, plaque accumulation, and discomfort during oral hygiene (Monje et al., 2019; Ravida et al., 2022). However, conflicting evidence from Wennström & Derks (2012) suggests that, while KM may foster peri-implant health, effective plaque control can mitigate the adverse effects of its absence. This ongoing debate in the literature stems from findings that adequate KM does not substantially affect probing depth, soft tissue recession, or marginal bone loss when compared to insufficient keratinised mucosa (Ravida et al., 2022).

Nevertheless, failure to establish optimal peri-implant mucosal thickness during implant placement can lead to supracrestal tissue attachment, which often results in bone loss (Linkevicius et al, 2010; Linkevicius et al., 2015). Bone-level implants placed in areas with naturally thick mucosal tissues (over 2 mm) experience significantly less peripheral bone loss than those with thinner mucosal types, with expected bone loss of around 0.25 mm for thicker tissues and 1.38 mm for thinner ones (Linkevicius et al., 2015). Consequently, thinner mucosal layers over time may increase the risk of implant surface exposure, food impaction, and foster bacterial colonisation (Linkevicius et al., 2010; Linkevicius et al., 2015). There is possibly a higher MBL in thinner KM as a result of remodelling processes to establish biological width during the phase of adaptation.

Meanwhile, the hard tissue component consists of alveolar bone in direct contact with the implant surface. This bone undergoes a unique process termed osseointegration, in which a direct functional and structural connection is established without the interposition of soft tissue (Albrektsson et al., 1981). This integration is critical for implant stability and load-bearing function.

The crestal bone, or the alveolar crest, refers to the most coronal portion of the alveolar bone that surrounds and supports the teeth or dental implants. In the context of

dental implants, it is the bone that encircles the neck of the implant fixture at the level of the alveolar ridge (Berglundh et al., 2003). This bone plays a critical role in the initial and long-term success of implant therapy, as it forms the primary interface between the implant and the surrounding osseous structure. The crestal bone is typically located at or just below the implant-abutment junction, depending on the implant design and surgical placement. The crestal bone supports the implant collar and defines the biological width.

Following implant placement, the surrounding bone undergoes remodelling influenced by factors such as surgical trauma, implant design, and biomechanical loading. Initially, this remodelling involves the formation of woven bone, which is subsequently replaced by mature lamellar bone (Lang et al., 2004). This transformation typically occurs within the first year (Buser et al., 1991) and may result in a certain degree of physiological crestal bone loss (Adell et al., 1981). The remodelling process continues throughout the implant's lifespan, maintaining a dynamic equilibrium between bone resorption and apposition. The stabilisation of the peri-implant bone is vital for ensuring long-term implant stability and success.

In dental implantology, the significance of peri-implant tissue (PIT) cannot be overstated. The primary roles of PIT include creating a biological seal that effectively prevents microbial entry, preserving the aesthetic appearance of dental restorations, and promoting long-term peri-implant health. Healthy mucosal tissue plays a vital role in enhancing patient comfort and maintaining proper hygiene, while the stability of the crestal bone is essential for providing the structural support necessary for both the implant and the surrounding soft tissues. This stability directly influences the longevity of the prosthesis, highlighting the importance of a well-maintained peri-implant environment. A summary of functional roles of PIT is as in Table 2.18.

Table 2.18
Functional Roles of Peri-implant Tissues

Roles	Structure involved	Description	Factors influence	Importance
Formation of Biological Seal	Supracrestal tissue attachment (STA)- the biological width that forms around dental implants refers to the dimension of the soft tissue attachment.	STA consists of: - Peri-implant epithelium and - Connective tissue zone, similar to natural teeth but with distinct differences in attachment due to the implant's non-biological surface (Berglundh & Lindhe, 1996). - Spans approximately 3 – 4 mm from the gingival margin to the first bone-to-implant contact, which peri-implant epithelium typically spans ~ 2.0 – 3.2 mm and connective tissue (~1.1 – 2.4 mm thickness) (Zaccheo et al., 2025). - In natural teeth, STA averages ~1.7 – 2.7 mm, including ~0.7–1.35 mm JE and 1.06– 1.99 mm CT (Rios-Osorio et al., 2025).	- Crestal bone level stability • Adequate height and volume → maintaining proper gingival contours for functional and aesthetic outcomes (Rios-Osorio et al., 2025). • Resorption of crestal bone →soft tissue recession, exposure of implant components, and aesthetic concerns, particularly in the anterior region. - Insufficient space for soft tissue attachment → the body to resorb crestal bone, to restore necessary biological dimensions (Hermann et al., 2000). - Implant designs, surgical techniques, or prosthetic connections, such as micro-gaps at the implant-abutment interface, can influence early crestal bone remodelling. - Peri-implantitis, biomechanical stress, or suboptimal prosthetic design → progressive bone loss and compromised implant survival (Schwarz et al., 2018).	- Serves as a functional protective barrier between the oral environment and the underlying bone. - Provide mechanical support to both the soft tissue and the dental implant. - Resists the ingress of oral pathogens. - Absence of fibre insertion and weaker epithelial adhesion mean this seal is more fragile than the natural tooth structure, increasing vulnerability to microbial invasion and inflammation (Berglundh & Lindhe, 1996; Berglundh et al., 2024). - However, this is compensated by an increase in STA dimension (Hermann et al., 2000; Zaccheo et al., 2025)

Roles	Structure involved	Description	Factors influence	Importance
Host Defence and Immune Regulation	Peri-implant epithelium (PIE)	- Acts as a physical barrier against microbial infiltration. - The junctional epithelium forms a hemidesmosomal attachment to the implant surface, limiting pathogen entry (Berglundh et al., 1991)		Primary biological protection around dental implants
	Mucosal seal ("biological seal")	- The mucosal barrier, serving as a physical barrier, helps to prevent microbial leakage along the implant-abutment interface (Berglundh et al., 2018; Lang & Berglundh, 2011)		
	Connective tissue zone	- Contains fewer fibroblasts and more collagen fibres, but lacks a periodontal ligament. - The dense connective tissue surrounding implants may help resist early microbial penetration (Choe et al., 2024; Rios-Osorio et al., 2025)		
	Innate immune cells (neutrophils, macrophages)	- Neutrophils are recruited during the early stages to neutralise pathogens, - Macrophages orchestrate inflammation and wound healing (Sculean et al., 2014)		
	Cytokines and chemokines	- Pro-inflammatory cytokines (IL-1β, TNF-α, IL-6) are released		

Roles	Structure involved	Description	Factors influence	Importance
		during the early response to regulate defence and healing. - However, excessive levels may lead to tissue breakdown (Klinge et al., 2018)		
Load Distribution and Mechanical Support	Crestal bone	- First bone to be subjected to mechanical load. - Transferring occlusal forces from the prosthesis to the jawbone (under loading) - Overload can lead to bone microdamage and progressive marginal bone loss (Winkler et al., 2003)	The success of this function depends on: - Implant design, - Surface characteristics, - Quality of bone-implant contact. - Magnitude & type of force applied	
Remodelling and Adaptation	Crestal bone, soft tissue attachment	- Natural biological process following dental implant placement. - Involves the adaptation of bone tissue in response to surgical trauma, implant loading, and the establishment of biological width. - Some degree of crestal bone resorption is anticipated and deemed physiological (bone loss of less than 1.5 mm in the first year following loading, with subsequent annual bone loss of less than 0.2 mm. (Albrektsson et al.,1986). - Most remodelling takes place within the initial year following implant placement, especially after abutment connection and	Multiple factors regulating the continual adaptation of the tissues to the functional environment (Lang et al., 2004): - Mechanical stimuli - Micro-motion - Inflammation - Implant design - Surgical methods - Prosthetic connections - Positioning of microgaps	

Roles	Structure involved	Description	Factors influence	Importance
		prosthetic loading (Berglundh et al., 2018). - Establishment of a biologic width, plays a vital role in initiating early crestal bone changes. Alteration of soft-tissue attachment caused by the implant-abutment interface and microgap leads to vertical bone remodelling (Hermann et al., 2000).		

2.8.4 Factors Affecting Peri-Implant Soft Tissue Health

Peri-implant tissue health is a parameter observed after implant placement that significantly affects implant success and longevity. It is influenced by a combination of surgical technique and implant-related factors, such as surface topography and abutment connection; for instance, platform switching reduces crestal bone loss and enhances soft tissue volume (Insua et al., 2023). Additionally, host-related factors, including oral hygiene, smoking, and systemic health status, as well as biomechanical factors (Albrektsson et al., 1986; Clementini et al., 2014; Schwarz & Ramanauskaite, 2022), further influence outcomes.

2.8.4.1 Surgical Factors and Their Effects on Peri-implant Tissues and Marginal Bone Loss

Surgical techniques used during implant placement can significantly impact the biological environment around the implant, thereby influencing the extent of marginal bone loss (MBL). Surgical aspects such as implant placement depth and angulation, flap versus flapless approaches, and the timing of implant loading each play critical roles.

a) Implant Placement Depth and Angulation

The vertical and depth positioning of dental implants is crucial for establishing the implant–bone interface. Whether placed supracrestally, equicrestally, or subcrestally has garnered increasing attention due to its potential influence on peri-implant hard and soft tissue stability. While implant design, surface characteristics, and loading protocols contribute to clinical outcomes, the precise crestal positioning plays a critical role in the re-establishment of biological width, marginal bone remodelling, and the risk of peri-implantitis.

Supracrestal placement refers to positioning the implant platform above the alveolar crest. While this orientation facilitates hygiene, it might result in metal exposure or aesthetic issues, particularly in patients with thin gingival biotypes. Equicrestal placement of the implant shoulder is aligned with the alveolar bone crest and is typically regarded as the standard method. Subcrestal placement refers to positioning the implant platform below the alveolar crest, typically 1–2 mm apically. In

aesthetic areas, this method can enhance emergence profiles and prosthetic shaping. This technique is frequently utilised with platform-switching implants and in situations with thin soft tissue.

The clinical outcomes of vertical implant placement demonstrate that subcrestally implants (approximately 1–2 mm below the bone crest) result in slightly greater initial bone remodelling than equicrestal implants (Valles et al., 2018). Particularly with platform-switching implants, subcrestal placement results in significantly reduced crestal bone loss and superior marginal bone preservation compared with equicrestal placement, especially in thick soft-tissue biotypes (Canullo et al., 2016). Significantly reduces crestal bone loss with platform switching and subcrestal positioning in the early phases, possibly due to the inward position of the implant-abutment interface, which is farther from the bone crest (Canullo et al., 2016).

Furthermore, subcrestal placement facilitates the early establishment of a soft tissue seal, which protects against microbial infiltration. It also allows for the re-establishment of biological width (Chiyun, 2024). Influencing biological width reformation is associated with more favourable outcomes, optimal tissue conditions, and improved aesthetics (Berglundh & Lindhe, 1996; Puisys et al., 2023). They emphasised the necessity for the peri-implant soft tissue to reorganise around the implant-abutment junction. Regardless of placement depth, implants in areas with inadequate soft-tissue thickness (<2 mm) often result in increased marginal bone loss and additional bone remodelling to accommodate the biological width (Linkevicius et al., 2015). However, when soft tissue thickness exceeds 2 mm, subcrestal implants demonstrate stable marginal bone levels (Linkevicius et al., 2010, 2015).

Although deeper placement (subcrestal) can enhance aesthetics and support bone preservation, it may also restrict access for hygiene and increase the risk of soft tissue and technical complications, particularly if positioned at an improper angle or with overcontouring of the prosthesis (Puisys et al., 2025). If monitoring and intervention are not implemented, plaque buildup around implants can trigger an inflammatory response, leading to peri-implant soft tissue inflammation and bone loss (Lang & Berglundh, 2011). The presence of anaerobic bacteria, including *Porphyromonas gingivalis* and *Treponema denticola*, is well established in peri-implantitis (PI) (Chun Giok & Menon, 2023; Mombelli & Lang, 1998). Despite no significant difference in the occurrence of peri-implantitis across vertical implant placements, deeper implants may be more prone to plaque accumulation if not

adequately maintained (Noguera-Fernandez et al., 2014). Meanwhile, poor angulation may lead to unfavourable mechanical stress concentration, especially on the buccal bone plate, which is naturally thinner and more susceptible to resorption (El-Zawahry et al., 2016; Kim et al., 2025). Excessive buccal angulation can thin the surrounding bone or expose implant threads, predisposing the area to early bone remodelling and resorption (Buser et al., 2004).

During implant placement, bone temperature may rise due to friction between the surgical tool and the bone and the insertion torque applied during implant installation. Excessive heat generated during the meticulous preparation of an osteotomy, combined with improper torque application or insufficient irrigation, can severely compromise the integrity of both the peri-implant bone and the surrounding soft tissues. This trauma not only initiates a cascade of inflammatory responses but also poses a significant threat to the delicate process of osseointegration, potentially leading to the detrimental breakdown of peri-implant tissues. Notably, bone exposed to temperatures exceeding 47°C for more than 1 minute sustains irreversible damage, inducing bone necrosis that profoundly affects the vital interface between the implant and bone, leading to early bone resorption (Eriksson & Albrektsson, 1984). Meanwhile, dull drills or insufficient irrigation further exacerbate this phenomenon. Tribocorrosion, caused by worn material from the implant or drill due to excessive friction during osteotomy or implant placement, triggers a foreign body response, leading to bone loss and implant failure (Suárez-López del Amo et al., 2018; Insua et al., 2023).

The choice of surgical access, whether through a traditional full-thickness flap or a flapless procedure, has significant biological implications that merit consideration. Lifting a mucoperiosteal flap to expose the underlying bone can temporarily disrupt the periosteal blood supply, which is crucial for nourishing cortical bone (Kotsakis & Romanos, 2022). This ischaemia associated with flap elevation may lead to increased bone remodelling, early marginal bone loss (MBL), and potential soft tissue recession (Kotsakis & Romanos, 2022).

On the other hand, flapless implant placement offers several advantages. By minimising surgical trauma and preserving the periosteal blood supply, this approach can reduce postoperative inflammation and help maintain soft-tissue contours. Studies have shown that flapless implant placement results in significantly less crestal bone loss over a 3-year follow-up period (Crespi et al., 2018). However, it is essential to remain aware of potential risks, such as impaired visualisation, which could increase the

likelihood of implant malpositioning or incomplete seating (Chrcanovic et al., 2014). Therefore, a balanced approach that considers the benefits and risks of each technique is crucial for achieving optimal surgical outcomes.

The timing of functional loading, defined as the application of masticatory forces following implant placement, plays a crucial role in managing marginal bone level (MBL). Immediate loading involves attaching a prosthesis within 48 hours of implant placement. When primary stability is achieved (with an insertion torque greater than 35 Ncm) and micromotion is minimised (to less than 100 μm), immediate loading can promote successful osseointegration without significant bone loss (Darriba et al., 2022). This approach helps to preserve the natural contours of both soft and hard tissues. However, if micromotion exceeds acceptable limits, it may impede the establishment of a stable bone-implant interface, jeopardise healing, and lead to fibrous encapsulation instead of osseointegration, ultimately resulting in MBL (Albrektsson et al., 2019; Albrektsson & Wenneberg, 2018; Chrcanovic et al., 2015). Although immediate placement offers aesthetic advantages, careful patient selection and surgical expertise are essential to prevent adverse outcomes.

Conversely, delayed loading represents a conventional approach that involves a healing period of approximately 3 to 6 months before loading, allowing for more complete tissue maturation and potentially reducing complications. This method enables complete primary osseointegration to occur prior to the introduction of functional stress, thereby minimising early MBL. However, the drawbacks of delayed loading are extended treatment time and increased patient morbidity.

2.8.4.2 Effect of Implant Design on Marginal Bone Loss

The design of a dental implant plays a crucial role in maintaining stability and preserving marginal bone. Essential design features such as implant geometry, thread pattern, surface texture, and platform configuration dictate the distribution of mechanical forces and the biological response at the bone-implant interface over time.

a) Implant Surface Texture

The texture of implant surfaces, their material composition, and both macro- and micro-geometries directly affect peri-implant bone remodelling and tissue integration.

Implants with moderately rough surfaces, such as sandblasted or acid-etched surfaces, have been linked to improved bone-implant contact (BIC) and enhanced soft-tissue adhesion (Albrektsson & Wenneberg, 2004). The incorporation of micro- and nanotopography increases the surface area available for cellular adhesion, including osteoblast activity, thereby promoting better bone integration. This process contributes to quicker and more robust osseointegration; however, it may also raise the risk of bacterial colonisation if the implant is exposed (Albrektsson & Wennerberg, 2004). A detailed examination of the surface topography of implant fixtures will be thoroughly addressed in the forthcoming section on implant biomaterials.

In addition to enhancing surface topography to improve bone-to-implant interaction, considerable attention has been devoted to modifying the implant neck surface, which influences peri-implant soft and hard tissue responses. The implant collar or neck region acts as the essential interface between prosthetic components and biological tissues. Its surface topography affects the nature of epithelial and connective tissue attachment, bacterial colonisation, and marginal bone maintenance (Canullo et al., 2020). Advances in implant design increasingly emphasise bioactive or topographically enhanced surfaces for better outcomes. Surface modifications, including smooth, microgrooved (Rompen, 2012), laser-treated (Ahamed et al., 2021), and micropore textures (Mangano et al, 2018), influence tissue integration, collagen fibre orientation, and resistance to bacterial colonisation. While smooth surfaces are hygienic, they provide weak biological sealing. The microgrooved and laser-treated collars enhance soft-tissue integration, while the porous necks offer exceptional potential for osseointegration, promoting bone and soft-tissue ingrowth. At the same time, porous surfaces pose challenges for hygiene and inflammation control when exposed (Mangano et al., 2018; Rompen, 2012).

b) Implant Geometry and Thread Design

Compressive forces positively influence bone tissue by enhancing bone density and improving strength. In contrast, tensile and shear forces can weaken bone, with shear forces being the least advantageous (Misch et al., 2008). The forces produced vary with implant geometry and thread configurations; therefore, an optimal implant design must balance compressive and tensile forces while minimising shear forces (Abuhussein et al., 2010). For instance, tapered implants tend to distribute force more

uniformly than cylindrical implants, which create higher stress in the crestal and apical regions (Gehrke et al., 2016). In cases where bone quality is favourable and primary stability is readily achieved, specific implant design features may not play a crucial role in the overall success of the procedure. However, when primary stability is compromised due to factors such as poor bone quality or elevated occlusal stresses, certain design modifications may be advantageous. Utilising implants with a smaller pitch, additional threads, deeper threads, a reduced thread helix angle, a longer length, or a wider diameter can enhance the surface area in contact with the surrounding bone, thereby improving stability and promoting successful outcomes (Abuhussein et al., 2010; Ao et al., 2010; Dos Santos et al., 2011; Insua et al., 2023).

Apart from primary stability, the design of threads significantly impacts how occlusal forces are transmitted to the surrounding bone. Research indicates that variations in thread pitch, depth, shape, and angle can significantly influence peri-implant bone preservation and the long-term health of adjacent tissues (Abuhussein et al., 2010). Implants featuring deeper threads and a tapered design tend to reduce peak stress concentrations at the crestal bone level (Abuhussein et al., 2010; Gehrke et al., 2016; Kreve et al., 2024). V-shaped and square threads are known to mitigate stress concentrations compared to thinner, narrower square threads, particularly in cancellous bone, thereby aiding in the preservation of marginal bone (Abuhussein et al., 2010). Cortical bone does not exhibit significant variation among thread designs. Unfortunately, V-shaped threads can concentrate stress at the thread apex, whereas square threads distribute stress more evenly (Al-Sanea et al., 2023).

Thread designs may enhance the adaptation of epithelial and connective tissues, potentially leading to a more effective biological seal (Berglundh et al., 2003). In contrast, aggressive thread designs could induce micro-movements at the bone crest, interfering with the biological width and accelerating bone remodelling (Abuhussein et al., 2010). Macro-designs incorporating microthreads are particularly effective at maintaining peri-implant bone levels, especially during the early healing phase (Akkocaoglu et al., 2005). Improper thread geometry can lead to surgical trauma or uneven load distribution, increasing the risk of peri-implantitis in susceptible patients.

c) Implant-Abutment Connection

In addition to other factors discussed earlier, the implant-abutment interface plays a pivotal role in both biomechanical stability and peri-implant bone preservation. Two critical yet distinct components at this interface are the implant-abutment platform and the implant-abutment connection. The platform refers to the horizontal surface at the coronal end of the implant where the abutment is seated, and its configuration, whether platform-matched (PM) or platform-switched (PS), significantly influences crestal bone preservation. In contrast, the implant-abutment connection refers to the internal or external mechanical geometry that joins the implant and abutment. Both the platform and the abutment connection influence microbial sealing, load transmission, and joint stability. Advancements in both platform design and connection types have been driven by the goal of minimising marginal bone loss (MBL), reducing mechanical complications, and optimising peri-implant soft tissue outcomes.

The distinction between platform switching (PS) and platform matching (PM) is based on the diameters of the implant platform and the abutment. In PM, the abutment and implant platform have the same diameter, resulting in no horizontal offset; thus, the abutment fits flush against the implant shoulder. In PM, the microgap is situated at the implant's edge, nearer the bone, which could allow inflammatory responses from the microgap to affect the crestal bone, potentially causing increased bone remodelling or loss.

Whereas PS refers to an abutment with a smaller diameter than the implant platform. This adjustment in the implant-abutment connection creates a horizontal shift, moving the junction inward from the edge of the implant platform. This strategy helps to maintain the microgap by relocating the implant-abutment interface inward, away from the crestal bone, and alleviating mechanical stress on the bone-implant interface (Atieh et al., 2010; Chrcanovic et al.,2015). Thus, inflammatory cells are kept away from the bone crest, which, in turn, helps preserve crestal bone levels. When paired with subcrestal placement, this technique is thought to be more effective in preserving bone by minimising horizontal stress transmission. Additionally, it enhances prosthetic adaptability and improves the emergence profile. As a result, the peri-implant tissue can establish a more stable biological width (Blanco et al., 2017).

A FEA study by Liu et al. (2014) demonstrated that PS reduced stress at the crestal bone, supporting clinical observations of improved marginal bone preservation

(Blanco et al., 2017; Maceiras et al., 2024). PS in subcrestal implants results in a more apically located connective tissue zone and a more coronal bone crest than platform-matched configurations (Canullo et al., 2016).

Clinical trials have reinforced these biomechanical and histological observations. PS significantly reduced MBL compared to platform matching (PM), with a mean difference of approximately 0.3 mm (Atieh et al., 2010), resulting in a reduction of approximately 0.6–1.2 mm at 5–10 years versus PM (~1.1–1.3 mm) (Tomar et al., 2025). When stratified by placement depth, the benefit was more pronounced in subcrestally placed implants, particularly during the first year of loading (Atieh et al., 2010). This aligns with other findings indicating that PS implants significantly better preserve the mesial marginal bone and reduce biomechanical loading on the peri-implant bone compared with PM implants (Canullo et al., 2016; Liu et al., 2014; Tomar et al., 2025). In a systematic review, subcrestal implants with platform switching exhibited less marginal bone loss (MBL) than equicrestal implants without platform switching, suggesting a combined protective effect (Pellicer-Chover et al., 2019).

The characteristics of the implant-abutment connection significantly influence the positioning of microgaps, stability, load distribution, and seal integrity. The external hex design, used in an early implant system, connects the abutment to the implant via a hexagonal interface, offering improved handling but also increasing stress at the crestal bone level. This heightened stress increases the likelihood of screw loosening, microgaps, and micromovements at the junction, which can lead to bacterial infiltration and subsequent bone loss (Liu & Wang, 2017).

In contrast, modern internal conical connections reduce the microgap size, improve joint stability, and minimise bacterial leakage (Jansen et al., 1997). The internal hex design, for example, allows the abutment to fit into the implant fixture via a hexagonal interlock, thereby improving mechanical stability, promoting uniform stress distribution, reducing the risk of screw loosening, and providing a superior microbial seal (Bozkaya & Müftü, 2003). On the other hand, Morse taper (conical) connections employ a friction-fit tapered interface. Comprehensive analyses, including finite element assessments, animal studies, and clinical outcomes, suggest that Morse taper connections demonstrate superior biomechanical engagement, reduced micromovement, and enhanced marginal bone stability (Canullo et al., 2016; Macedo et al., 2018; Schmitt et al., 2014).

2.8.4.3 Prosthetic and Biomechanical Factors

a) Emergence Profile and Crown Contour

Inappropriate prosthetic contours can eliminate the papilla, leading to tissue collapse and marginal inflammation (Tarnow et al., 2000). Any excessively convex or non-anatomical emergence profile creates soft tissue pressure that disrupts the mucosal seal and hinders effective oral hygiene, thereby promoting plaque accumulation and inflammation. In cantilevered prostheses, excessive cantilever length, particularly when associated with improper implant angulation, significantly increases bending moments on implants, resulting in greater peri-implant stress and associated bone loss (Berzaghi et al., 2025; İleri et al., 2025). Furthermore, a microgap resulting from prosthetic misfit at the implant–abutment interface exacerbates the condition, serving as a nidus for microbial infiltration. This colonisation can lead to chronic inflammation and crestal bone loss (Jansen et al., 1997). Simultaneously, even small misfits can generate continuous microstrain that cumulatively leads to bone remodelling and resorption.

When a functional occlusal load is applied to an implant, it triggers the remodelling of the adjacent alveolar bone. A light load initiates a response that enhances bone remodelling and the development of reactive woven bone. In contrast, excessive loading can cause microfractures that promote osteoclastogenesis (Elsayed, 2019). If the capacity for bone remodelling cannot keep pace with microdamage, these minor defects accumulate and eventually merge into larger ones. Consequently, these larger defects may be filled with fibrous tissue and microorganisms (Hämmerle & Tarnow, 2018). Significant bone loss can ultimately ensue, reducing the bony support around the implant and increasing the likelihood of implant failure (Hämmerle & Tarnow, 2018). Any excessive mechanical forces from parafunctional habits, such as bruxism or poor occlusion, can place stress on the bone–implant interface, disrupting the balance between bone formation and resorption (Elsayed, 2019; Hämmerle & Tarnow, 2018). This stress may result in bone remodelling, microfractures, and weakened soft tissues, inducing marginal bone loss without signs of infection. A summary of implant factors affecting peri-implant soft and hard tissues is shown in Figure 2.19.

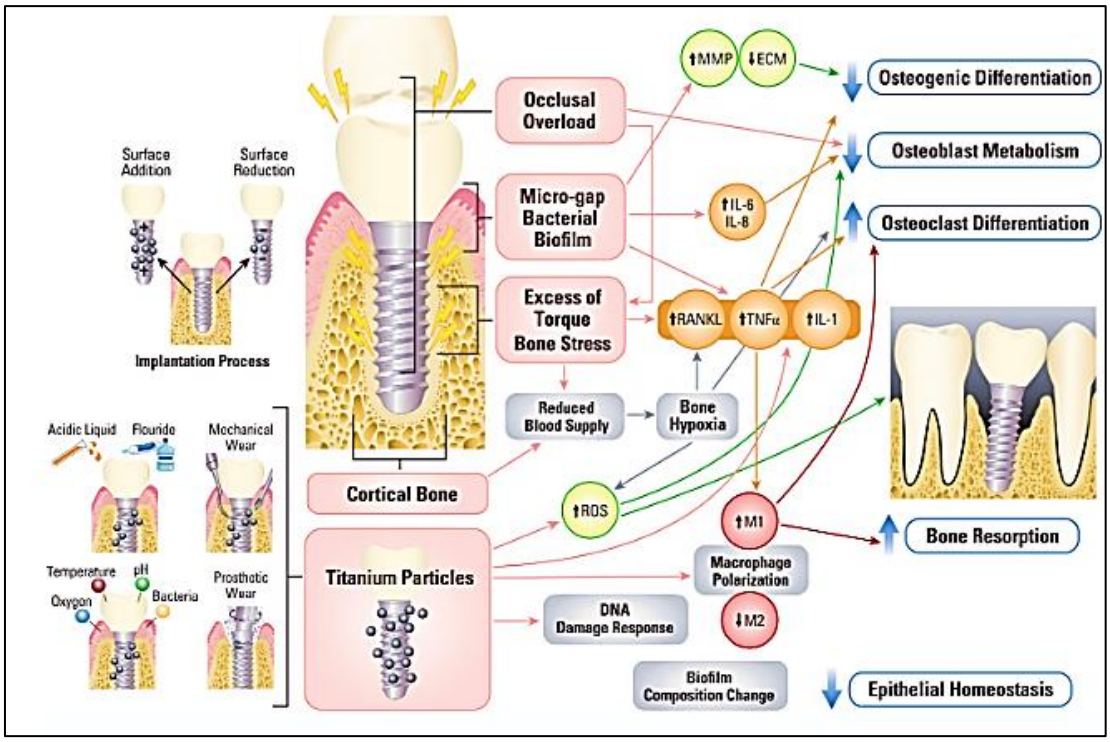

Figure 2.19 Implant Factors Affecting Hard and Soft Peri-implant Tissue Response (Insua et al., 2023)

2.8.4.4 Host-Related Factors Affecting Peri-Implant Tissue (PIT)

The integrity and longevity of peri-implant tissues (PIT) are crucial for the success of dental implants. While surgical and prosthetic factors are often the primary focus in implant planning, host-related factors significantly influence healing dynamics, osseointegration, and the risk of peri-implant diseases. Local factors, including soft tissue thickness and keratinised tissues, systemic health conditions, behavioural habits, genetic predispositions, and immunological competence, can modulate the host response to implants and affect outcomes. Recognising and managing these variables is essential for reducing biological complications and enhancing implant survival.

a) Local Factors - Soft Tissue Thickness and Marginal Bone Loss

As previously mentioned regarding the anatomy and biology of the PIT, the thickness of peri-implant soft tissue plays a crucial role in influencing marginal bone levels. Thicker mucosal tissue (>2 mm) helps maintain crestal bone by providing enhanced protection, reducing inflammation, and improving long-term stability. In contrast, thinner tissue often triggers bone remodelling as the body works to re-establish

the biological width required for a stable soft-tissue seal. Likewise, the width and presence of keratinised mucosa (KM) surrounding implants are linked to the preservation of marginal bone. KM contributes to a stable mucosal seal and provides resistance against mechanical and microbial threats. Sufficient KM (≥ 2 mm) promotes better plaque control, lowers inflammation, and minimises marginal bone resorption. Conversely, a lack of KM leads to increased marginal bone loss (MBL), heightened inflammation, and greater patient discomfort.

b) Systemic Health Conditions

Systemic diseases such as uncontrolled diabetes mellitus and habits like smoking impair microvascular function, collagen synthesis, and immune response. This leads to increased susceptibility to infection and delayed wound healing. Summary of the potential effect of systemic diseases on wound healing following implant placement, as in Table 2.19.

Table 2.19
Significant Systemic Factors Affecting Peri-implant Tissue Healing

Systemic Factor	Key Findings	Clinical Implications	References
Diabetes Mellitus	3× increased risk of peri-implantitis in poorly controlled diabetics. Impaired healing, increased MBL, and higher peri-implantitis prevalence	Strict glycemic control is recommended (HbA1c <7%).	Chrcanovic et al., 2014; Monje et al., 2017
Smoking	Vasoconstriction, reduced healing, increased bone loss, increased bone loss, deeper pockets, and failure rate.	Smoking cessation is crucial for pre- and post-implant therapy.	Chrcanovic et al., 2015; Costa et al., 2022
History of Periodontitis	2–4× higher peri-implantitis rate than healthy individuals.	Manage periodontitis before implant placement.	Chrcanovic et al., 2014; Schwarz et al., 2018
Obesity/Metabolic Syndrome	Linked with elevated inflammatory cytokines affecting healing.	Monitor systemic inflammation and stress, as well as oral hygiene.	De Oliveira et al., 2020

Systemic Factor	Key Findings	Clinical Implications	References
Alcohol Consumption	Higher peri-implantitis risk in chronic users.	Assess alcohol use in medical history.	Guabello et al., 2023
Osteoporosis / Anti-resorptive	Reduced bone quality, potential MBL, bisphosphonate-related complications of MRONJ with bisphosphonates/ denosumab use.	Avoid IV bisphosphonates; coordinate care with a physician.	Guabello et al., 2023; Otomo-Corgel, 2012; Stavropoulos et al., 2018;
Cardiovascular Disease (CVD)	CVD and hypertension increase inflammation, affecting PIT.	Comprehensive medical evaluation is advised.	Monje et al., 2023; Orlandi et al., 2024; Ustaoglu & Erdal, 2020;
Autoimmune Disorders or immunocompromised	RA, lupus may impair healing and immune regulation. Higher infection risk, impaired soft tissue defence	Careful monitoring and interdisciplinary care.	Chitumalla et al., 2025; Esimekara et al., 2022; Hyldahl et al., 2024
Genetic Polymorphisms	Altered cytokine expression, increased inflammatory response		Januzzi et al., 2024
Medications (PPIs, SSRIs)	Associated with impaired osseointegration in some reviews.	Evaluate long-term medication effects during planning.	Chawla et al., 2022; Kotsailidi et al., 2023;

Notes: MRONJ: Medication-related osteonecrosis of the jaw, such as bisphosphonates; PPI: proton pump inhibitors such as omeprazole, esomeprazole, pentoprazole; SSRI: Selective serotonin reuptake inhibitors such as Fluoxetine, Sertraline, citalopram.

2.8.5 Healthy vs Pathological Changes of Peri-Implant Tissue

In oral implantology, pathological alterations in peri-implant tissue (PIT) are primarily caused by peri-implant infectious diseases (PIIDs), ranging from reversible inflammation of the peri-implant mucosa to irreversible loss of supporting bone. The two main entities, peri-implant mucositis (PIM) and peri-implantitis (PI), are primarily caused by bacterial biofilm accumulation, often exacerbated by mechanical and systemic risk factors. Clinically, their presentation can resemble gingivitis and periodontitis due to overlapping risk factors.

Histologically, peri-implantitis is characterised by ulcerated epithelium and inflammatory infiltrates (Lindhe & Meyle, 2008). The summary of precipitating and

aggravating factors in the development of PIIDs is illustrated in Figure 2.20, adopted from Pokrowiecki et al. (2017). The subsequent tables present a comparison of clinical presentations between healthy and diseased peri-implant tissue (Table 2.20), along with a table summarising the aetiologies, clinical presentations, associated microbial pathogens, and histological findings of PIIDs (Table 2.21).

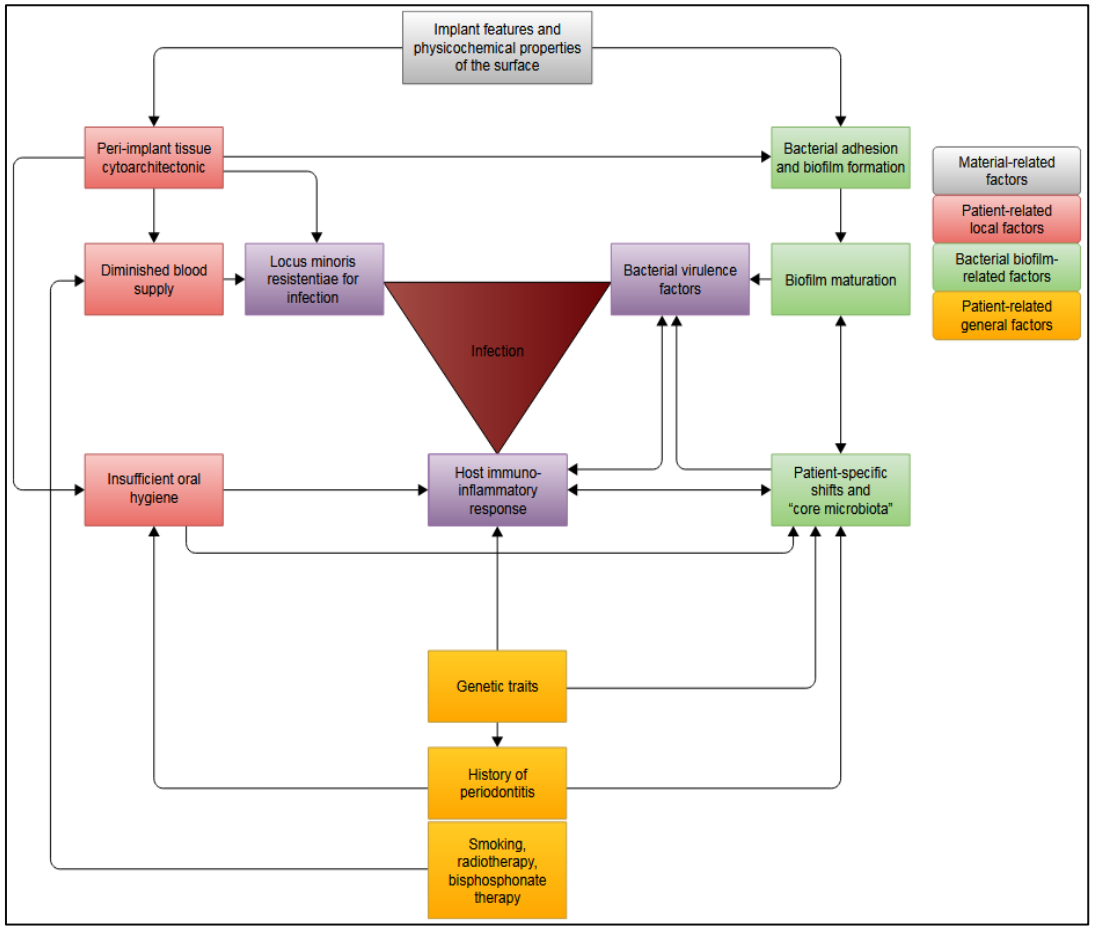

Figure 2.20 Factors Influencing Peri-Implant Diseases.

Notes: The characteristics of implants significantly influence the immunological responses observed in peri-implant tissues and facilitate bacterial infiltration, predominantly due to the compromised nature of the peri-implant tissue (PIT). Moreover, smoking diminishes blood flow within the peri-implant capillaries, thereby heightening the risk of infection. Additionally, inadequate hygiene practices and a pertinent history of "periodontitis" represent substantial risk factors for the manifestation of peri-implant infectious diseases (PIIDs). Furthermore, genetic factors may modulate the host's immunoinflammatory response, leading to individual variations in the oral biofilm**.** The probability of infection occurring at the implant–tissue interface is significantly increased when these three primary components coalesce concurrently (Pokrowiecki et al., 2017).

Table 2.20
Healthy vs Diseased Peri-Implant Tissue (Comparison of Healthy Peri-Implant Tissue, Peri-Implant Mucositis (PIM), and Peri-Implantitis (PI))

Parameter	**Healthy Peri-Implant Tissue**	**Peri-Implant Mucositis (PIM)**	**Peri-Implantitis (PI)**
Definition	Stable, inflammation-free tissue around a functional implant	Inflammation of the peri-implant mucosa without bone loss	Inflammation of the peri-implant mucosa with progressive bone loss
Tissue Involvement	Peri-implant mucosa only (no inflammation)	Soft tissue only	Soft and hard tissues
Clinical Signs	Normal colour (pale pink), firm and well-adapted gingiva, no swelling, or BOP	Redness, swelling, BOP	BOP, suppuration, possible mobility
Probing Depth	1–3 mm (varies by biotype and implant type)	Increased, but no attachment loss	≥ 6 mm
Bleeding on Probing (BOP)	Absent	Present	Present
Suppuration	Absent	Absent or minimal	Often present
Radiographic Bone Loss	None after initial remodelling	No bone loss	Progressive bone loss beyond initial remodelling
Histopathology	Minimal inflammatory infiltrate; intact epithelium and bone	Inflammatory infiltrate in connective tissue (plasma cells, lymphocytes)	Apical epithelial migration, granulation tissue, and bone resorption
Common Pathogens	Commensals: *Streptococcus spp., Actinomyces spp.*	*F. nucleatum, P. intermedia, P. gingivalis*	*P. gingivalis, T. forsythia, T. denticola, A. actinomycetemcomitans*
Reversibility	Not applicable	Yes, if addressed early	No, requires surgical and regenerative interventions
Treatment Approach	Routine hygiene and maintenance	Mechanical debridement, antiseptics, and hygiene reinforcement	Mechanical + surgical debridement, antibiotics, regenerative therapy

Table 2.21
Aetiology, Clinical and Histological Presentations of Peri-Implant Tissue Pathologies

Peri-Implant Pathology	Primary Aetiology	Clinical Presentation	Histological Findings	Common Pathogens	References
Peri-Implant Mucositis (PIM)	Inadequate maintenance i.e., poor oral hygiene, smoking, poor prosthetic design	Bleeding on probing (BOP) Erythema Edema No radiographic bone loss	Infiltration of inflammatory cells (predominantly lymphocytes and plasma cells) into intact bone. Intact junctional epithelium	*Streptococcus spp.* *Fusobacterium nucleatum* *Prevotella intermedia* *Porphyromonas gingivalis*	Berglundh et al., 2024; Heitz-Mayfield 2018;.
Peri-Implantitis	Persistent bacterial biofilm Residual cement Excessive biomechanical occlusal overload Implant surface contamination Systemic disease (e.g., diabetes)	BOP and/or suppuration Deep probing depths (≥ 6 mm) Radiographic MBL Implant thread exposure	Apical migration of epithelium, granulation tissue, and fibrosis Dense inflammatory infiltrate (neutrophils, plasma cells, macrophages) Osteoclast activation and bone resorption	*Porphyromonas gingivalis* *Tannerella forsythia* *Treponema denticola* *Aggregatibacter actinomycetemcomitans* *Fusobacterium spp.*	Berglundh et al.,2024; Heitz-Mayfield & Salvi,. 2018
Retrograde Peri-Implantitis	Contamination of the implant surface by residual endodontic lesion, bone overheating during implant placement	Pain with or without swelling, Periapical radiolucency, No MBL bone loss Early post-op symptoms	Apical inflammatory infiltration (Neutrophils) Necrotic bone Absence of MBL	*Klebsiella penumaniae* *Streptococcus spp.* *Porphyromonas gingivalis* *Corynecbacterium*	Marshall et al., 2019
Implant-Related Cysts (E.G., Implant Periapical Lesion)	Residual cysts Apical trauma during placement Infection of pre-existing lesions	Asymptomatic or swelling Radiolucent periapical lesion Implant mobility (late)	Lining epithelium (in cysts) Chronic inflammatory cells May mimic odontogenic cyst histology		Marshall et al., 2019
Titanium Particle-Induced Osteolysis Or Foreign Body Reaction (FBR)	Microparticles from the implant abutment friction, Titanium or metal debris (e.g., from drills) Corrosion products or surface wear	May have no apparent symptoms early progressive bone loss Radiographic changes Persistent inflammation Non-healing pocket or fistula Implant failure without infection	Presence of titanium particles in peri-implant tissue, Multinucleated giant cells (MNGCs). Chronic macrophage infiltration Bone resorption around particles, Fibrosis around debris particles Non-infectious granulomatous response		Chen et al., 2023; Mombelli et al., 2018; Suárez-López del Amo et al., 2018;

2.8.6 Peri-Implant Tissue (PIT) Assessment

The assessment of peri-implant tissue (PIT) is essential for ensuring the long-term success and health of dental implants. Unlike natural teeth, dental implants lack a periodontal ligament and mainly rely on osseointegration for stability. This makes the early detection of soft tissue inflammation and marginal bone loss critical. Regular evaluation of peri-implant tissues allows clinicians to identify early signs of peri-implant diseases such as mucositis and peri-implantitis, guiding timely interventions and maintaining implant longevity.

2.8.6.1 Importance of Peri-Implant Tissue (PIT) Assessment

The primary goal of PIT assessment is to identify any signs of inflammation or bone loss around dental implants before they progress to irreversible damage. The objectives include monitoring soft tissue health, assessing the stability of bone levels, and evaluating the integrity of the peri-implant biological seal. Timely diagnosis helps to prevent peri-implantitis, which is a leading cause of implant failure.

The objectives of the PIT assessment include:

i. Early diagnosis of peri-implant diseases (mucositis and peri-implantitis)
ii. Monitoring soft tissue integrity and keratinised mucosa
iii. Assessing marginal bone level stability over time
iv. Evaluating implant success and guiding treatment decisions
v. Preventing irreversible bone loss through proactive care

2.8.6.2 Methods of Peri-Implant Tissue Assessment

The long-term success of dental implants is influenced not only by osseointegration but also by the stability and health of the surrounding peri-implant tissues. These tissues, comprising both soft and hard components, are essential for maintaining a biological seal, preventing microbial invasion, and supporting the functional and aesthetic aspects of the

implant. Given their significance, it is crucial to conduct systematic and periodic assessments of peri-implant tissues for the early detection of pathological changes, such as peri-implant mucositis and peri-implantitis, which could lead to implant failure if left unmanaged.

A variety of diagnostic tools and clinical protocols are available for evaluating peri-implant health. These methods range from simple clinical indices and probing techniques to advanced radiographic imaging and molecular analyses. Each approach presents distinct advantages and limitations regarding accuracy, invasiveness, cost, and clinical practicality. Integrating multiple assessment tools often yields a more comprehensive understanding of the biological status of the implant.

This section outlines the current methods for assessing peri-implant tissues, detailing their principles, strengths, weaknesses, and relevance in both routine practice and research. A summary of these methods is presented in Table 2.22.

a) Clinical Methods

Clinical evaluation includes probing depth (PD), bleeding on probing (BOP), plaque index, and suppuration. These assessments are typically performed during regular maintenance visits using either plastic or metal periodontal probes. Gentle probing (≤0.25N) is advised to prevent trauma to the peri-implant tissues.

b) Radiographic Methods

Standardised periapical radiographs are used to evaluate marginal bone levels (MBL) around implants. Cone-beam computed tomography (CBCT) provides detailed three-dimensional imaging and is useful in complex cases. Annual radiographic assessments are recommended to monitor changes in bone support over time.

c) Biochemical and Microbiological Methods

Peri-implant sulcular fluid (PISF) analysis and microbiological testing can offer insights into the inflammatory and microbial status of the peri-implant tissues. These methods are more common in research or specialist settings due to their cost and technical requirements.

d) Mechanical Methods

Implant stability can be assessed using resonance frequency analysis (e.g., ISQ) or Periotest. These tools help evaluate osseointegration and guide loading protocols, especially in immediate or early loading scenarios.

Table 2.22
Methods for PIT Assessment

Method	Pros	Cons
Probing Depth (PD) & BOP	Simple, non-invasive, inexpensive; detects early inflammation (Coli & Sennerby, 2019; Monje & Salvi, 2024; Monje et al., 2021;)	May underestimate PD; force-sensitive; needs skill (Coli & Sennerby, 2019)
Plaque Index	Easy to perform; indicates oral hygiene status (Mombelli & Lang, 1998)	Subjective; does not reflect subgingival biofilm (Mombelli & Lang, 1998)
Suppuration	Confirms infection presence; quick to observe (Buser et al., 1997; Monje & Salvi, 2024;)	May not be present in early disease; subjective (Heitz-Mayfield & Lang, 2010)
Periapical Radiograph	Objective bone loss measurement; easy to standardise (Monje & Salvi, 2024)	2D image; no buccal/lingual info; technique sensitive (Brägger et al., 2004)
CBCT	3D imaging of all bone surfaces; detects buccal/lingual bone loss (Bornstein et al., 2014; Monje & Salvi, 2024)	Higher radiation, costly, not for routine use.

Method	Pros	Cons
PISF Biomarker Analysis	Early inflammation marker detection, a non-invasive method for early diagnosis, monitoring and personalised treatment, useful in research (Lumbikananda et al., 2024; Rakic et al., 2014)	Not routine; cost and lab need limit use, require standard sample collection method and storage for reliability, may be misinterpreted with certain local (smoking, periodontitis) and systemic (DM or other chronic inflammation diseases) (Lumbikananda et al., 2024; Rakic et al., 2014)
Microbiological Sampling	Identifies specific pathogens; aids targeted treatment (Anitua et al., 2024)	Costly; microbial communities depending on sampling technique, mixed up with normal oral microbiota, lab time required (Anitua et al., 2024)
ISQ (Resonance Frequency)	Non-invasive; quantifies stability; repeatable over time (Meredith, 1998)	
Periotest	Provides a numeric stability value; quick and easy (Olivé & Aparicio, 1990)	

2.8.7 Patient-centred Outcomes as an Additional Tool Measuring Treatment Outcome

Implant-supported prostheses have emerged as the preferred treatment modality for restoring missing teeth, owing to their favourable long-term outcomes, functional effectiveness, and aesthetic appeal. While traditional indicators of dental implant success, such as implant survival rates, marginal bone levels, and peri-implant conditions, are significant, they do not encompass the full spectrum of patient experiences and expectations. A considerable gap exists between how clinicians and patients define success. Clinicians tend to measure prosthetic performance against technical standards; however, these criteria often overlook patients' unique needs, attitudes, and expectations. In contrast, patients typically prioritise aesthetics and comfort, often overlooking other critical clinical factors (Zavanelli et al., 2017). Failing to meet patients' expectations may lead to significant psychosocial challenges, including anxiety, feelings of insecurity, and reduced self-esteem (Cibirka et al., 1997). Consequently, patient satisfaction is crucial for achieving a successful treatment outcome (Zarb & Albrektsson, 1998). This is where patient-centred

outcome measures come into play, offering a pathway to more tailored and satisfying prosthetic solutions in modern implantology.

The oral health-related quality of life (OHRQoL) captures individuals' perceptions of orofacial disorders and dental treatments (John, 2021). The concept of OHRQoL encompasses various dimensions of oral health, influenced by biological, psychological, and social factors. This aligns with the World Health Organisation's broad definition of health, which covers overall physical, mental, and social well-being (Locker & Allen, 2007). There is a growing trend towards integrating patient-reported outcome measures and prosthesis-related factors alongside clinical success when evaluating treatment efficacy and patients' overall quality of life (Yusof et al., 2016). Two validated patient-reported outcomes, including the Oral Health Impact Profile (OHIP) and the Patient Satisfaction Questionnaire (PSQ), were used to gauge overall quality of life and subjective satisfaction, respectively (Yusof et al., 2016; Layton & Walton, 2011).

2.8.7.1 OHIP-14 and Patient Satisfaction Questionnaire (PSQ) as a Tool in Implant Dentistry

The OHIP is a validated tool commonly utilised to assess the pre- and post-treatment effects of oral health on overall quality of life by subjectively evaluating how prostheses affect patients' daily activities, social interactions, pain, and psychological health. It stands out as the gold standard among OHRQoL instruments and is widely recognised for its sophistication and comprehensiveness (Su et al., 2021). Created by Slade and Spencer in 1994, the original OHIP consisted of 49 items (OHIP-49) based on patient interviews and targeted seven essential domains outlined in Locker's model: functional limitation, physical pain, psychological discomfort, physical disability, psychological disability, social disability, and handicap (Slade & Spencer, 1994). The OHIP-14, introduced by Slade in 1997, provides a more concise and reliable method for measuring these dimensions (Slade, 1997). This tool is extensively used worldwide and has been translated into several languages, confirming its cross-cultural equivalence. This includes Saub (2005), who worked to establish the reliability and validity of the adaptation for the Malaysian population, known as OHIP-14 (M) (Saub et al., 2005).

The assessment employs a 5-point Likert scale ranging from "never" to "very often". A low OHIP-14 score post-treatment indicates better perceived oral health and satisfaction. Patient satisfaction with implants is multifactorial, often overlapping with the OHIP-14 domains, and is influenced by clinical, psychological, and aesthetic factors. The OHIP-14 is increasingly utilised as a measurable tool in implantology to assess patients' OHRQoL (Lang & Zitzmann, 2012; Manfredini et al., 2024; Nickening et al., 2016; Yunus et al., 2013).

In contrast, the PSQ concentrates on treatment-specific metrics, evaluating patient satisfaction across various dimensions of dental care and treatment outcomes (Lim & Ariff, 2020; Dong et al., 2019). This emphasis makes it particularly useful for assessing treatment outcomes based on factors such as implant appearance, masticatory performance, hygiene practices, costs, and overall satisfaction with the institution's treatment.

Patient satisfaction has become a crucial factor in evaluating treatment success in dentistry (Dong et al., 2019). The Patient Satisfaction Questionnaire (PSQ) addresses the limitations of Oral Health-Related Quality of Life (OHRQoL) measures, as these may not accurately reflect patient satisfaction with prosthetic devices. Satisfaction is typically gauged using a Likert scale ranging from "strongly disagree" to "strongly agree," with higher scores indicating greater satisfaction (Layton & Walton, 2011).

Research indicates a direct correlation between patient satisfaction and the quality of oral care received (Lim & Ariff, 2020). Furthermore, satisfaction levels are also influenced by factors such as pre-treatment expectations, age, gender, and previous dental experiences. Despite the importance of understanding patient satisfaction following dental implant rehabilitation, research in this area remains limited (Lang & Zitzmann, 2012). Employing both the Oral Health Impact Profile (OHIP) and the PSQ can yield valuable insights into patient-centred outcomes in implant therapy.

Furthermore, psychological predispositions and socio-economic status may influence perceived treatment outcomes. Katsoulis et al. (2011) found that individuals with realistic expectations reported higher satisfaction and greater reductions in OHIP-14 scores. This highlights the necessity for clear communication and managed expectations in dental care to improve patient satisfaction.

2.9 Early Dental Implant Failure

Osseointegrated oral implants have been in use for over five decades (Buser et al., 2016; Albrektsson & Wenneberg, 2019). While dental implants exhibit long-term survival rates exceeding 85 % over 25 years of placement in turned surfaces, and 95 % of moderately rough surfaces in 10 years (Jemt, 2019), failures still happen (Chranovic et al., 2016; Esposito et al., 1999; Malm et al., 2018; Wahbelrg et al., 2025). Clinical evidence indicates that the overall implant failure rate was 2.21%, while the early failure rate was 1.56% (Tobias et al., 2025). Nonetheless, systematic reviews and cohort studies indicate an overall failure rate of about 3% to 5% over 5 to 10 years (Jung et al., 2012).

Early failure remains a significant clinical concern, as a substantial percentage of these devices are lost within the first six months after placement, before the implant is loaded (Chranovic et al., 2015; Esposito et al., 1999; Wåhlberg et al., 2025). Early implant failure primarily results from the formation of fibrous scar tissue and ongoing inflammation (Abrishami et al., 2023), which interfere with osseointegration and can lead to implant mobility or loss (Esposito et al., 1999). Conversely, late failures occur after successful bone integration, usually due to mechanical problems or peri-implant diseases (Jemt, 2019).

2.9.1 Prevalence and Factors of Early Implant Failure

Rates of early implant failure vary widely across studies (Wåhlberg, 2025). Reports indicate that at the patient level, failure rates range from 1.6% to 3.7%, and at the implant level, from 1.2% to 2.4%, based on 6,113 implants placed in 3,785 patients (Wu et al., 2021). More detailed data from retrospective studies of single implants show that the rate of early failure can be as high as 4.4% at the implant level (Kang et al., 2019) and 6.68% (Mohajerani et al., 2017). This variability underscores the complexity of the implant-body response and the numerous factors that may influence its success in the initial months.

A comparative analysis of two different periods, implants placed in 2007 versus those inserted in 2017, revealed a concerning increase in early failure rates. Specifically, the early failure rate was only 1.1% for implants from 2007, whereas the rate for those installed in 2017 was significantly higher at 2.4%, reflecting a 1.3% rise. This variation in

failure rates over time may be due to several factors. These include the rapid development and diversification of implant systems, the adoption of more varied surgical protocols and placement techniques, such as those used in cases with poor bone volume or in augmented bone, and varying levels of surgical experience (Wåhlberg et al., 2025; Wu et al., 2021).

For example, in implant dentistry, early systems mainly used commercially pure titanium (CP Ti) (Albrektsson et al., 1981). While CP Ti Grade 4 remains the standard, newer materials such as titanium-zirconium alloys (TiZr) are gaining popularity due to their higher strength, which allows for narrower implants (Wåhlberg et al., 2025). The macro design of implants has also improved to enhance primary stability, with the surface microstructure aimed at biological stabilisation. Different macro features, including tapered shapes, deeper threads, and longer implants, have been studied to improve stability by increasing bone-to-implant contact (Abuhussein et al., 2010; Gehrke et al., 2016; Kreve et al., 2024) and are often recommended for patients with poor bone quality (Gehrke et al., 2016; Kreve et al., 2024). These modifications apply not only to CP Ti but also to newer materials, influencing clinical outcomes at micro- and nanoscales (Albrektsson & Wennerberg, 2004; Albrektsson & Wennerberg, 2019; Wennerberg & Albrektsson, 2009), thereby affecting implant failure rates (Wåhlberg et al., 2025).

Furthermore, patient-related factors also play a vital role, such as smoking habits, impaired healing in patients with systemic diseases, infections, or a history of periodontitis. These are particularly concerning when comparing the current situation of early failure to the early years of dental implant use, when only a limited range of implant systems was available to practitioners.

2.9.2 Pathophysiology of Early Implant Failure

The process involved in placing dental implants is complex, involving a series of biological steps: 1. the formation of an initial blood clot and subsequent inflammation immediately after implant placement; 2. the recruitment of osteogenic cells and the formation of woven bone; and 3. a remodelling phase resulting in the development of lamellar bone. During this period, the implant bed is highly vulnerable, as the implant's primary stability often declines significantly before biological stability is established. The

body typically reacts in one of two ways: successful integration via osseointegration, in which a bony barrier forms to encapsulate the implant and establish a stable bond, or an immune response that may lead to fibrous encapsulation and potential implant rejection (Albrektsson et al., 2018). In cases of early implant failure, it is suggested that the failure results from wound healing dysregulation involving the innate immune system and persistent inflammation (Albrektsson et al., 2018; Babensee et al., 1998; Trindade et al., 2018).

Studies indicate that various factors influence early implant success and can also cause early failure. Local and systemic patient-related factors (Chrcanovic et al., 2016, 2015, 2014), surgeon skills and protocols (Jermt et al., 2016), and implant factors (Tomasi & Derks, 2022) are all important. These factors can lead to immune dysregulation, micromotion, infection, ischaemia, or unresolved inflammation, which disturbs the delicate osseous bed system. This disruption causes immune imbalances that weaken the bond between bone and implant (Albrektsson et al., 2018; Anderson & McNally, 2011; Babensee et al., 1998). Such issues hinder stable bone integration, often resulting in fibrous encapsulation of the implant (Albrektsson et al., 2018; Tomasi & Derks, 2022). A detailed overview of these factors and their mechanisms is provided in Table 2.23 and Figures 2.21 and 2.22.

Table 2.23
Pathophysiology in Early Implant Failure

Factor	Cause	Mechanism	References
Surgical Factors	Overheating of bone during drilling due to frictional heat or inadequate irrigation	• A 47°C exposure for 1 minute is sufficient to cause bone necrosis, and the temperature at which bone becomes irreparable is approximately 60°C for 1 minute, leading to thermal osteonecrosis and impairing osseointegration. • Surgery and overheating will traumatise tissues and cell surfaces, with the release of mediators (cytokines, oxygen radicals, lysosomal enzymes); these could produce a widening zone of necrosis with the presence of fibrous tissue at the interface	Ericksson & Albrektson, 1984; Kotsakis & Romanos, 2022; Er et al., 2018; Piattelli et al., 1998
	Inadequate primary stability, especially in low-density bone	• Micromovement > 50 – 100 μm	Chrconovic et al., 2015, Javed et al., 2013
	Contamination of the metal debris	• Friction between implant-bone, or surgical tool-bone, or corrosion due to exposure to biological fluid • cause metal debris or ion leaching into the peri-implant tissue	Bernabeu-Mira et al., 2020; Chen et al., 2023, Toledano-Serrabona et al., 2022
	Surgeon's experience, attitude and behaviour	• e.g, excessive trauma during surgery, improper angulation	Jemt et al., 2016
	Excessive IT	• Bone compression → local ischaemia, bone microfractures, necrosis→healing impairments	Antonacci et al., 2023
Patient-Related Factors:	Smoking	• impairs vascularisation due to arteriolar vasoconstriction and decreased blood flow, toxic by-products (nicotine, carbon monoxide, hydrogen cyanide) • inhibitory effect on osseogenesis	Alrowis et al., 2025; Chrcanovic et al., 2015; Costa et al., 2022
	Uncontrolled diabetes mellitus, postmenopausal estrogen therapy, head & neck radiation,	• Affects bone metabolism and immune response, delaying healing and decreasing bone quality.	Chrcanovic et al., 2014; Januzzi et al., 2024; King et al., 2016; Monje et al., 2017;

Factor	Cause	Mechanism	References
	genetic predispositions	• Impairment of single mucleotide polymorphisms → affects bone metabolisms & inflammatory cytokines especially if involve with IL-1, TNF-α	
	Existing periodontal disease	• Increases bacterial load and inflammatory risk	Chrconovic et al., 2015 Schwarz et al., 2018; Zhang et al., 2024
Implant-Related Factors:	Surface characteristics	• Influence protein adsorption and early cellular attachment. Too reactive surfaces may induce immune sensitisation	Hanawa et al., 2019; Wennerberg & Albrektsson, 2010
	Implant design and thread geometry	• Affect insertion torque and primary stability	Dos Santos et al., 2011; O'Sullivan et al., 2000.
	Titanium or any metal particles	• Affect immune response, causing periimplantitis	Schwarz et al., 2018

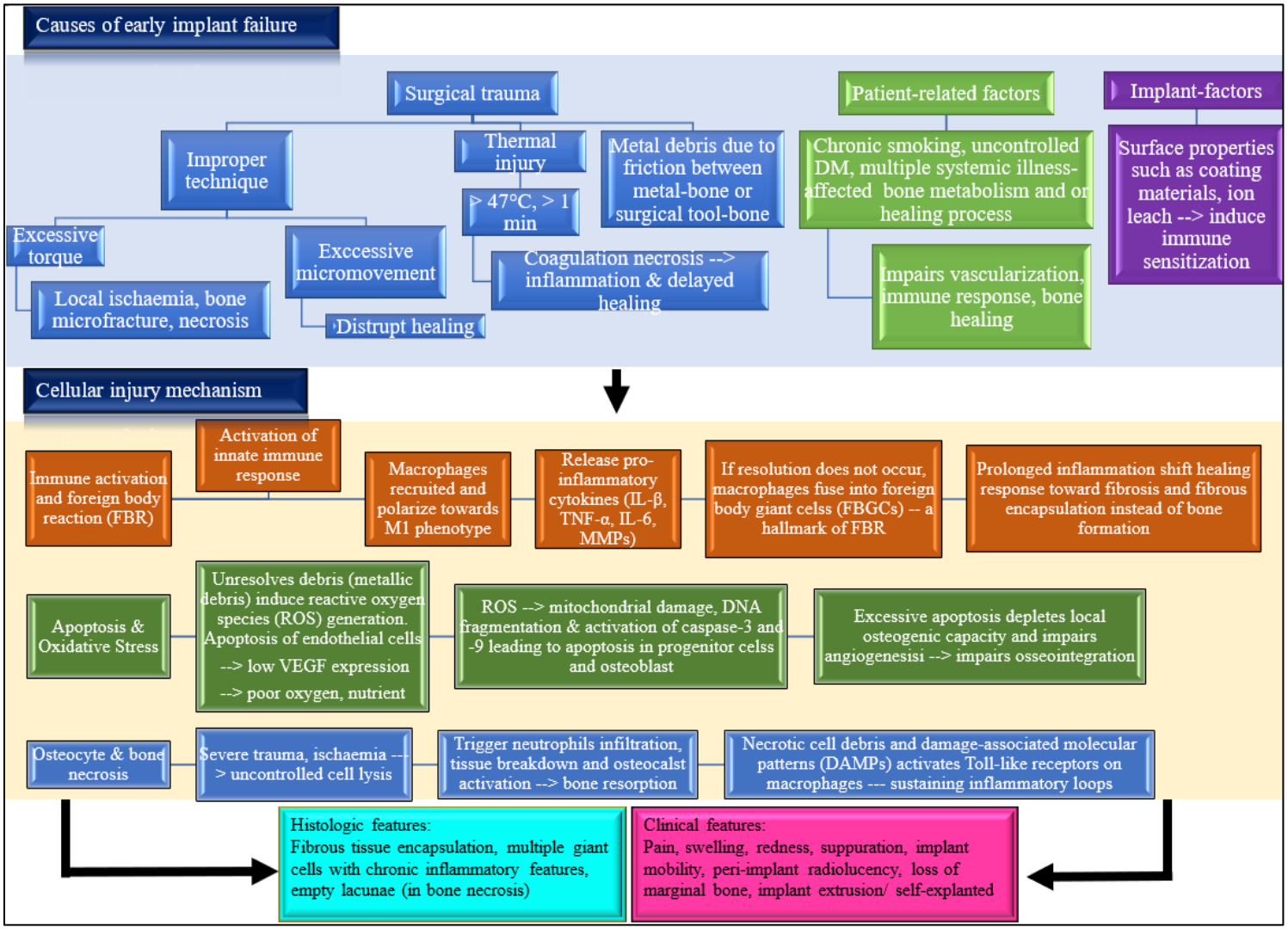

Figure 2.21 Summary of Causal Factors of Early Implant Failures, Cellular Injury Mechanism, with Histological and Clinical Presentations

2.9.3 Clinical Symptoms and Diagnostic Indicators

Early implant failure can often occur without any apparent symptoms. However, various clinical signs can provide crucial insights into potential complications. Pain, swelling, fistula, implant mobility, and peri-implant radiolucency are among the clinical signs indicating implant failure (Esposito, 1999; Piattelli et al., 1998). Additionally, auditory cues, such as dull sounds on percussion, can be observed (Esposito, 1999). One of the most concerning indicators is implant mobility prior to prosthetic restoration fitting, which can be detected using Periotest® or resonance frequency analysis (RFA). This mobility is typically observed when an abutment or transducer peg is engaged or disengaged during RFA on the implant (Esposito, 1999). Any movement detected at this stage may suggest insufficient integration with the surrounding bone, a phenomenon known as osseointegration.

However, clinicians should stay alert for signs of inflammation in the peri-implant soft tissues. From acute to chronic inflammation, an excessive inflammatory response can result in peri-implantitis. This may present with erythema (redness), noticeable swelling, and bleeding on gentle probing. Such inflammatory reactions might indicate infection or rejection and must be addressed swiftly to prevent further complications.

In chronic cases, increased osteoclast activity leads to significant bone resorption, which directly causes implant mobility. When mobility is noticed during the healing phase, it strongly indicates that the implant has not been securely integrated into the bone. Clinicians should be alert to critical radiographic signs, such as peri-implant radiolucency, which clearly indicates bone loss around the implant. Additionally, marginal bone loss is characterised by a noticeable reduction in the bone height surrounding the implant, or by the implant appearing elevated relative to neighbouring teeth, suggesting an intraoral projection issue (Piattelli et al., 1998). These clinical and radiographic signs collectively emphasise the importance of continuous monitoring and assessment of dental implants to ensure patient safety and maximise implant longevity (Esposito et al., 1999).

2.9.4 Are Oral Implants a Foreign Body Reaction (FBR)?

While osseointegration generally refers to the direct structural and functional union of bone with an implant, Donath et al. (Albrektsson et al., 2020) proposed an alternative viewpoint. Titanium is considered a foreign material, and osseointegration essentially reflects a foreign body response. After implantation, the immune system initiates a series of reactions that can result in two outcomes: either successful osseointegration or rejection. The bone that forms around the implant creates a barrier, isolating the CP-Ti implant from surrounding tissues. This process enables long-term implant loading. During haemostasis, even CP-Ti implants can elicit a mild immune response, whereas metals like copper and PEEK tend to provoke a stronger reaction; therefore, a pronounced inflammatory response is expected (Albrektsson et al., 2020, 2018). If the inflammation persists, the body is likely to reject it.

The foreign body reaction (FBR) is a complex, chronic inflammatory response that occurs after the implantation of synthetic materials into biological tissues. This reaction reflects the host's biological efforts to isolate and break down foreign objects, which play a vital role in the long-term success of biomedical implants. Despite notable progress in materials science and implant design, FBR still poses challenges in clinical practice, particularly when it leads to fibrous encapsulation or implant failure.

Although many materials are biocompatible, factors such as friction between the implant or surgical instruments and the bone surface can cause complications. Moreover, the dynamic interactions with bodily fluids, which vary in pH, may lead to corrosion and the release of metal particles into surrounding tissues (Chen et al., 2023). This chain of events can further initiate immunological responses.

2.9.5 FBR and Biological Significance

FBR describes the body's ongoing inflammatory response to an implanted biomaterial. It is an active immune process, not a passive one (Anderson & Cramer, 2015), involving several biological steps starting with protein adsorption on the implant surface, followed by immune cell recruitment, macrophage activation, and ultimately the formation

of foreign body giant cells (FBGCs) and fibrotic tissue encapsulation (Anderson & McNally, 2011; Anderson & Jiang, 2017). This response aims to isolate the foreign material from surrounding tissue, thereby reducing the risk of integration and functionality impairment (Anderson et al., 2008). When the body recognises the implant as foreign, it may trigger a reaction that includes multinucleated giant cell formation and the release of inflammatory cytokines like IL-1β, IL-6, TNF-α, and RANKL (Albrektsson et al., 2019; Chen et al., 2023), potentially leading to bone resorption and aseptic implant loosening (Serrabona et al., 2022).

2.9.6 Cellular Mechanisms

Macrophages (M) play a vital role in the FBR, as they are precursors of multinucleated giant cells (Chen et al., 2017; Serrabona et al., 2022). When they detect a foreign surface, they adhere, become activated, and may fuse into FBGCs. Macrophages polarise into either M1 (pro-inflammatory) or M2 (pro-healing) phenotypes, which influence whether the response leads to healing or ongoing inflammation (Anderson et al., 2008; Anderson & McNally, 2011; Anderson & Jiang, 2017; Serrabona et al., 2022). The formation of FBGCS is common in persistent FBR and is often surrounded by fibrotic tissue. Additionally, cells such as neutrophils, dendritic cells, and lymphocytes can also affect the inflammatory response (Anderson et al., 2008; Chand Yadav & Akash Bachuka, 2023). The sequential stages of FBR formation are illustrated in Figure 2.22, and the mechanisms of cellular activation and lysosomal activities are depicted in Figures 2.23 and 2.24.

2.9.7 Molecular Signalling Pathways

FBR involves multiple molecular signalling pathways (Anderson et al., 2008; Chen et al., 2023; Yadav & Bachuka, 2023). Key pro-inflammatory cytokines such as interleukin-1 beta (IL-1β), tumour necrosis factor-alpha (TNF-α), and transforming growth factor-beta (TGF-β) play roles in macrophage recruitment and fibrosis (Serrabone et al., 2022). The transcription factor nuclear factor of kappa light chain enhancer (NF-κB) plays

a crucial role in regulating the expression of numerous inflammatory mediators. Additionally, integrins and pattern recognition receptors (PRRs) contribute to macrophage adhesion and surface recognition of biomaterials (Chen et al., 2023).

2.9.8 Intracellular Changes in Foreign Body Response

The cellular response to a foreign body involves recruiting and activating immune and stromal cells, as well as various intracellular changes that influence their behaviour and fate. These internal processes encompass signal transduction, transcriptional activation, cytoskeletal rearrangements, and metabolic adaptations, all of which shape the foreign body response (FBR).

2.9.8.1 Neutrophils – Acute Inflammation Phase

Neutrophils recognise foreign substances through pattern recognition receptors (PRRs), such as Toll-like receptors (TLRs). When these receptors detect pathogens, they activate the NF-κB pathway, leading to the production of pro-inflammatory cytokines such as TNF-α, IL-1β, and IL-6 (Takeuchi & Akira, 2010). Activation of NADPH oxidase triggers a respiratory burst, producing reactive oxygen species (ROS) that help eliminate microbes and degrade materials (Yadav & Bachuka, 2023). Inside the cell, neutrophil granules containing enzymes such as myeloperoxidase and elastase either fuse with phagosomes or are secreted extracellularly (Yadav & Bachuka, 2023). At the same time, chemokines such as transforming growth factor-beta (TGF-β), platelet-derived growth factor (PDGF), CXCL4, leukotriene B4 (LTB4), and IL-1 exhibit chemoattractive properties that draw macrophages to the implantation site, resulting in macrophage infiltration (Piatnitskaia et al., 2024).

2.9.8.2 Macrophages – Chronic Inflammation Phase

The accumulation of macrophages around the implant initiates a cascade of immune responses, further attracting macrophages. These immune cells secrete various cytokines,

including PDGF, TNF-α, IL-6, G-CSF, and GM-CSF, which play a crucial role in enhancing inflammation and the foreign body reaction. Chemokines such as CCL2, CCL4, CCL13, and CCL22 further facilitate the recruitment of additional macrophages to the implant site. The incoming macrophages may adhere to the implant and participate in subsequent foreign body responses (FBR) and wound healing, thereby supporting the various stages of inflammation. Additionally, implants can trigger an inflammatory response by activating various receptors on immune and non-immune cells, which detect endogenous signals produced during cellular injury. The principal receptors involved include Toll-like receptors (TLRs), C-type lectin receptors (CLRs), RIG-I-like receptors (RLRs), NOD-like receptors (NLRs), as well as IL-1 receptor (IL-1R), IL-6 receptor (IL-6R), and TNF receptor (TNFR) (Piatnitskaia et al., 2024). Activation of these receptors initiates intracellular signalling pathways that lead to the nuclear translocation of transcription factors such as activator protein-1 (AP-1), NF-κB, and interferon regulatory factor 3 (IRF3) (Piatnitskaia et al., 2024).

Macrophages interact with substrates through integrin proteins such as CR3, αβ3, and α5β1. They produce TNF-α, IL-1β, and IL-6 during the acute inflammatory phase, followed by the resolution, clearance, and matrix reconstruction phases. Besides, this reconstruction can also lead to tissue fibrosis (Albrektsson, 2018).

Macrophages play a crucial role in the body's response to foreign materials, such as implants. They attach to the implant surface and can fuse to form multinucleated cells known as foreign body giant cells (FBGCs). These FBGCs exhibit many macrophage-like functions, including the ability to phagocytose foreign particles, generate oxygen radicals and nitrogen species, and produce a variety of cytokines and growth factors (Chen et al., 2023; Yadav & Bachuka, 2023).

High concentrations of growth factors, such as TGF-β, surrounding the biomaterial play a crucial role in the transformation of fibroblasts into myofibroblasts (Piatnitskaia et al., 2024). Additionally, macrophages facilitate osteogenesis during the early and middle stages of healing by promoting the production of key factors such as BMP-2 and RUNX2.

2.9.8.3 Foreign Body Giant Cells (FBGCs)

Insufficient degradation of biomaterials through phagocytosis can result in the formation of foreign body giant cells (FBGCs). These large multinucleated macrophages arise from the fusion of multiple macrophages in response to implanted materials or foreign objects (Kim et al., 2023). FBGCs tend to adhere to biomaterial surfaces, where they release various enzymes, including acid hydrolases and proteases, as well as reactive oxygen species. This release can lead to chronic inflammation and negatively affect the functionality of the biomaterial (Chen et al., 2023; Kim et al., 2023; Yadav & Bachuka, 2023).

Additionally, macrophages can amplify the inflammatory response by activating transcription factors such as nuclear factor-κB (NF-κB). This activation promotes the production and release of further pro-inflammatory cytokines and chemokines. The presence of these signalling molecules stimulates fibroblast recruitment to the implantation site, contributing to the formation of a fibrous encapsulation around the biomaterial (Kim et al., 2023; Noskovicova et al., 2021; Takeuchi & Akira, 2010).

During normal wound healing, various cells in the wound environment, such as macrophages, platelets, and adipocytes, secrete growth factors that promote the recruitment and activation of fibroblasts (Noskovicova et al., 2021). These growth factors, including platelet-derived growth factors (PDGF), TGF-β, and vascular endothelial growth factors (VEGF), play a crucial role in stimulating the replacement of weak fibrin cells with a stronger collagenous extracellular matrix (ECM) (Noskovicova et al., 2021)

During the FBR, macrophages release profibrotic growth factors, thereby promoting fibroblast proliferation and migration to the biomaterial–tissue interface (Noskovicova et al., 2021). At the implant site, fibroblasts differentiate into myofibroblasts and commence excessive synthesis and deposition of collagen fibres, gradually forming a dense network that surrounds the biomaterial (Noskovicova et al., 2021). The thick fibrous capsulation isolates the biomaterial from the surrounding tissue environment, which interferes with proper wound healing, prevents integration of the biomaterial into the tissue, and impairs the biomaterial's compatibility and efficacy (Noskovicova et al., 2021).

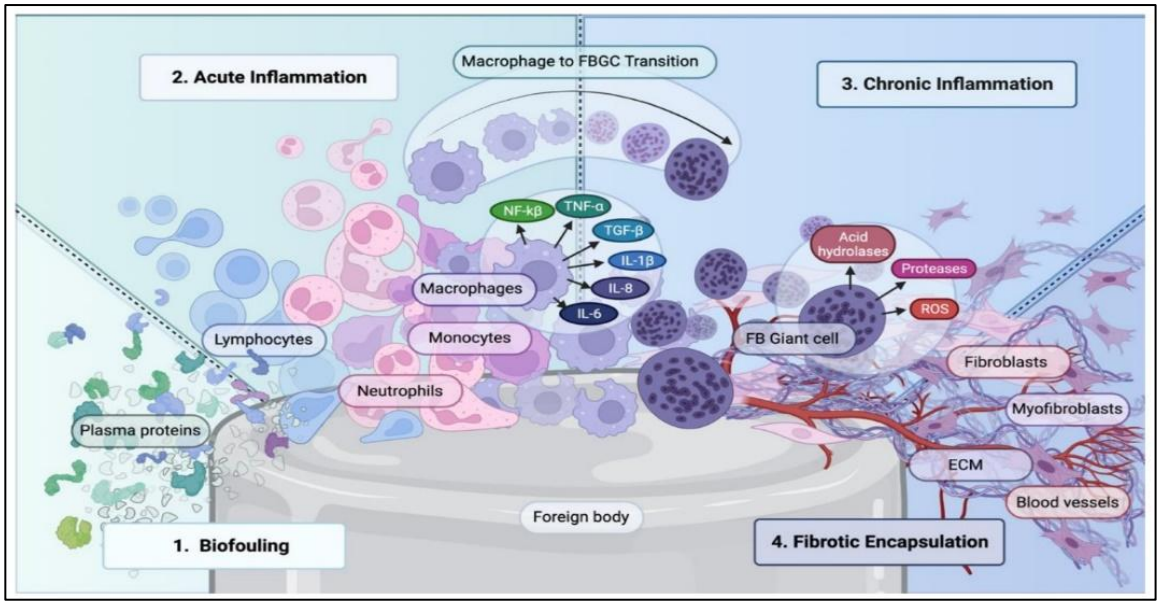

Figure 2.22 Sequential Steps of Immune-Foreign Body Reaction.

Notes: Plasma proteins in the body interact with the biomaterial, initiating the recruitment of immune cells, including lymphocytes, neutrophils, monocytes, and ultimately macrophages. In turn, macrophages release various cytokines, such as NF-κB, TNF-α, TGF-β, IL-1β, IL-6, and IL-8, which further enhance macrophage recruitment, promote phagocytosis, and contribute to the formation of foreign body giant cells (FBGCs). The presence of FBGCS leads to the secretion of proteases, acid hydrolases, reactive oxygen species (ROS), fibroblasts, and the generation of extracellular matrix (ECM), ultimately resulting in the development of a fibrotic capsule surrounding the biomaterial (Kim et al., 2023).

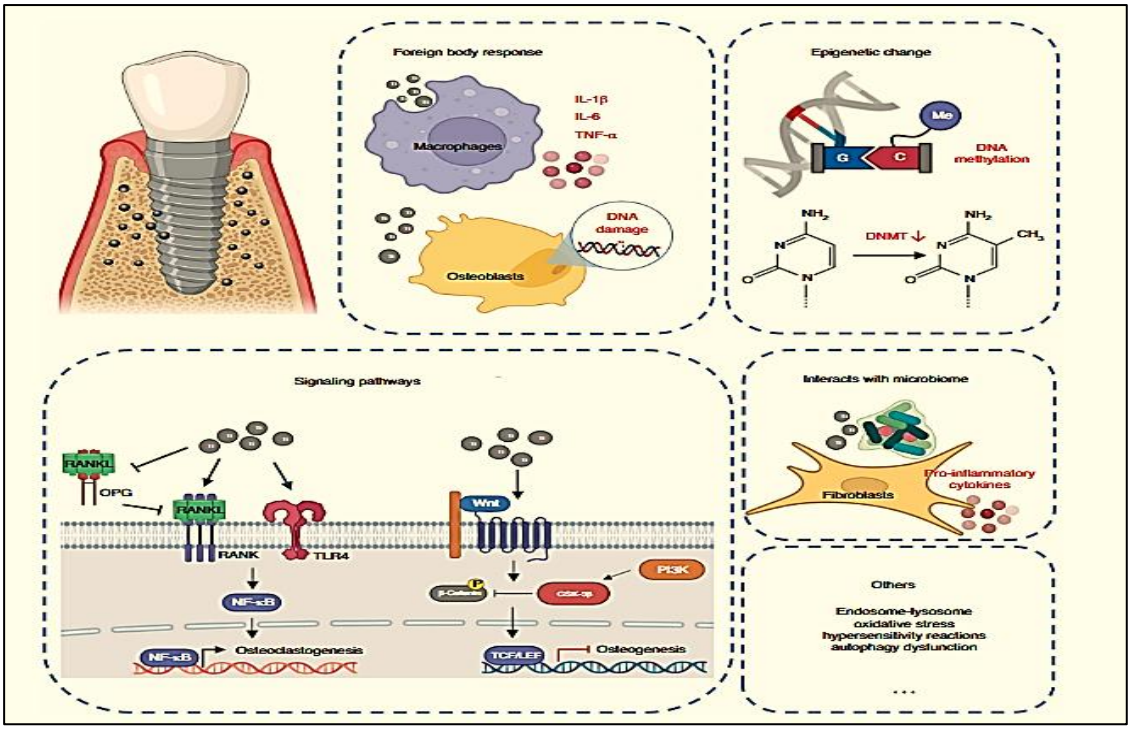

Figure 2.23 The Potential Role of Titanium Particles in the Development of Inflammation.

Notes: Titanium particles, commonly used in biomedical applications, can provoke significant inflammatory responses in the body. When introduced, they trigger a foreign body reaction, causing macrophages to engulf them and polarise towards the pro-inflammatory M1 phenotype. This process releases factors that can damage DNA and impair cellular function. Ti and its oxides can modify the epigenetic landscape by influencing DNA methylation patterns, thereby shaping inflammatory responses in surrounding tissues. Ti particles also affect various signalling pathways, particularly the NF-κB pathway, by modulating the RANKL-to-OPG ratio, which is vital for bone homeostasis. They can further amplify inflammation through proteins from the Toll-like receptor (TLR) family. Conversely, the Wnt/β-catenin pathway may protect against titanium-induced inflammation by inhibiting the NLRP3 inflammasome, thereby reducing osteolysis. The interaction between titanium particles and the microbiome complicates the inflammatory response, as bacterial corrosion can increase the release of titanium particles, thereby intensifying inflammation in peri-implant tissues. Other factors, such as oxidative stress and autophagy, also contribute to this process. (Chen et al., 2023)

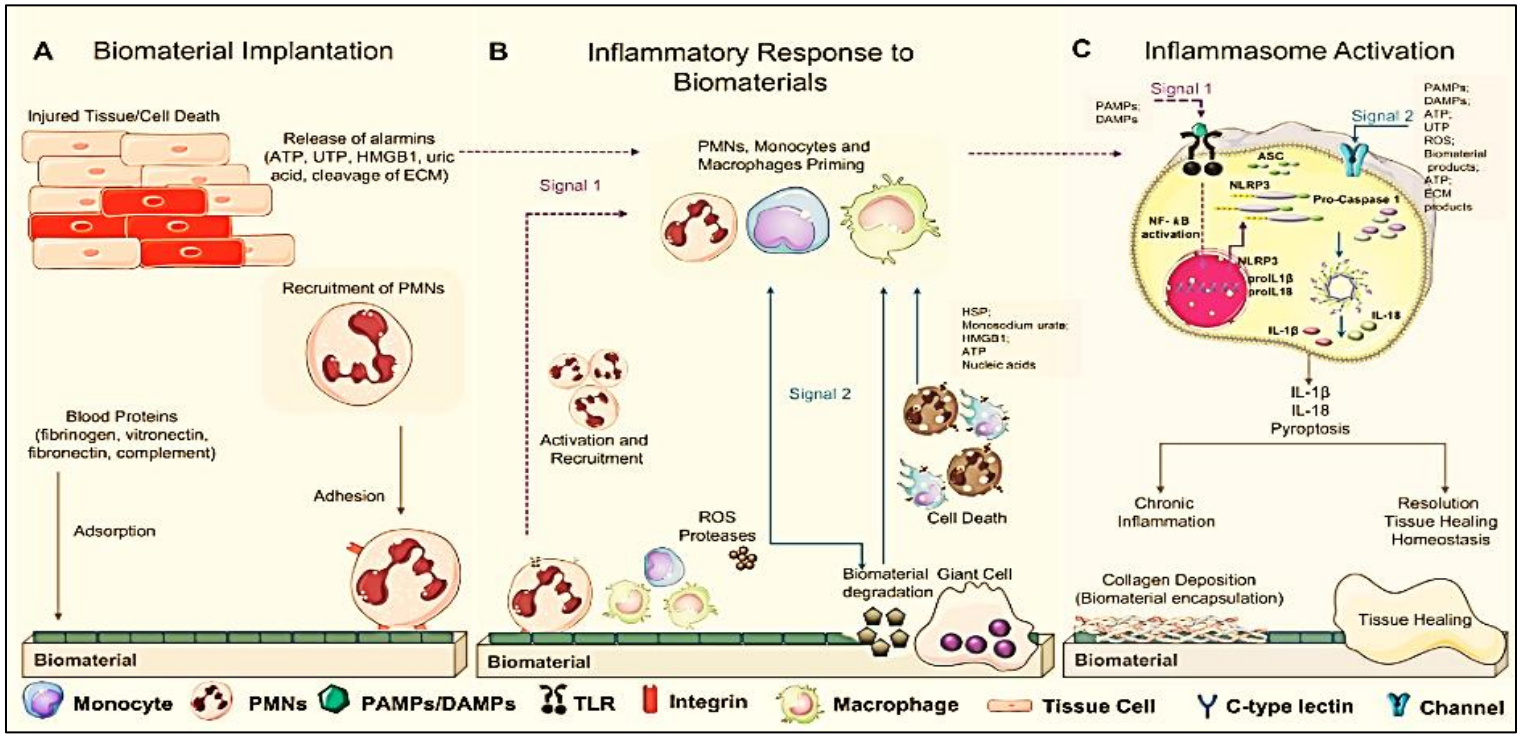

Figure 2.24 The Inflammasomal Role in the Immune Response towards an Implanted Biomaterial

Notes: (A) During biomaterial implantation, the process damages cells, which release danger signals such as alarmins, HMGB1, ATP, and UTP. These signals recruit and activate immune cells, such as polymorphonuclear leukocytes (PMNs), monocytes, and resident macrophages, through pattern recognition receptors (PRRs). Common damage-associated molecular patterns (DAMPs) include ATP, nucleic acids, HSP, monosodium urate, HMGB1, and inflammatory cytokines. Blood proteins adsorbing onto the material surface further attract immune cells. (B) The acute inflammatory response involves immune cells secreting proteolytic enzymes and reactive oxygen species (ROS) that degrade the biomaterial surface and extracellular matrix (ECM). During this phase, endogenous danger signals are released from stressed or necrotic cells and damaged ECM. (C) Inflammasome activation involves the NLRP3 inflammasome, composed of NLRP3, ASC, and pro-caspase-1, which is regulated by two signals. The first signal (signal 1) originates from danger signals released by injured tissues and immune cells, enhancing inflammasome component expression through NF-κB activation. The second (signal 2) promotes assembly through mechanisms like ROS generation, lysosomal damage from phagocytosed biomaterial degradation products, and potassium efflux. Inflammasome assembly activates caspase-1, which cleaves the cytokines IL-1β and IL-18, as well as gasdermin D, resulting in pyroptotic inflammatory cell death. The inflammatory response then either resolves, restoring homeostasis and healing, or progresses to chronic inflammation and biomaterial failure encapsulation (Vasconcelos et al., 2019).

CHAPTER 3
RESEARCH METHODOLOGY

3.1 Study Design

This was a multicentre, observational pilot clinical trial conducted at the Prosthodontic Clinic of the Universiti Teknologi MARA (UiTM, ethics number: REC/11/2020 (FB/365)-Appendix C) and Universiti Kebangsaan Malaysia (UKM, ethics number: DD-2021-010- Appendix D) involving patients with missing single posterior mandibular teeth who volunteered for this study. The study was registered under ClinicalTrials.gov (U.S. National Library of Medicine, ID: NCT04618055) and adhered to the ICH GCP and ISO 14155:2011 guidelines and regulations.

As previously explained in Chapter 1, this study incorporated both clinical (Part A) and laboratory (Part B) components, with the primary purpose of evaluating the clinical performance of the investigational dental implant (NiTiDent Porous NiTi) in restoring single-tooth gaps in the posterior mandible. For Part A, all implants were placed using a two-stage surgical approach. The implants were completely embedded after surgery, and a healing abutment was connected after 18 weeks post-insertion. The mucogingival area was left to heal for approximately 4 weeks. In the 19th week after implant surgery, a master impression was taken for prosthesis fabrication (a monolithic zirconia crown). The crown was delivered in the 20th week. Implant stability, peri-implant tissue health, crestal bone level, and implant survival were evaluated.

The secondary aim of Part B was to identify the possible cause of early implant disintegration by qualitatively evaluating the failed implants and their peri-implant tissues histologically. *In vitro* analysis was conducted on the surgical drill, followed by an assessment of potential nickel ion release. The ability of bone marrow-derived human mesenchymal stem cells (hMSCs) to proliferate and differentiate into osteoblast-like cells, as well as produce a mineralised matrix on porous NiTi dental implants, was also observed and evaluated. The study timeline is presented in Figure 3.1, and the study design is illustrated in Figure 3.2.

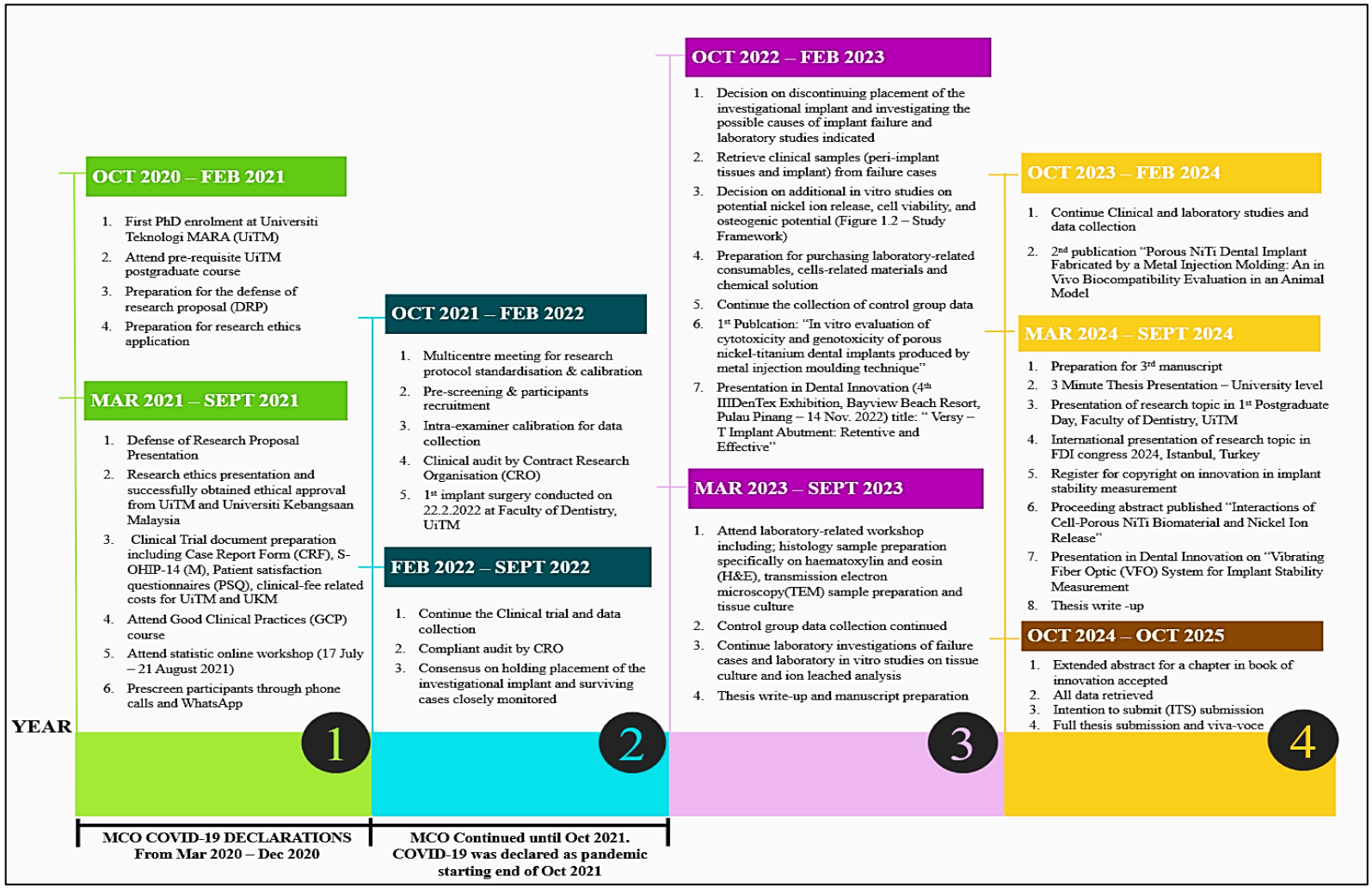

Figure 3.1 Overview of Research Timeline and Achievements

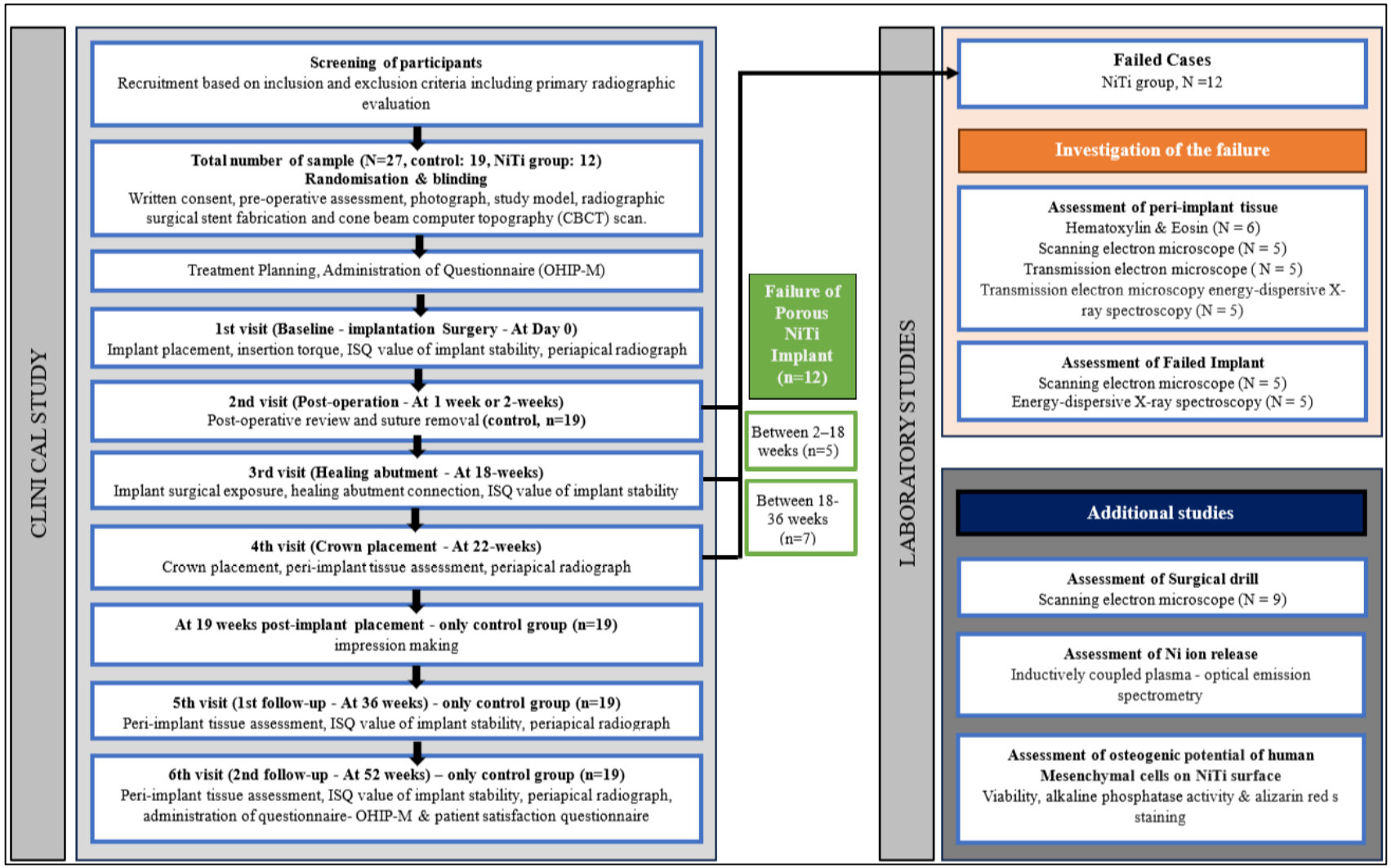

Figure 3.2 Study Framework

3.2 Part A – Clinical Trial Study

3.2.1 Biomaterial Used for This Study

In this Phase 1 clinical trial, a newly developed NiTiDent Tuah porous NiTi tapered dental implant, measuring 4.5 mm in diameter and 10 mm in length, was manufactured by Nitium Technology Sdn Bhd using the MIM technique. Manufacturing comprised injection moulding, solvent and thermal debinding, and sintering, all performed at a certified facility (Nitium Technology Sdn. Bhd, Selangor, Malaysia, ISO 13485:2016), consistent with previous studies (Mustafa et al., 2023; 2024). Further details on this experimental biomaterial are available in an unpublished investigator's brochure (NTSB/MD/01-01-IB-01) (Khushaini & Ahmad, 2021). Concurrently, a similarly sized dental implant, AnyRidge® (Megagen, Korea), served as the control.

3.2.2 Sample Size Calculation

The sample size was calculated using NCSS PASS (Power Analysis and Statistical Software) based on the study design framework of the superiority randomised controlled trial. By assuming a 10% improvement margin of the survival rate for Group A of 98 % and Group B of 88 %, and a 20 % dropout rate, with a significance of 0.05 and a power of 90 %, a total of 105 patients (75 test group and 30 control group) will be needed. The sample size ratio is set to (Gr A: B = 3:1).

The following formulas were used for the sample size and power calculation, respectively (Chow et al., 2008):

$$n_A = \kappa n_B \; and \; n_B = \left(\frac{p_A(1-p_A)}{\kappa} + p_B(1-p_B)\right)\left(\frac{z_{1-\alpha} + z_{1-\beta}}{p_A - p_B - \delta}\right)^2 \tag{3.1}$$

$$1-\beta = \Phi\,(z - z_{1-\alpha/2}) + \Phi\,(-z - z_{1-\alpha/2}), z = \frac{p_A - p_B - \delta}{\sqrt{\frac{p_A(1-p_A)}{n_A} + \frac{p_B(1-p_B)}{n_B}}} \tag{3.2}$$

Where,

$\kappa = nA/nB$ is the matching ratio
Φ is the standard normal distribution function
Φ^{-1} is the standard normal quantile function
α is Type I error
β is Type II error, meaning $1-\beta$ is power
δ is the testing margin

3.2.3 Participant Selection and Recruitment

Ethical approval was obtained at each centre (UiTM and UKM) (Appendix 3 and 4). A total of 30 patients (18 from UiTM and 12 from UKM), aged 18 years or older, attending the Faculty of Dentistry at UiTM and UKM who requested restoration of a single-tooth gap in the posterior mandible, were screened. Eligible patients were informed of the detailed treatment plan and any associated risks. Written consent was obtained.

The patient's detailed information and demographic data were recorded and reviewed. The preoperative evaluation, including an intraoral examination, panoramic radiograph (Fig. 3.3A), cone-beam computed tomography (CBCT) (Fig. 3.3B, C, and D), and diagnostic casts, was assessed accordingly.

Before CBCT scanning, a laboratory-fabricated tooth-borne radiographic template was fabricated using PETG co-polyester thermoforming resin (Erkodent Erich Kopp GmbH, Germany). 7 g of high-density barium in 5 mL of varnish mixture as the radiopaque marker was coated to fill within the crown space area (Israelson et al., 1992). The predetermined location of the future implant was established by creating a vertical hole along the planned crown's height. Sectional scanning of the posterior mandibular bone was performed using CBCT (CS 9300C, Carestream Dental LLC, Atlanta, United States) at 90 kV, 3.5 mA, 5 x 5 FOV, slice thickness of 90 µm with a 90 µm interval. Analysis of the scan images was performed in cross-sectional, axial, and panoramic views, with the radiograph marker visible to ensure the implant's correct position.

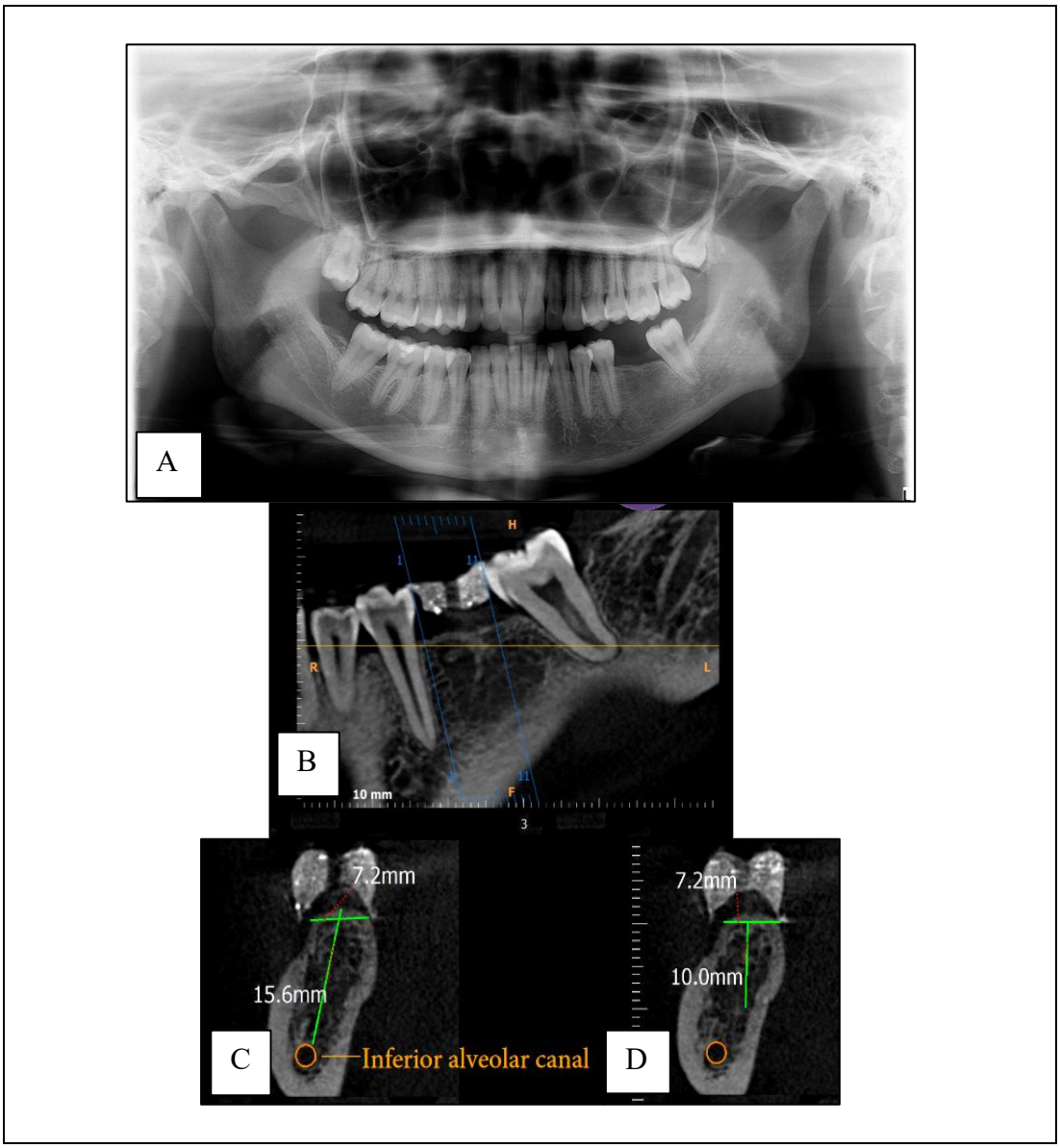

Figure 3.3 Radiographic Assessment of the Patient Before Including or Excluding, Either of the Patients in this Study.

Notes: Orthopantomogram (OPG) in a, assessing general oral tissue condition. A 3-D evaluation of CBCT images (B, C and D) evaluates the local bone of the planned future implant (B and C) and the relation of a future implant with vital structure (inferior alveolar nerve) in D.

3.2.4 Inclusion and Exclusion Criteria

The inclusion and exclusion criteria are tabulated in Table 3.1.

Table 3.1
Inclusion and Exclusion Criteria for this Study

Inclusion criteria
1. Patients of either sex and at least 18 years of age
2. Ability to understand and provide informed consent before starting the study.
3. Ability and willingness to comply with all study requirements and be physically able to tolerate conventional surgical and restorative procedures.
4. The patient has a negative urine pregnancy test.
5. Good oral hygiene.
6. Adequate bone volume for placement of a 4.5 mm in diameter and 10 mm in length endosseous dental implant and interocclusal distance (crown height space) of at least 6 mm measured from the alveolar crest to the occlusal table.
7. Intact buccal table as verified by Cone Beam Computed Tomography (CBCT).
8. Missing one tooth in the posterior mandible, surrounded by two natural teeth (one anterior and one posterior to it and the presence of opposing dentition with a functional occlusion
9. Primary stability of implant consistent with standards of care is achieved at the time of implant placement.
Exclusion criteria
Presurgical:
1. Patient is a tobacco user within the last five years (more than 10 cigarettes per day)
2. History of alcoholism or drug abuse within the past 5 years.
3. Severe wear with an etiology of bruxism or clenching habits.
4. Patients in need of bone grafting at the site of the intended implantation site.
5. Patients who have previously failed implants at the site intended for study implant placement.
6. Patients in need of other treatments or surgeries at a site adjacent to the intended implantation site.
7. Patients with active infection or severe inflammation in the areas intended for implant placement.
8. Patient has significant untreated periodontal disease, severe recession, caries, clinical or radiographic signs of infection within two adjacent tooth positions of implant area.
9. History of HIV infection, Hepatitis B or C.
10. Patients has history of systemic disease with ASA (American Society of Anesthesiologists) III classification (including cardiovascular, hepatic, renal, gastrointestinal, metabolic, neurologic, pulmonary, endocrine, autoimmune, or psychiatric disorders).
11. Presence of local inflammation or mucosal diseases such as lichen planus.
12. Patient has a history of consistent high risk for subacute bacterial endocarditis.

Exclusion criteria
13. Current haematological disorder or warfarin (or similar) therapy.
14. Patient has a history of disease that affects bone metabolism, congenital connective tissue disorders (e.g., osteogenesis imperfecta), or Paget's disease.
15. Patient is taking medications or having treatments known to affect bone turnover, including thiazide diuretics, calcitonin, systemic steroids, bisphosphonates, vitamin D (>800 IU/day), estrogen or progesterone therapy.
16. History of steroid treatment of duration of 2 weeks or longer in the past 2 years.
17. Patient currently undergoing chemotherapy.
18. Patient has a history of radiation treatment to the head or neck.
19. Physical or mental handicaps that would interfere with the patient's ability to exercise good oral hygiene regularly.
20. Use of any investigational drug or device within the 30 days immediately before implant surgery.
21. Patient is pregnant and lactating.
Post-Implant Surgery:
1. Lack of implant primary stability
2. Inappropriate implant position for prosthetic requirements.
3. Major simultaneous augmentation procedures at surgery.
4. X-ray does not show the implant from the first bone contact to the apical tip.

3.2.5 Participant Randomisation and Grouping

The randomisation process for participants adhered to the CONSORT 2010 guidelines, which involved three (3) steps (http://www.consort-statement.org/consort-2010). The first randomisation was to create a list of unpredictable allocation sequences of sampling numbers, and the second was for subsequent allocation concealment. The random sequence of numbers from 1 to 35 was generated using a website (https://stattrek.com/statistics/randomnumber-generator.aspx). Using the same generator, the sequences were generated once again. The first twenty-five numbers were assigned to the intervention group, and the remaining to the control group.

The procedure was conducted at each centre by an independent examiner who was not involved in the implant surgical placement. Then, 35 opaque, sealed envelopes, labelled 1 to 35, were prepared, each containing a chit marked "A" or "B". A designated A for the control (Anyridge®, Megagen, Korea) and B for the tested groups (NiTiDent Tuah, Nitium Technology Sdn, Bhd., Malaysia).

The randomisation took place just before the implant surgical procedure. The sealed envelope was opened by an independent, recruited dental assistant, and the chit

note was revealed to the clinician; therefore, only the clinician and their assistant knew which arm was allocated. The participants were kept blinded to the allocation. All participants' information was kept in a case report form (CRF) (Appendix E).

3.2.6 Implant Surgical Procedure

The implant surgery was performed by an experienced surgeon or prosthodontist who had calibrated the implant systems prior to the study. Under local anaesthesia with mepivacaine hydrochloride 2 % and epinephrine 1:100 000 (Scandonest, Septodont, France) and strict adherence to sterile technique protocol, a mid-crestal incision was made with a scalpel blade #15 extended through interproximal and sulcular tissues of the adjacent teeth, followed by a full-thickness mucoperiosteal flap elevation to expose the proposed implant site. As recommended by the manufacturer, the osteotomy procedure began with a 2-mm-diameter pilot drill, guided by a surgical template, at the centre of the crestal bone. A direction indicator gauge was inserted after the osteotomy had reached the desired depth (10 mm in the bone) to determine the proper position and angulation of the osteotomy concerning the adjacent tooth roots, which was confirmed with a periapical radiograph. To reach the desired depth, end-cutting twist drills with diameters up to 4.5 mm were used to increase the osteotomy diameter. The osteotomy position and angulation were checked after each drill size. A large amount of saline solution was used for irrigation during the procedure. The implant fixture was placed with a maximum torque of 50 Ncm (Lemos et al., 2021), leaving one or two threads above the crest, as recommended by the manufacturer. Finally, the platform was adjusted to 1 mm subcrestally using a ratchet wrench (Valles et al., 2018).

The insertion torque value (ITV) was recorded, and primary implant stability was evaluated by measuring the implant stability quotient (ISQ) with an ISQ device (Mega ISQ® II, Megagen, Korea) (Fig. 3.4D). A low-profile cover screw was secured onto the implant fixture after the subcrestal placement of the implant (Fig. 3.4E). The mucoperiosteal flap was subsequently adjusted and secured with a 4/0 absorbable, coated, undyed, braided Vicryl suture for primary closure (EthiconTM, Johnson & Johnson, USA) (Fig. 3.4F), followed by a post-insertion periapical radiograph to establish bone level baseline data (Fig. 3.4 G). Postoperative instructions were provided, including avoiding strenuous exercise, using a dental prosthesis (for patients with removable partial dentures), adhering to a soft diet, and implementing an oral hygiene

program to reduce the risk of trauma from brushing. The participant was informed about the possibility of pain, oedema, and bleeding. Analgesics were administered, starting with etoricoxib 90 mg on day one and paracetamol 1000 mg if needed, on subsequent days. The patient also received oral irrigation with 0.12% chlorhexidine (CHX) three times daily for seven days (Morris et al., 2000).

3.2.7 Postsurgical Review Procedure

All participants were reviewed within 7–14 days post-operatively (Adell et al., 1980). Any adverse events, such as pain, swelling, bleeding, and surgical site infection, were evaluated and treated accordingly, as shown in Table 3.2. Suture removal was performed during this follow-up visit (Fig. 3.4H).

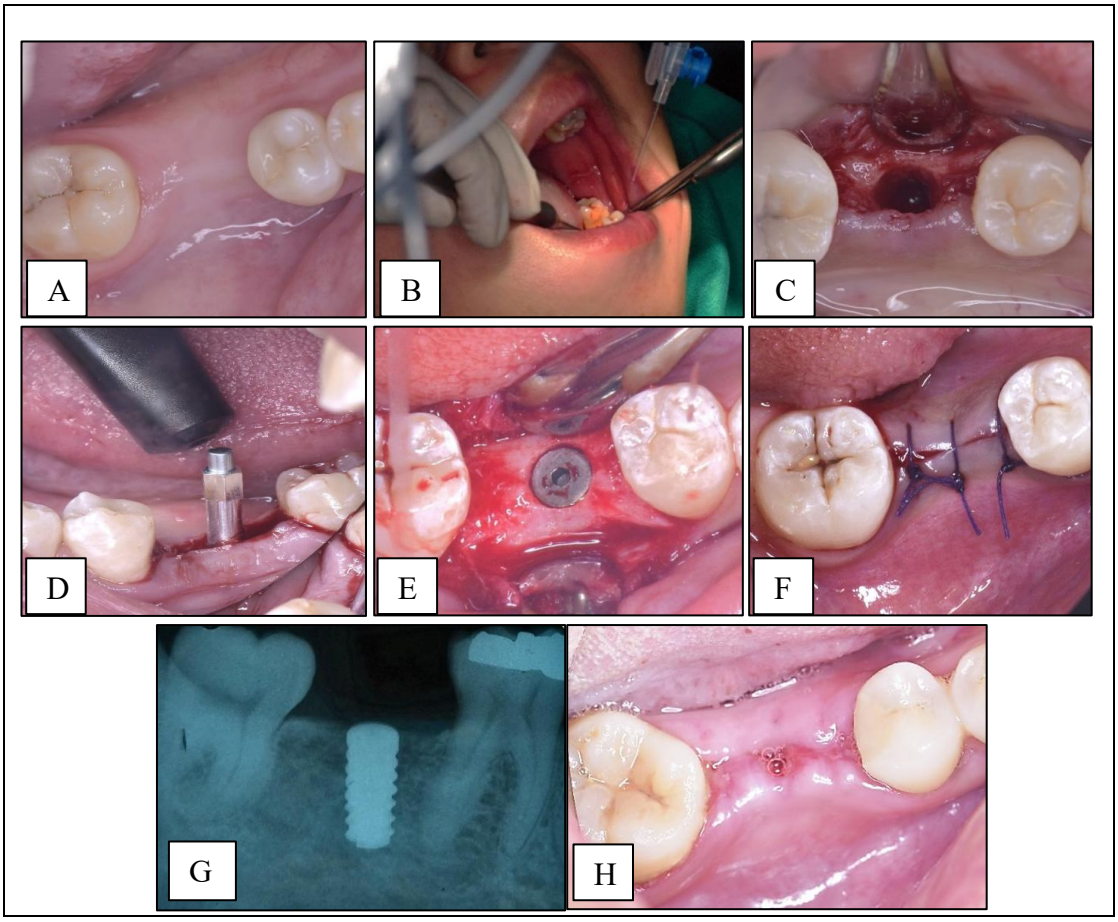

Figure 3.4 Procedures Involved During Intra- and Post-operative Visits 1 (V_1) and 2 (V_2) in this Study.

Notes: A) photo of the planned surgery area. B) Copious irrigation of the surgery site before the incision is made. C) The prepared implant bed condition before implant placement. D) ISQ device probe over the smart peg affixed to the implant fixture to

measure implant stability (ISQ). E) The cover screw in situ covering the implant fixture. F) Flap repositioned and secured with sutures. G) Baseline periapical radiograph and g) post-operative photo after removal of sutures.

Table 3.2
Management of Post-operative Complications (Bryce et al., 2014)

Event	Post-operative procedure	Post-operative complication management
Management of postoperative haemorrhage	Physical pressure using CHX-soaked gauze for 30 minutes. Avoidance of exercise to prevent disruption (including appropriate oral hygiene methods). Management of post-operative bleeds using pressure.	1. Minor bleeds: site examination, LA placement with a vasoconstrictor, dampened gauze pressure. 2. Moderate to severe haemorrhages: In addition to the treatment for mild bleeds, incorporate supplementary sutures and haemostatic agents (tranexamic acid-impregnated gauze).
Management of post-operative swelling	Cold compress for 4 hours: 10 minutes on, 20 minutes off. Tell them applying the compress repeatedly for 48 hours will diminish oedema. If required, prescribe a non-steroidal anti-inflammatory drugs (NSAIDs).	Prolonged post-operative swelling: 4 mg of dexamethasone daily for 7 days will be prescribed.
Reduction of the risk of postoperative infection	Chlorhexidine (CHX) mouth rinses 3 times daily for 7 days or until sutures are removed. Advice on the use of soft-bristled brushes to assist plaque control within the surgical site.	If symptoms and clinical signs persist, use Amoxycillin 500 mg TDS for 5 days or 300 mg Clindamycin TDS for 5 days (for penicillin-sensitive patients).
Neurosensory disruption	Report changed sensations in patient records. The patient and dexamethasone (6–8 mg daily for 7 days) prescription will be reviewed.	Reversal or explantation of the implant away from the neurovascular structure if problems are detected early.

3.2.8 Restorative Procedure

Re-entry surgery was performed within 18 weeks post-implantation (third visit - second stage) to remove the cover screw (Fig. 3.5C), as described by Branemark et al. (1983), with a minimum of 3–4 months. A healing abutment was affixed to the implant and allowed to heal for 4 weeks (Fig. 3.5D, E, F) (DeAngelo et al., 2007). Subsequently, during the 19th week of this healing phase, the implant position is ready to be captured in an impression. The healing abutment was removed, and an impression coping was attached. An individualised open tray technique was employed to capture the implant position at the osseous level, utilising vinyl polysiloxane impression material (Dentsply

Sirona, USA). The implant analogue was thereafter affixed to the transfer post prior to fabrication of the master cast (Fig. 3.5G). A maxillomandibular jaw relationship was then recorded utilising vinyl polysiloxane bite registration material (Regisil, Dentsply Sirona, USA). The impression was sent to the laboratory for production of a CADCAM screw-retained monolithic zirconia crown.

The crown's anatomical form, marginal fit, colour compatibility, relationship to adjacent teeth, and occlusion with opposing teeth in centric, lateral, and protrusive movements were meticulously assessed. If modification is necessary, the crown was repolished using coarse to finer burs to smooth out its surface. The retaining screw was tightened to a final torque of 35 Ncm, as advised by the manufacturer, using a torque wrench.

3.2.9 Follow-up Visits

The participants were scheduled for follow-up at 14 weeks after crown insertion (36 weeks post-implant placement at the 5^{th} visit, V_5) and 52 weeks (6^{th} visit, V_6) post-implant placement (Dahlin et al., 2013). The health of peri-implant tissues (presence of infection such as peri-implantitis, discomfort, bleeding, inflammation, and suppuration), complications related to crowns (screw loosening, screw fracture, and chipped porcelain), and implant characteristics (stability and crestal bone loss) were assessed. All dependent variables were documented in the CRF for each follow-up visit.

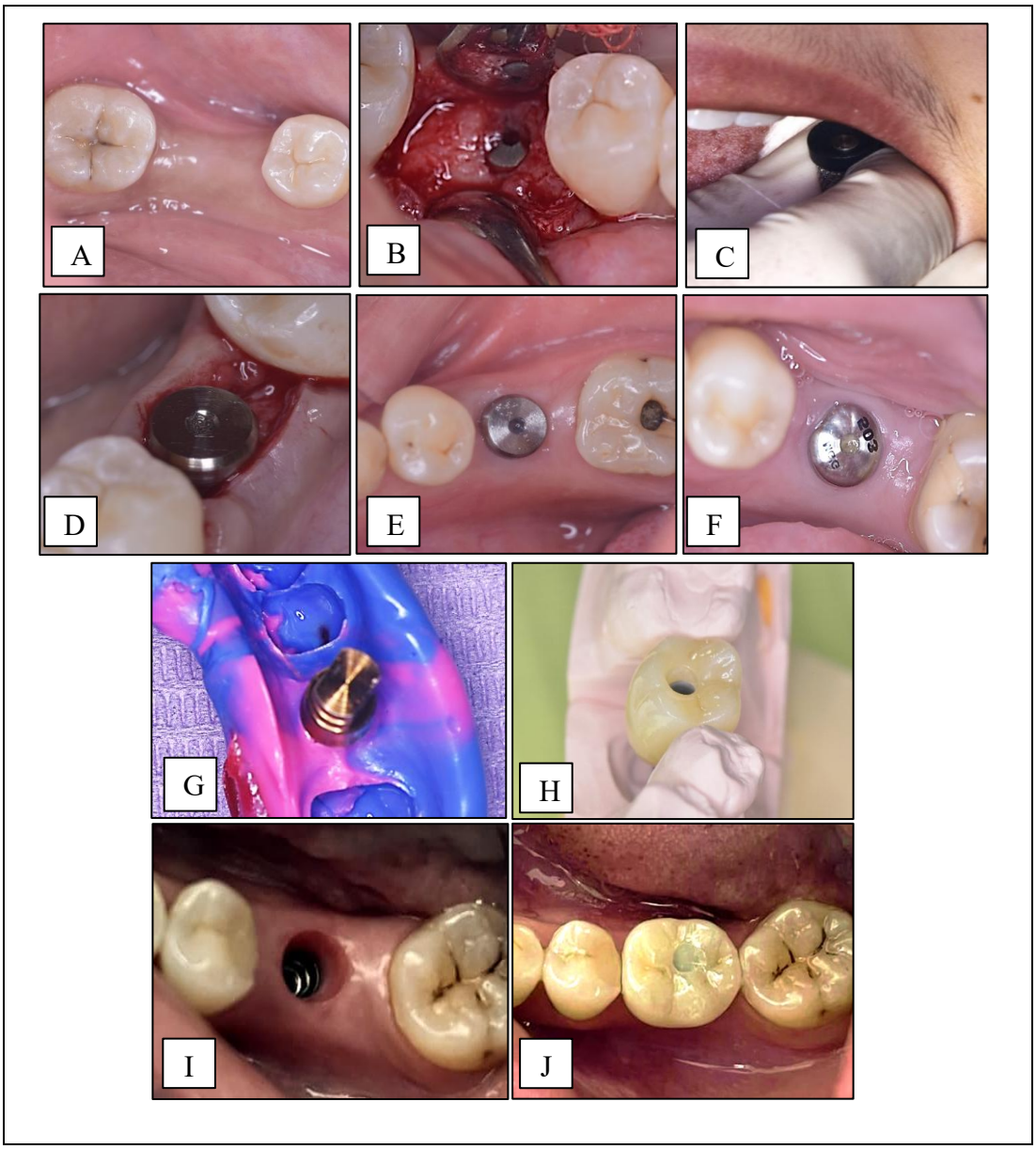

Figure 3.5 Photo Taken During the Second-Stage Visits.

Notes: A) Residual ridge condition before exposure of the cover screw. B) Bone overgrowth over the cover screw was seen after the flap was raised. C) removal of a cover screw with a hand driver and replacement with a healing abutment (D). Healing abutment in situ with E) NiTiDent and F) Megagen dental implant systems. G) Completed impression with implant analogue secured into the impression material. H) Crown on the working cast, I) peri-implant tissue conditions prior to crown placement and J) crown in situ, intraorally (Megagen system).

3.2.10 Data Collection for Part A

3.2.10.1 Implant Stability Assessment by Resonance Frequency Analysis

The implant stability quotient (ISQ) is a value on a scale generated by resonance frequency analysis (RFA) that indicates the level of stability and osseointegration of dental implants. The scale ranges from 1 to 100. This measurement was done using an ISQ device (Mega ISQ® II, Megagen, Korea). The sterile, disposable Smart Peg (transducer) was carefully affixed to the implant fixture, and the probe was maintained at a right angle to the alveolar crest. The measurement was conducted 3 times on the mesial, distal, buccal, and lingual sides, and a single average value was computed. The measurements were documented at implant placement (1st visit, V_1), 18 weeks (3rd visit, V_3), and 22 weeks (4th visit, V_4) for the control group, whereas for the tested group, data were gathered only on V_1 (n = 12) and V_3 (n = 7) post-implant placement. Following the initial assessment after crown placement in the review visit, data concerning implant stability were not retrieved. Although the abutment screw was successfully removed from the control group's abutment system, we had challenges in detaching the screw from its fixture; hence, the ISQ value was not assessed at the initial (V_5) and subsequent review (V_6) visits.

3.2.10.2 Evaluation of Peri-Implant Soft Tissues

Prior to data collection, evaluations for both intra- and inter-examiner reliability were conducted to ensure the accuracy and validity of the measurements. A total of ten dental implants were selected for the assessment of peri-implant probing depth (PD). To establish inter-examiner calibration, two examiners independently measured the PD. In terms of intra-examiner reliability, a single evaluator recorded the PD at two different time points. Measurements were taken using a manually graded UNC-15 periodontal probe from Hu-Friedy (Chicago, IL, USA). The reliability of the measurements was analyzed using the intraclass correlation coefficient (ICC), yielding scores of 0.894 and 0.931 (refer to Appendices F & G). Both scores exceed the threshold of 0.80, indicating excellent agreement. With the reliability satisfactorily confirmed, the main data collection commenced.

The conditions of peri-implant soft tissue, including the presence of mucositis (inflammation of the peri-implant mucosa without progressing to crestal bone loss), probing pocket depth, bleeding on probing, suppuration, and dehiscence, were evaluated (Buser et al., 1990). Peri-implant bleeding on probing (BOP) and probing depth were measured at six sites of the peri-implant tissue using a UNC-15 periodontal probe (Hu Friedy, Chicago, IL, USA). These six sites were: mesiobuccal, mid-buccal, distobuccal, mesiolingual, midlingual, and distolingual. All peri-implant soft-tissue variables were collected at 22 weeks (4th visit, V_4), 36 weeks (5th visit, V_5), and 52 weeks (6th visit, V_6) in all participants with Anyridge® dental implants only. The assessment of peri-implant tissue health could not be performed in the tested group due to premature biological failure.

3.2.10.3 Evaluation of Crestal Bone Levels

The intraoral periapical radiograph was used to evaluate crestal bone levels related to the implant. Similar to the peri-implant soft-tissue probing-depth data collection, a comprehensive intra- and inter-examiner reliability test was conducted. To assess inter- and intra-examiner consistency, ten periapical radiographs of single dental implants were selected. A simple randomisation method was employed by generating a sequence of random odd numbers, each corresponding to a patient record with a single implant in the posterior mandible. Radiographs matching these randomly generated odd numbers were then retrieved and used for reliability testing. The mesial and distal bone levels were measured as the distance from the implant shoulder to the first visible bone contact; each measurement was repeated three times to obtain an average value. Intra- and inter-examiner agreement was assessed between two assessors (inter-examiner) and on two occasions by the same investigator (intra-examiner). In this study, reliability was excellent, with values of 0.996 and 0.997 (Appendices H and I). Following the agreement, data collection then commenced.

In UiTM, the periapical radiograph was taken using an intraoral digital sensor (EzSensor Classic, Vatech, Korea). Meanwhile, at UKM, the periapical radiograph was obtained using conventional radiographic film (Kodak Ultraspeed Dental Film, Eastman Kodak). A digital sensor and radiographic film were positioned intraorally using a radiographic positioner (RINN XCP-Posterior, DENTSPLY, Des Plaines, Ill., U.S.). The long-cone paralleling technique was adopted, using a bite registration

material (Aquasil Soft Putty/Regular Set, Dentsply, Germany), to facilitate consistent image reproducibility across consecutive visits (Lago et al., 2018). The dental radiology system was set at 70 kV and 7 mA at 0.16 s. The image should show the implant, including the mesial and distal adjacent teeth, with at least 2 mm of apical bone visible below the implant apex.

Linear measurements of implant length, mesial and distal of the crestal bone level of the control and tested groups were performed using the Easydent 4 software (Vatech, Korea). A direct measurement using a digital calliper under an X-ray magnifier was performed for images taken via conventional radiographic film. The measurement description is as follows:

Implant length: A vertical line was traced across the midportion of the implant from the coronal to its apex (IL). This measurement was used to calibrate radiographs taken digitally or conventionally. Each radiograph's measurements were adjusted for a coefficient derived from a ratio of the implant's true length to IL.

Crestal bone level: A horizontal line was drawn to locate the implant shoulder (line 0), and two vertical lines were traced perpendicular to line 0 to the first bone-to-implant contact on the mesial (M) and distal (D) aspects of the implant (Lago et al., 2018).

The measurements were conducted at baseline (during implant placement, 1st visit, V_1) (M0, D0), at 22 weeks (4th visit - during placement of the crown, V_4) (M1, D1), 36 weeks (5th visit), V_5, (M2, D2), and 52 weeks (6th visit, V_6), (M3, D3) post-implant placement. The average bone level of the respective study visit was computed and statistically analysed.

3.2.10.4 Patient Satisfaction and Patient-Related Outcome Satisfaction using a validated Patient Satisfaction Questionnaire (PSQ) and validated Oral Health Impact Profile-14 (Malay version)

The validated Malay version of the Patient Satisfaction Questionnaire (PSQ) was used to assess patient satisfaction following prosthodontic treatment, particularly with respect to dental implants used to replace missing teeth. This questionnaire was carefully translated from English to Malay by researchers and later evaluated by two prosthodontists, Lim and Ariff, in 2020. To enhance the study, supplementary insights from Dong et al. (2019) were incorporated and validated by three prosthodontists

through expert assessments. The questionnaire comprises nine items (Q1-Q9) assessed on a 7-point Likert scale. It encompasses several dimensions, including i. aesthetics and functionality; ii. maintenance and cleanliness; iii. comfort and behaviour iv. acceptance and recommendation of the prescribed treatment; and v. readiness to undergo the same procedure again in the future.

The questionnaire was provided to all participants during the second follow-up meeting (52 weeks, 6th visit) in a guided, self-administered, closed-ended manner. Overall satisfaction will be determined by summing and ranking the scores, with the findings interpreted as follows: 1-2 (low), 3-4 (medium), and 5-7 (high).

As for the patient-related outcome, patients were evaluated using a shortened Malaysian version of the Oral Health Impact Profile-14 (OHIP-14 (M)), for which validity and reliability have been tested by Saub et al. (2005). This oral health-related quality of life (OHRQoL) questionnaire assesses the adverse effects of the treatment provided. It consists of 14 items covering seven domains, including functional limitation, physical pain, psychological discomfort, physical disability, social disability, and handicap. A 5-point Likert-type scale comprises 0: Never, 1: Hardly, 2: Occasionally, 3: Fairly often and 4: Very often. The total mean value for each domain will be calculated by summing the mean values assigned to the questions. The relationship between the two groups, both before and after the intervention, was also assessed, along with demographic and clinical parameters. A low score indicates a better patient's OHRQoL. This questionnaire was administered using a guided, self-administered technique and distributed to patients before implant placement (at the screening visit, once the patient had signed the informed consent document) and at 52 weeks (second visit post-implant placement). The questionnaires were thereafter gathered independently from the treating operators involved in delivering surgical and prosthodontic procedures.

3.2.10.5 Implant Success and Survival Rates Evaluation

The survival rate was assessed solely by the presence of the implant in the mouth, regardless of any biological or technological issues. The success criteria were determined using the principles proposed by Buser et al. (1990). Papaspyridakos et al. (2012) included an additional element (prosthodontic and patient satisfaction metrics). The success criteria are as follows: no persistent subjective discomfort, such as pain, foreign-body sensation, or dysesthesia; no recurrent peri-implant infection with suppuration; no detectable implant mobility on manual palpation; no continuous peri-implant radiolucency; no prosthodontic technical complications; and overall patient satisfaction.

3.2.10.6 Adverse Events

Any adverse event, whether related to the device or not, and regardless of its severity, was documented in the Case Report Form (CRF) and reported to both the manufacturer and the ethics committee in accordance with the established protocol (Ahmad & Lim, 2021). Discontinuation of the study treatment occurred when the investigator, based on clinical judgment, determined that it was in the subject's best interest to cease treatment for safety reasons. Participants were monitored at both scheduled and unscheduled visits until satisfactory clinical resolution was achieved. In cases of implant failure, whether early or late, the implant was retrieved, and its associated peri-implant soft tissue was evaluated ultrastructurally, following the methods outlined by Albrektsson et al. (1981), Esposito et al. (1997), Piatelli et al. (1998), and Faeda et al. (2019). The participants were subsequently excluded as a secondary exclusion criterion, and options for replacing the missing tooth were offered, including an implant, bridge, or removable prosthesis.

3.2.10.7 Data Analyses

All the data were analysed using IBM SPSS version 29.0.1.0 (177) (IBM Corp, Armonk, NY), based on the objectives:

i. Implant stability
ii. Peri-implant tissue health (signs of inflammation, bleeding on probing, probing depth, suppuration and dehiscence)
iii. Crestal bone level
iv. Patient-related outcome (PSQ & OHIP-14)
v. Implant success and survival rates

Descriptive statistics were performed for all parameters. The demographic characteristics, like age, sex, and occupation, were summarised and tabulated. The statistical analyses for each objective are listed in Table 3.3 below:

Table 3.3
Data Analyses of Part A Study

Objective	Variable		Data collected	Descriptions
	Independent variable/s	**Dependent variable/s**		
1. To determine the implant stability of the NiTiDent Tuah implant compared to the control group (Anyridge®) by Resonance Frequency Analysis	Gr A: control group (AnyRidge® dental implant, MegaGen, Korea) Gr B: Investigational implant (NiTiDent Tuah porous NiTi dental implant, Nitium Technology Sdn. Bhd, Malaysia)	Implant stability quotient, ISQ	- At implant placement (1st visit, V_1), - 18th -week (V_3), & - 22nd -week (V_4) (Anyridge® only)	The mean, standard deviation, and 95% confidence interval for implant stability (ISQ) were derived. A repeated measures ANOVA was conducted for Anyridge® group to test the time effect within the group. A paired t-test was performed for NiTiDent Tuah to compare the mean difference at two different intervals
2. To assess the conditions of the peri-implant soft tissues of porous NiTi implant compared to the control group by probing depth, bleeding on probing, suppuration and dehiscence at 16 weeks, 26 weeks, and 52 weeks after implant placement.	Gr A only: control group (AnyRidge® dental implant, MegaGen, Korea)	Signs of inflammation, probing depth, bleeding on probing, suppuration & dehiscence	3 times: - 22nd -week (V_4), - 36th -week (V_5) & - 52nd -week (V_6) after implant placement	For objective number two, the incidence of inflammation and its degree (mild, moderate, severe), bleeding on probing (BOP), suppuration, and dehiscence were reported as percentages. A repeated-measures analysis of variance (ANOVA) was performed to evaluate mean differences in probing depth and objective no. 3 (crestal bone level) across continuous dependent variables from day 0 (baseline) to the specified weeks following implant installation. The F-test for significance was used to assess the effect of time.
3. To evaluate crestal bone loss associated with porous NiTi implant compared to the control group by serial periapical radiography at the time of implant placement and 16 weeks, 26 weeks and 52 weeks after implant placement.		Crestal bone level measurement	4 times: - At implant placement (1st visit, V_1), - 22nd -week, V_4, - 36th -week, V_5 & 52nd -week, V_6 after	

Objective	Variable		Data collected	Descriptions
	Independent variable/s	Dependent variable/s		
			implant placement	
4. To compare the patients' satisfaction and oral health-related quality of life between NiTi implant and control group for single missing molar replacement.	Gr A only: control group (AnyRidge® dental implant, MegaGen, Korea)	1. Patient satisfaction, PSQ 2. OHIP (before & after)	PSQ: 52nd -week after implant placement OHIP: - 2nd screening visit - 52nd -a week after implant placement	For PSQ and OHIP, only the control group proceeded in this study, descriptive analysis was performed for PSQ and paired t-tests were conducted to compare means within Group B
5. To Evaluate implant success and survival rates	Gr A: control group AnyRidge® dental implant, MegaGen, Korea) and Gr B: Investigational implant (NiTiDent Tuah porous NiTi dental implant, Nitium Technology Sdn. Bhd, Malaysia)	**Implant success criteria:** presence/absence of implant discomfort, recurrent peri-implant infection, implant mobility on manual palpation and continuous peri-implant radiolucency **Implant survival**: Presence of implant in bone within an expected period		Implant success: Categorical study variables such as presence/absence of implant discomfort, recurrent peri-implant infection, implant mobility on manual palpation and continuous peri-implant radiolucency, and cumulative implant success were descriptively summarised by percentages. Implant survival rate: Survival rates of implants were analysed over a 12-month period, and Kaplan-Meier plots were generated for both the intervention dental implant and the control group. The log-rank test was employed to assess significant differences between the two implants

3.3 Part B – Laboratory Studies

3.3.1 Retrieval of Disintegrated Implant and Peri-implant Tissue

The procedure for retrieving failed implants was performed in accordance with the protocols of Esposito et al. (1997), Faeda et al. (2019) and Piatelli et al. (1998). A total number of 12 porous NiTi implant had been removed in events of clinically evident failure, which included one of the following two major scenarios: 1 - an expression of inflammation in the peri-implant tissue, marked by symptoms including swelling, discomfort, fistula formation, and/or the presence of purulent discharge; 2 - a partial or total displacement of the implant fixture from its osseous bed, with or without peri-implant tissue pathology, and with or without pathological indications on intraoral and periapical radiographs.

All procedures were performed following the administration of a local anaesthetic. The implants were carefully unscrewed to preserve as much of the peri-implant tissue as possible. Subsequent to the removal of the failed implants, the areas were curated, carefully cleaned and sutured (Esposito et al., 1997). The retrieved samples of implant and peri-implant tissues were prepared for further analysis following Albrektsson et al. (1981), Esposito et al. (1997), Faeda et al. (2019), and Piatelli et al. (1998). Post-operative instructions were delivered, and patients were evaluated within one to two weeks. All implant sites have healed without problems during the review visit, and patients were offered alternative treatment to replace the failed implant.

3.3.2 Sample Preparation

Subsequent to retrieval, the disintegrated implants and selected peri-implant tissue were instantly preserved in 10% neutral buffered formalin at a pH of 7.2 – 7.4 (implants: n = 5, peri-implant tissue: n = 6) and in 4 % glutaraldehyde (implants: n = 5, peri-implant tissue: n = 5) (Figure 3.6). All samples underwent further procedures for qualitative analysis: the peri-implant tissues were prepared for light microscopy using haematoxylin and eosin (H&E) staining, and for scanning electron microscopy (SEM), transmission electron microscopy (TEM), and energy-dispersive X-ray spectroscopy (EDS). Concurrently, the retrieved implants were examined using SEM and analysed using EDS.

3.3.2.1 Haematoxycillin and Eosin Staining (H & E)

Following fixation with 10 % neutral buffered formalin, the peri-implant tissues (n = 6) were put in cassettes (Fig. 3.7B). The samples were processed using an automated tissue processor (Leica ASP300S Biosystems, USA). The processing approach strictly adhered to the Leica guidelines, which involved dehydrating the samples by exposing them to a series of graded ethanol concentrations, beginning at 70%, then increasing to 90%, and finally to 100%. The ethanol was subsequently cleaned using xylene. The sample matrix and structure were subsequently preserved by infiltration and embedding in paraffin to generate a paraffin block (Tissue Embedding Console System, Tissue-Tek®, USA) (Fig. 3.7C). Serial sections of approximately 3 µm were cut from paraffin blocks using a microtome (Leica RM2255, United States) (Fig. 3 .7E and F). The floating tissue ribbon in the water bath (10 °C) was then captured on a glass slide (Fig. 3.7G). Before staining, the tissue was dried in an oven at 37 °C for 24 hours (Fig. 3.7H and I).

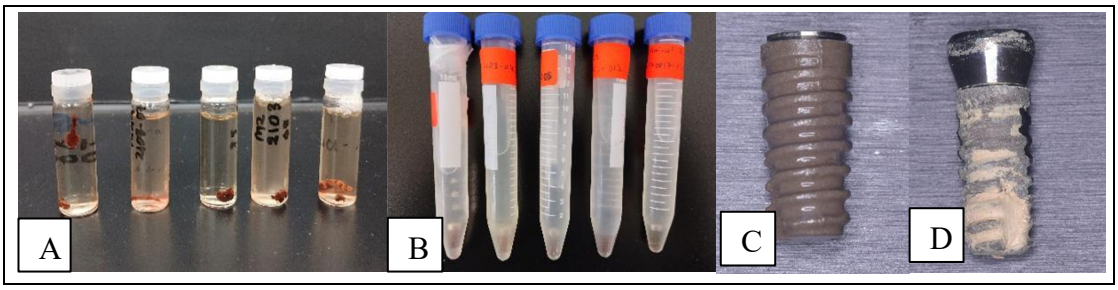

Figure 3.6 Collected Samples and Preparation before Further Processing for Histology Evaluation Under Light Microscopy, SEM or TEM.

Notes: Fixation of peri-implant tissue and implant in 4 % glutaraldehyde in A) and B), respectively. Photo of disintegrated porous NiTiDent implant taken after completing SEM analysis. C) The implant with the cover screw and D) the implant with healing abutment with gross bone tissue still present (after the second stage was commenced). The implant size: 4.5 mm in diameter and 10 mm in length.

The staining procedures started with the de-paraffinization of the samples with a clearing agent (xylene) to remove paraffin that adhered to the glass slide. Next, the samples were slowly dipped into a series of decreasing alcohol concentrations to rehydrate the tissue and then rinsed with distilled water. For primary staining, the samples were incubated with haematoxylin for 5 minutes, then washed under running tap water for 5 minutes to bluish, followed by distilled water. Then, the samples were

counterstained with eosin for 5 minutes, and dehydration was followed by exposure to alcohol at increasing concentrations (95% for 20 seconds, then 100% for 3 minutes) (Fig. 3 .7J, K, and L). Finally, the alcohol was cleared with xylene, and the slides were allowed to dry before viewing under the light microscope (M205, Leica, United States) (Fig. 3.7 M), (Lisowski, n.d).

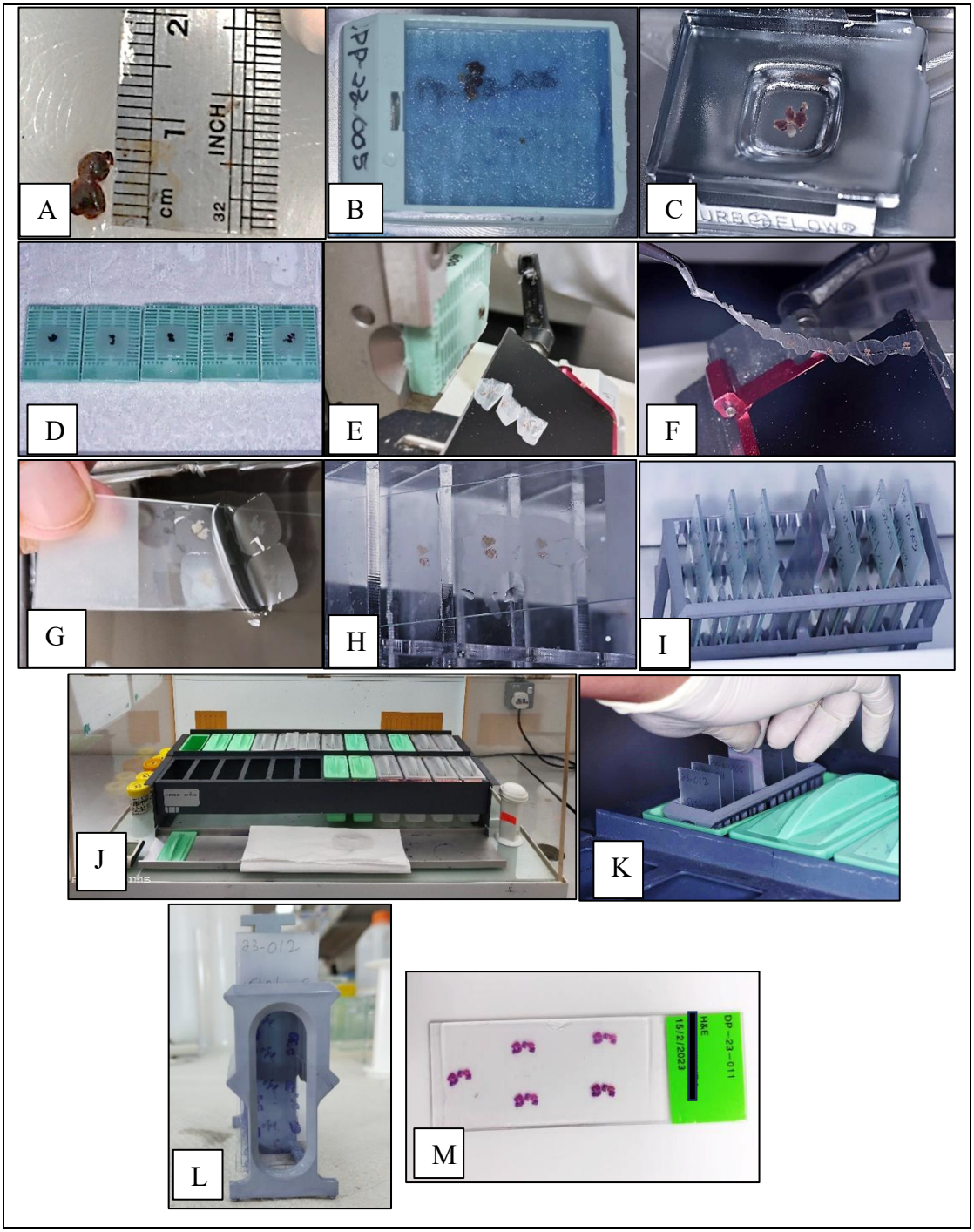

Figure 3.7 Sample Preparation for H&E.

Notes: A) The fixed tissue sample measured by a pathologist. B) Tissue sample in cassette after overnight processed in an automatic machine tissue processor. C) The sample in liquefied paraffin in the mould during an embedding process. D) Samples in the paraffin blocks. E) Sample trimmed to reach the whole sample from the paraffin block. F) End of the initial section held with a tweezer to prevent the folding of the sections and allow them to float in a water bath. G) The floated sample ribbons in a water bath caught using a glass slide. H) glass slides dried up in the oven. I) Tissue sample slides on the rack. J) Staining chemical equipment in the fume cabinet. K) Immersion of the sample in decreasing alcohol concentrations series after de-paraffinization and before staining with haematoxylin, then eosin. L) Sample to dry up at room temperature and M) glass slide with completed H & E sample staining.

3.3.2.2 Scanning Electron Microscopy (SEM)

Samples analysed under SEM (peri-implant tissue, n = 5, disintegrated implant, n = 5) and TEM (peri-implant tissue, n = 5) were primarily fixed with 4 % formaldehyde and kept in a refrigerator at 4°C before processing. The samples were transferred to the vial and washed three times with 0.1 M sodium cacodylate buffer (3 minutes each). Then, they were immersed in 1% osmium tetroxide at 4°C for 2 hours for post-fixation and rinsed with 0.1 M sodium cacodylate buffer, as before (Fischer et al., 2012).

Next, the fixed samples were dehydrated by immersion in acetone at increasing concentrations over the respective times to gently remove water from the samples without causing defects. Subsequently, 1 mm^3 of each tissue sample was excised for TEM analysis. The remaining tissues (~ 1 cm^2) were infiltrated with acetone and hexamethyldisilazane (HMDS) at different mixture ratios (acetone: HMDS, 1. at 2:1 for 1 hour, 2. at 1:2 for 1 hour, 3. at 100 % HMDS in 3 consecutive solutions for 30 minutes each, and finally 100 % acetone overnight). The samples were then placed in a desiccator and allowed to air-dry overnight at room temperature (Fischer et al., 2012).

The dried samples were then mounted on the SEM sample stub using double-sided sticky tape, followed by a 50-second platinum coating in a sputter coater before viewing. Similar procedures were done for the disintegrated implant. The samples were examined using an FEI Quanta 200 SEM (Germany) at 15 kV. The disintegrated implants (n = 6) were coated with a gold-palladium coating material ~ 1.5–3.0 nm thick, and the mapping of elements over the implant samples was analysed.

3.3.2.3 Transmission Electron Microscopy (TEM) and Energy-Dispersive X-Ray Spectroscopy (EDS)

Following dehydration (as described earlier), the tissues prepared for TEM were infiltrated with an acetone and resin mixture at a prescribed time interval in a different acetone: resin ratio mixture. A decanted initial infiltration was done with a 1:1 ratio (1 hour). Then, with a ratio of 1:3 (2 hours), 100% resin (overnight), and finally replenished with new 100 % resin (2 hours). The infiltration was conducted while the tissue was placed on a rotator. The samples were then positioned into beam capsules and fully impregnated with resin embedding medium for 24–48 hours in an oven (60–70 °C) to allow the resin to polymerize completely and form a sample block (Fig. 3.8A and B) (Mascorro & Bozzola, 2007; Webster, 2007).

Several sections of ~ 800 nm of the sample block were cut using a wet glass knife on the ultramicrotome (Fig. 3.8C) (Hagler, 2007). The thick sections floated in the boat were transferred to a labelled glass slide and dried on a 70 °C hot plate (Fig. 3.8D and E). Once the glass slide was dried, the sample was stained with a mixture of 1% toluidine and 1% sodium borate. The toluidine blue stain was applied to the dried section using a filtered syringe so that, the samples' peripheral border was surrounded with a small amount of stain (Ellis, 2007). The slide was then allowed to dry on the hot plate until the edge of the sample turned green (Fig. 3.8F). Then, an excess stain was removed with distilled water and allowed to air-dry before being examined under a light microscope to determine the area of interest. A thin section of the area of interest (based on the previous thick section) was cut using a diamond knife that was integral to a boat and attached to the knife holder of the ultramicrotomy (Leica UM UC7, United State) (Fig. 3.8G).

The sectioning was conducted at a speed of 0.7 mm/s, and the ribbon was made to ~ 70 nm thickness when these floated sections exhibited a silver interference colour (Fig. 3.8H). Subsequently, a grid was cleaned in the diluted nitric acid solution before picking up the floated sections in the boat. Using cross-action EM forceps, the grid was submerged below the water surface in the boat to pick up the section. Once the section was in place, the grid was gently lifted vertically from the water and transferred to dry filter paper to remove the water from the grid. With forceps, the grid was picked up and floated side-down on a uranyl acetate stain. After 15 minutes, the grid was washed with warm, freshly boiled, deionised water. This procedure was repeated three times using

fresh deionised water. Then, a few drops of lead citrate (one drop for each grid) were placed on parafilm in a petri dish prepared in a CO_2-free chamber. The grid was placed on a drop of lead citrate and floated side down with a carefully opened dish cover (only enough to insert the grid). Then the petri dish cover was immediately closed. After 10 minutes, the grids were removed and swirled in the beaker containing newly freshened boiled deionised water. The procedure was repeated three times with new solutions. Along with the staining procedures, the grids were kept in a wet condition. After completing the staining procedures, the grids were allowed to dry using filter paper. The structural and elemental analyses were conducted with TEM (Tecnai G2 Spirit Bio TWW, ThermoFisher Scientific, United State) (Fig. 3.9) and energy-dispersive X-ray spectroscopy. The procedures are as shown in Fig. 3.8.

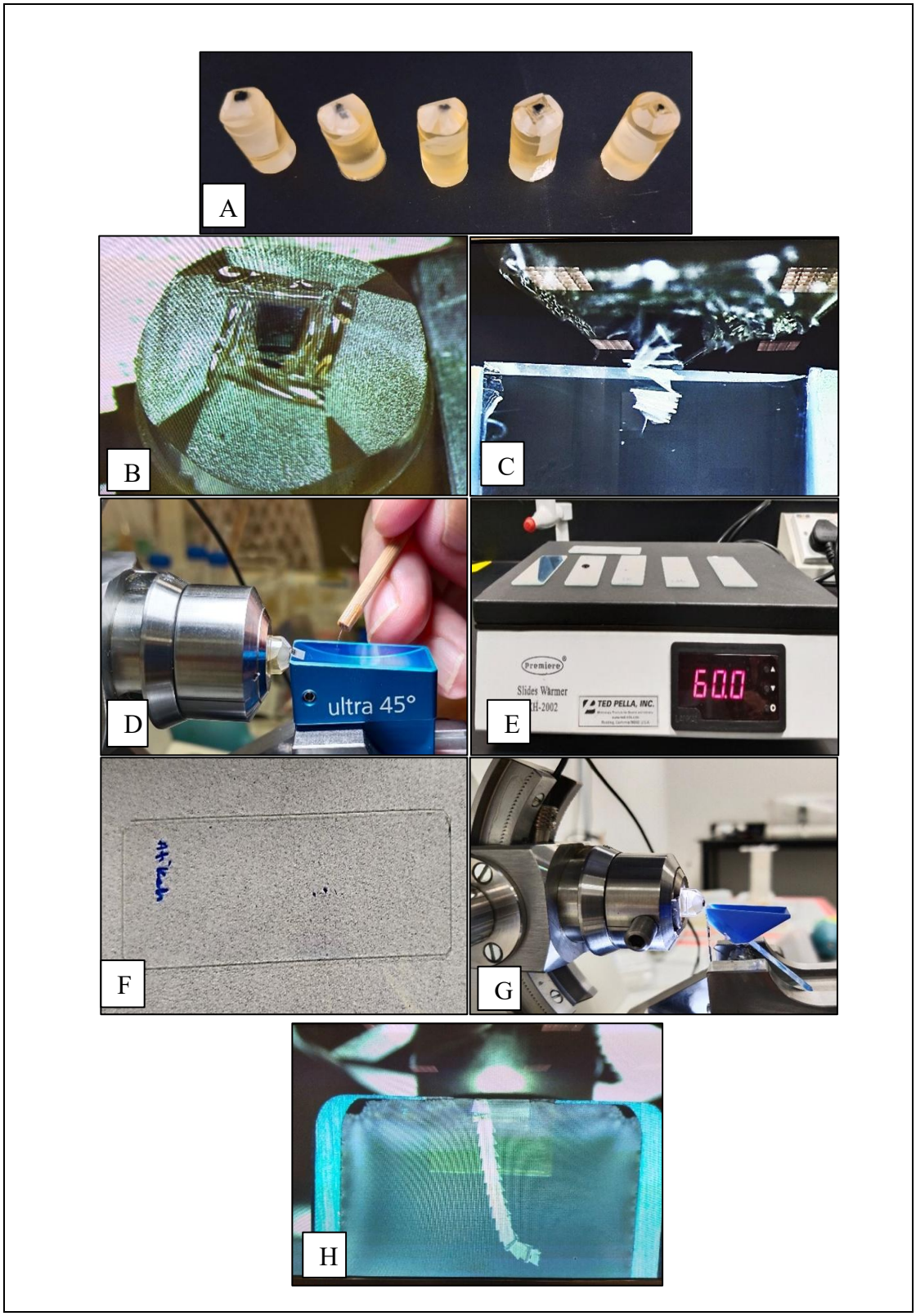

Figure 3.8 Sample Preparation for TEM Analysis

Notes: A) Resin block with samples. B) Sample mounted in sample ultramicrotome holder C) The sample block face to the prepared blade sealed to the boat. D) A Close-up photo showed trimming of the sample block until the desired whole sample was reached. E) The floated section is caught and transferred to the glass slide. F) The sample dried up after being stained with Toluidine blue. G) Sample after drying up and

ready for assessment under light microscopy. H) A thin section of the sample was prepared, and the reflected interference colour was observed to ensure the correct sample thickness was obtained

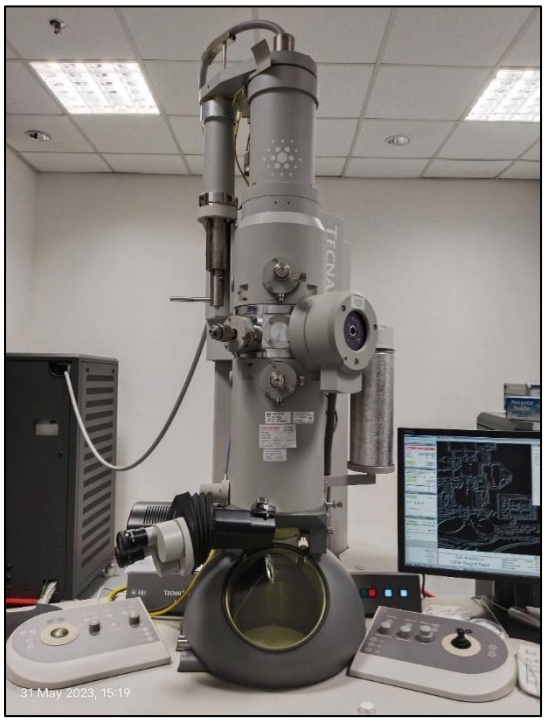

Figure 3.9 Transmission Electron Microscopy Operating Machine.

3.3.3 Assessment of Surgical Drill

3.3.3.1 Synthetic Blocks Preparation

The study utilised a standardised synthetic block (Implant training plate, Biomechanicals Models®, SelModels SL, Barcelona, Spain) measuring 140 × 90 × 15 mm. This block consists of a consistent 2 mm cortical plate covering the cancellous part, replicating human bone condition type 1 as per the Lekholm and Zarb classification. A clamp firmly held the bone block in place on the table.

3.3.3.2 Operational Procedure

The implant surgical drill (NiTiDent, Malaysia), implant motor (Azdent, China), and handpiece (NSK, Japan) were used in the same manner as for placing a porous nickel-titanium dental implant in a clinic. The maximum motor speed was set to 800

rpm, and a single operator completed the operation. The surgical implant drill was made of twisted stainless steel (n = 3). Initially, a pilot drill (2 mm diameter x 10 mm) was used to make the initial puncture at a depth of 10 mm. The drilling sequence was then gradually increased to 2.8, 3.2, 4.2, and 4.4 mm at comparable depths, following the manufacturer's instructions. Throughout the operations, extensive direct irrigation was used to prevent overheating at the interface between the surgical drill and the synthetic block. An optical microscope and a scanning electron microscope (SEM) were used to test the drills before their first use and at 5× and 10× magnification thereafter.

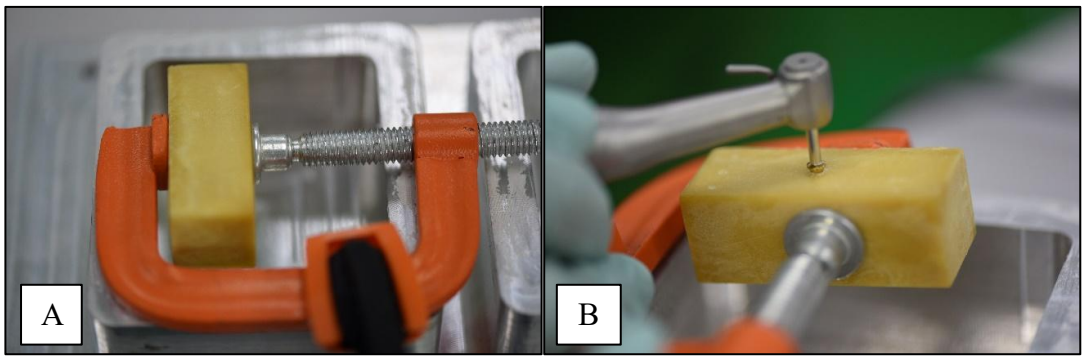

Figure 3.10 A Model for *In Vitro* Surgical Drill Evaluation.

Note: B) Drilling with NiTiDent Tuah implant surgical drill (copious irrigation was done but not shown in this photo).

3.3.4 Monoculture with Human Mesenchymal Cell

3.3.4.1 Initiation of Cell Culture and Seeding on Biomaterials

The Poietic™ human mesenchymal stem cells (hMSCs), labelled as PT-2501 from Batch 22TL301024, were commercially obtained from Lonza, a leading biotechnology firm based in Walkersville, Maryland, USA. These stem cells, known for their potential in regenerative medicine and tissue engineering, reached passage 2, ensuring they were in a suitable condition for further research and applications. Thawing of the cells and subsequent subculture were strictly followed by Lonza's technical instructions until the cells reached passage 5. Briefly, the thawed cell suspension was added to a 15 mL centrifuge tube containing 5 mL of temperature-equilibrated medium using a micropipette. Then, the tube was centrifuged at 500 x g for 5 minutes at room temperature. The supernatant was discarded while the pellet was

resuspended with 1 mL of temperature-equilibrated human mesenchymal stem cell growth medium (MSCGM™, Lonza Walkersville, Inc., Walkersville, MD, USA) by gently pipetting up and down. The total cell viability was counted (95%), and the volume of suspended cells needed for each prepared 25 cm^2 flask containing 5 mL of MSCGM™ was calculated (6 x 10^3 cells per cm^2). The flask was gently rocked after seeding to disperse the cells evenly, and then incubated at 37 °C with 5% CO_2 and 90% humidity. The culture medium was replaced every 3 days until the cells reached approximately 90% confluence, at which point they were subcultured.

For this study, a 4.5 mm-diameter, 10 mm-long porous NiTi dental implant (pNT), which was the same implant used in this clinical, was utilised. The similarly sized dense, machined-surface Ti6Al4V and machined-surface NiTi (mNT), fabricated through casting, served as controls; both were supplied by the same company involved in this research. All specimens came with sterilised packaging and were further sterilised with UV light for 20 minutes prior to each test.

At passage 5, 50 µL of MSCGM™ media consisting of 1.5 × 10^4 cells was dropped wisely on each sterile biomaterial (negative control: directly seeded into the 24-well, positive control: machined surfaces of NiTi (mNT), and Ti6AL4V (Ti)) and tested dental implant (porous NiTi Dent Tuah dental implant (pNT)) that were already placed in a 24-well plate. 950 µl of the osteogenic medium was added after 15 minutes of incubation of the seeded hMSCs on the biomaterials in a humidified atmosphere with 5% CO2 at 37 °C to promote initial cell attachment (Gotman et al., 2013). The osteogenic media (OM) responsible for inducing osteogenic differentiation in this cell comprises Dulbecco's Modified Essential Medium (DMEM, Sigma-Aldrich, Germany), supplemented with 10 % foetal bovine serum (Sigma-Aldrich, Germany), 100 units/ml penicillin-streptomycin (Gibco, Thermo Fisher Scientific, United States), 50 nM dexamethasone, 0.2 mM ascorbic acid, and 10 mM b-glycerophosphate. On another 24-well plate, another 1.5 × 10^4 cells were suspended in 1 ml of osteogenic medium as a negative control. After 1 day of incubation, all biomaterials were transferred to the new well, the plate on which the negative control had previously been suspended. Fresh OM was added (1 ml per well) and replaced every 3 days.

3.3.4.2 Cell Viability Assay

The cellular metabolic activity was assessed by determining cell viability using a colourimetric assay with (3-(4,5-dimethylthiazol-2-yl)-2,5-diphenyl tetrasodium bromide) (MTT Merck, Germany). This assay measures dehydrogenase activity in viable cells, resulting in the formation of purple formazan crystals from the pale-yellow tetrazolium salt of MTT. Following the manufacturer's instructions, 100 µl of the MTT mixture was added to each cell-seeded well for both the control and NiTi dental implants. The plate was gently tapped to mix the solution, covered with aluminium foil, and incubated for 4 hours at 5% CO_2 and 37°C. Subsequently, isopropanol with 0.04 NHCl was added to each well and thoroughly mixed. The absorbance was then measured at a wavelength of 570 nm using an ELISA plate reader. The assay was performed in replicates on days 1, 7, 14, 21, and 28.

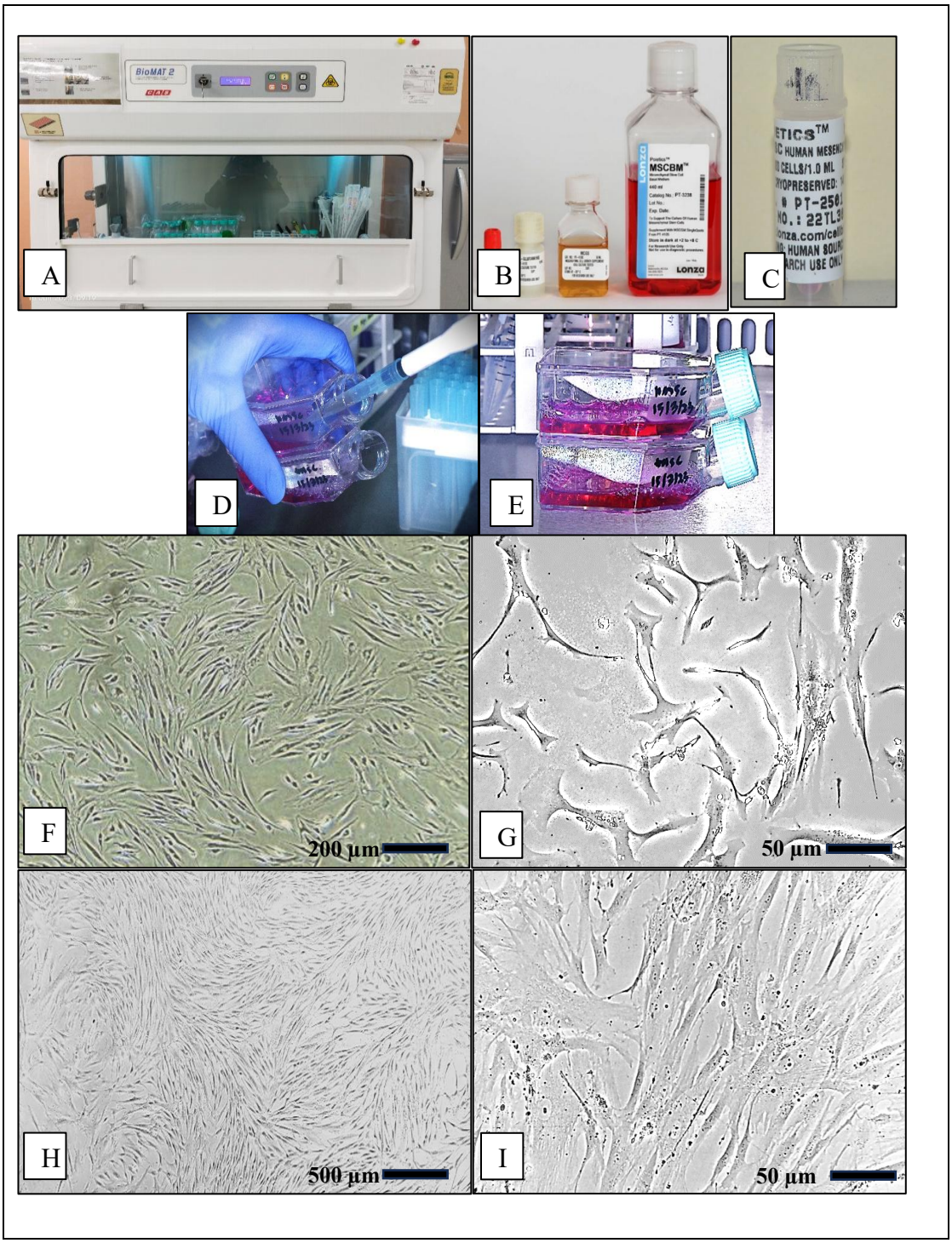

Figure 3.11 Instruments, Media and hMSCs Used in this Study.

Notes: Mesenchymal cells under inverted microscopy at passage 4, ~50% confluence, at 10x (F) and 40x (G) magnification. The same cells are at ~80% confluence at magnifications of 4x (H) and 40x (I).

3.3.4.3 Alkaline Phosphatase Activity

This study assessed the osteogenic differentiation of hMSCs in osteogenic media by measuring alkaline phosphatase (ALP) activity using the ALP assay with MAK 447 (Merck KGaA, Darmstadt, Germany). ALP activity was evaluated 7 and 14 days after seeding. The cells were washed twice with 1 ml of PBS and then lysed by shaking for 20 minutes in 0.5 ml of 0.2% Triton X-100 (Sigma-Aldrich) in purified water at room temperature. Subsequently, 50 µl of each sample was transferred into a 96-well plate containing 150 µl of working reagent in triplicate. This working reagent comprises a mixture of assay buffer, 0.2 M Mg acetate, and 1 M p-nitrophenol phosphate solution, prepared in accordance with manufacturing guidelines. Additionally, 200 µl of purified water and 200 µl of calibrator liquid were transferred into separate wells of the 96-well plate. The plate was gently tapped to ensure thorough mixing. The optical density (OD) of each prepared mixture was measured immediately on a plate reader at 405 nm (T = 0 minutes) and repeated after 4 minutes (T = 4 minutes). The ALP activity was calculated following this formula:

$$\text{ALP } (\mu\text{mol}/(\text{L.min}) \quad \frac{(OD_{T4} - OD_{T0}) \times 1000 \times \text{RxnVol}}{\varepsilon_{PNP} \times L \times (OD_{cal} - OD_{Blank}) \times \text{SmplVol} \times T} \qquad (3.3)$$

3.3.4.4 Alizarin Red S staining

Calcium deposition indicating mineralisation in this monolayer cell culture was assessed using the Alizarin Red S assay (ScienCell's ARS Staining Quantification Assay, Ared-Q, catalogue #8678, Faraday Ave, Carlsbad). Following the 21st and 28th post-seeding days, the culture medium from each well was removed, and the cells were gently rinsed three times with 1 mL of phosphate-buffered saline (PBS). The cells were then fixed in 4% formaldehyde for 15 minutes at room temperature. Next, the fixative was aspirated, and the container was rinsed three times with distilled water. Once the distilled water was completely removed, 1 mL of 40 mM ARS was added to each well, and the plate was incubated at room temperature and gently shaken at 40 rpm for 20–30 minutes. Then the dye was removed, and the cell was rinsed five times with distilled water. The plate was tilted for approximately 2 minutes to facilitate the removal of excess water, then stored at –20 °C before dye extraction. Quantification of

mineralisation was performed by acid extraction of the ARS stain, following the protocol of Gregory et al. (2004).

200 µL of 10 % acetic acid was added to each well, followed by incubation at room temperature and gentle shaking with a shaker for 30 minutes. At this point, cell monolayers on negative controls, including the other samples (positive control and NiTi), are now loosely attached. The samples were transferred into a 50 mL centrifuge tube and vortexed for 30 seconds. Then each tube was sealed with Parafilm, heated at 85 °C for 10 minutes, and transferred to ice for 5 minutes. The slurry was then centrifuged at 20,000 g for 15 minutes. After that, 200 µL of supernatant was transferred to a new tube. 75 µL of 10 % ammonium hydroxide (pH 4.1–4.5) was added to neutralise the acid. Then, 50 µL of each sample was transferred into each well of a 96-well plate in triplicate. The absorbance of aliquots was measured at 405 nm with a plate reader. Figure 3.11 exhibits staining of the cells following Alizarin Red S staining.

3.3.4.5 Visualisation of The Cultured Cells on Biomaterials

For visualisation, the cells were seeded onto a glass slide cover (Corning®, Merck, Germany) as a negative control. All negative, positive and tested samples were collected at predetermined intervals on days 7, 14, 21, and 28, and initially fixed in a 4% glutaraldehyde solution for 24 hours at 4°C. Subsequently, the samples were washed in 0.1 M sodium cacodylate buffer at pH 7.2, then post-fixed in 1% osmium tetroxide for 2 hours. The washing step was then repeated with a similar solution, followed by a series of dehydration steps using graded acetone solutions ranging from 35% to 100%. The samples were then infiltrated with a mixture of acetone and HMDS, dried, mounted on a stub, sputter-coated with platinum, and viewed under a scanning electron microscope (SEM-FEI Quanta 200, US) operating at 15 kV.

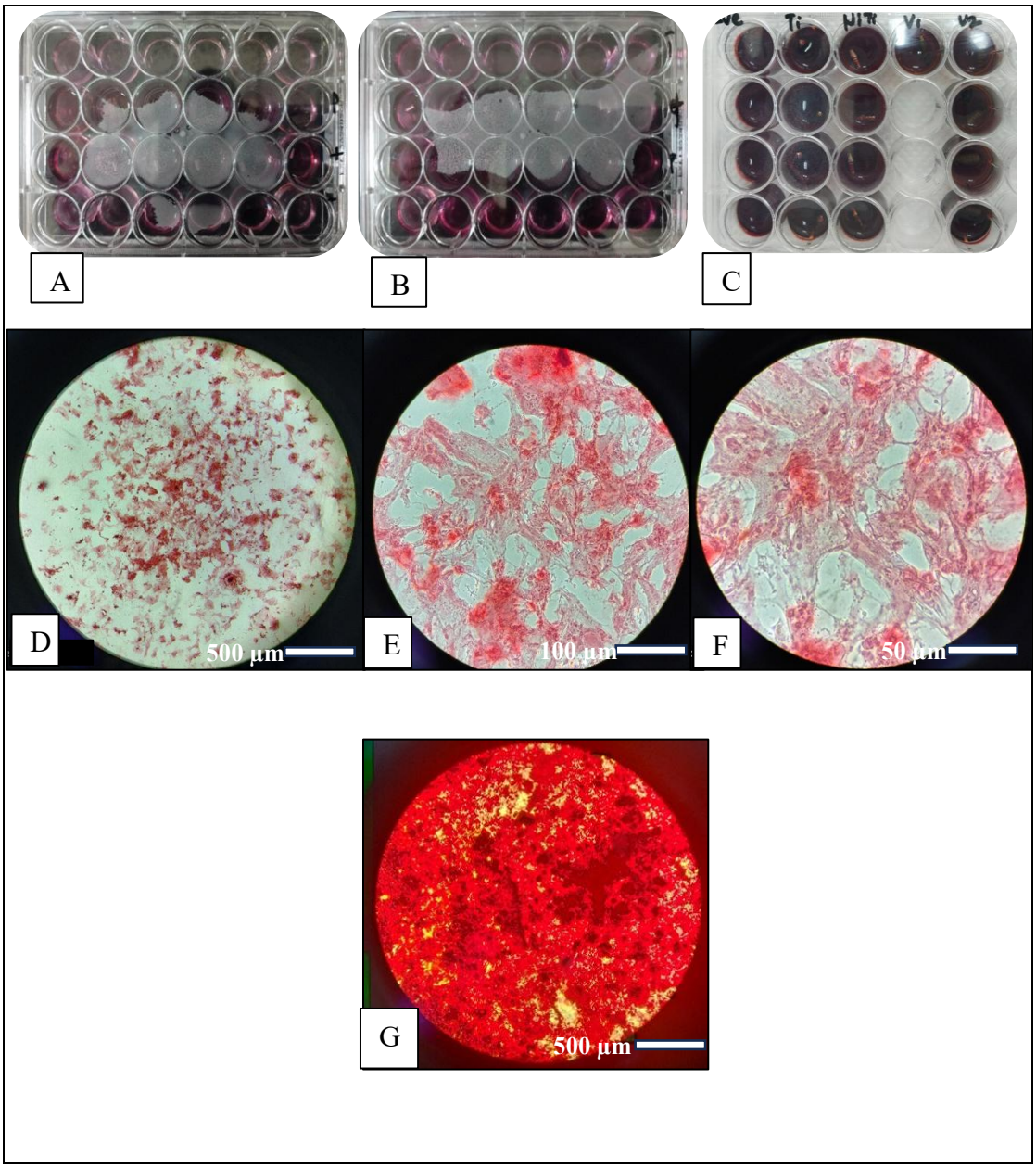

Figure 3.12 Assessing Cell Viability Using MTT and Calcium Deposition in Monolayer Cultured Cells Using Alizarin Red Staining ARS).

Notes: A purplish-coloured formazan crystal formation was seen in 7 days (A) and 14 days (B). C) showed fixation of the samples in 4 % formaldehyde. The image of the negative control under inverted light microscopy showed calcium deposition in this mesenchymal monolayer cultured in osteogenic media. An osteogenic-like cell image taken at 21 days at 4 x (D), 20 x (E), and 40 x (F) magnifications. G) ARS staining at 28 days of incubation (image at 4 x magnification)

3.3.5 Ni Ion Release

Nickel ion release was assessed in three solutions: osteogenic media, DMEM at pH 7.2, where the medium was collected from conventional NiTi (control) and porous NiTi dental implants (tested) at days 1, 3, 7, 14, 21, and 28 after seeding; and 0.9% NaCl at pH levels of 6 (± 0.2) and 7.2 (± 0.2). For both NaCl pH conditions, the implants (n = 6) were individually placed in 50 mL of the NaCl solution and stored at 37 °C. At predetermined intervals, 10 mL aliquots were taken from each test bottle, and the solution was replenished with fresh NaCl. Ion release was measured on days 1 and 3 (immediate), 14 (intermediate), and 28 (late). The nickel ion concentration was determined using inductively coupled plasma optical emission spectroscopy (ICP-OES, OPTIMA 2100DV, United States). Figure 3.13 illustrates several procedures performed during the analysis.

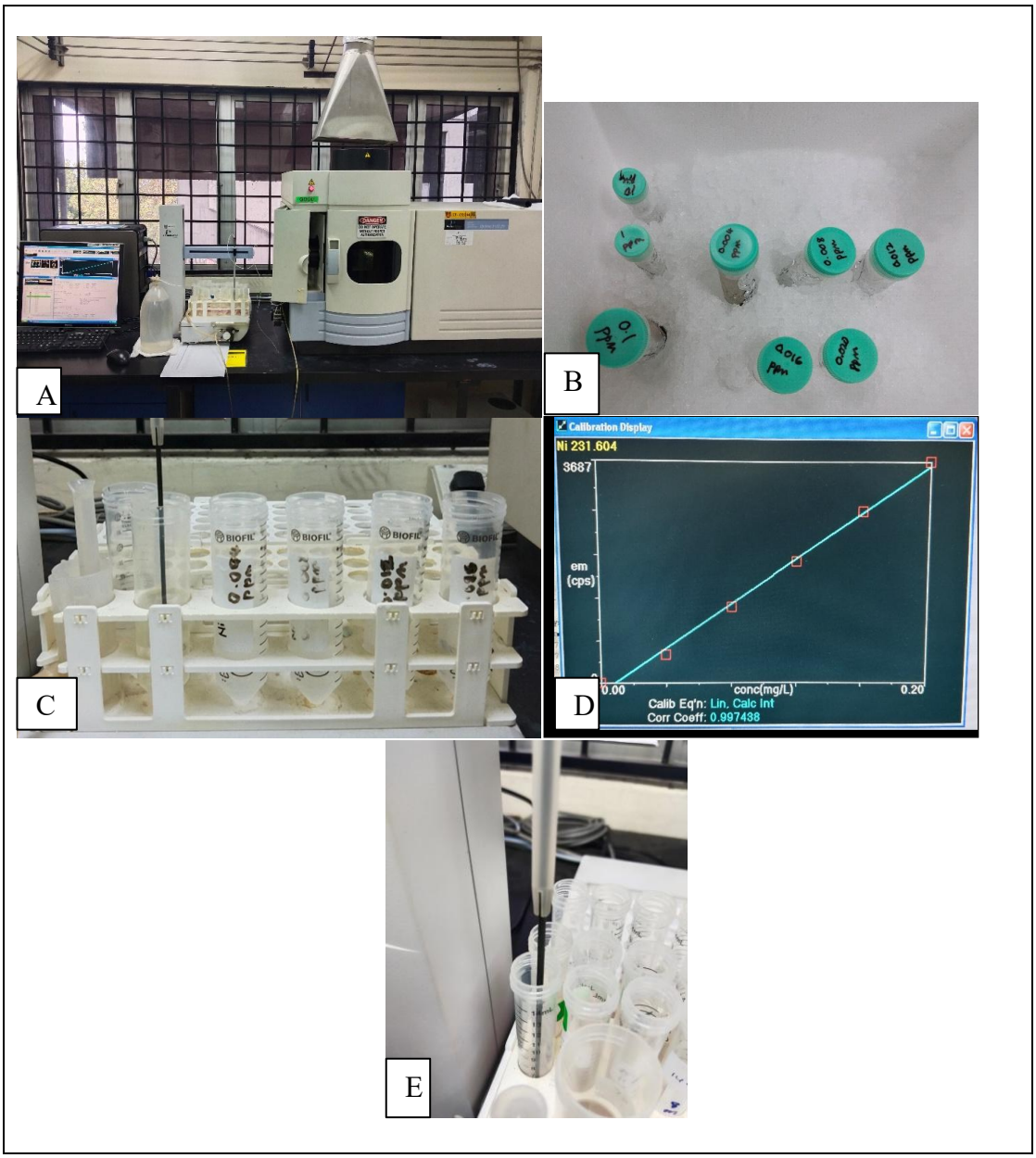

Figure 3.13 A) An Inductive Coupled Plasma Optical Emission Spectroscopy.

Notes: Calibration procedure prior to the actual analysis of the collected samples (B to D). B) The standard Nickel solution is prepared using ultrapure water at different Ni concentrations, starting at 0.002 to 0.020 ppm. C)The Ni content measurement process where the probe moves from one to another over the prepared standard solution, automatically. D) An acceptable correlation coefficient result was generated based on the standard solution prepared. E) Measurement of Ni (if present) in the collected samples.

3.3.6 Data Collection for Part B

A comprehensive qualitative analysis was conducted using scanning electron microscopy (SEM), transmission electron microscopy (TEM) and energy-dispersive X-

ray spectroscopy (EDS) on peri-implant tissue, implants retrieved from failed cases, and surgical drills. Additionally, data on viability (MTT) and osteogenic potential of hMSCs (ALP and ARS) on porous NiTiDent Tuah dental implants were collected at specific time points, as outlined in the respective sections. All datasets underwent thorough statistical processing using IBM SPSS version 29.0.1.0 (177) (IBM Corp., Armonk, NY). A repeated-measures ANOVA was conducted for all dependent variables, and pairwise comparisons with Bonferroni correction were used to identify significant differences in the prescribed treatment, subjects, and treatment-time interaction. In cases where differences in variances were detected, statistical significance was set at $p < 0.05$.

CHAPTER 4
RESULTS

4.1 Chapter Outline

The primary aim of this study (Part A) focuses on a clinical trial; to evaluate the safety and performance of a porous NiTi dental implant (NiTiDent Tuah, Nitium Technology Sdn. Bhd, Malaysia) in comparison to a dense, non-porous dental implant for the restoration of single-tooth gaps in the posterior mandible. Key factors assessed were implant stability, peri-implant tissue health, crestal bone level, patient satisfaction, and oral health-related quality of life. The study also monitored the implant's success and survival rates.

The secondary aim in Part B entailed the detailed laboratory analyses of the peri-implant soft tissue surrounding the explanted implants and the implants themselves to gain a deeper insight into identifying causes of biological osteointegration failure involving porous NiTi dental implant. Additionally, the study examined the porous NiTi implant's ability to promote the proliferation and differentiation of bone marrow-derived hMSCs into osteogenic-like cells, facilitating the production of a mineralised matrix. The potential release of nickel ions from the implant and its biological effects were also explored.

4.2 Results for Part A

4.2.1 Demographic Data of Participants in This Study

Table 4.1 presents the demographic information of 30 participants who successfully enrolled in this study. Overall, female participants comprised a higher proportion at 70% (n = 21), compared to males at 30% (n = 9). The average age of participants was similar across genders, with females having a mean age of 39.3 years (± 10.5) and males having a mean age of 39.6 years (± 7.2).

In terms of education, 73.3% (n = 22) of participants held tertiary qualifications, while an equal number had primary or secondary education, each accounting for 13.3%

(n = 4). Occupationally, the majority of participants were in the professional category, totalling 16 (53.3%). This was followed by the clerical category, with 8 participants (26.7%), and other occupations, with 6 participants (20%). This distribution illustrates a diverse range of employment types among the participants.

Household income was categorised into four categories as in Table 4.1. Most participants had an income of less than RM4,850 (14 participants, 46.7%) and the RM4,850 to RM10,959 range (12 participants, 40%). Only a small number of participants (2 each, 6.7%) fell into the higher-income categories of RM10,959 to RM15,040 and above RM15,040. This indicates a predominance of participants from lower- to middle-income groups.

Table 4.1
Descriptive Analysis of Participant Demographic Data from Universiti Teknologi MARA and Universiti Kebangsaan Malaysia

			Total (n)				**Total Participant**
Sex	**Female**		**Male**				**30**
n	21		9				
Age (Year)	**18 - 24**	**25 - 34**	**35 - 44**	**45 -55**	**55 - 64**	**65 and above**	
n	2	6	14	4	2	1	
Mean (SD)	39.4 (9.4): Female: 39.3 (10.5), Male: 39.6 (7.2)						
Education	**Primary**		**Secondary**	**Tertiary**			
n	4		4	22			
Occupation	**Professional**		**Clerical**	**Others**			
n	16		8	6			
Income (RM)	**< 4850**		**4850 - 10959**	**10959-15040**		**>15040**	
n	14		12	2		2	

4.2.2 Insertion Torque Value (ITV) and Implant Stability Assessment between AnyRidge® and NiTiDent Tuah Dental Implants

Table 4.2 presents a comparison of insertion torque values (ITV) and primary stability between the control group (AnyRidge®, Megagen, Korea) and the tested group (NiTiDent Tuah, Nitium Technology, Malaysia). The control group exhibited a

significantly higher median ITV of 38.00 Ncm (IQR: 7.75) compared to the tested group's median of 35.00 Ncm (IQR: 0.00), with a *p*-value of 0.01.

Regarding primary stability, as measured by the implant stability quotient (ISQ), the AnyRidge® dental implant had a significantly higher mean ISQ of 64.18 ± 10.19 compared with the NiTiDent Tuah dental implant, which had a mean ISQ of 52.18 ± 13.63. This difference yielded a t-value of 2.76 and a *p*-value of 0.01, with a mean difference (MD) of 11.95 and a 95% confidence interval ranging from 3.09 to 20.90 (Table 4.3).

Additionally, a correlation analysis indicated a weak negative correlation between ITV and ISQ value, with a correlation coefficient of -0.36 and a *p*-value of 0.31. This suggests that ITV does not directly predict ISQ values.

Table 4.2
A Comparison of Insertion Torque Value (ITV), Primary Stability between AnyRidge® and Porous NiTiDent Tuah Dental Implants and Correlation between ITV and Implant Stability

Type of Implant	**Insertion Torque Value (Ncm)[a]**		**Primary Implant Stability (ISQ)[b]**		**Correlation[c]**		
	Median (IQR)	***p*-value**	**Mean ± SD**	***p*-value**	**Parameter Observed**	**Correlation Coefficient**	***p*-value**
Anyridge®	38.00 (7.75)	0.01	64.18 ± 10.19	0.01	ITV – ISQ	-0.36	0.31
Porous NiTi Dent Tuah	35.00 (0.00)		52.18 ± 13.63				

Notes: [a] Independent-Samples Mann-Whitney U Test. [b] Independent T-test, F = 1.35 (28). [C] Spearman's rho Correlation. The *p*-value was set at 0.05.

Table 4.3
Implant Stability Quotient (ISQ) Between AnyRidge® and Porous NiTiDent Tuah Dental Implants

Type of Implant	**Total Sample (n)**	**Mean ± SD**	**Mean Difference (MD)**	**95 % Confidence Interval**		**t-statistic (df)**	***p*-value**
				Lower	**Upper**		
AnyRidge®	18	64.18 ± 10.19	11.99	3.09	20.90	2.76 (28)	0.01
Porous NiTi Dent Tuah	12	52.18 ± 13.63					

Note: Independent T-test. F = 1.37 (28). Significant level set at 0.05

Further comparison of the ISQ values was conducted at three key time points for AnyRidge® and two time points for NiTiDent Tuah. The key predetermined times observed, namely, V_1 (day of implant placement), V_3 (day of second-stage surgery), and V_4 (day of crown placement), are listed in Table 4.4. In a repeated-measures ANOVA, the mean ISQ value of the AnyRidge® dental implant significantly increased over time ($p < 0.001$). Multiple comparisons with Bonferroni correction revealed significant differences in ISQ values with the following MD: V_1–V_3: -8.94 (95% CI: -13.19, -4.67), $p < 0.001$; V_1–V_4: -14.74 (95% CI: -20.19, -2.29), $p < 0.001$; and V_3–V_4: -5.80 (95% CI: -8.78, -2.82), $p < 0.001$. The increase in ISQ values for the Anyridge® implant across all time points indicates a consistent improvement in implant stability.

In contrast, a paired t-test comparing ISQ values at two observation times (V_1 and V_3) showed that the ISQ values for the NiTiDent Tuah implant were significantly lower at V_3 (7.33 ± 11.67) than at V_1 (52.18 ± 13.63), with a p-value < 0.001. At V_3, five participants were excluded due to early implant disintegration before reaching the second stage.

Table 4.4
Descriptive Analysis and Comparison of the Effect of Time on Implant Stability Quotient Value Between AnyRidge® and Porous NiTiDent Tuah Dental Implants

Time	Total sample (n)	Mean ± SD	*p*-value
AnyRidge®[a]			
$V_1^{A,B}$	18	64.18 ± 10.19	< 0.001
$V_3^{A,C}$		73.12 ± 8.41	
$V_4^{B,C}$		78.92 ± 7.29	
NiTiDent Tuah[b]			
V_1	12 (V_1) 7 (V_3)	52.18 ± 13.63	< 0.001
V_3		7.33 ± 11.67	

Notes: V_1 –Visit 1: Day of implant placement, V_3 – Visit 3: Day of second surgery, V_4 – Visit 4: Day of crown placement. [a] A Repeated Measure ANOVA. F(df) = 41.12 (2). Pairwise comparison using Bonferroni correction. A similar capital, superscript letter indicates a significant difference between the measured time points. [b] Paired t- test. The mean difference is statistically significant at $p < 0.05$.

4.2.3 Evaluation of Peri-Implant Soft Tissues of AnyRidge® Dental Implant

The evaluation of peri-implant soft tissues focused on the incidence of inflammation, bleeding on probing (BOP), and probing depth at three predetermined

time points: V_4 (the day of crown placement), V_5 (the day of the first review, three months post-crown placement), and V_6 (the day of the second review, six months post-crown placement), as summarised in Table 4.5. This parameter was collected only for participants in the control group.

Throughout the observation period, no reported inflammation was observed at V4, with 100% of cases indicating "No" inflammation. At V_5, following three months of crown placement, a small percentage (16.7%, n = 3) developed inflammation—two cases were mild (11.1%), and one case was categorised as moderate (5.6%). In V_6, the incidence of inflammation further decreased to 11.1% (n = 2), with all cases classified as mild.

Regarding bleeding on probing, no cases of BOP were observed at V_4 (100% "No"). However, BOP was noted in three cases (16.7%) at V_5. This percentage declined to 11.1% (n = 2) at V_6, which aligned with the observed inflammation results.

In terms of probing depth (PD), the mean PD values remained relatively stable across visits: V_4 (1.6 ± 0.7 mm), V_5 (1.8 ± 0.9 mm), and V_6 (1.8 ± 0.7 mm). Multivariate analysis indicated a significant difference in PD over time (p = 0.02). A pairwise multiple comparison with Bonferroni correction revealed a significant increase in PD from V_4 to V_5 (p = 0.04). Overall, the findings indicate that there were no significant associations between inflammation, bleeding on probing (BOP) and probing depth during the observation period ($p > 0.05$).

Table 4.5
Peri-implant Soft Tissue Conditions within Observation Periods and Association between Inflammation, Bleeding and Probing on Peri-implant Probing Depth in AnyRidge® Dental Implant.

Parameter		**Incidence**		
		Present: Yes (Y) / No (N)	**Percentage (%)**	**Total (n)**
Inflammation (I)				
Time Observed	V_4	No	100	18
		Yes	0.0	0
	V_5	No	83.3	15
		Yes	16.7	3
		Mild	5.6	1
		Moderate	11.1	2
	V_6	No	88.9	16
		Yes	11.1	2

Parameter			Incidence		
		Present: Yes (Y) / No (N)		Percentage (%)	Total (n)
			Mild	11.1	2
			Moderate	0.0	0
Bleeding on Probing (BOP)					
Time Observed	V_4	No		100	18
		Yes		0.00	0
	V_5	No		83.3	15
		Yes		16.7	3
	V_6	No		88.9	16
		Yes		11.1	2

Peri-implant Tissue Probing Depth (PD)[a]

Time observed		Mean ± SD	*p*-value	Interaction*	Mean Difference (95 % CI)	*p*-value
	V_4	1.6 ± 0.7	0.02	$V_4 – V_5$	-0.20 (-0.45, 0.04)	0.13
	V_5	1.8 ± 0.9		$V_4 – V_6$[#]	-0.20 (-0.40, -0.01)	0.04
	V_6	1.8 ± 0.7		V_5 -V_6	0.00 (-0.15, 0.15)	1.00

Notes: V_4 – Visit 4: for crown placement; V_5 – Visit 5: the first (three months); and V_6 – Visit 6: the second (six months) post-placement. [a]A Repeated-Measure ANOVA of peri-implant tissue probing depth, F = 4.19 (2). *Pairwise multiple comparison using Bonferroni correction. [#] Indicates a significant difference in PD between two time-points. Association between inflammation, bleeding and peri-implant probing depth using Fisher-Freeman-Halton Exact Test. I – PD, p = 0.23, BOP – PD, p = 0.35. The significance was set at 0.05.

4.2.4 Evaluation of Crestal Bone Levels of AnyRidge® Dental Implant

Similar to the peri-implant soft tissue condition evaluation, Table 4.6 illustrates the changes in mesial and distal crestal bone levels of the AnyRidge® group at four evaluation time points: V_1 (baseline during surgical placement), V_4 (crown placement), V_5 (first review), and V_6 (second review after 3 and 6 months of crown placement). Observations indicated that the mesial and distal bone levels exhibited a similar pattern. Initially, there was crestal bone resorption at V_4 compared with baseline (V_1), with measurements of -0.22 ± 0.81 mm mesially and -0.39 ± 0.91 mm distally. Over time, the means of the crestal bone levels gradually improved in V_5 and V_6, although they remained slightly lower than the baseline (V_1) values (mesial: -0.62 ± 0.54, distal: -0.51 ± 0.73).

A repeated-measures ANOVA indicated a significant difference in bone levels across time points for both mesial and distal measurements ($F(3) = 11.11$, $p < 0.001$). Pairwise multiple comparisons with Bonferroni correction revealed significant differences: $V_1 – V_4$ ($p < 0.001$; mean difference (MD): -0.53, 95% CI: -0.87, -0.20) and $V_4 – V_6$ ($p < 0.001$; MD: 0.58, 95% CI: 0.21, 0.96). However, the difference between mesial and distal crestal bone levels was not statistically significant (MD: 0.018, 95% CI: -0.37, 0.41; $p = 0.93$).

Table 4.6
The Mean and Standard Deviation of Mesial and Distal Bone Levels Across Time in AnyRidge® Dental Implant Group

Time Evaluated[a]	**Location[b]**		**F (df)**	***p*-value**
	Mesial (mm)	**Distal (mm)**		
	Mean ± SD	**Mean ± SD**		
V_1^A	-0.62 ± 0.54	-0.51 ± 0.73	11.11 (3)	< 0.001
$V_4^{A,B}$	-0.22 ± 0.81	-0.39 ± 0.92		
V_5	-0.36 ± 0.79	-0.43 ± 0.75		
V_6^B	-0.56 ± 0.70	-0.67 ± 0.66		

Note: A Repeated-Measure ANOVA. V_1: surgical placement visit, V_4: crown placement visit, V_5: first review after 3 months and V_6: second review after 6 months of crown placement visits. Negative values indicate the bone level was above the abutment-implant fixture platform. [a] Time effect. A similar capital letter indicates multiple pairwise comparisons with Bonferroni correction, with significant differences between the time–to–time interactions. [b.] Location effect. The mean difference was set at a significance level of 0.05.

4.2.5 Patient Satisfaction and Patient-Related Outcome Satisfaction of Participants Receiving AnyRidge® Dental Implants

Table 4.7 illustrates the means and standard deviations of the Patient Satisfaction Questionnaire (PSQ) scores after 52 weeks of observation for participants who received AnyRidge® dental implants. The overall mean PSQ score was notably high, at 6.01 ± 1.54, signifying a generally high level of satisfaction with the treatment among all participants.

In particular, the scores for aesthetics (Q1), masticatory performance (Q2), phonetics (Q4), and comfort (Q6) were exceptional, all exceeding a score of 6. Hygiene practices (Q5) garnered a mean score of 5.83 ± 1.10, reflecting a favourable assessment of satisfaction. Conversely, food impaction (Q3) and the tendency to play around the

implant crown (Q7) received the lowest mean PSQ scores, at 4.78 ± 1.86 and 4.39 ± 2.43, respectively; however, these still indicate a medium level of satisfaction.

With regard to participants' willingness to recommend the treatment to others (Q8) and their readiness to undergo similar treatment at the same institution (Q9), the scores demonstrated strong agreement, recording means of 6.61 ± 1.20 and 6.28 ± 1.49, respectively. This indicates that approximately 94.4% of participants selected the highest scores, 7 (n = 16) and 6 (n = 1), for these questions.

Table 4.7
Descriptive Analysis of Patient Satisfaction Towards AnyRidge® Implant Treatment

Question No:	Description	Mean	SD
Q1	How would you rate the appearance of the implant tooth today? *Bagaimana anda menilai keadaan gigi implant anda, sekarang?*	6.50	0.62
Q2	How would you rate your present capacity to chew with th implant tooth? *Bagaimana anda menilai keupayaan anda mengunyah sekarang*	6.28	1.07
Q3	How would you rate your present capacity to speak? *Bagaimana anda menilai keupayaan anda bertutur sekarang?*	6.72	0.46
Q4	Do you experience of food impaction with your implant tooth? *Adakah anda mengalami makanan terlekat pada gigi implan anda?*	4.78	1.86
Q5	How easy do you find it to clean your implant tooth and gums? *Adakah mudah bagi anda membersihkan gigi implan dan gusi?*	5.83	1.10
Q6	Do you feel comfortable with your implant tooth today? *Adakah anda berasa selesa dengan gigi implan anda, sekarang?*	6.72	0.46
Q7	Do you play around the implant tooth with your tongue? *Adakah anda sering menyentuh gigi implan anda dengan lidah?*	4.39	2.43
Q8	Would you like to recommend this treatment to another patient? *Adakah anda akan mencadangkan rawatan ini kepada orang lain?*	6.61	1.20
Q9	In hindsight, would you undergo the treatment you had for your implant tooth, again here? *Pada pendapat anda, adakah anda ingin mengulangi rawatan gigi implant, disini?*	6.28	1.49
	Total Mean Score	6.01	1.54

Note: The range scores of 1 - 2, 3 - 4, and 6 - 7 are considered low, medium, and high satisfaction, respectively.

The mean OHIP-14 scores for the Anyridge® implant group at pretreatment baseline (T_0) and 52 weeks post-treatment (T_1) are shown in Table 4.8. In general, the mean OHIP-14 score decreased from T0 to T1, with values of 3.21 ± 1.11 and 1.36 ± 0.96, respectively. A paired t-test for each domain revealed significant improvements in participants' oral health-related quality of life (OHRQL) after treatment, with p-values of 0.001 and 0.05.

Although the mean OHIP-14 scores showed a weak positive correlation between pre- and post-treatment (r = 0.30), this correlation was not statistically significant (p = 0.63). Furthermore, most domains showed weak negative correlations in OHIP-14 scores between pre- and post-treatment, except for the physical and psychological disability domains, which exhibited only weak correlations ($r < 0.2$).

Table 4.8
Mean and Standard Deviation of Oral Health Impact Profile Score and their Relationship before and after Treatment with AnyRidge® Dental Implant

OHIP[a] Descriptions	**T_0**	**T_1**	**Mean Difference (95 % CI)**	**t-statistic (df)**	***p*-value**	**Paired Samples Correlation**	
						Correlation Coefficient	***p*-value**
	Mean ± SD	**Mean ± SD**					
Functional limitation							
Have you experienced difficulty chewing any food because of problems with your teeth, mouth or implant? *Pernahkah anda mengalami kesukaran mengunyah sebarang makanan disebabkan masalah gigi, mulut atau implan anda? 1*	3.33 ± 0.96	1.06 ± 0.87	2.28 (1.58, 2.98)	6.87 (17)	< 0.001	-0.16	0.52
Have you felt problems related to your teeth, mouth or implant cause bad breath? *Pernahkah anda merasakan yang masalah gigi, mulut atau implan anda menyebabkan nafas anda berbau?*	3.56 ± 0.62	1.50 ± 1.25	2.06 (1.30, 2.81)	5.76 (17)	< 0.001	-0.23	0.36
Physical Pain							
Have you experienced discomfort eating any food because of problems with your teeth, mouth or implant? *Pernahkah anda mengalami rasa tidak selesa untuk makan sebarang makanan disebabkan masalah gigi, mulut atau implan anda?*	3.00 ± 1.08	1.11 ± 0.76	1.89 (1.21, 2.57)	5.86 (17)	< 0.001	-0.72	0.78
Have you experienced ulcers in your mouth? *Pernahkah anda mengalami tompok-tompok putih yang pedih (Ulser) di dalam mulut?*	3.39 ± 0.98	1.28 ± 1.13	2.11 (1.35, 2.87)	5.86 (17)	< 0.001	-0.50	0.84
Psychological discomfort							
Have you felt discomfort due to food getting stuck in between your teeth or implant? *Pernahkah anda merasa tidak selesa disebabkan makanan terlekat di celah gigi atau implan anda?*	2.28 ± 1.27	0.72 ± 1.02	1.56 (0.72, 2.40)	3.91 (17)	0.001	-0.73	0.77

OHIP[a] Descriptions	T_0	T_1	Mean Difference (95 % CI)	t-statistic (df)	*p*-value	Paired Samples Correlation	
						Correlation Coefficient	*p*-value
	Mean ± SD	Mean ± SD					
Have you felt discomfort due to food getting stuck in between your teeth or implant? *Pernahkah anda merasa tidak selesa disebabkan makanan terlekat di celah gigi atau implan anda?*	3.39 ± 1.04	1.33 ± 0.91	2.06 (1.32, 2.79)	5.92 (17)	< 0.001	-0.15	0.56
Physical disability							
Have you avoided eating certain foods because of problems with your teeth, mouth or implant? *Pernahkah anda mengelak daripada memakan makanan tertentu disebabkan masalah gigi, mulut atau implan anda?*	2.28 ± 1.41	1.17 ± 0.99	1.11 (0.37, 1.85)	3.16 (17)	0.006	0.26	0.29
Have you avoided smiling because of problems with your teeth, mouth or implant? *Pernahkah anda mengelak daripada senyum disebabkan masalah gigi, mulut atau implan anda*?	3.44 ± 0.86	1.06 ± 1.11	2.33 (1.61, 3.06)	6.80 (17)	< 0.001	0.01	0.98
Psychological disability							
Has your sleep been disturbed because of problems with your teeth, mouth or implant? *Pernahkah tidur anda terganggu disebabkan masalah gigi, mulut atau implan anda?*	3.44 ± 0.86	0.83 ± 0.79	2.61 (2.07, 3.15)	10.14 (17)	< 0.001	0.12	0.65
Has your concentration been disturbed by problems with your teeth, mouth or implant? *Pernahkah tumpuan anda terganggu disebabkan masalah gigi, mulut atau implan anda?*	3.44 ± 0.98	0.88 ± 0.90	2.56 (1.91, 3.20)	8.38 (17)	< 0.001	0.06	0.82
Social disability							
Have you avoided going out because of problems with your teeth, mouth or implant? *Pernahkah anda mengelak daripada keluar berjalan-jalan*	3.56 ± 0.98	1.00 ± 1.19	2.56 (1.83, 3.28)	7.41 (17)	< 0.001	0.10	0.69

OHIP[a] Descriptions	T_0	T_1	Mean Difference (95 % CI)	t-statistic (df)	*p*-value	Paired Samples Correlation	
						Correlation Coefficient	*p*-value
	Mean ± SD	Mean ± SD					
disebabkan masalah gigi, mulut atau implan anda?							
Have you experienced problems in carrying out your daily activities because of problems with your teeth, mouth or implant?	3.39 ± 1.04	0.83 ± 0.86	2.56 (1.85, 3.26)	7.62 (17)	< 0.001	-0.12	0.63
Pernahkah anda mengalami masalah untuk menjalankan kerja-kerja harian anda disebabkan masalah gigi, mulut atau implan anda?							
Handicap							
Have you had to spend a lot of money due to problems with your teeth, mouth or implant?	3.11 ± 1.37	0.83 ± 0.79	2.28 (1.60, 2.96)	7.09 (17)	< 0.001	0.29	0.24
Pernahkah anda terpaksa mengeluarkan perbelanjaan yang tinggi disebabkan masalah gigi, mulut atau implan anda?							
Have you felt less confident of yourself due to problems with your teeth, mouth or implant?	3.33 ± 1.14	1.00 ± 1.25	2.44 (1.76, 3.13)	7.51 (17)	< 0.001	-0.23	0.93
Pernahkah anda merasa kurang yakin dengan diri anda disebabkan masalah gigi, mulut atau implan anda?							
Total	3.21 ± 1.11	1.36 ± 0.96	2.17 (1.99, 2.35)	23.81 (251)	< 0.001	0.30	0.63

Notes: OHIP score was assessed using Likert's Scale 0: Never, 1: Hardly, 2: Occasionally, 3: Fairly often and 4: Very often. T_0 – before implant placement, T_1 – after treatment completed. [a] Paired sample T-Test. The significant level was set at $p = 0.05$.

Table 4.9 examines the relationship between patient satisfaction (PSQ score) and the impact of oral health on quality of life (OHIP-14 score) across various demographic and clinical parameters.

The analysis reveals no significant correlation between age and either score (PSQ: $p = 0.74$; OHIP-14: $p = 0.52$), suggesting that age does not influence patient satisfaction or quality of life post-treatment. While sex does not significantly affect the PSQ score ($p = 0.11$), it is significantly associated with the OHIP-14 score ($p = 0.026$), suggesting a potential influence on perceived quality of life.

Education level has no significant effect on either score (PSQ: $p = 0.47$; OHIP-14: $p = 0.42$), nor do occupation (PSQ: $p = 0.13$; OHIP-14: $p = 0.12$) and income (PSQ: $p = 0.55$; OHIP-14: $p = 0.14$), suggesting these socioeconomic factors are not key determinants of satisfaction or quality of life.

In terms of clinical parameters, there is no significant correlation between implant stability and either satisfaction ($p = 0.14$) or quality of life ($p = 0.85$). A weak positive correlation exists between crestal bone level and PSQ score ($r = 0.17$; $p = 0.34$), but crestal bone level does not significantly affect the OHIP-14 score ($p = 0.95$). No significant relationships were found between probing depth (PSQ: $p = 0.33$; OHIP: $p = 0.97$) or inflammation (PSQ: $p = 0.37$; OHIP-14: $p = 0.97$) and either score, suggesting that minor clinical findings do not directly affect perceived satisfaction or quality of life.

Table 4.9
Relationship Between Patient Satisfaction and the Impact of Oral Health Following Treatment, Considering Patient Demographics and Clinical Parameters in the AnyRidge® Dental Implant Group

Variables	**PSQ Score**					**OHIP Score**				
	Correlation Coefficient	**Mean Difference (95 % CI)**	**F (df)**	**t-statistic (df)**	***p*-value**	**Correlation Coefficient**	**Mean Difference (95 % CI)**	**F (df)**	**t-statistic (df)**	***p*-value**
Demographic Variables										
Age [a]	-0.08				0.74	0.522				0.026
Sex [b]		-1.89			0.11		0.43			0.44
		(-4.28, 0.50)					(-0.72, 0.58)			
Education [c]			0.79 (2)		0.47			2.25 (2)		0.12
Occupation [c, d]				4.17	0.13				0.50	0.62
				(2)					(2)	
Income [c, d]				2.13 (3)	0.55				2.02 (3)	0.16
Clinical Variables										
Implant Stability [a]	-0.203				0.14	0.64				0.65
Crestal Bone Level [a]	0.17				0.04	-0.28				0.74
Peri-implant Probing Depth [a]	-0.08				0.33	-0.04				0.95
Inflammation [c]			1.01		0.37				0.11 (2)	0.90
			(2)							
Bleeding on Probing [b]		-0.05			0.95		0.02			0.97
		(-1.76, 0.66)					(-0.72,0.76)			

Note: Significance level of p = 0.05 was used. [a] Spearman's Correlation. [b] Independent T-Test. [c] One-way ANOVA, [d] Kruskal-Wallis Test.

4.2.6 Implant Success and Survival Rates Evaluation

Life table analysis of implant success, based on the criteria defined by Buser et al. (1990), was presented in Table 4.10. This table assesses the success rate of two dental implants, denoted as AnyRidge® and NiTiDent Tuah, over specific time intervals, considering various clinical and patient-centred outcomes up to 52 weeks.

Based on the criteria in subchapter 3.3.1, one implant was retrieved due to swelling and a purulent exudate (n = 1). Five implants (n = 5) were retrieved on the day of the planned abutment connection; two had implant exposure in the mouth, and the other three showed radiolucency along the implant fixture on the periapical radiograph and mobility after flap exposure. Two implants were spontaneously explanted from the patient's implanted site (n = 2). Another 4 implants were retrieved after the abutment connection (n = 4). In these instances, movement was observed alongside pain during attempts to release the implant. During the 18–22-week interval, 6.5% of participants with the NiTiDent Tuah reported discomfort, while 2.2% experienced recurrent peri-implant inflammation. Notably, 12.0% showed perceptible implant mobility, and 83.3% exhibited peri-implant radiolucency, indicating potential bone loss or osseointegration failure. During this period, the cumulative success rate for NiTiDent Tuah decreased to 25.0%. Conversely, Anyridge reported no discomfort, infections, or mobility issues, achieving a 100% success rate without technical complications.

Table 4.11 presents a Kaplan-Meier survival analysis comparing implant survival distributions. The estimated overall survival time was 37.75 weeks, with NiTiDent Tuah at 16.38 weeks and AnyRidge® at 52 weeks, showing significant differences ($p < 0.01$). Similar findings were confirmed by Breslow and Tarone-Ware tests (both: $p < 0.001$). Figure 4.1 illustrates a declining survival proportion for NiTiDent Tuah, with a median survival time of 20 weeks, whereas AnyRidge® survived for up to 52 weeks post-implantation.

Table 4.10
Life Table Analysis of NiTiDent Tuah and AnyRidge® Implant Success (Buser et al.,1990; Papaspyridakos et al., 2012)

Implant type	Total Participants (n)	Interval (Week)	Incidence of Signs and Symptoms Observed (n, %)						Failures During an Interval (n, %)	Cumulative Success (%)
			Discomfort (pain, foreign body perception or dysaesthesia)	Recurrent Peri-Implant Infection with Suppuration	Perceptible Implant Mobility on Manual Palpation	Peri-implant Radiolucency	Prosthodontic Technical Complication	Overall Patient Satisfaction		
NiTiDent Tuah	12	< 2	6, 50 %	2, 20 %	12, 100 %	10, 83.3 %	Not evaluated	Not evaluated	0	100
		2 - 18							5, 41.7 %	58.3
		18 - 22							4, 33.3 %	25.0
		22 - 36							3	0
		36 - 52								
Anyridge®	18	< 2	0	0	0	0	0	(6.01)	0	100
		2 - 18						High satisfaction	0	100
		19 - 22							0	100
		23 - 36							0	100
		37 - 52							0	100

Table 4.11
Survival Analysis of NiTiDent Tuah and Anyridge® within 52 Weeks of Observation

Implant type	Median Survival				Chi-Square (df)			*p*-value
	Estimate	Std. Error	95 % Confidence Interval		Log-Rank (Mantel-Cox)	Breslow (Generalised Wilcoxon)	Tarone-Ware	
			Lower	Upper				
NiTiDent Tuah	16.38	2.24	11.985	20.781	38.36 (1)	33.23 (1)	35.78 (1)	< 0.001
Anyridge®	52.00	0.00	52.000	52.000				
Overall	37.75	3.36	31.176	44.331				

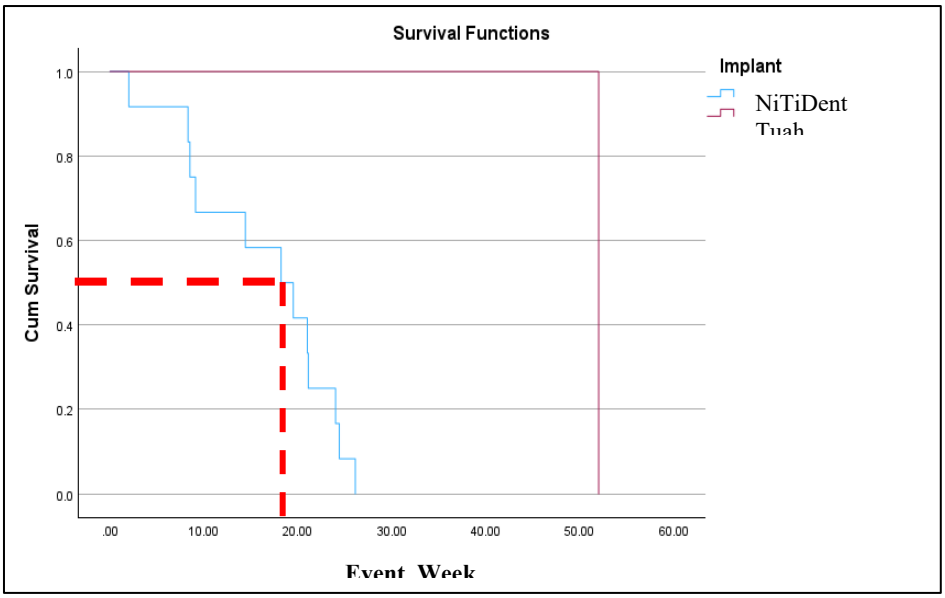

Figure 4.1 The Cumulative Survival Proportion with Time (Week)

4.3 Part B

4.3.1 Assessment of Peri-implant Tissue

4.3.1.1 Histopathology Evaluation of Peri-implant Tissue

Figure 4.2 exhibits histopathological evaluation of peri-implant tissue sections stained with Haematoxylin and Eosin (H&E). Under light microscopy, all samples showed diffuse chronic inflammatory infiltrates, including lymphocytes, plasma cells, and multinucleated giant cells, consistent with a foreign body reaction. Notably, small

red-stained areas in all samples represented engorged blood vessels or capillaries containing extravasated erythrocytes due to increased vascular permeability in response to active inflammation. The observation of a pale-pink network suggests the presence of fibrous or collagen deposition (indicated by the yellow arrow), along with large multinucleated giant cells (*). Figures B and C illustrate granuloma formation, characterised by clusters of large cells surrounded by densely packed smaller cells and numerous small blood vessels.

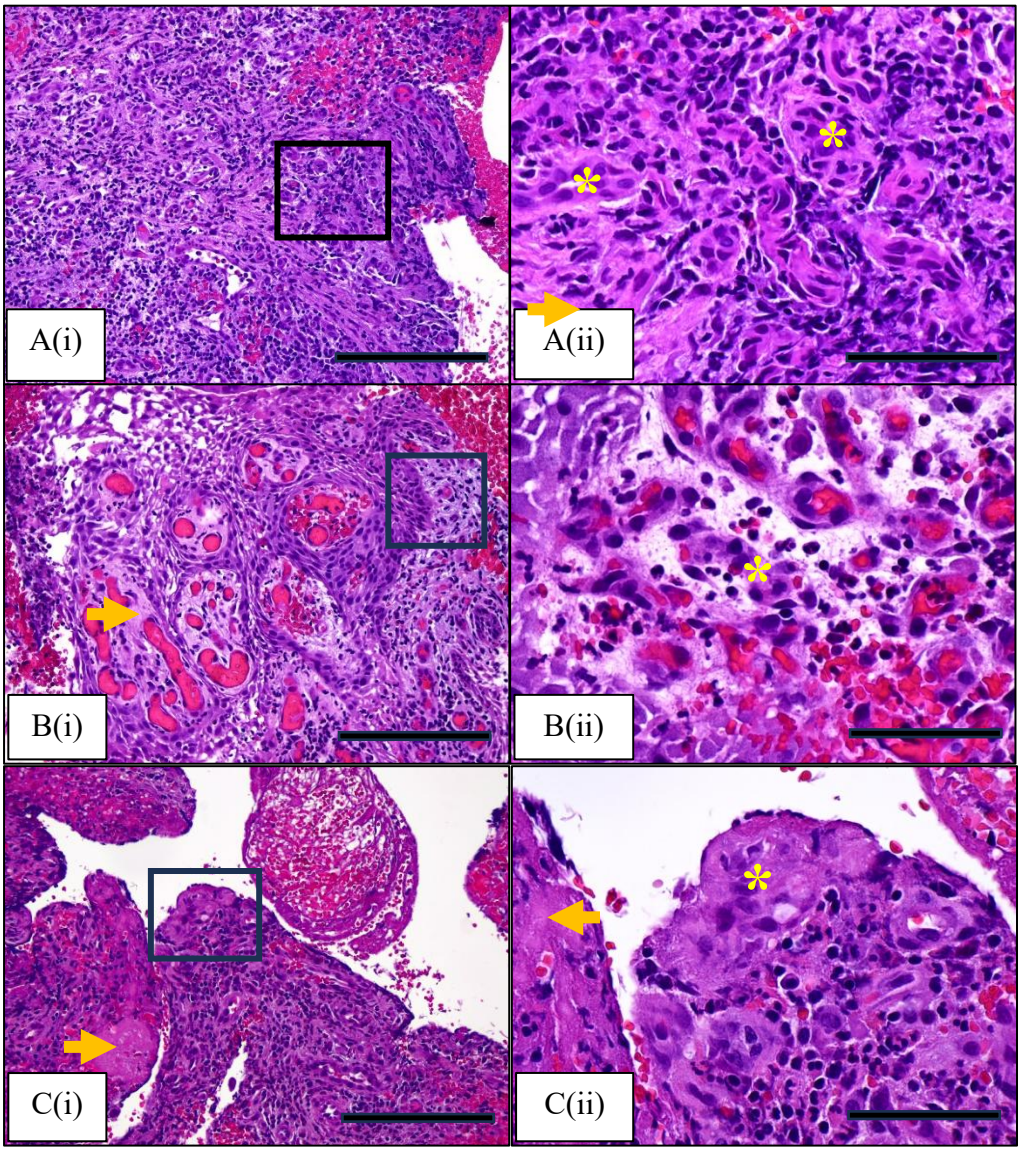

Figure 4.2 Peri-implant Tissue Associated with a Disintegrated Implant, Examined Under Light Microscopy, Stained with H&E.

Notes: i) images at 20x magnification (left), scale bar = 100 µm. ii) a close-up view of the boxes at 60x magnification (right), scale bar = 20 µm. * Denotes multinucleated giant cell (MGC), yellow arrow - fibrous or collagen deposition.

4.3.1.2 Scanning Electron Microscopy (SEM)

The scanning electron microscopy (SEM) images of the failed peri-implant tissue samples, shown in Figure 4.3, provide a detailed view of the tissue's cellular architecture. In these images, a noticeable aggregation of inflammatory cells, accompanied by extravasated erythrocytes, is characterised by biconcave-shaped cells. At a magnification of 3000x (B and D), irregularly shaped and clumped cells were observed, indicating the presence of macrophages and multinucleated giant cells (yellow arrows). Prominent apoptotic blebs, represented by small, rounded protrusions (red arrows), were suggestive of apoptosis. Additionally, a distinctive meshwork-like structure of the extracellular matrix, denoted by an asterisk (*), likely reflecting fibrous encapsulation, surrounds the inflammatory site.

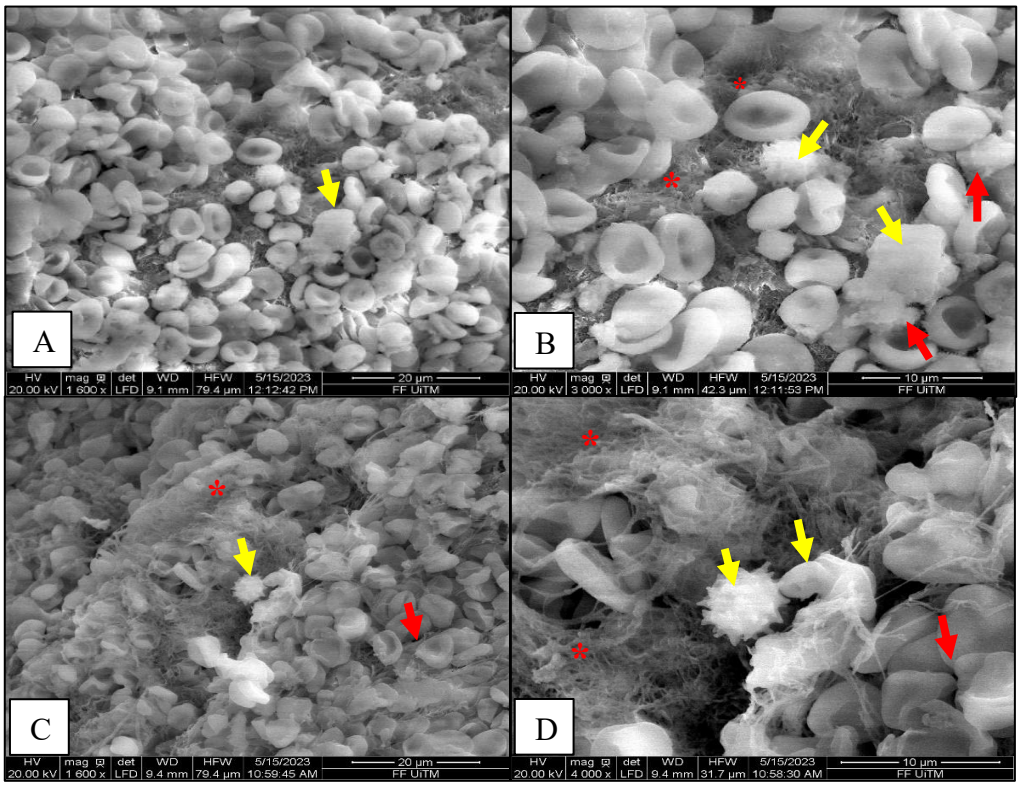

Figure 4.3 Peri-implant Tissue Related to Disintegrated Implant under SEM.

Note: Yellow Arrow – MGC or Activated Macrophage, Red Arrow – Apoptotic Bleb and * Indicates Extracellular Matrix.

4.3.1.3 Transmission Electron Microscopy (TEM)

Figures 4.4 and 4.5 present transmission electron microscopy (TEM) images that provide a comprehensive view of the intra- and extracellular compartments of failed peri-implant tissues. The figures are displayed at varying magnifications, represented by distinct colour bands: blue for 2 µm, orange for 1 µm, yellow for 200 nm, and green for 500 nm.

Image A indicates an activated macrophage, highlighted by a yellow dashed circle. Surrounding this macrophage, an erythrocyte and several dark materials, likely metallic, differing markedly in size and shape, and dispersed throughout the interstitial compartment were observed. Transitioning to image B, where the yellow dashed circle is magnified to a scale of 500 nm, a large, irregularly shaped cell characterised by a well-defined central structure was identified. The centre of this cell features densely packed with black granular components at its periphery, which hint at high electron absorbance. This heavily electron-dense area likely represents the nucleus in an advanced stage of apoptosis. Meanwhile, the cytoplasmic region appears less dense and exhibits remarkable porosity, with distinct mitochondria, indicated by the label "m." The cell membrane exhibited multiple projections, possibly indicating an active phagocytic process aimed at engulfing foreign particles (as marked by the red dashed circle) and the aggregation of metal particles, as indicated by a yellow arrow. Image C, a close-up of image A (marked by the red box), reveals a spectrum of degraded foreign entities ranging in size from under 500 nm to 2 µm. A vacuole-like structure was observed, characterised by a darker region, in images B and D (marked by the blue arrow), This further suggests phagolysosomal activity, indicating the cell's engagement in engulfing and degrading foreign materials. This illustrates the macrophage's active role in processes crucial for foreign material reaction and immune response within the compromised peri-implant environment.

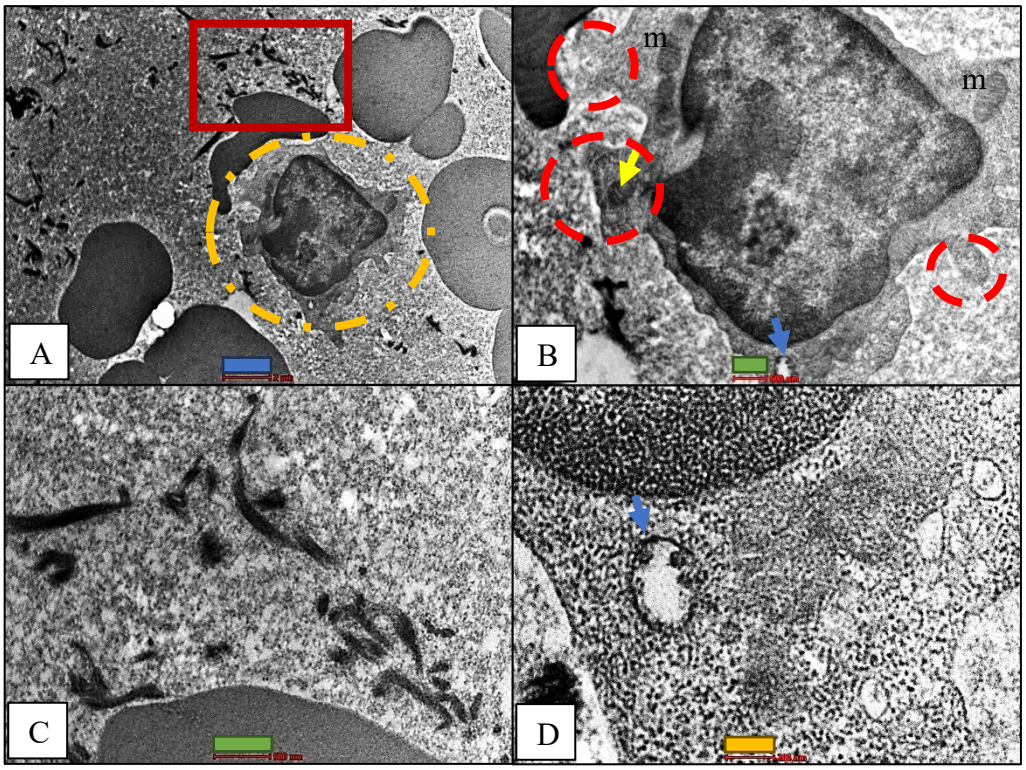

Figure 4.4 Transmission Electron Microscopy (TEM) Images of Peri-implant Tissues Related to Disintegrated Implants.

Notes: A) An activated macrophage (yellow dashed circle), magnified view in (B) (green band, 500 nm), C: close-up (red box) displays degraded foreign entities (500 nm to 2 µm). D: highly granulated and porous cytoplasmic milieu. Blue arrows mark vacuole-like structures of phagolysosomal activity.

An in-depth analysis of ultra-subcellular organelles is presented in Figure 4.5. A pronounced cellular compartmentalisation was identified in A, characterised by numerous large vacuolar spaces (v) forming within the intracellular environment. The endoplasmic reticulum (ER) appears disorganised, and the compromised state of the organelles in the central region signals a state of cellular distress and degradation.

In image B, the activity of intracellular organelles during protein synthesis is vividly illustrated. A yellow arrow directs to a densely packed, dark, lamellated structure identified as the Golgi apparatus, with prominent staining indicative of its active engagement in processing proteins and lipids. The red arrow highlighted the cell, which contained multiple dark circular structures scattered throughout its cytoplasm. These structures resemble vesicles or vacuoles, which are crucial for storage and transport. The granular texture of the cytoplasm indicates the presence of ribosomes and other molecular complexes essential for protein synthesis.

Image C highlights a multinucleated giant cell (MGC) with distinctly visible nuclei within a single cellular boundary, positioned adjacent to foreign bodies (FB). The cell highlighted by the yellow arrow appears to be undergoing apoptosis, characterised by the presence of various vacuole-like structures of differing sizes and shapes, alongside noticeable cell shrinkage (~550 µm). The multiple dark, dense entities observed may represent chromatin condensation, lysosomal remnants, or degraded organelles. In image D, the MGC actively engaged in phagocytic activities, including endocytosis and exocytosis (*), in response to foreign material. This cell is enveloped by a fibrous capsule, indicating a robust immune response to the surrounding foreign substances.

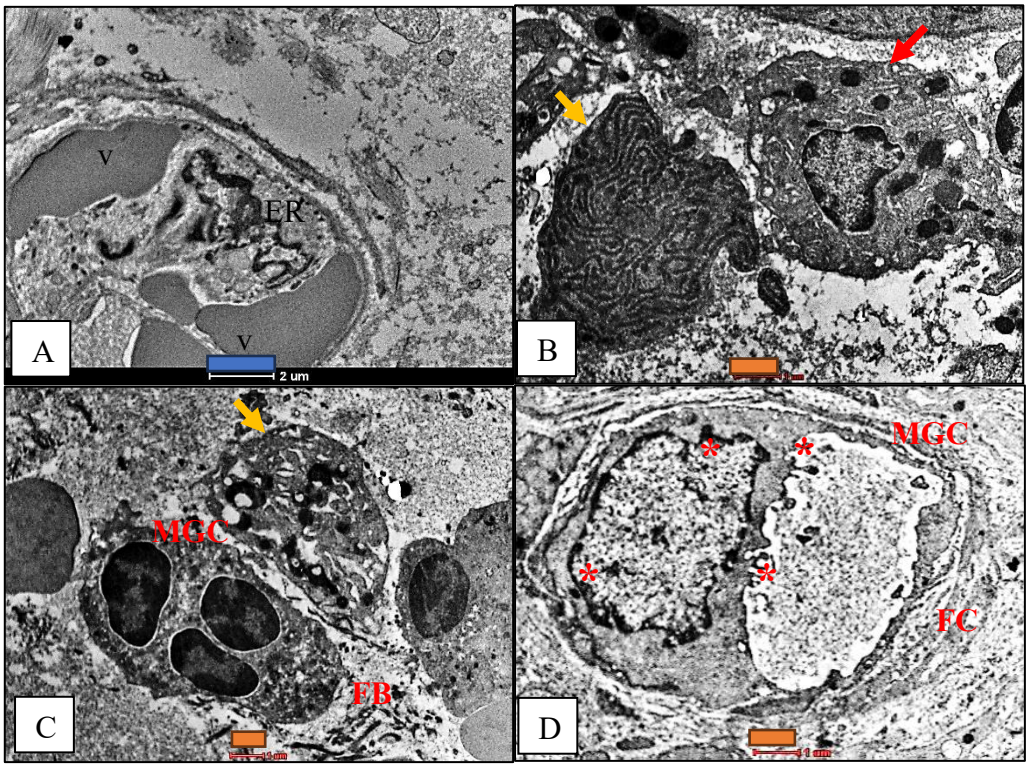

Figure 4.5 Transmission Electron Microscopy (TEM) Images of Peri-Implant Tissues Related to Disintegrated Implant.

Notes: A) v - vacuolar spaces, ER - endoplasmic reticulum. B) Yellow arrow - an active Golgi apparatus, red arrows – a cell actively involved with protein synthesis and transportation. C) MGC - multinucleated giant cell, FB -foreign bodies. D) FC - fibrous encapsulation, * - sites of endocytosis and exocytosis.

4.3.1.4 Energy-Dispersive X-Ray Spectroscopy (EDS)

The EDS analysis results, as illustrated in Figure 4.6, along with the corresponding elemental map in Figure 4.7 and the detailed elemental percentages in Table 4.12, shed light on the intricate elemental composition of the failed peri-implant tissue. In Figure 4.6, the most predominant elements within the sample are oxygen (O), carbon (C), and calcium (Ca). These key elements, along with others such as sodium (Na), magnesium (Mg), and potassium (K), indicate the presence of a complex biological matrix actively involved in calcium incorporation. This suggests ongoing cellular activities critical for maintaining the ionic environment, with Na, K, and Mg playing significant roles in cellular function. Furthermore, the presence of sulphur (S) suggests the involvement of protein structures in cellular mechanisms.

On the other hand, the identification of elements such as silica (Si), aluminium (Al), manganese (Mn), and iron (Fe) suggested potential external contamination in these biological samples. Furthermore, the multiple-minute peaks of platinum (Pt) observed in the analysis likely originate from the coating materials applied during scanning electron microscopy (SEM). The distribution of these elements is shown in Figure 4.7, which provides a comprehensive visual representation of their spatial relationships within the tissue.

Table 4.12
Analysis of the Elements Present in the Peri-Implant Tissue Related to a Disintegrated Implant

Element	Weight (%)
C	25.64
O	50.07
Na	0.11
Mg	0.19
Al	1.54
Si	5.68
S	0.22
K	0.33
Ca	15.16
Mn	0.10
Fe	0.97

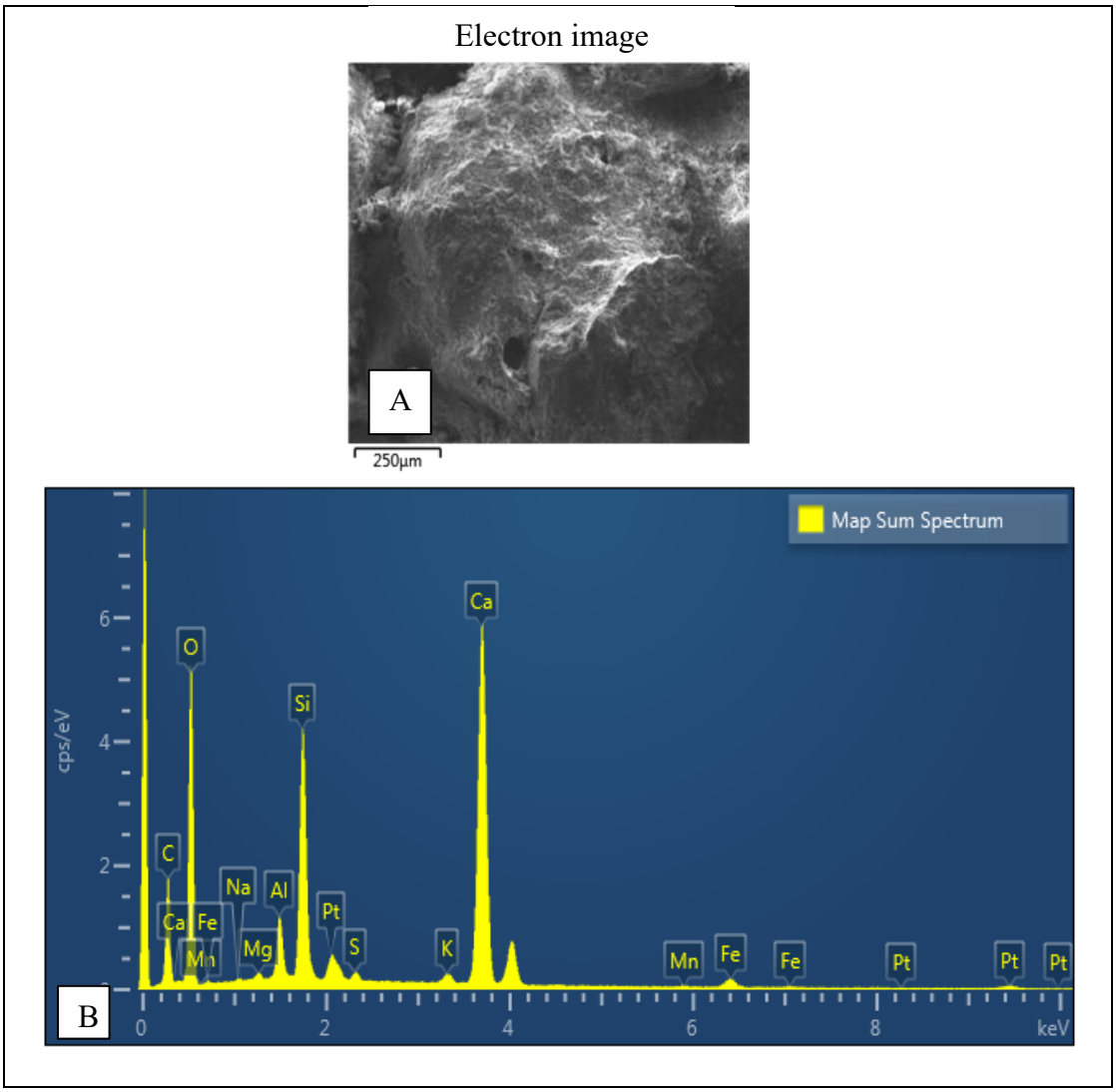

Figure 4.6 Elemental Analyses of Peri-implant Tissue Related to the Disintegrated Implant.

Note: A: Electron image of the sample, B: EDS analysis of the sample

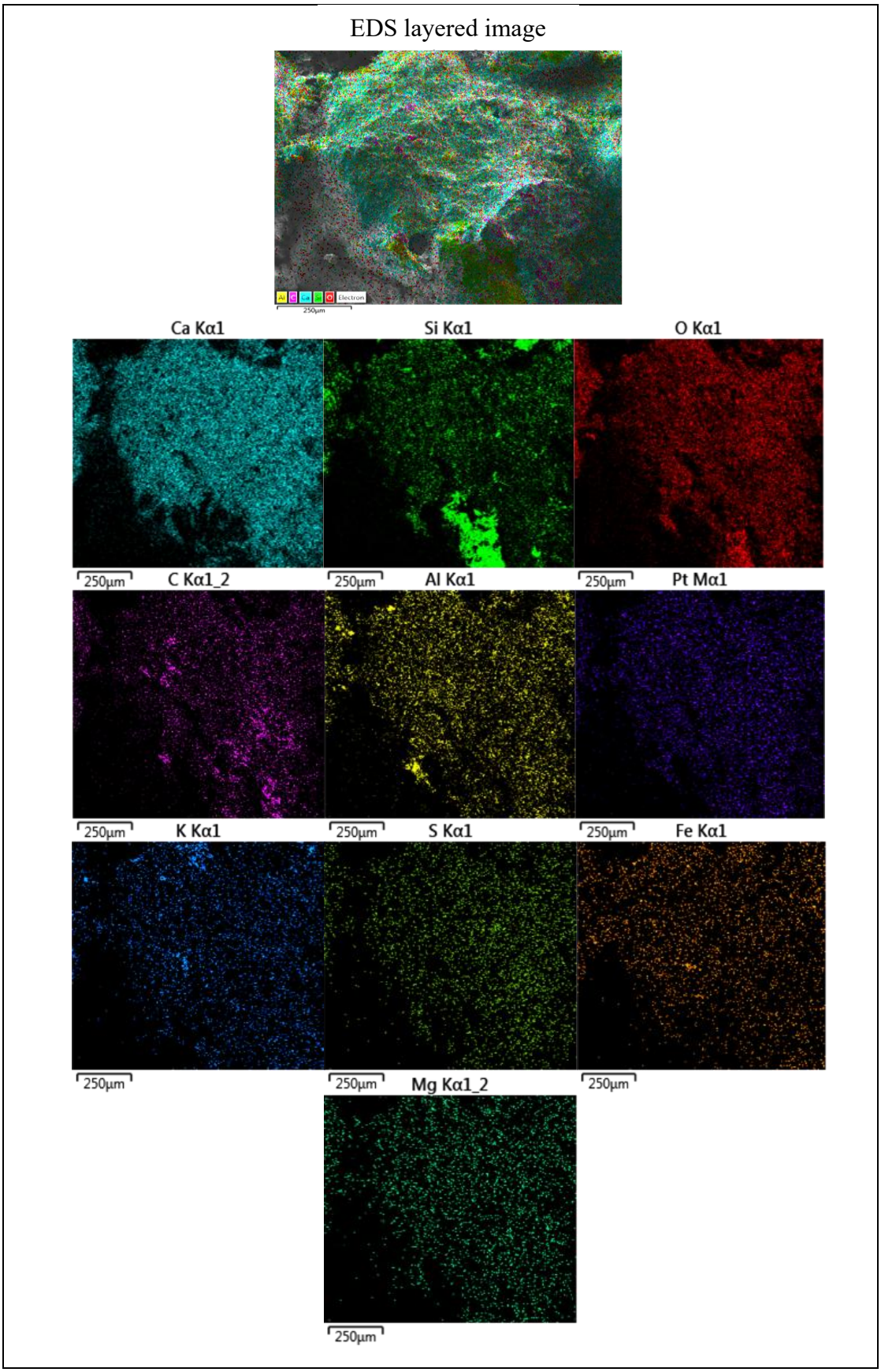

Figure 4.7 The Distribution of Elements Found in the Sample Retrieved from the Peri-implant Tissue of the Disintegrated Implant

4.3.2 Assessment of Failed Implant

4.3.2.1 Scanning Electron Microscopy (SEM)

The scanning electron microscope (SEM) images presented in Figure 4.8 illustrate the surface of the original porous NiTiDent Tuah (Figure 4.8) and the failed implant (Figure 4.9). Close-up images A (i) highlight the red box of section A, while A (ii) exhibits a close-up image of the red box in A (i). Similar to the image in B (i) and B (ii). In image A (ii), generalised network-like structures and filamentous appearance, likely representing a fibrous network, indicative of fibrous encapsulation, were observed. This image also features cell aggregation (highlighted by the yellow circle), multinucleated giant cells (MGCs), and apoptotic blebs (indicated by the red arrow). Furthermore, debris is present, possibly resulting from cellular activity or the degradation of foreign body material.

Image B (ii) revealed a filamentous, band-like structure that suggests fibrous tissue (F) overlaying a trabeculated, spongy bone matrix (BM). The small, rounded particles visible within the network were possibly remnants of inflammatory cells or degradation products related to the foreign body (red arrow).

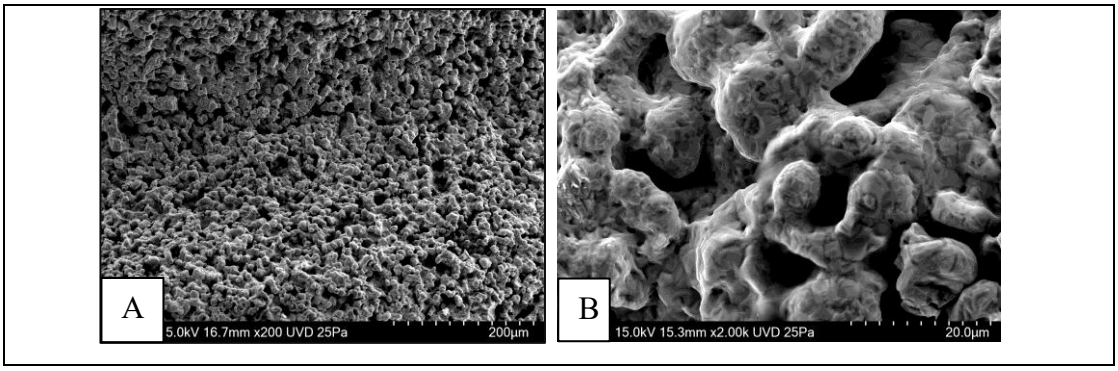

Figure 4.8 SEM Images of Porous NiTi Microstructure

Note: (A) at 200 µm Magnification; and (B) at 20 µm Magnification (Mustafa et al., 2023).

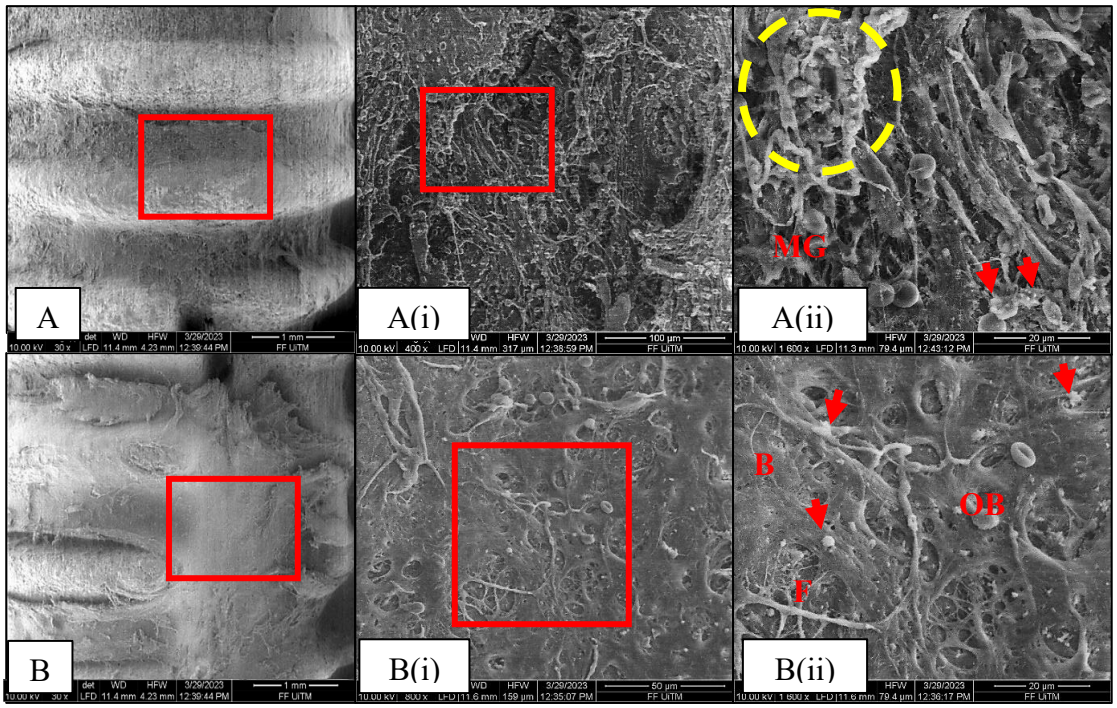

Figure 4.9 Scanning Electron Microscopy of Disintegrated Implants.

Notes: The SEM images were taken at the middle (A) and apical (B) sections. Yellow circle – inflammatory cell aggregation, red arrow – debris derived from inflammatory cells or degraded foreign body material, MGC – multinucleated giant cell, BM – bone matrix, OB – osteoblast.

4.3.2.2 Energy-Dispersive X-Ray Spectroscopy (EDS)

A detailed elemental analysis was conducted on the surface of NiTi Dent Tuah implants before failure (as shown in Figure 4.10 and Table 4.13) and on the failed implants displayed in Figure 4.11 and 4. 12. The primary elements found on the surface of the intact implants were titanium (55.42% and 60.92%) and nickel (32.04% and 27.47%). Other elements detected at spot 2 included oxygen, carbon, and silica.

In contrast to the results shown in Figure 4.10, the disintegrated implants from different samples (A and B) presented in Figures 4.11 and 4.12 contained additional elements indicative of external contamination. In sample A, three external metallic elements were identified, including ferum (6.0 %), chromium (1.2%), and phosphorus (1.0%). While sample B exhibited a higher phosphorus content (6.8%), and sulfur was about 0.4%. Other elements observed from both samples were derived from the implant material itself and remnants of peri-implant tissues that remained attached to the implant surface.

Table 4.13
Weight (%) of Elements Present on the Surface of the NiTiDent Tuah Porous NiTi Dental Implant

Spot 1		Spot 2	
Element	**Weight (%)**	**Element**	**Weight (%)**
Ti	55.42	Ti	60.95
Ni	32.04	Ni	27.47
O	5.20	O	6.30
C	7.34	C	5.07
		Si	0.22

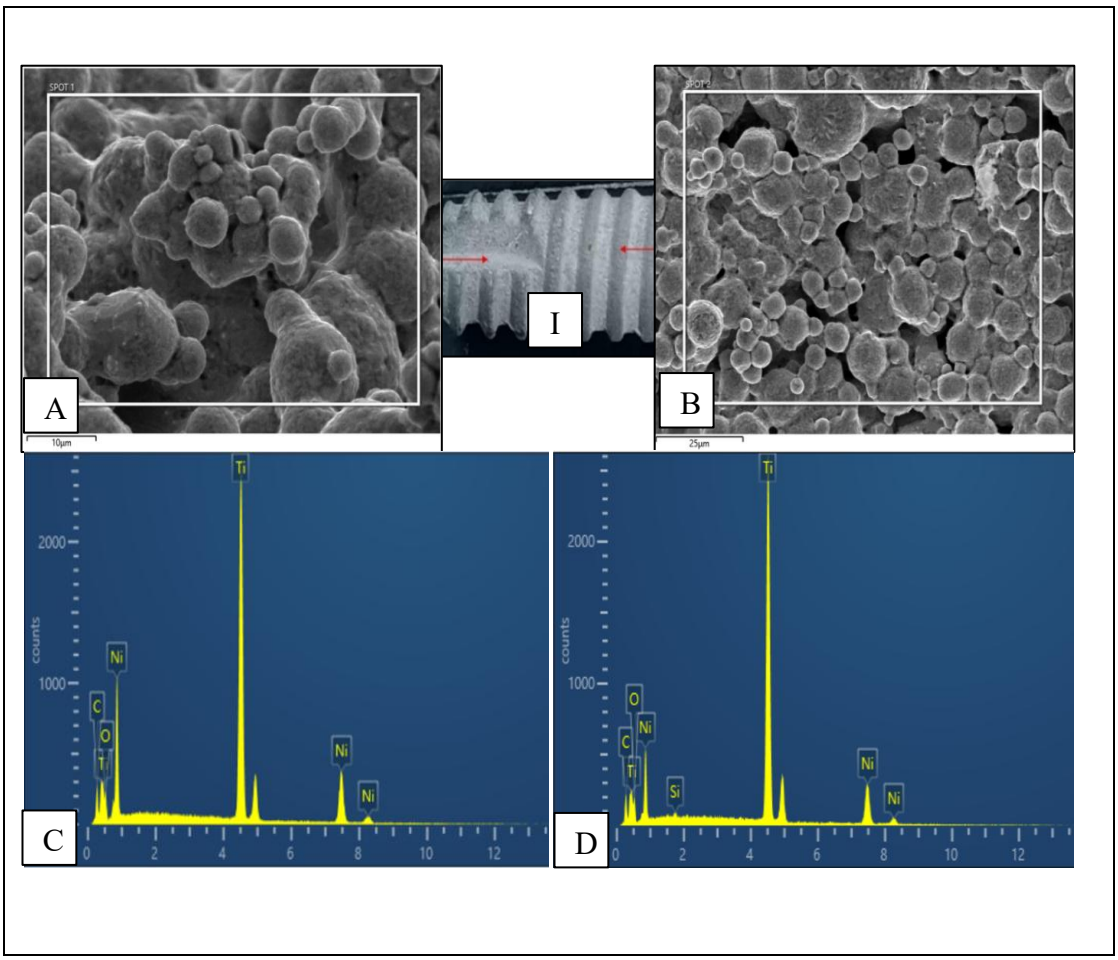

Figure 4.10 Elemental Surface Analyses of NiTi DenTuah Porous NiTi Dental Implant by EDS.

Note: A) Spot 1 at the apical region, B) Spot 2 at the middle region of the implant. I – implant, C) EDS analysis for spot 1 and D) for spot 2.

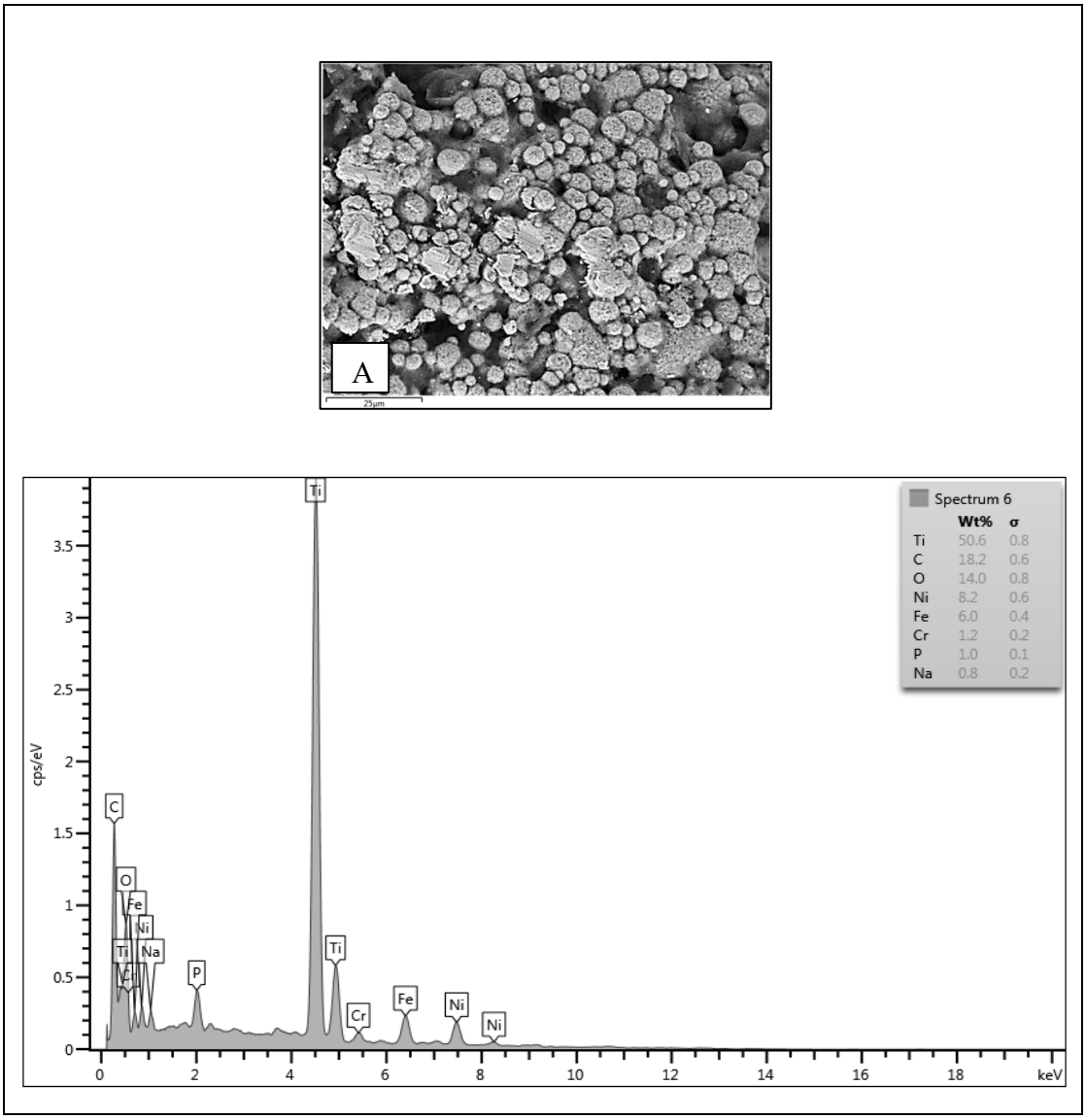

Figure 4.11 Elemental Analysis by EDS of Sample 1.

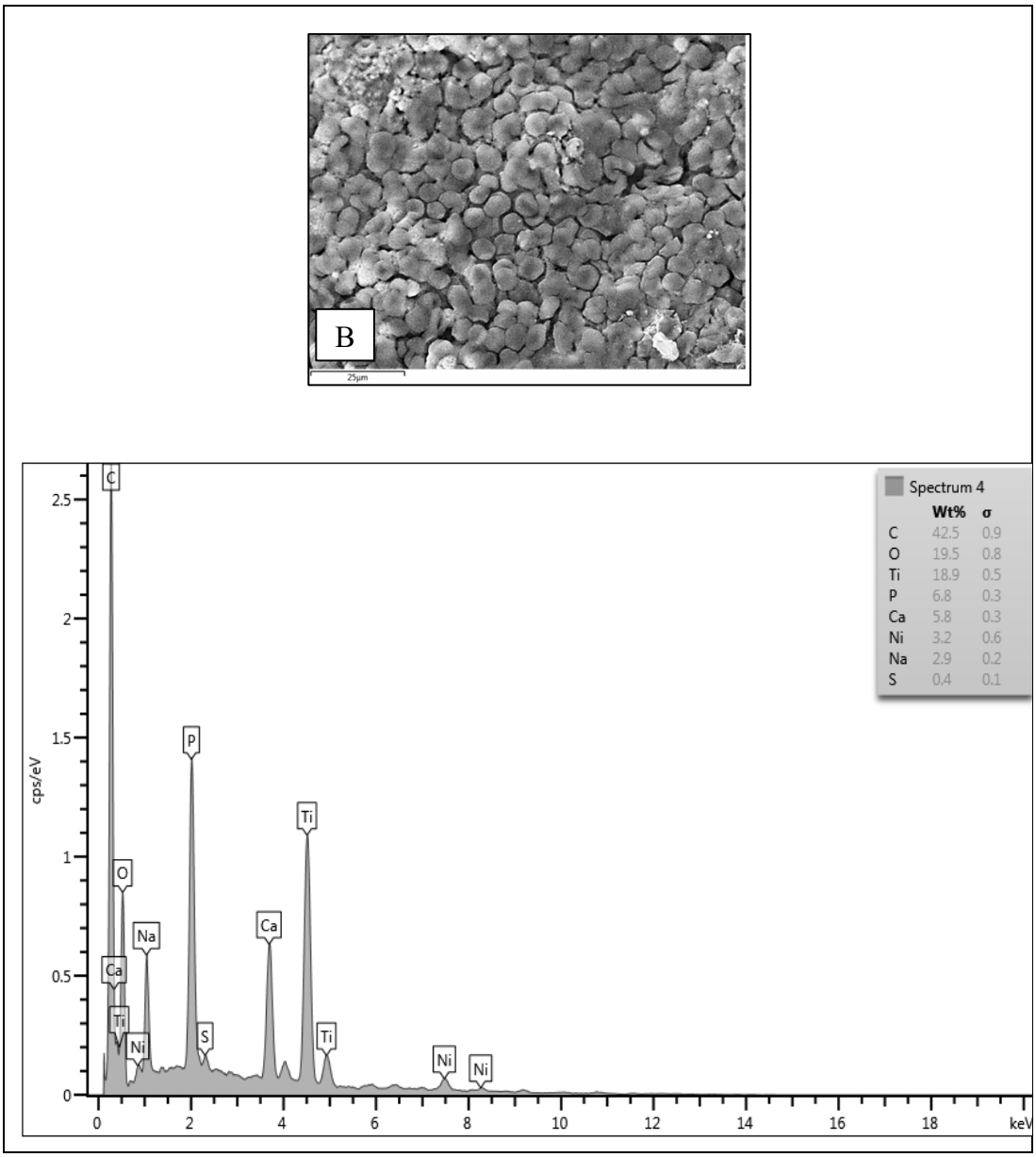

Figure 4.12 Elemental Analysis by EDS of Sample 2.

4.3.3 Assessment of Surgical Drill

4.3.3.1 Micrograph and Scanning Electron Microscopy (SEM)

This study observed the integrity of the implant surgical drill and its potential contribution to the biological failure of the implant treatment. The observation focuses on the cutting-edge and surface conditions. Figure 4.13 refers to the surgical drill made of stainless steel that had been used for the preparation of the implant cavity for placement of the NiTiDent Tuah dental implant, while Figure 4.14 exhibits the surgical drill used for the control group.

Observation of the cutting-edge in Figure 4.13 revealed an obvious sign of wear and degradation (red arrow) in B and C. Close-up views under SEM in B (i) and C (i) exhibited chipping, pitting and roughened surfaces. The drill surface was identified with a micro-crack (circled) and an irregular surface (yellow arrow). These conditions would compromise the sharpness and cutting precision during surgery.

In contrast, the cutting edge and surface integrity of the surgical drill used in the control group remained intact after use five (B) and ten (C) times, Figure 4.14.

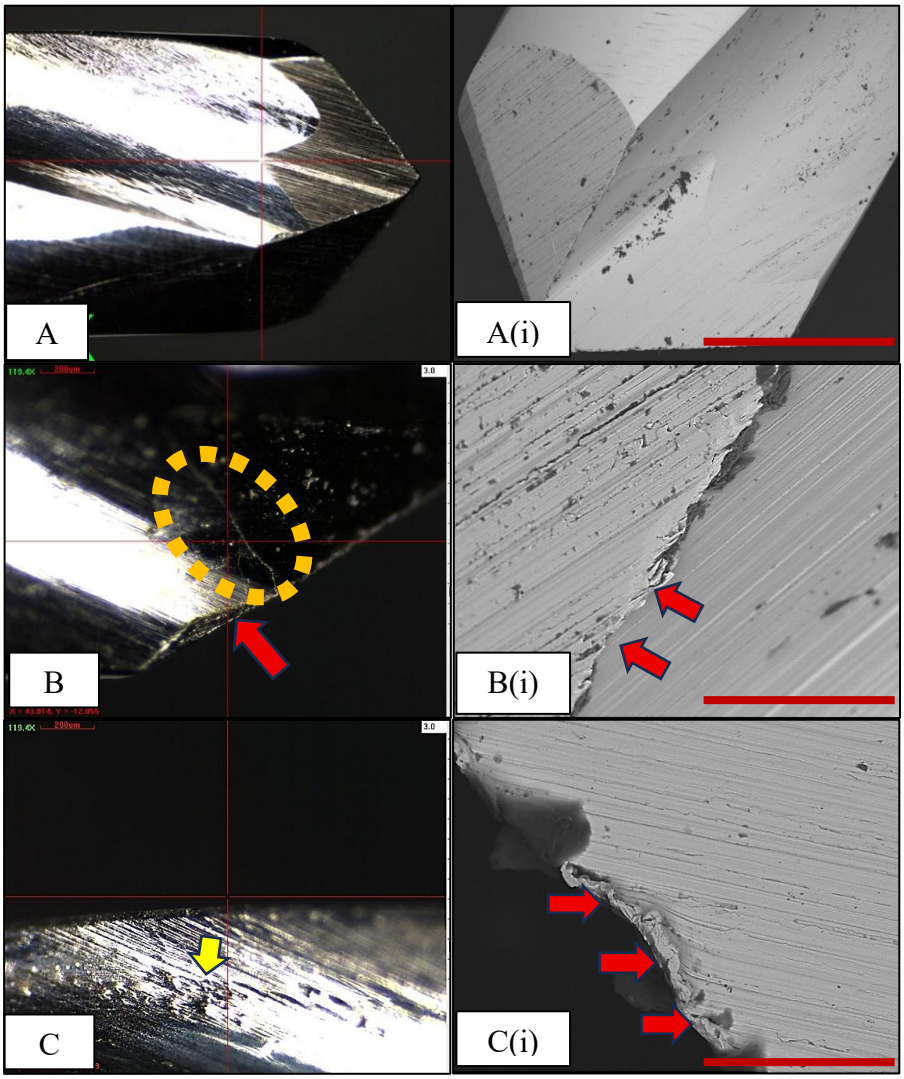

Figure 4.13 The Images of Surgical Drill Used for NiTi Dent Tuah Porous NiTi Dental Implants.

Notes: Left-side images viewed under a micrograph, right-sided images viewed under SEM at (10x) magnification. A) before drilling, B) after five times, and C) after ten times of usage. Red arrow – worn cutting-edge, yellow arrow – irregular surface, circled – micro-crack

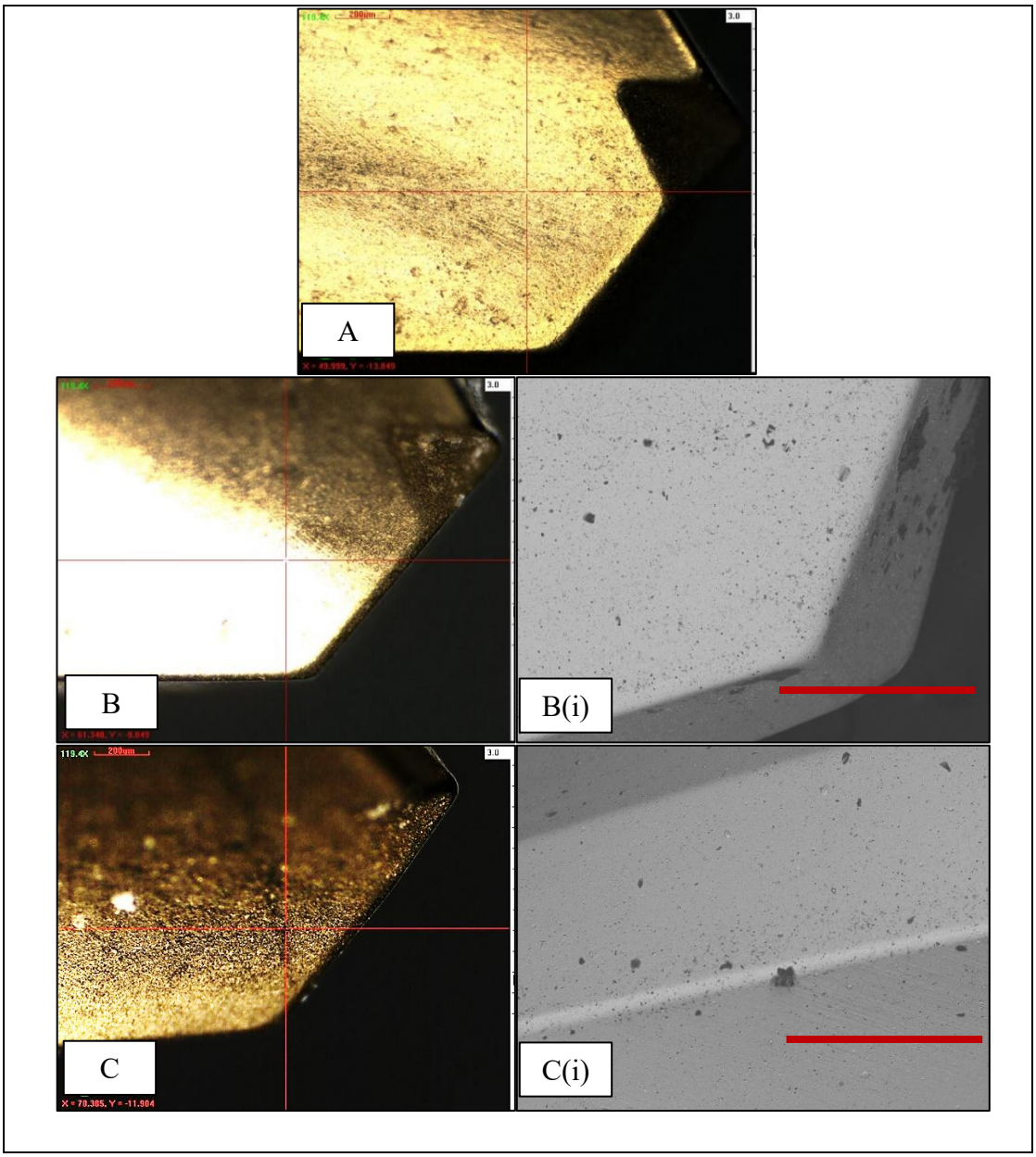

Figure 4.14 The Images of Surgical Drill Used for the Control Group (Anyridge®, Megagen).

Notes: Left-side images viewed under a micrograph, right-sided images viewed under SEM at (10x) magnification. A) before drilling, B) after five times, and C) after ten times of usage.

4.3.4 Monoculture with Human Mesenchymal Cell

4.3.4.1 Cell Viability Assay

The descriptive analysis, including mean values and standard deviations of cell viability, is summarised in Figure 4.15. All tested biomaterials exhibited a higher mean

optical density than the negative control group, indicating that the cells remained viable and proliferated over time, with pNiTi showing the highest viability.

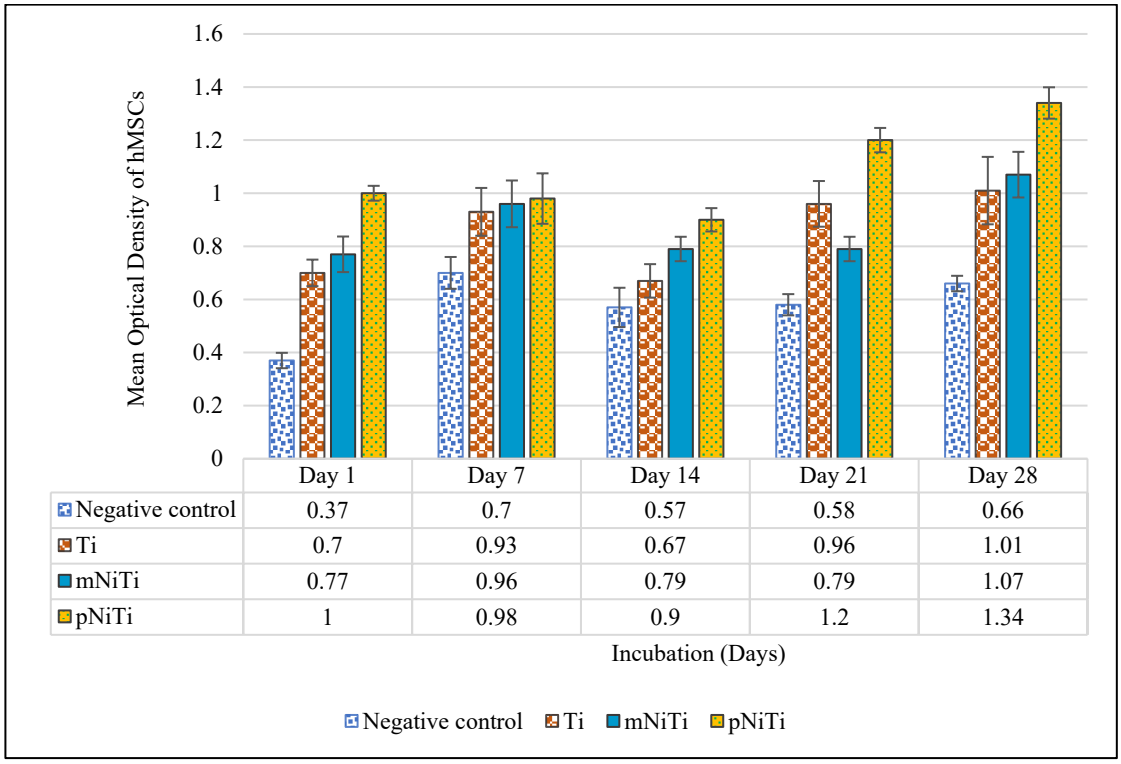

	Day 1	Day 7	Day 14	Day 21	Day 28
Negative control	0.37	0.7	0.57	0.58	0.66
Ti	0.7	0.93	0.67	0.96	1.01
mNiTi	0.77	0.96	0.79	0.79	1.07
pNiTi	1	0.98	0.9	1.2	1.34

Figure 4.15 Cell Viability Assays Across Different Biomaterials (n = 6/ sample)

A repeated-measures ANOVA was conducted to evaluate cell viability using mean optical density across various biomaterials at specific time points (days 1, 7, 14, 21, and 28). The analysis of the effect of time on cell viability across different groups revealed a significant statistical result, with an F(df) = 11.74 (4), p-value < 0.001. Post-hoc pairwise comparisons, adjusted using the Bonferroni method, are outlined in Table 4.14. Significant increases in cell viability were observed in several comparisons: Day 1 vs Day 7, Day 1 vs Day 21, Day 1 vs Day 28, and Day 14 vs Day 28.

Additionally, as shown in Table 4.15, the effects of various biomaterials on cell viability were significant. Across all time points, the mean optical density values for different biomaterials differed significantly ($p < 0.001$). Post hoc comparisons indicated that the mean optical density of the negative control was significantly lower than those of all three tested biomaterials. Similar significant differences were found between pairs such as Ti vs mNiTi, Ti vs pNiTi, and mNiTi vs pNiTi ($p < 0.001$).

Table 4.14
Comparisons of Mean Optical Density of hMSCs Based on Incubation Time Regardless of Biomaterial Type

Time Comparison		Mean Difference	95 % Confidence Interval		*p*-value
			Lower Bound	Upper Bound	
Day 1	Day 7	- 0.18	- 0.35	- 0.03	0.035*
	Day 14	- 0.02	- 0.13	0.08	1.000
	Day 21	- 0.18	- 0.29	- 0.06	0.001*
	Day 28	- 0.31	- 0.45	- 0.16	< 0.000*
Day 7	Day 14	0.16	- 0.01	0.33	0.083
	Day 21	0.01	- 0.17	0.19	1.000
	Day 28	- 0.13	- 0.33	0.07	0.592
Day 14	Day 21	- 0.15	- 0.31	0.01	0.067
	Day 28	- 0.29	- 0.46	- 0.11	< 0.001*
Day 21	Day 28	- 0.13	- 0.31	0.04	0.281

Notes: A Repeated measures ANOVA within-group analysis for time effect comparison regardless of the biomaterial, followed by pairwise multiple comparisons with confidence interval adjustment and Bonferroni correction. *: denotes a significant mean difference at the 0.05 level. (n = 24/ time).

Table 4.15
Mean Difference of hMSCs Optical Density Among Biomaterial Groups

Group Comparison		Mean Difference	95% Confidence Interval		*p*-value
			Lower Bound	Upper Bound	
Negative control	Ti	- 0.28	- 0.379	- 0.180	< 0.001*
	mNiTi	- 0.30	- 0.402	- 0.204	< 0.001*
	pNiTi	- 0.51	- 0.607	- 0.409	< 0.001*
Ti	mNiTi	- 0.02	- 0.123	0.076	0.913
	pNiTi	- 0.23	- 0.330	- 0.129	< 0.001*
mNiTi	pNiTi	- 0.21	- 0.304	- 0.106	< 0.001*

Notes: F = 5424.30 (1), $p < 0.001$. A repeated-measures ANOVA between-group analysis was applied to assess the effect of biomaterial type on mean optical density, followed by post hoc multiple comparisons. *: denotes the mean difference significant at the 0.05 level (two-tailed), (n = 6/ group).

4.3.4.2 Alkaline Phosphatase Activity (ALP)

The means and standard deviations of alkaline phosphatase (ALP) activity are presented in Table 4.16. On day 7, the Ti group exhibited the highest mean ALP level (41.22 ± 14.84), while the negative control group showed the lowest mean (36.18 ± 9.98). By day 14, mean ALP levels had increased compared with day 7, with the pNiTi group showing the highest mean ALP of 67.86 ± 18.43.

A repeated-measures ANOVA indicated that extending the incubation time of hMSCs on biomaterials significantly increased ALP activity, with a mean difference (MD) of -21.67 (95% CI: -28.02 to -15.32), $p < 0.001$. However, the type of biomaterials did not significantly influence ALP secretion by hMSCs ($p = 0.12$).

Table 4.16
Descriptive Statistics and Pairwise Comparisons of Alkaline Phosphatase Secreted by hMSCs Between Day 7 and Day 14

Time (Day)[a]	Group[b]	Mean (SD)	F(df)[b]	*p*-value
7	Negative control	36.18 (9.98)	2.14 (3)	0.12
	Ti	41.22 (14.84)		
	mNiTi	25.55 (4.29)		
	pNiTi	36.27 (4.77)		
14	Negative control	50.79 (15.22)		
	Ti	52.87 (8.71)		
	mNiTi	54.36 (9.30)		
	pNiTi	67.86 (18.43)		

Notes: Repeated Measures ANOVA. [a] A significant difference within days. [b] Group Effect. The significance level was set at $p = 0.05$

4.3.4.3 Alizarin Red S staining (ARS)

The mean and standard deviation of the Alizarin Red S (ARS) assay, which evaluates calcium deposition by hMSCs across various biomaterial groups and time points, are presented in Table 4.17. A repeated-measures ANOVA revealed a significant

increase in the ARS assay on day 28 across all tested groups, with a mean difference (MD) of -0.07 (95% CI: -0.08, -0.05), $p < 0.001$.

Additionally, there were significant differences between the groups influencing the ARS assay results ($p < 0.001$). Multiple pairwise comparisons, corrected with the Bonferroni method, indicated that the interactions were between the pNiTi group and all other groups ($p < 0.001$), as well as between the Ti and mNiTi groups ($p < 0.05$).

Table 4.17
The Mean and Pairwise Comparisons for ARS Assay between Day 21 and Day 28 Across Different Groups

Time (Day)[a]	Group[b]	Mean ± SD	F(df)[b*]	*p*-value	Group Interaction[c]	Mean Difference (95 % CI)	*p*-value
21	Negative control	0.03 ± 0.02	75.52 (3)	< 0.001	Negative control – Ti	0.02 (-0.01, 0.05)	0.19
	Ti	0.01 ± 0.00			Negative control - mNiTi	-0.01 (-0.03, 0.01)	0.78
	mNiTi	0.08 ± 0.01			Negative control - pNiTi	-0.17 (-0.20, -0.13)	< 0.001
	pNiTi	0.03 ± 0.02			Ti - mNiTi	-0.03 (-0.06, -0.01)	0.01
28	Negative control	0.13 ± 0.03			Ti - pNiTi	-0.19 (-0.22, -0.15)	< 0.001
	Ti	0.12 ± 0.04			mNiTi - pNiTi	-0.15 (-0.19, -0.20)	< 0.001
	mNiTi	0.12 ± 0.04					
	pNiTi	0.24 ± 0.03					

Note: Repeated Measures ANOVA. [a] A significant difference within days. [b] Between-group effect. [b*]Multivariate Tests. [c] Multiple pairwise comparisons using Bonferroni correction. The significance level was set at $p = 0.05$

4.3.4.4 Scanning Electron Microscopy (SEM)

The image in Figure 4.16 presents a series of scanning electron microscopy (SEM) images of hMSCs cultured on various biomaterials in osteogenic media.

Following a 7-day incubation period, small cell aggregates adhered to all evaluated biomaterials, as evidenced by panels A (Titanium), B (mNiTi), and C (pNiTi). Furthermore, the progression of hMSCs' activity and surface interaction on pNiTi over time is represented through points C1 to C4. The orange arrows in the images indicate areas of particular interest, including cell attachment sites, extracellular matrix formation, and interactions with the biomaterial surface. Collectively, the images demonstrate the compatibility and biological response of hMSCs to titanium and NiTi throughout the incubation period.

In C1 (day 7), the early stage exhibits scattered cell adhesion alongside initial extracellular matrix formation, as indicated by the arrows. C2 (day 14) reveals an increase in cell attachment and proliferation, accompanied by noticeable extracellular matrix deposition (orange arrows). C3 (day 21) shows a well-developed, dense extracellular matrix, highlighting enhanced cellular activity and interaction (orange arrows). C4 (day 28) presents a mature and compact extracellular matrix characterised by dense cellular coverage, indicating successful cell proliferation and integration.

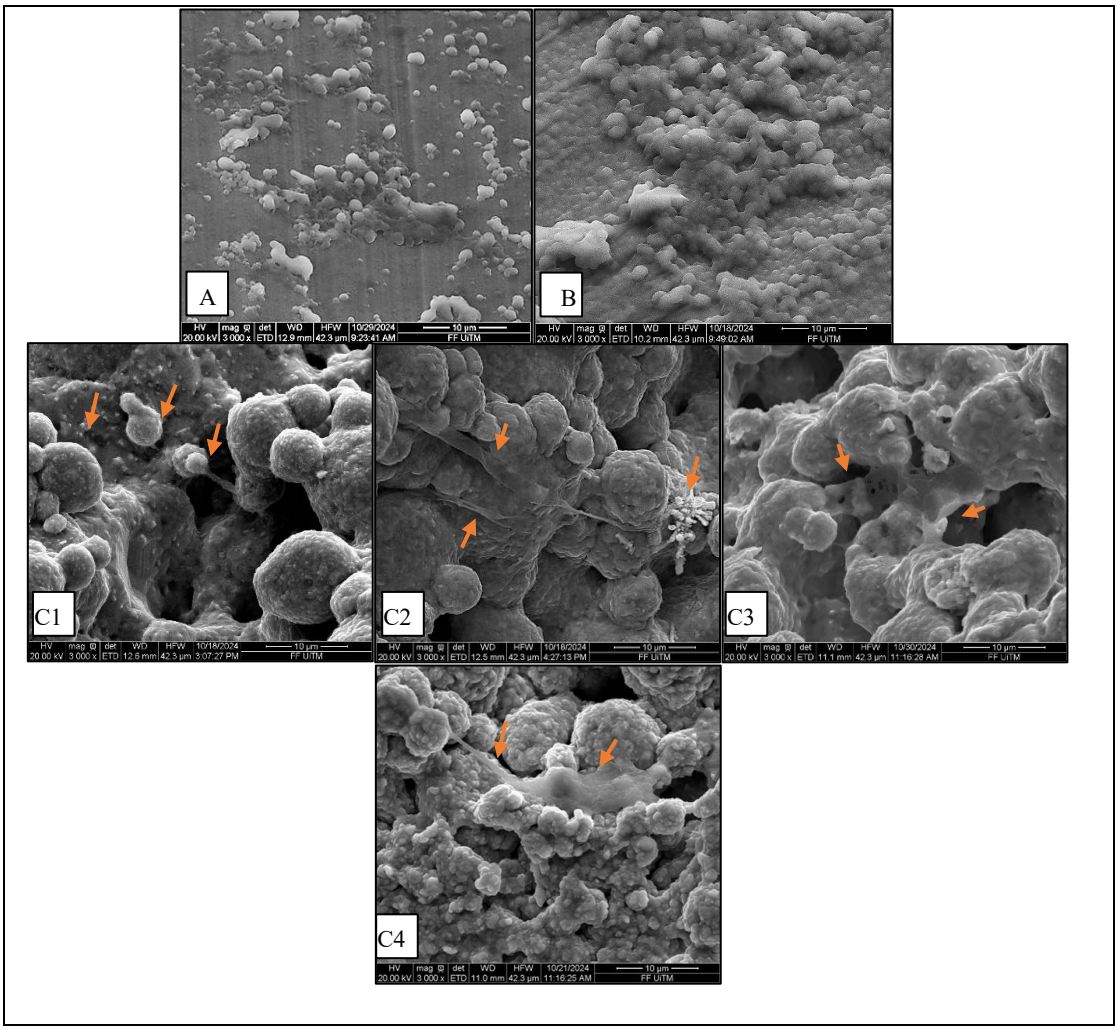

Figure 4.16 SEM Images of hMSCs Incubated on Different Biomaterial Groups.

Note: A on titanium, Ti (day 7); B on mNiTi (day 7); C on pNiTi at different time intervals – C1: day 7, C2: day 14, C3: day 21, and C4: day 28.

4.3.5 Nickel Ion Release

4.3.5.1 Nickel Ion Release in Different Types of Media

Table 4.18 demonstrates the mean and standard deviation of nickel ion release based on exposure (day 1, 2, 14 and 28), media (DMEM at pH 7.2, 0.9 % NaCl at pH 6 and 7) and NiTi-based biomaterials; dense-machined (mNiTi) and porous (pNiTi) surfaces fabricated by conventional casting and metal injection moulding techniques.

Regardless of the media type and NiTi surface, the highest average release of nickel ions was on day 14 at 0.020 ± 0.019 µg/L, while the lowest occurred on day 28 at 0.005 ± 0.007 µg/L. Based on the media used, the 0.9% NaCl solution at pH 7 showed

a nickel concentration of approximately 0.015 ± 0.016 µg/L, which was higher than at pH 6 and in DMEM (pH 7.2). Meanwhile, considering the NiTi surface, pNiTi released more nickel than mNiTi, with a value of 0.014 ± 0.017 µg/L.

The trend in nickel ion release from both NiTi groups is illustrated in Figure 4.17. In DMEM, higher levels of nickel ions were observed on days 1 and 3, followed by a declining trend by day 28. The pH 6 and pH 7 0.9% NaCl solutions showed inconsistencies, with mean release peaking on day 14 before dropping back to day 1 levels.

Multivariate analyses revealed significant differences by exposure duration ($p < 0.001$) and by the type of media used in the NiTi groups ($p = 0.02$). Detailed post hoc analyses with Bonferroni correction are presented in Table 4.19.

Table 4.18
Descriptive Analysis of Nickel Release (µg/L) Based on Days Evaluated, Media and NiTi Group

Variables[a]	**Mean**	**SD**	**F(df)**[b]	***p*-value**
Day Exposure				
1	0.013	0.014	21.12 (3)	< 0.01
3	0.011	0.008		
14	0.020	0.019		
28	0.005	0.007		
Media				
DMEM	0.010	0.014	9.99 (2)	< 0.001
NaCl (pH 6)	0.012	0.012		
NaCl (pH 7)	0.015	0.016		
NiTi Group				
mNiTi	0.010	0.010	5.76 (1)	0.020
pNiTi	0.014	0.017		

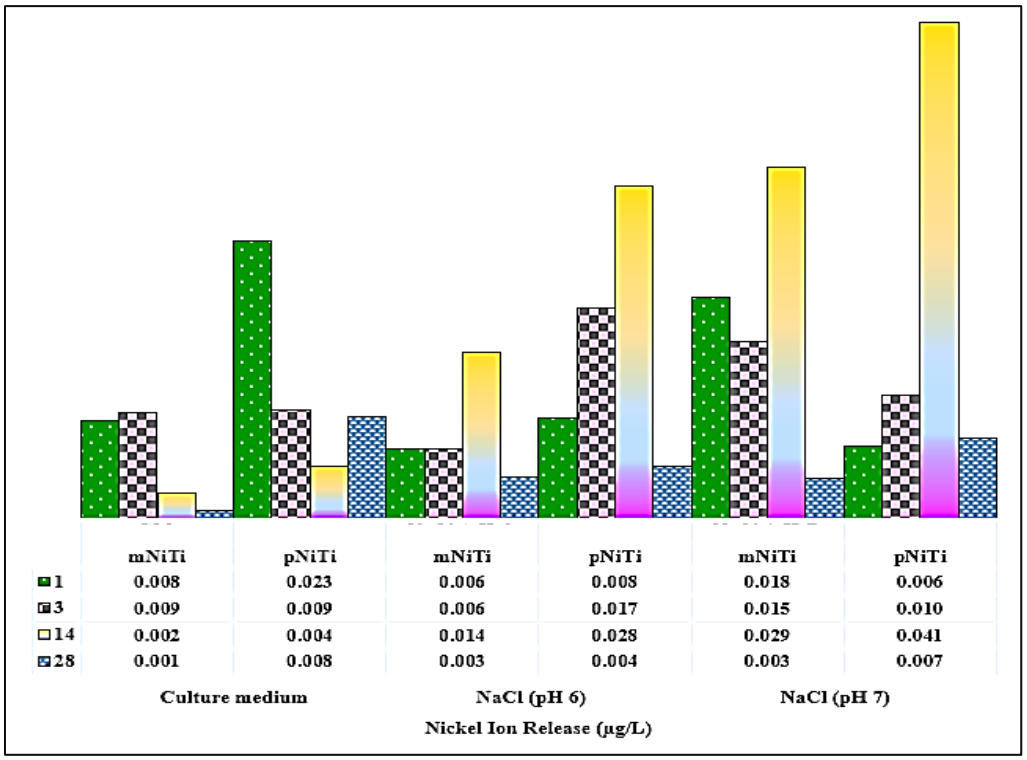

Figure 4.17 Mean of Nickel Ion Release (µg/L) by NiTi Biomaterial into Different Types of Media at Different Time Intervals

Table 4.19
Multiple Pairwise Comparisons of the Effect of Day Exposure, NiTi Group, and Media Used on Nickel Ion Release (µg/L)

Interactions		**Mean Difference**	**95 % Confidence Interval for Difference**		***p*-value**
			Lower	**Upper**	
The Effect of Time Exposure (Days)					
Day	Day				
D1	D7	0.002	-0.003	0.008	1.000
	D14	-0.007	-0.013	-0.001	0.018
	D28	0.008	0.003	0.013	< 0.001
D7	D14	-0.009	-0.015	-0.003	< 0.001
	D28	0.006	0.002	0.010	0.001
D14	D28	0.015	0.010	0.020	< 0.001
The Effect of the Group of NiTi Used					
Group	Group				
mNiTi	pNiTi	-0.004	-0.007	-0.001	0.020

Interactions		Mean Difference	95 % Confidence Interval for Difference		*p*-value
			Lower	Upper	
The Effect of Media					
Media	Media				
DMEM	NaCl (pH 6)	-0.003	-0.008	0.002	0.380
	NaCl (pH 7)	-0.009	-0.013	-0.004	< 0.001
NaCl (pH 6)	NaCl (pH 7)	-0.006	-0.010	-0.001	0.019
The Effect of Groups Soaking on Different Types of Media					
Group	Media				
mNiTi	DMEM	0.005	0.001	0.009	0.124
	NaCl at pH6	0.008	0.004	0.012	0.189
	NaCl at pH7	0.017	0.013	0.021	< 0.001
pNiTi	DMEM	0.011	0.007	0.015	0.008
	NaCl at pH6	0.014	0.010	0.018	< 0.001
	NaCl at pH 7	0.016	0.012	0.020	< 0.001

4.3.5.2 Nickel Release to the Culture Media and Its Relationship on hMSc Viability

An evaluation of nickel ion release in culture media (DMEM, pH 7.2) at different time intervals and its influence on hMSCs viability is demonstrated in Table 4.20. pNiTi showed a higher amount of nickel ions released into the DMEM culture media than mNiTi, $p = 0.03$, especially on day 1. Over time, a significant difference was observed ($p < 0.05$). Post-hoc analysis with the Bonferroni correction showed a significant difference between day 3 and day 14; MD (95% CI): 0.01 (0.00, 0.01), $p = 0.03$. Based on Spearman's rank correlation, there was a very weak positive association between the release of nickel ions into the DMEM and hMSCs viability ($r = 0.07$). Nonetheless, no significant difference was observed $p = 0.48$.

Table 4.20
Nickel Ion Release (μg/L) in Culture Media by NiTi Biomaterials and Its Relationship to hMSCs Viability

Group	Time (Day)[a]	Mean ± SD	Group Effect		Time Effect		Correlation[b]	
			F(df)	*p*-value	F(df)	*p*-value	Correlation Coefficient	*p*-value
mNiTi	1	0.008 ± 0.005	8.794 (1)	0.009	3.814 (5)	0.048	0.07	0.48
	3[A]	0.009 ± 0.006						
	7	0.003 ± 0.002						
	14[A]	0.002 ± 0.003						
	21	0.002 ± 0.003						
	28	0.000 ± 0.003						
pNiTi	1	0.023 ± 0.028						
	3[A]	0.009 ± 0.004						
	7	0.006 ± 0.007						
	14[A]	0.004 ± 0.006						
	21	0.007 ± 0.007						
	28	0.008 ± 0.013						

Notes: [a] A Repeated Measure ANOVA. Multivariate analyses found a significant difference (p = 0.048), followed by pairwise comparisons with Bonferroni correction. A similar letter "A" indicates a significant difference, $p = 0.03$; [b] Spearman's Correlation. The significant difference is at 0.05.

CHAPTER 5
DISCUSSION

5.1 Chapter Outline

This chapter presents a comprehensive discussion of the research conducted to assess the clinical performance of a newly developed porous nickel-titanium dental implant known as NiTiDent Tuah (NT). This investigational implant is compared with a well-established commercial implant, AnyRydge® (AR), aimed at a single-tooth replacement in the posterior mandible. The study, conducted with meticulous attention to detail, assessed several critical parameters, including implant stability, peri-implant tissue health, crestal bone levels, patient satisfaction, and oral health-related quality of life (OHRQoL).

While the control group demonstrated successful integration throughout the 1-year study, the NiTiDent Tuah implant had a median survival time of 20 weeks. Failures associated with this implant were predominantly linked to foreign-body reactions, traced to external metal contamination from degradation of the surgical drill. These findings were substantiated through histopathological examinations and energy-dispersive X-ray spectroscopy (EDS) analysis.

In vitro analyses demonstrated that porous NiTiDent Tuah exhibited positive biocompatibility and osteogenic potential, as evidenced by alkaline phosphatase (ALP) and calcium secretion, and the formation of a mature bone matrix after 28 days of incubation. However, this promising *in vitro* result, as reported in subchapter 4.3.4, and the previous animal study (Rahimi, 2023; Mustafa et al., 2024) did not translate into clinical success, potentially due to unforeseen extrinsic instrumentation factors rather than the intrinsic material properties of the porous implant.

This chapter's discussion is divided into two sections. Part A delves into the key findings from the clinical trial. The preceding chapter, Part B, dissects the underlying factors contributing to the biological failure observed in the NiTiDent Tuah porous NiTi dental implant.

5.2 Discussion for Part A - The Clinical Trial Study

5.2.1 Participants' Demographic Distribution in This Study

The study was initially planned to include 105 participants, with 75 in the test group (NT) and 30 in the control group (AR). However, after 5 months, the NT group experienced early implant failures (n=3), prompting a temporary pause in the study to closely monitor the remaining participants with the tested implant. One year after the study commenced, all participants in the NT group were excluded due to early implant disintegration, leading to the study's early termination. The focus then shifted to investigating the causes of these failures. Meanwhile, data collection continued for the remaining participants randomly assigned to the control group. Hence, due to premature termination of this study, only 30 participants were included: n=12 in the test group and n=18 in the control group.

The demographic data illustrated in Table 4.1 reveal significant insights into the participant diversity in this study, encompassing various aspects such as gender, education level, occupation, and income. The gender distribution shows a predominant female representation, with 21 participants (70%) compared to 9 males (30%). This disparity may suggest that females are generally more proactive in seeking dental care, thus indicating differences in health-seeking behaviour.

Regarding age, the participants exhibited a relatively homogeneous distribution, with an average age of 39.3 years (± 10.5 years). Notably, males exhibited an average age slightly higher at 39.6 years (± 7.2). Furthermore, educational status was a significant feature of the study population, where a substantial majority (73.3%) possessed tertiary education. The occupational analysis indicated that the professional sector comprised the largest group (16 participants, 53.3%), followed by clerical positions (8 participants, 26.7%) and other occupations (6 participants, 20%). This reflects a correlation between educational attainment and professional background, a key insight that enhances participants' awareness and understanding of dental treatments, especially implant treatment.

In terms of income, the majority (86.7%) of participants fell within the lower-to middle-income bracket, with household incomes of less than RM11,000. This demographic detail suggests that the study primarily attracted participants from average

income backgrounds, potentially influenced by the subsidies provided for the survey, thereby reflecting socioeconomic factors in dental care accessibility.

5.2.2 Insertion Torque Value (ITV) and Implant Stability Assessment between Anyridge® and NiTiDent Tuah Dental Implants

Achieving primary stability prevents micromovement and supports physiological and biological bone healing after implant placement. Primary stability is a mechanical phenomenon that reflects the direct engagement between the bone and the implant during initial placement (Javed et al., 2011). In this study, the primary stability of the implant was assessed by insertion torque (IT) and resonance frequency analysis (RFA). While IT indicates the resistance of an implant during its insertion into the prepared osseous bed, RFA measures resistance to lateral movement, expressed as an implant stability quotient (ISQ). These parameters can serve as predictive measures for long-term implant success. Overall, IT and RFA values showed that both implants used in this work demonstrate acceptable primary stability, with the control group consistently performing better than the tested group.

The AR dental implant's higher ITV and ISQ values suggest better mechanical engagement within its osseous bed. Influential factors affecting IT and ISQ values, specifically bone factors and surgical protocols, were systematically controlled throughout the study. All surgeries were conducted under standardised conditions by experienced and calibrated surgeons. This was evidenced by the consistent outcomes in the control group, which showed variability in ITV (IQR = 7.75), whereas the tested group displayed no such fluctuations (IQR = 0.00). Significantly, the participant selection was restricted to the posterior mandible, owing to its favourable bone quality, which allows better control of primary stability and reduces confounding factors. This setting ensures a safer environment for first-in-human evaluations of new implant systems. Although not quantified in the present study, the authors believe that the participants predominantly consisted of D2 bone types, with minor contributions from D3 bone types (Truhlar et al., 1997). In this work, all participants also experienced a period of edentulousness exceeding four months without any local or systemic conditions that could interfere with post-extraction bone healing.

In this investigation, the mean insertion torque (IT) recorded for both types of implants ranged from 35 to 38 Ncm, categorising them within the intermediate torque

range of 32 to 50 Ncm, which is believed to be safe for restorative survival (Lemos et al., 2021; Ottoni et al., 2005). The role of torque values in influencing the success of dental implants is a topic of ongoing debate in the literature (Berardini et al., 2016). High torque levels (50 – 176 Ncm) and regular or low torque levels <30 Ncm have both been discussed as factors essential to achieving implant success (Atieh et al., 2012; Berardini et al., 2016; Lemos et al., 2021).

Research suggests that high torque may be necessary to achieve primary stability, particularly in cases of immediate loading and single-crown applications (Cannizzaro et al., 2012). However, applying excessive torque could pose risks to the bone-implant interface. It may lead to the formation of microfractures in the bone and exert compressive forces that could adversely affect bone microcirculation, ultimately affecting osteocyte activities (Bashutski et al., 2009; Cory et al., 2010; Insua et al., 2023; Ueda et al., 1991) and early marginal bone loss due to the compression of the cortical bone (Marconcini et al., 2018; Oskouei et al., 2023). Such complications might increase the chances of implant failure (Bashutski et al., 2009). Moreover, utilising a high insertion torque could compromise the microgeometric characteristics of the implant itself (Cannizzaro et al., 2012). Recent studies have suggested that there may be no significant differences in IT values with respect to implant survival (Berardini et al., 2016; Norton et al., 2017). Clinical evidence shows that low torque (less than 30 Ncm) can achieve osseointegration regardless of the treatment protocol used (Darriba et al., 2022; Lee et al., 2019; Rodrigo et al., 2010). Conversely, other research has indicated that maintaining an intermediate torque (greater than 35 Ncm but less than 50 Ncm) may be vital for optimising the survival of single restorations (Darriba et al., 2022).

The AR group demonstrated an average ISQ of 64.18 ± 10.19, which is 10 % higher than the NT group's average of 52.18 ± 13.63. Unlike the AR group, the NT group exhibited greater variability in ISQ values. While bone quality was not evaluated in this study, the variance observed in IT value and ISQ was likely attributable to inherent differences in macro design, specifically thread geometry and material type, and may also stem from inaccuracies in the osteotomy procedure resulting from the imprecision of NT's surgical bur.

Furthermore, the findings from both IT and ISQ directly influenced the correlation analysis conducted in this study. They showed a weak inverse relationship between implant torque (IT) and initial stability quotient (ISQ) values, with a correlation coefficient of -0.36 and a non-significant *p*-value of 0.31. Although other studies agree

that there is no relationship between ITV and ISQ (Akca et al., 2006; Levin et al., 2016), this intriguing finding contrasts with previous research, which has consistently suggested a positive correlation (Makary et al., 2019; Sarfaraz et al., 2019), as higher torque values (ITV) are expected to be linked with increased primary stability, as measured by ISQ (Sarfaraz et al., 2019).

The thread design, including pitch, depth, and morphology, has a dramatic effect on implant-bone interaction (Abuhussein et al., 2010; Dos Santos et al., 2011; Insua et al., 2023; Menini et al., 2020; Vollmer et al., 2022). Implants featuring deeper threads, a smaller pitch, and a reduced helix angle have been shown to improve primary stability by increasing bone-to-implant contact while reducing osseointegration compression (Abuhussein, 2010). The AR group utilised a more aggressive thread design in our analysis, featuring a knife-edge depth of 0.6 mm consistent across the entire fixture. In contrast, the NT group had a thread depth ranging from 0.2 to 0.4 mm, with a rounded V-shaped configuration in the apical region that transitioned to square threads from the middle third towards the top.

The aggressiveness of the V-shaped thread design facilitates bone cutting. It allows smoother implant insertion into the osseous bed (Dos Santos et al., 2011), potentially contributing to increased bone condensation during insertion and enhancing both initial stability biometrics (IT and ISQ) (Menini et al., 2020). Additionally, finite element analysis has shown that thread depth plays a pivotal role. Implants with thread depths between 0.2 and 0.6 mm exhibit diverse stress distributions. Those with deeper threads, particularly those exceeding 0.44 mm in diameter, exhibit enhanced biomechanical performance. The most favourable outcomes were noted, with depths ranging from 0.34 to 0.5 mm, indicating that this may provide further insight into the improved initial stability observed in the control group (Ao et al., 2010).

While the smooth, rounded V-shaped threads in the NT group facilitate easier insertion, and the square threads enhance bone-to-implant contact (BIC) by providing a better grip (Ryu et al., 2014), neither thread type is likely to cause localised bone fracturing during insertion. Similarly, from a biomechanical perspective, the thread depth of NT is shorter than that of AR, and the smooth, rounded thread tip edge makes it unlikely to cause microfractures in bone; however, this does not explain why the IT and ISQ values are lower. Two possible factors could contribute to this: first, the NT group is made of a NiTi-based material, which has inherent elastic and shape-memory properties (Jani et al., 2014; Shabalovskaya, 1996), allowing it to change shape under

compression and strain and recover after full seating in the osseous bed. Second, there was also a potential for imprecise osseous bed preparation with the NT surgical bur, which may contribute to a more destructive implantation process compared to the control group, despite careful control of the surgical osteotomy.

This study's correlation findings suggest that, in addition to prior discussions concerning the macro design of implants and the type of material utilised, the small sample size may significantly influence these results. A skewed distribution of variability in NT ISQ values could adversely affect the outcomes observed. Furthermore, as previously discussed, aggressive thread design in AR was positively associated with increased mechanical engagement. This observation aligns with earlier studies on similar implant types, highlighting elevated IT and ISQ values during initial assessments and the subsequent one-month evaluation period. (Makary et al., 2019).

Moreover, the weak, non-significant correlation identified suggests that IT and ISQ assess fundamentally different aspects of stability. It concerns the shear force exerted during implant insertion, whereas ISQ assesses resistance to micromotion via resonant frequency. This latter metric indicates the quality or density of the surrounding osseous structure. Makary et al. (2019) reported a robust correlation between IT and ISQ only in soft bone (D4) instances, with no significant correlation in denser bone types classified as D2 and D3. Interestingly, even in type D1 bone, an inverse correlation was observed, although it was not statistically significant. These nuanced distinctions highlight the complexity of measuring and interpreting initial or primary stability in implant systems, and the relationship remains inconclusive.

Implant stability progresses from mechanical fixation to biological integration. The subsequent evaluation of ISQ values for both implant types revealed a consistent improvement in secondary implant stability over time in the AR group, beginning at implant placement and continuing until crown insertion, approximately 5 months post-implantation.

The AR group exhibited impressive IT and ISQ values, indicating implant stability with minimal or no micromotion, possibly below the 50 μm threshold, thereby facilitating osseointegration. While a temporary decline or fluctuation in implant stability, known as the "dip" phenomenon, is common during the initial healing phase, particularly within the first month post-insertion, evidence from previous studies confirms that the AR implant remains stable throughout this critical period (Makary et al., 2019). At the 4-month review before the second-stage surgery, the implant showed

a marked improvement in ISQ, rising from an initial stability of 64.18 ± 10.19 to 65 and an impressive 81. This significant enhancement indicates successful biological changes and a robust transition from primary mechanical stability to secondary biological stability through bone remodelling and integration. Moreover, existing studies indicate that implant stability may fluctuate in the early phases; however, by 3-4 months, stability consistently improves as new bone encases the implant (Barewel et al., 2003; Smeets et al., 2016; Wang et al., 2018). By the crown placement visit, approximately 5 months after insertion, the ISQ of the AR group consistently ranged from 71 to 85, indicating a solid transition to biological stability, with mature bone undoubtedly adapting around the implant.

These two key intervals, ~ 4 and 5 months after implant placement, are crucial for ensuring a predictable outcome, guiding the decision to proceed with prosthetic loading, and assessing the long-term success of the implant treatment. This enhancement highlights the reliability of AR implants in achieving and maintaining stability throughout this critical healing phase. In addition to the progressive thread design, the ample inter-thread space has increased the surface area of the wound chamber, thereby improving blood circulation (Makary et al., 2019). Furthermore, AR features a special surface treatment that involves the hydrothermal incorporation of calcium ions, which activates osteoblasts and expedites osseointegration. This surface characteristic accelerates biological interactions and establishes implant stability (Mangano et al., 2017). Moreover, allowing the implant to heal in its osseous bed for an adequate period permits bone integration without compromise.

In contrast, the implant stability quotient (ISQ) for the NT group was recorded only twice: at the initial assessment (V_1) and at the third visit (V_3). By V_3, ISQ values were obtainable for only 7 implants due to early implant failures. Notably, this observation revealed a significant decline in stability in the NT implant group, with measurements dropping to a concerning value of 7.00. The observed variations in ISQ within the NT group may indicate an adverse healing response of the peri-implant tissue, rather than shape changes resulting from intrinsic micromovement. NiTi material exhibits superelastic and shape-memory properties due to its martensite-austenite transformation (Duering et al., 2017). However, in this study, no functional stress-strain was applied, as the implants were fully embedded in bone before the second stage, and no changes in body temperature occurred that could trigger intrinsic changes. As a result, in the absence of functional stress-strain or significant temperature variations,

the NT is expected to maintain its austenite form (Krämer et al., 2017). Therefore, Part B of this chapter will explore the NT group's performance and further discuss the investigations conducted. Hence, in the paragraphs that follow, only the clinical performance of the AnyRidge® implants will be considered, specifically the peri-implant soft tissue, crestal bone levels, patient satisfaction, and patient-related outcome satisfaction.

5.2.3 Peri-Implant Soft Tissues

This study evaluates peri-implant soft tissues, focusing on the incidence of inflammation, bleeding on probing (BOP), and probing depth at three predetermined time points. V_4 corresponds to the day of crown placement; V_5 corresponds to the day of the first review, three months after crown placement; and V_6 corresponds to the day of the second review, six months following crown placement, as delineated in Table 4.5.

Peri-implant tissue health is critical for the long-term success of dental implants. Probing depth (PD) and bleeding on probing (BOP) are key indicators of peri-implant health (Berglundh et al., 2024 & 2018; Ramanauskaite et al., 2018). BOP strongly predicts peri-implant mucositis but is unreliable in detecting peri-implantitis (Lindhe & Meyle, 2008). PD increases with peri-implant disease severity, while BOP is more prevalent in peri-implantitis compared to mucositis (Ramanauskaite et al., 2018). Probing force significantly affects BOP and PD measurements, with 0.15 N suggested as the optimal pressure to avoid false positives (Coli & Sennerby, 2019; Gerber et al., 2008). Early soft tissue healing around one-stage implants shows stable PD from 4 to 12 weeks post-surgery, with no significant association between flap thickness or papilla height and bleeding sites (DeAngelo et al., 2007).

Our evaluation of peri-implant soft tissue health around AR implants showed a temporary increase in inflammation, bleeding on probing (BOP) and a significant increase in PD at three months post-placement (V_5), which subsided by six months (V_6). This pattern aligns with previous studies indicating that early soft tissue adaptation occurs around similar implants, followed by stabilisation as the peri-implant mucosal seal matures (Rossi et al., 2021). The observed mild, transient inflammation and an increase in BOP, along with slight increases in PD, suggest a post-crown-placement response leading to early mucosal remodelling, which does not signify peri-implant

disease. The decrease in BOP at V_6 indicates successful soft tissue adaptation and maturation, a positive indicator of long-term implant success.

It is essential to consider that patient factors may affect these results, as only 3 of 18 participants showed signs of inflammation (2 with mild and 1 with moderate). Lang & Berglundh (2011) reported that early inflammation around implants can be reversed with proper intervention. In these cases, participants were re-educated and encouraged to adhere to a comprehensive oral hygiene regimen. The effectiveness of this approach became evident after six months, as evidenced by a subsequent reduction in inflammation, suggesting that the peri-implant mucosa may improve with targeted interventions.

Additionally, several factors may contribute to improving tissue health. The knife-edge thread design of AnyRidge implants maintains peri-implant tissue stability, minimising long-term risks of inflammation (Farronato et al., 2021) and promoting soft-tissue stability (Farronato et al., 2020). The implant-abutment interface also plays a crucial role in supporting soft tissue healing. The platform-switched design of AnyRidge implants prevents micro gaps, stabilising the crestal bone to support the soft tissue (Farronato et al., 2021). Rossi et al. (2021) noted that AnyRidge implants display mild early mucosal inflammation due to fibroblast attachment, which stabilises over time.

Within six months of evaluating peri-implant tissues, this study demonstrates that transient peri-implant inflammation stabilised, with minimal changes in probing depth. Our PD values (1.6–1.8 mm) suggest healthy peri-implant conditions, as a healthy soft implant is reported to have an average PD of 1.5–2.5 mm. At the same time, peri-implantitis is often associated with PD > 4 mm (Heitz-Mayfield & Salvi, 2018).

5.2.4 Crestal Bone Levels

Evaluating changes in crestal bone levels is essential for assessing the long-term stability of dental implants. In this study, bone levels were measured from the implant fixture neck to the first bone-implant contact. Negative values indicate that the bone level is above the implant neck, which may suggest favourable bone adaptation or osseointegration.

The results suggest that bone levels remain favourable throughout the observation period, consistently above the implant neck, with some fluctuations. The

slight reductions observed after three months of implant installation (V_1–V_4) may reflect healing and adaptation. We observed a slight, albeit minimal, increase in crestal bone in V_5, followed by a further increase in V_6, likely due to a normal bone response to functional adaptation to occlusal forces rather than peri-implant bone loss.

Following implant placement, the crestal bone undergoes remodelling as an integral component of osseointegration. During this phase, a marginal bone loss (MBL) ranging from 0.5 to 1.5 mm is anticipated, which is a consequence of surgical trauma associated with osteotomy preparation (Berglundh & Lindhe, 1996), disruption of blood supply during flap preparation (Kotsakis & Romanos, 2022), and the natural bone remodelling process within the first year (Albrektsson et al., 1986; Kotsakis & Romanos, 2022).

This study reveals fascinating insights into how crestal bone undergoes consistent remodelling following crown placement. These changes stem from the bone's dynamic biological response to various influencing factors. Among these, the design of the implant-abutment connection plays a crucial role, as highlighted in research by Atieh et al. (2013), Kim K et al. (2020) and Kim J et al. (2020). Other factors include implant surface characteristics, implant dimensions, surgical techniques, peri-implant soft-tissue thickness, and loading protocols.

The type of implant-abutment connection is a standout factor that significantly impacts marginal bone stability. In this study, the AnyRidge® implant system, featuring a Morse taper connection, demonstrated exceptional mechanical stability. This design minimises bacterial microleakage and creates a friction-fit connection that eliminates micro-movements (Fuda et al., 2023). This reduces stress at the bone-implant interface, effectively helping to prevent crestal bone loss, as supported by Kim J et al. (2020).

Moreover, the study employed the platform switching concept in its implant design, which may have contributed to the remarkable preservation of crestal bone levels. This innovative approach utilises a narrower abutment than the implant platform, effectively shifting the inflammatory zone away from the junction where the bone meets the implant. Evidence shows that this design can significantly reduce peri-implant bone loss compared to traditional implant designs, as found in studies by Canullo et al. (2016) and Lazzara & Porter (2006). A comprehensive meta-analysis by Mishra et al. (2021) even confirmed that platform-switched implants experience an average reduction of 0.5 mm in marginal bone loss compared to non-platform-switched options.

The implant's surface properties are also vital for osseointegration and bone preservation. Roughened surfaces, such as SLA or anodised finishes, promote enhanced bone-to-implant contact (BIC) compared to smoother alternatives (Li et al., 2002; Schwarz et al., 2009). As mentioned earlier in this discussion section, the AnyRidge was treated with calcium ions, which are believed to accelerate biological healing cascades; thus, an increase in BIC was anticipated. This effect is particularly pronounced during the early healing phase, where increased BIC translates into improved implant stability, ultimately reducing marginal bone loss.

Concerning implant dimensions, a 4.5 mm diameter and 10 mm length were utilised in this study. The diameter and length of the implant significantly affect stress distribution and bone remodelling at the crestal level. Wider implants (≥ 4mm) distribute occlusal forces more effectively, minimising stress on the crestal bone, whereas longer implants offer enhanced primary stability, decreasing early micromovements and subsequent bone remodelling (Atieh et al., 2012; Javed et al., 2011). Research comparing conventional implants with AnyRidge® has shown considerably lower marginal bone loss with AnyRidge®, attributed to superior stress distribution and improved primary stability (Hamed et al., 2020; Makary et al., 2019).

The selected delayed loading protocol for this investigation substantially affects the stability of the bone surrounding the implant. The timing of prosthetic loading is critical for peri-implant bone remodelling. Delayed loading provides sufficient time for osseointegration before applying functional occlusal stresses to the implant, thereby mitigating early bone loss and enhancing the observed stability of crestal bone in this study.

Bone density differs between the maxilla and mandible, influencing primary stability and marginal bone preservation. This study exclusively examines the replacement of a single molar tooth in the posterior mandible, where increased bone density provides superior implant stability and reduced marginal bone resorption compared with the posterior maxilla (Javed & Romanos, 2010). This may elucidate the advantageous bone-level results obtained. The selected delayed loading protocol for this investigation substantially affects the stability of the bone surrounding the implant. The timing of prosthetic loading is critical for peri-implant bone remodelling. Delayed loading provides sufficient time for osseointegration before applying functional occlusal stresses to the implant, thereby mitigating early bone loss (Cobo-Vázquez et

al., 2018; Darriba et al., 2022) and enhancing the observed stability of crestal bone in this study.

In addition to these factors, the thickness of the peri-implant tissue may significantly influence the maintenance of the crestal bone level. In this study, nearly 90% of participants exhibited adequate mucosal thickness, although this detail was not documented in the results chapter. A thicker peri-implant mucosa (greater than 2 mm) acts as a biological barrier, thereby mitigating crestal bone resorption (Linkevicius et al., 2015). Conversely, a thinner peri-implant mucosa (less than 2 mm) has been associated with increased marginal bone loss due to insufficient soft-tissue protection (Buser et al., 2016).

In this study, the likely preservation of crestal bone levels observed with the AR implant may be due to multiple interacting factors. The combination of Morse taper connection, platform switching, rough implant surfaces, wider dimensions, delayed loading, high bone density, and adequate mucosal thickness appears to have contributed to minimal marginal bone loss. These findings emphasise the multifactorial nature of bone preservation around implants, suggesting that biomechanical and biological factors are essential for long-term success.

5.2.5 Patient Satisfaction and Patient-Related Outcome Satisfaction Using a Validated Patient Satisfaction Questionnaire (PSQ) and Validated Oral Health Impact Profile (Malay version)

In addition to clinical parameters, this study also evaluated patients' reported outcomes regarding the impact of implant treatment. The Patient Satisfaction Questionnaire (PSQ) score evaluates overall satisfaction. This includes patient satisfaction assessments of aesthetics, masticatory performance, phonetics, and comfort. Patients' willingness to recommend the treatment to others and their readiness to undergo similar treatment at the same institution were also noted. The Oral Health Impact Profile (OHIP) score measures the perceived impact of oral health on quality of life, encompassing the biopsychosocial aspects of the patient's pre- and post-implant treatment.

The PSQ score fell within the "high satisfaction" range, indicating that most patients are generally satisfied with their implant treatment. Consequently, significant improvements in OHRQoL were also anticipated on the OHIP-14 assessment, as all

domains showed scores below 2 (some below 1), compared with pre-treatment scores below 4. Assessing patient satisfaction and the impact of oral health following implant treatment involves analysing various demographic and clinical factors. These data suggest dental implants significantly enhance oral function, aesthetics, and overall quality of life.

The general findings of this study indicate commendable levels of patient satisfaction with aesthetics, mastication, speech, and cleaning. This is consistent with existing research that highlights the natural appearance of dental implants and improvements in masticatory efficiency and phonetics, which significantly enhance patient satisfaction (Lim & Ariff, 2020).

Notably, a low score was recorded for food impaction, indicating that some patients occasionally experience difficulty getting food lodged around the implant. Additionally, some individuals reported a tendency to play with their implants using their tongues, which may suggest a varied experience with food impaction or a habitual reaction linked to long-term edentulousness. Despite this, the overall satisfaction remained moderate, suggesting that food impaction was not a significant concern. Patients generally found it relatively easy to maintain their implants (medium-high score) and reported high levels of comfort. Therefore, we believed that patients did not perceive this condition as a significant factor contributing to their psychological or social disability and felt less hindered by it, especially since their scores significantly improved following treatment. These experiences are consistent with findings from a previous study (Saad et al., 2023), which may indicate that the observed improvements in patients' oral health-related quality of life (OHRQoL) stemmed more from the treatment than the initial edentulous state. Nevertheless, the necessity for enhanced post-treatment counselling and the promotion of proper maintenance and professional cleaning was emphasised to prevent peri-implant diseases (Monje & Salvi, 2024; Monje et al., 2021).

OHIP-14 showed significant improvements across multiple domains after treatment, with a general improvement of 1.36 (after treatment) and 3.21 (before treatment). Since a smaller score indicates greater improvement, the feeling of food sticking does not affect the patient’s psychological discomfort (0.72). Hence, feelings of psychological disability were not affected. Avoidance of certain foods, social events, and daily activities decreased significantly post-treatment. This indicated that chewing difficulty was significantly reduced post-treatment. This is because the implants restore

occlusal function, improving the ability to eat a wider variety of foods (Adell, 1981; Boven et al., 2015; Wang et al., 2021). Psychological and social well-being improved, and patients reported lower levels of embarrassment. Additionally, feelings of discomfort and the risk of ulcers decreased after treatment, indicating that the implants successfully alleviated pain from missing teeth. This aligns with research showing that implant-supported restorations enhance self-confidence and quality of life (Buser et al., 2016).

The patient's willingness to recommend this treatment to others and their likelihood of choosing the procedure again received overwhelmingly positive responses. This trend reflects a high level of confidence among patients regarding the effectiveness and safety of the treatment process. Furthermore, the feedback reinforces a strong sense of overall satisfaction with their care, highlighting the clinical results, supportive environment, and attentive service provided throughout their experience.

Among demographic variables, age showed a statistically significant correlation with OHIP scores ($p = 0.026$), indicating that older patients perceive a greater impact on their oral health. However, age did not significantly affect patient satisfaction (PSQ), indicating that while ageing influences oral health perceptions, it does not necessarily alter satisfaction with treatment outcomes.

Sex differences were not significant in either the PSQ or OHIP scores ($p = 0.14$), indicating that male and female patients report similar satisfaction levels and oral health-related quality of life. Similarly, education and income did not show significant effects, suggesting that socioeconomic factors may not strongly influence post-treatment perceptions.

Occupation, however, significantly affected PSQ scores ($p = 0.02$), indicating that employment status may shape satisfaction levels. This could be due to differences in lifestyle, expectations, or access to healthcare resources. However, occupation did not significantly influence OHIP scores ($p = 0.62$), implying that while it affects satisfaction, it does not necessarily impact perceived oral health conditions.

The study also explored the influence of various clinical factors on patient satisfaction and oral health perceptions. Implant stability showed a weak negative correlation with PSQ scores (-0.203), which was not statistically significant. Similarly, OHIP scores did not significantly correlate with implant stability ($p = 0.65$), suggesting that objective measures of implant success may not directly align with patient perceptions.

Other factors, such as crestal bone level, peri-implant probing depth, and inflammation, also showed no significant correlations with either PSQ or OHIP scores. This suggests that although these parameters are critical for clinical assessments, they may not substantially affect patient satisfaction or perceived oral health outcomes.

Notably, bleeding on probing, a standard indicator of peri-implant health, showed no significant association with patient satisfaction (-0.05) or OHIP scores (0.02, $p = 0.97$). This highlights that minor clinical signs of inflammation may not translate into patient-reported dissatisfaction or discomfort.

This analysis highlights the complex relationship between patient satisfaction, oral health perceptions, and demographic/clinical factors. Age and occupation emerged as significant influencers, with older individuals reporting a greater impact on their oral health and employed individuals exhibiting different levels of satisfaction. However, clinical parameters, such as implant stability, bone levels, and peri-implant health, did not significantly affect patient satisfaction or OHIP scores. These findings emphasise the importance of incorporating patient-reported outcomes into evaluations of implant success, as traditional clinical indicators may not always reflect patients' experiences (Papaspyridakos et al., 2012). Future research could explore psychological and behavioural factors in greater depth to better understand patient satisfaction and the perceived impact of oral health.

5.2.6 Implant Success and Survival Rates

Implant treatment has emerged as one of the most effective approaches for replacing single or multiple missing teeth, with long-term success rates generally ranging from 89% to 97% over 10 years (Adler et al., 2019; Pjetursson et al., 2012). Evaluating implant success and survival is therefore critical in assessing the reliability of different implant systems. This study compared NiTiDent Tuah (NT) and AnyRidge (AR) implants over a 52-week observation period, analysing complication rates, survival probability, and patient-reported outcomes.

The success of an implant is determined by its ability to remain free from biological complications, such as pain, infection, and mobility issues, as well as prosthetic complications (Esposito, 1999; Piattelli et al., 1998). In this study, AR implants demonstrated favourable short-term outcomes, with no failures observed over 52 weeks, aligning with previously reported success rates for this system. NT implants,

however, demonstrated early complications and progressive failure during the study period. Importantly, these outcomes must be interpreted with caution, as subsequent analysis suggested that the failures were strongly associated with the performance of the outsourced surgical drill, rather than solely attributable to the implant material or design.

Clinical observations in the NT group included pain or discomfort, peri-implant suppuration in isolated cases, and radiographic evidence of peri-implant bone loss. Affected implants became mobile and were eventually explanted, with most failures occurring between 16–36 weeks. The median survival time for NT implants was 16.38 weeks, compared with 52.00 weeks for AR implants. However, these findings seem to reflect procedural and technical issues rather than inherent implant performance. Indeed, microbial cultures from the explant sites showed no bacterial growth, indicating aseptic failure, likely due to inadequate osteotomy preparation and poor primary stability.

On the other hand, AR implants consistently achieved favourable outcomes, reflecting their well-documented macro- and micro-design advantages. Features such as KnifeThread® for enhanced initial stability and the Xpeed® calcium-treated surface promote rapid bone integration and long-term survival (Mangano et al., 2017). These design features likely contributed to the absence of complications and the high patient satisfaction observed in the AR group.

While AR implants showed excellent short-term survival, consistent with published reports (Makary et al., 2019), the higher complication rates observed in NT implants during this study should be interpreted in consideration of technical factors, particularly the use of non-proprietary surgical drills. Future studies using system-specific instrumentation and optimised surgery tools are necessary before the clinical potential of NT implants can be thoroughly assessed.

5.3 Part B

5.3.1 Investigation of the Failure of Porous NiTi Implants

The present study showed that all porous nickel–titanium (NiTi) implants failed during the early healing phase, with a median survival time of about 16 weeks. Clinically, this indicates reduced osseointegration, as evidenced by a steady decline in

implant stability quotient (ISQ) values and early implant loss. Implant stability is a vital factor for successful osseointegration, encompassing both mechanical engagement and biological integration over time (Javed et al., 2011). At first glance, these results may suggest impaired biological performance of the porous NiTi material in humans.

Prior to this Phase 1 clinical trial evaluating the safety and performance of this material, a comprehensive preliminary biocompatibility study was conducted by a laboratory adhering to the OECD principles and Good Laboratory Practice (GLP), in accordance with the ISO standard detailed in Table 1.1 of Chapter 1 (Khushaini & Ahmad, 2020). The results showed that this tested material was biologically safe, including being non-toxic, compliant with ISO 10993-Part 5 and ISO 10993-Part 12, non-mutagenic (ISO 10993-Part 3, ISO 10993-Part 33, ISO 10993-Part 12), non-irritant (ISO 10993-Part 10, ISO 10993-Part 12, ISO 10993-Part 2), not inducing systemic toxicity (ISO 10993-Part 2, ISO 10993-Part 11), and not provoking any adverse biological reactions in a rabbit model after three months of implantation, comparable to the conventional commercialised implant material (Khushaini & Ahmad, 2020; Mustafa et al., 2023; Rahimi, 2023; Mustafa et al., 2024). This is further supported by an in-depth analysis that combines the laboratory findings from Part B of this study, which reveal contrasting biological responses to those of Part A. Our *in vitro* evaluation using human mesenchymal stem cells (hMSCs) demonstrated favourable cellular attachment, proliferation, and osteogenic differentiation on the porous NiTi surface. These findings align with previous research indicating that porous implant structures promote cell infiltration and bone ingrowth due to increased surface area and interconnectivity (Nakaş et al., 2011; Gotman et al., 2013; Wang et al., 2018). Furthermore, nickel ion release analysis confirmed that the concentration of released ions remained well below cytotoxic levels and did not harm cell viability, as the European Food Safety Authority (2020) advised that the tolerable daily intake ranges from 2.8 to 13 micrograms per kilogram of body weight (https://www.efsa.europa.eu/en/topics/topic/metals-contaminants-food#). This supports existing evidence suggesting that controlled nickel release from NiTi alloys does not necessarily compromise biocompatibility (Geetha et al., 2009).

This apparent discrepancy between unfavourable clinical outcomes and favourable biological performance warrants further interpretation. Histological examination of peri-implant tissues revealed multinucleated giant cells and dense fibrous encapsulation, consistent with a foreign body reaction (FBR). Such responses

are typically associated with the presence of foreign particulate matter and indicate the body's attempt to isolate it (Anderson et al., 2008). Ultrastructural analysis using scanning and transmission electron microscopy further demonstrated macrophage activation, cellular stress responses, and active phagocytosis of particulate debris. Notably, energy-dispersive X-ray (EDX) analysis identified metallic particles within both peri-implant tissues and implant surfaces, with elemental composition consistent with stainless steel rather than nickel–titanium.

These findings provide critical evidence that the compromised osseointegration observed *in vivo* was not primarily attributable to the intrinsic properties of the porous NiTi implant. Instead, the results strongly suggest that the failure was secondary to exogenous contamination, specifically tribochemical debris originating from the surgical drilling process. Metallic wear debris has been widely reported to induce inflammatory responses and impair bone healing, ultimately leading to fibrous encapsulation and implant failure (Hallab et al., 2001). In this context, the presence of stainless-steel particles likely triggered a sustained inflammatory cascade, resulting in disruption of bone-to-implant contact and inhibition of osseointegration.

Therefore, the preliminary *in vivo* findings do not reflect a true biological incompatibility of porous NiTi as a biomaterial. Rather, they highlight the significant impact of surgical and procedural factors on implant outcomes. The foreign body reaction observed in this study is a contamination-driven response that masked the material's inherent osteogenic potential. This interpretation is further supported by the absence of cytotoxic nickel-ion levels and a positive *in vitro* osteogenic response.

This finding is particularly important in the context of implant biomechanics and material design. Porous NiTi has been proposed as a potential solution to stress shielding because of its lower elastic modulus, which more closely matches that of cancellous bone (Huiskes et al., 1992; Pilliar et al., 1981). However, the clinical translation of such materials is highly dependent on the integrity of the surgical environment and instrumentation. Without appropriate system-specific tools, the evaluation of novel biomaterials may be confounded by external variables unrelated to the material itself.

Consequently, the findings of this study should be interpreted within the context of this identified limitation. Future investigations should prioritise the development of compatible surgical instrumentation and strict control of operative variables to enable a more accurate assessment of porous NiTi implants under clinical conditions. To

determine the cause of failure, we conducted histological analysis of the peri-implant tissues retrieved from the failure case. This includes scanning electron microscopy (SEM), transmission electron microscopy (TEM), and energy-dispersive X-ray (EDS) analysis.

In early implant failure, the introduction of biomaterials triggers a series of host responses, collectively known as the foreign body reaction (FBR), which can ultimately result in implant failure. This response includes the adsorption of host proteins onto the implant surface, the recruitment of immune cells, and subsequent chronic inflammation, often leading to fibrosis and a loss of implant functionality (Abrishami et al., 2023; Albrektsson et al., 2019; Anderson & Jiang, 2017; Serrabona et al., 2022).

The observation of multinucleated giant cells (MGCs) in H&E-stained tissue sections in this study underscores a profound chronic inflammatory response, as these prominent cells are situated in the peri-implant tissue and on the surface of the failed implant (Figures 4.2, 4.3, 4.4 and 4.9). These findings indicate a vigorous attempt by the body's immune system to phagocytise the foreign material, a critical aspect of the healing process. Moreover, the dense collagen deposition observed in the tissue suggests the formation of a resilient fibrous capsule around the implant. This encapsulation reflects the host tissue's proactive strategy to isolate and effectively manage foreign materials, demonstrating the dynamic interplay between the implant and the surrounding biological environment.

Using ultrastructural observations with scanning electron microscopy (SEM), we detected apoptotic blebs on the surfaces of peri-implant cells. These blebs may signify programmed cell death, likely instigated by stress induced by the implant. The remodelling of the extracellular matrix, characterised by a distinct meshwork-like structure, emerges as an encouraging response, indicating tissue adaptation and healing in response to the implant.

Meanwhile, the activation of macrophages adhering to the implant surface plays a crucial role in orchestrating the foreign body reaction (FBR), underscoring the body's multifaceted response to foreign materials. Our transmission electron microscopy (TEM) analysis revealed several indicators of cellular stress, including dilated endoplasmic reticulum and vacuolisation within peri-implant cells. The heightened lysosomal activity observed in macrophages indicates effective degradation of implant debris, which is pivotal to the healing process.

Overall, TEM images of PIT validated the successful formation of a fibrous capsule composed of densely packed collagen fibres surrounding the implant, vividly illustrating the body's adaptive response to the challenges posed by foreign objects. The findings of this study unequivocally demonstrate the critical role that the foreign body reaction plays in the early failure of implants. Multinucleated giant cells (MGCs) and activated macrophages indicate the body's determined response to phagocytose and isolate the implant material. While the formation of a fibrous capsule serves as a natural protective mechanism, it often leads to the implant's isolation and eventual failure.

Our further analysis also revealed metallic debris, including Cr, Mn, Fe, and C, within the peri-implant soft tissues and on implant surfaces, as identified by energy-dispersive X-ray spectroscopy (EDX). These elements are among the major constituents of stainless steel and likely originate from the surgical drill. This further confirms that only the elements Ni, Ti, C, and O were identified in the original NT implant (Figure 4.10 and Table 4.13). Additionally, we encountered chipped burs during an intraoperative procedure once. These results strongly suggest that implant failure primarily stems from contamination by surgical bur debris, compounded by a material-induced FBR. This combination leads to impaired osseointegration and peri-implant fibrosis.

TEM and EDX confirmed the presence of stainless-steel debris, both inter- and intracellular, in the granulation tissue around porous NiTi implants, indicating that mechanical wear from the surgical drill contributed to unresolved local inflammation. EDX also showed that macrophages phagocytose metallic debris. Although not being investigated, it probably triggers the release of TNF-α, IL-6, and prostaglandins, which drive fibrosis and peri-implant osteolysis (Raines et al., 2019). Similar findings have been observed in orthopaedic implants, where metallic wear particles trigger chronic inflammatory responses and fibrotic tissue formation (Ude et al., 2021). Stainless steel debris acts as foreign particulate matter, leading to the fibrotic encapsulation of the implant. This fibrosis prevents direct bone-implant contact, reducing mechanical stability (Albrektsson et al., 2018; Anderson et al., 2011; Babensee et al., 1998; Tomasi & Derks, 2022). Metal debris has been linked to increased TGF-β signalling, which promotes fibroblast proliferation rather than osteoblast activity (Insua et al., 2023; Noskovicova et al., 2021).

5.3.2 Role of Surgical Drill in Dental Implantation

In the present study, scanning electron microscopy (SEM) analysis was conducted *in vitro* on both the NT drill system and the AnyRidge® (AR). This methodological approach may be seen as a limitation, as it restricts direct comparative analysis between the two systems used for osteotomy preparation in Part A and limits the ability to draw definitive conclusions about differences in drill design, material properties, or wear characteristics.

However, the main goal of the drill analysis in this study was not to compare different drill systems, but to explore the possible cause of the unexpected implant failure observed in the NT group. The investigation was therefore hypothesis-driven and aimed to identify the presence and source of metallic debris within peri-implant tissues, since PIT and the failed implant's EDX analyses strongly suggested that the metallic particles matched a stainless-steel composition, the material of the NT surgical drill system. This result directly linked the drill to the observed foreign body reaction.

Furthermore, clinical results showed a distinct difference between the two implant systems. The AR group achieved 100% survival with stable peri-implant conditions, while NT implants failed during the early healing phase. The lack of similar adverse outcomes in the AR group suggests that the drill system used in the control group did not produce comparable levels of biologically significant debris. Although this does not replace direct microstructural analysis, it offers clinical evidence supporting the proposed failure mechanism. Additionally, the surgical tool used in this clinical trial was different from the drill used in the animal study, which may explain why this finding was not observed earlier in animal research (Rahimi et al., 2023; Mustafa et al., 2024).

The images of the surgical drills used in this study reveal a stark contrast in wear, surface integrity, and potential generation of metal debris between the NT and AR implants. This contrast highlights the key differences that contribute to the failure mechanisms of NT implants and the success of AR implants, reinforcing the pivotal role of surgical instrumentation in implant outcomes.

The worn cutting edges, irregular surfaces, and micro-cracks observed under the microscope and in SEM images of the NT's surgical drill suggest that repeated use of this drill led to mechanical degradation, potentially contributing to implant failure. The cutting edges appear rounded and worn, which reduces cutting efficiency and may

increase heat generation. Worn drills generate excessive friction and heat during drilling, which can lead to thermal osteonecrosis and impair osseointegration (Er et al., 2018; Ericksson & Albrektson, 1984; Kotsakis & Romanos, 2022; Piattelli et al., 1998). Eriksson and Albrektsson (1984) demonstrated that bone exposed to temperatures above 47°C for 1 minute undergoes irreversible cell death, thereby impairing healing and osseointegration. While sharp drills create well-defined osteotomies, promoting primary stability, a key factor in implant success, a worn drill leads to irregular or oversized cavities, compromising initial fixation and increasing the risk of micromovement and implant failure (Chen et al., 2023; Chrconovic et al., 2015; Javed et al., 2013; Jemt et al., 2016; Toledano-Serrabona et al., 2022). This may be one reason for the lower primary stability in the NT group, as worn surgical drills significantly reduce primary implant stability due to excessive heat and bone damage (Er et al., 2018; Kotsakis & Romanos, 2022). Thus, surgical drill wear must be considered a critical factor in implant failure.

Microcracks and an uneven surface suggest that the drill experienced material fatigue, causing metal fragmentation. This supports our TEM-EDX findings of metal debris at the implant site, likely originating from the drill. Increased drill wear promotes the release of metal particles, which can impair osseointegration (Bernabeu-Mira et al., 2020; Er et al., 2018). The degraded surface of the drill poses a significant risk of implant failure, as particles embedded in the peri-implant tissue can trigger chronic inflammation and lead to fibrotic encapsulation rather than direct bone-implant contact (Albrektsson et al., 2018; Anderson et al., 2008; Insua et al., 2023). This explains the presence of multinucleated giant cells and fibrotic encapsulation, which are characteristic of the foreign body reaction (FBR) observed on histology. Undigested stainless-steel debris seen via TEM of peri-implant tissue appears to provoke a persistent inflammatory response, driven by active phagocytosis and apoptosis, resulting in increased osteoclastic activity and eventual peri-implant bone loss (Oliveira et al., 2023). Therefore, the mechanical degradation of the drill in the NT group impacted the drilling process, triggering a cascade of biological events. These changes collectively compromised the implant site, leading to bone osteolysis and poor osseointegration. Bone healing is considerably delayed, raising the risk of implant micromotion and early failure (Kotsakis & Romanos, 2022; Trisi et al., 2013).

In contrast, the AR implant group drill remained structurally intact even after multiple uses. The cutting surfaces remain sharp and functional, ensuring efficient

drilling with minimal heat generation. Unlike the NT drill, this drill does not exhibit significant irregularities or cracks, reducing the risk of metallic debris contamination.

The degraded condition of the drill in the NiTi group likely played a key role in implant failure by introducing metallic contaminants that hindered bone healing. This highlights a vital, often-overlooked factor in the deterioration of surgical drills and their biological effects. Literature confirms that excessive heat causes osteonecrosis (Ericksson & Albrektsson, 1984). Additionally, imprecision during osteotomy is a significant risk associated with worn drills. Several studies have demonstrated that the repeated use of implant drills leads to wear, reduces cutting efficiency, and increases heat production. For example, zirconia drills used for 30 cycles of use and sterilisation showed considerably more cutting-edge damage compared to unused drills (Alevizakos et al., 2025). Similarly, stainless steel drills generally maintained bone temperatures within safe limits when used up to 50 times with irrigation; however, heat generation increased notably with further reuse (Koo et al., 2015). To improve durability, protective coatings such as boron nitride, titanium boron nitride, and diamond-like carbon have been shown to enhance drill performance and reduce temperature rises, even with repeated use without irrigation (Er et al., 2018). The use of high-wear-resistant coatings may further prolong their lifespan, although routine monitoring remains crucial. It also improves wear resistance, reduces debris production, and enhances cutting efficiency (Er et al., 2018).

5.3.3 Monoculture with Human Mesenchymal Cell

As part of the investigation on NT implant failure, comprehensive insights into the cytocompatibility and osteogenic potential of human mesenchymal stem cells (hMSCs) exposed to different biomaterials, including Titanium (Ti), machined NiTi (mNiTi), porous NiTi (pNiTi) and the potential release of nickel ions over 28 days were explored in this study. Previous studies have demonstrated that the biocompatibility of this porous NiTi is comparable to that of Grade V Ti alloy (Mustafa et al., 2023). Each assay, cell viability, alkaline phosphatase (ALP) activity, Alizarin Red S staining (ARS), and SEM imaging, converges on the conclusion that pNiTi is the most effective substrate for supporting osteogenic differentiation and matrix mineralisation.

The results underscore the dual capacity of porous NiTi to foster osteoblast-like differentiation of human mesenchymal stem cells (hMSCs) and release nickel ions in a

controlled manner. The potential of porous NiTi to enhance cellular proliferation, alkaline phosphatase (ALP) activity, and calcium deposition while keeping nickel ion release below cytotoxic thresholds is a reason for optimism about its biocompatibility and clinical promise.

5.3.3.1 Osteoconductive Properties of Porous NiTi

The osteoconductive properties of porous NiTi were significantly enhanced compared to machined NiTi (mNT) and Ti6AL4V. Optical density (OD) measurements, indicative of cell viability and metabolic activity, provided clear evidence of cellular proliferation. Throughout the 28-day incubation period, all biomaterials exhibited higher OD values than the negative control group, with porous NiTi consistently leading. The surface structure and chemistry of biomaterials play a crucial role in mediating cellular responses, including adhesion, proliferation, and differentiation (Berglundh et al., 2003; Schell et al., 2017; Terheyden et al., 2012). The enhanced performance of pNT compared to Ti and mNT can be attributed to its porous architecture, which increases the surface area for cell interaction and provides a more favourable microenvironment that mimics cancellous bone. Porosity has been shown to enhance angiogenesis and osseointegration by facilitating the diffusion of nutrients, oxygen, and waste products (Karageorgiou & Kaplan, 2005). This significant finding highlights the unique ability of porous NT to sustain and promote cellular growth.

From the first day of observation, pNiTi demonstrated the highest OD values, suggesting that its unique properties effectively stimulated cell proliferation. The superior performance of pNiTi can be attributed to its porous architecture, which provides an increased surface area for cell attachment and interaction. Surface topography and pore structure have been shown to play crucial roles in guiding cellular responses (Karageorgiou & Kaplan, 2005; Karazisis, 2016; Smeets, 2016). This finding is consistent with those of Jian et al. (2015), who reported superior cellular attachment and growth on porous NT due to the improved topographical cues. The significant increases at later time points (days 21 and 28) suggest a transition from proliferation to differentiation, which is further supported by elevated ALP levels and ARS staining. The porous NiTi used in this study had an average pore size of 50 μm and a porosity of 20–30%, which may be considered adequate to facilitate nutrient transport and cellular infiltration (Karageorgiou & Kaplan, 2005).

Interestingly, other porous materials exhibited similar trends in cellular response, regardless of whether they underwent surface treatments (Iezzi et al., 2024). However, contrasting findings were reported by Yu et al. (2021), who observed diminished cell proliferation and increased apoptosis rates in porous NiTi compared to dense NiTi and titanium materials. These discrepancies highlight the importance of pore size, surface chemistry, and material properties in influencing the behaviour of hMSCs. Such variations emphasise the need to carefully optimise pore characteristics to balance biological and mechanical requirements.

As the incubation period progressed, the OD values for all groups plateaued around day 7 and began to decline slightly by day 14. This pattern, consistently observed across all biomaterials, reflects a shift in hMSCs' behaviour. It suggests cellular resources are redirected from proliferation to differentiation processes as osteogenic differentiation progresses. This competitive interplay between proliferation and differentiation underscores the dynamic nature of osteogenesis, in which one pathway becomes dominant as the other diminishes (Lossdörfer et al., 2004).

To further understand this transition, the study monitored ALP activity and calcium deposition, key markers of early and late stages of osteogenesis, respectively. While ALP is a transient marker associated with early-stage osteogenesis, its rise between days 7 and 14 indicates that differentiation was progressing (Gotman et al., 2013; Lian & Stein, 1992). ALP activity, an indicator of bone cell growth and specialisation, was first detected on day 7 and surged by day 14, reflecting the active phase of osteoblast differentiation. This is complemented by the ARS assay, which reflects calcium deposition, signifying advanced bone formation, and was observed across all biomaterials, with the strong ARS signal observed in the pNiTi group by day 28, implying that the cells not only differentiated but also achieved functional maturity in matrix production. These findings suggest that pNiTi provides an optimal environment for the early and late stages of bone formation.

Scanning electron microscopy (SEM) images further reinforced additional insights by visualising the morphological evolution of hMSCs on biomaterials. The images revealed robust cellular attachment, with hMSCs forming filopodia and lamellipodia that extended to interact with the porous architecture. The interconnected pores of pNiTi created a three-dimensional microenvironment conducive to cell infiltration and matrix deposition. This porous structure facilitated cell anchorage and enhanced osteogenic differentiation by mimicking the natural microarchitecture of

bone. By day 28, dense extracellular matrix (ECM) networks were evident on pNiTi, indicating adhesion, active-matrix remodelling, and mineralisation. The sequential development of ECM over 7–28 days mirrors physiological osteogenesis, where an early attachment is followed by ECM secretion and mineral deposition (Franz-Odendaal et al., 2005; Gotman et al., 2013). These findings highlight the importance of evaluating both quantitative and qualitative cell-biomaterial interactions.

5.3.3.2 Nickel Ion Release and Biocompatibility

The issue of nickel toxicity is of paramount concern in NiTi-based biomaterials. The release of nickel ions was monitored over 28 days, revealing a dynamic pattern across all tested media. Although pNiTi consistently exhibited slightly higher Ni ion release compared to machined NiTi, the levels remained well below cytotoxic thresholds (Buxton et al., 2019; Navratilova et al., 2024) and below the tolerant dietary intake (Cempel & Nikel, 2006; Gopikrishnan et al., 2015; Mudjari et al., 2019, https://www.efsa.europa.eu/en/topics/topic/metals-contaminants-food#). Porous NiTi releases higher nickel ions due to the increased surface area provided by its interconnected pores. These structures expose more material to the surrounding environment, promoting ion exchange. Interestingly, the lack of a significant correlation between Ni release and cell viability confirms its biosafety within this context. However, these results do not negate the potential for nickel hypersensitivity or long-term accumulation, particularly *in vivo*. Thus, surface treatments that form passive oxide layers or coatings could be explored to further mitigate ion release without compromising biocompatibility (Clarke et al., 2006).

This study examined nickel ion release under various conditions, including osteogenic medium (pH 7.2) and saline solutions at pH 6.0 and 7.0, simulating inflammatory and post-inflammatory environments, respectively. Following implant placement, local acidification due to inflammation can significantly influence the behaviour of implant materials. Acidic environments enhance osteoclastic activity while suppressing osteoblast function, making pH a critical factor in evaluating material performance (Arnett, 2008; Berkmann et al., 2020).

Nickel ion concentrations were initially low during the first seven days, likely due to the limited availability of free ions on the oxide layer. By day 14, nickel release peaked in saline solutions for pNiTi and mNiTi, then sharply declined by day 28. This

reduction suggests that the material's surface is stabilised, possibly due to the formation of a passive oxide layer that restricts further leaching. Notably, the osteogenic medium consistently demonstrated lower nickel ion release than saline solutions at both pH levels. This may be attributed to the medium's buffering capacity and the presence of proteins, calcium, and phosphate ions, which likely help create a bioactive layer that reduces corrosion and ion leaching. Interestingly, nickel ion release was unexpectedly higher in saline at pH 7.0 compared to pH 6.0, particularly on day 14. This observation may be due to the destabilising effects of chloride ions, which can promote localised corrosion. In contrast, at pH 6.0, self-limiting corrosion mechanisms might prevail, allowing corrosion products to form a stable protective barrier (Clarke et al., 2006).

The manufacturing process for porous NiTi is essential to effectively reduce impurities and optimise the formation of the NT phase (B2), thereby significantly enhancing corrosion resistance. By employing the Metal Injection Moulding (MIM) process, we can promote the formation of the complete NiTi phase (B2) while minimising the presence of undesirable impurities, such as carbon-oxygen and intermetallic phases (Dehghan-Manshadi et al., 2020). Furthermore, ongoing research efforts aim to improve the surface properties of NiTi to prevent the release of nickel ions, highlighting its promising potential as a bone implant material (Arnett, 2008). Our earlier research highlights the viability of V794 Chinese fibroblast cells when exposed to NiTi extract concentrations up to 200 mg/L, with USP grade 0 (Mustafa et al., 2023). This indicates that the cells remained intact after exposure, which is promising for future applications. Furthermore, evaluations conducted for 30 minutes under both open and cyclic polarisation show that porous NiTi exhibits impressive corrosion resistance (677mV) and notable re-passivation capabilities (Khushaini & Ahmad, 2021; Mustafa et al., 2024). Its higher breakdown potential complied with ASTM F2129, and it is recommended that implants exceeding 600 mV have acceptable corrosion resistance (U.S. Food and Drug Administration [FDA], 2019). These findings emphasise the effective self-healing properties of the TiO_2 layer, paving the way for advancements in material resilience (Clarke et al., 2006; Tian et al., 2011; Wever et al., 1997).

Despite fluctuations in nickel ion concentrations, the highest level recorded, around 0.045 µg/L, remained well below established cytotoxic limits (Buxton et al., 2019). This is notable because it highlights the material's good biocompatibility. The increased alkaline phosphatase (ALP) activity and significant calcium deposition with pNT further confirm its compatibility with biological systems, suggesting that nickel

ion release is minimal and unlikely to induce adverse biological effects (Wang et al., 2019) These results align with previous studies that have demonstrated the biocompatibility of nickel-titanium (NiTi) alloys with different surface treatments (Wang et al., 2019). Furthermore, as bone integration progresses, nickel ion release is expected to decrease further, eventually becoming negligible once the material reaches a stable equilibrium in the biological environment (Buxton et al., 2019). In reality, Ni is a silvery-white metal found naturally in the earth's crust, present in trace amounts and excreted by the kidneys (Cempel & Nikel, 2006). Under normal circumstances, nickel is readily available in soil, air, metals, and most foods, such as chocolate, nuts, grains, and fish. In the human body, according to the European Food Safety Authority (2026), the advised tolerable daily intake ranges from 2.8 to 13 micrograms per kilogram of body weight (European Food Safety and Authority [EFSA], 2026).

The findings of this study reveal a promising perspective: porous NiTi not only supports osteoconductive processes but also ensures that nickel ion release remains well within non-cytotoxic levels. While the study provides robust *in vitro* data, there are limitations. The culture conditions do not fully replicate the dynamic, vascularised environment of living bone. Furthermore, it is important to consider how immune cells, mechanical stress, and systemic responses to nickel release contribute to the process, which will require further *in vivo* studies. Future research should also explore the roles of surface roughness, hydrophilicity, and potential nano-patterning in enhancing cellular responses. Additionally, investigating surface modifications to optimise corrosion resistance while increasing osteogenic potential could offer significant benefits. Extended incubation periods in simulated physiological environments would also deepen our understanding of the material's long-term performance. Such comprehensive studies are essential for bridging the gap between *in vitro* findings and their clinical applications.

5.4 Differentiating Intrinsic Material Effects from Extrinsic Factors in the Mechanism of Failure in This Study

When interpreting observed complications related to implants, it is important to distinguish between intrinsic material-related effects and extrinsic procedural factors. Through our findings, the clinical outcomes of early implant failure are in line with evidence of procedural complications of the surgical drill.

Histological and ultrastructural analyses in this study revealed features indicative of a foreign body reaction, including multinucleated giant cells, macrophage activation, and fibrotic encapsulation in all peri-implant tissues examined, as well as a disintegrated implant surface. While such features may be associated with both material-related and particulate-induced responses, further analyses were undertaken to determine the underlying cause. The possibility of microbial infection was ruled out. Although the porous structure may pose a risk of bacterial colonisation, this implant came with an intact seal pre-surgery and was sterilised by gamma radiation with a minimum dose of 25 kGy and a maximum dose of 45 kGy, in compliance with ISO 11737-2:2019 (Sanichem Resources Sdn. Bhd., 2022). Intra-orally, this implant was completely buried and not exposed to the oral environment. Neither participant developed signs and symptoms of infection, and ultrastructural findings did not indicate microbial colonisation. Additionally, swabs taken from the sockets of two patients, streaked onto nutrient agar and incubated under both aerobic and anaerobic conditions at 37°C for 7 days, yielded no growth on the agar plates.

It was unlikely that the debris originated from the NT itself. Under static loading, this material, with a 3.5 mm diameter, can withstand a load of 596.2 N before fracture and has a compressive strength of 5-7 kN. It is compliant with ISO 14801 and ASTM E9 (Khushaini & Ahmad, 2021). Energy-dispersive X-ray (EDX) analysis identified metallic particles in the peri-implant tissues and the retrieved implant, with elemental compositions consistent with stainless steel rather than nickel–titanium, as evidenced by multiple trace elements in the EDX analyses of the PIT and the failed implant surface. This finding provides strong evidence of exogenous contamination originating from the surgical drilling system. The detection of debris in multiple analysed specimens supports a significant association between the presence of stainless-steel particulates and the observed biological response. The reproducibility of both the elemental findings and the characteristic histological feature across several samples enhances the likelihood of a causal relationship.

Analysis of nickel ion release showed concentrations well below cytotoxic thresholds, and in vitro studies in human mesenchymal stem cells demonstrated robust cellular attachment, proliferation, and osteogenic differentiation on the porous NiTi surface, confirming its inherent biocompatibility. These findings indicate that the material's inherent properties were not associated with any adverse biological response.

This suggests that nickel leaching was unlikely to significantly influence the observed biological response.

It is recognised that definitive causality cannot be established due to the absence of a controlled comparative analysis and the limited sample size. Although the role of intrinsic factors cannot be entirely dismissed, the combined evidence from elemental, biological, and histopathological analyses over the study timeframe suggests that the observed foreign body reaction was more likely attributable to debris accumulation than to intrinsic rejection of the NiTi implant material.

Nevertheless, the author did not entirely rule out a possible contributing factor in the implant itself. The porous nickel–titanium implant evaluated in this study is characterised by its internal porosity, which fundamentally distinguishes it from conventional titanium implants that rely primarily on surface modifications. In this system, porosity is predominantly generated through bulk structural design rather than superficial surface treatment. Specifically, the implant was fabricated using metal injection moulding (MIM), a process that produces interconnected pores throughout the implant body, resulting in a three-dimensional porous network.

This bulk porosity differs significantly from surface roughness modifications commonly employed in conventional titanium implants, such as sandblasting, acid etching, or plasma spraying. While surface-modified implants primarily enhance micro- and nanoscale roughness to improve protein adsorption and osteoblast attachment, bulk porous implants aim to facilitate bone ingrowth into the implant's internal structure, thereby promoting mechanical interlocking and potentially improving long-term stability (Albrektsson & Wennerberg, 2019; Edelmann et al., 2019).

From a biological perspective, bulk porosity plays a vital role in facilitating cell migration, vascular infiltration, and nutrient diffusion (Zheng et al., 2019). Interconnected pores enable osteogenic cells to penetrate the implant structure and support new bone tissue formation within the porous network. This process, often called three-dimensional osseointegration, offers a potential advantage over traditional surface-based integration, which is mainly limited to the bone–implant interface (Edelmann et al., 2019). However, the effectiveness of this mechanism heavily relies on pore size, interconnectivity, and overall porosity, as inadequate pore dimensions may hinder cellular and vascular infiltration (Karageorgiou & Kaplan, 2005).

In contrast, surface modifications mainly influence early-stage biological interactions. Micro- and nanoscale roughness enhances the adsorption of proteins, such

as fibrin and fibronectin, that mediate osteoblast attachment and differentiation (Berglundh et al., 2003; Bosshardt et al., 2016; Lang et al., 2011). This promotes rapid initial bone formation and plays a key role in early implant stability (Smeets et al., 2016). However, these surface features do not promote deep bone ingrowth within the implant body (Assad, 2004).

In the present study, the porous NiTi implant combines the theoretical benefits of bulk porosity with inherent material properties, including superelasticity and a lower elastic modulus. These features aim to reduce stress shielding and encourage more physiological load transfer to the surrounding bone. However, unlike hybrid systems that include both surface modification and optimised pore architecture, the performance of bulk porous implants is highly sensitive to structural design parameters (Elahina et al.,2012; Ismail et al., 2012; Sun et al., 2025; Zhang et al., 2021).

Therefore, while the porosity in the NiTi implant mainly results from bulk structural design rather than surface modification, both factors work together to support bone regeneration. Bulk porosity allows for long-term bone ingrowth and mechanical interlocking, while surface features influence early biological responses and initial osseointegration. Identifying the ideal built-in pore sizes for bony implants poses challenges (Sun et al., 2025). Without optimised pore architecture or proper control of surgical variables, these benefits may not be fully realised in clinical practice. The porous NiTi implant examined in this study had a reported pore size of around 50 μm and an overall porosity of 20–30%. From a biomaterial's perspective, these structural parameters are key in influencing the amount of bone ingrowth, vascularisation, and long-term osseointegration. Previous research indicates various pore sizes suggested for bone ingrowth generally range between 100–600 μm (llister, 2005), with larger interconnected pores promoting not only osteoblast migration but also vascular penetration, which is vital for sustained bone remodelling and maturation (Karageorgiou & Kaplan, 2005; Nakaş et al., 2011). While larger pores enhance biological performance, they can reduce strength, particularly in bone implants.

The Haversian system plays a vital role in supporting bone, and effective bone formation requires pore sizes of 50-300 μm (Zheng et al., 2019). Although pores at least 35 μm in diameter enable proper cell and blood vessel migration, the relatively small pore size of approximately 50 μm in the present implant system may be suboptimal for promoting extensive bone ingrowth. While pores of this size may support limited cell

attachment and surface-level bone apposition, they are generally inadequate to enable deep penetration into vascularised bone.

Consequently, osseointegration may be limited primarily to the implant surface rather than to true three-dimensional bone ingrowth within the porous network. This limitation could diminish the biological advantage usually associated with porous implant designs. In contrast, the AnyRidge® implant system does not rely on macroporosity but instead utilises advanced surface modification techniques and macrodesign features, including aggressive thread geometry, knife-edge threads, and platform switching. These features enhance primary stability and promote favourable stress distribution while maintaining a controlled healing environment at the bone–implant interface. Surface roughness at the micro- and nanoscale has been shown to enhance protein adsorption, osteoblast attachment, and early bone formation, thereby supporting rapid and predictable osseointegration (Wennerberg & Albrektsson, 2009).

From a mechanistic standpoint, porous NiTi and conventional titanium implants such as AnyRidge® differ fundamentally in how they achieve osseointegration. Porous NiTi aims to reduce stress shielding through a lower elastic modulus and facilitate mechanical interlocking via bone ingrowth. However, this approach is highly dependent on achieving optimal pore size, interconnectivity, and structural integrity. In contrast, titanium implants rely on surface-mediated osseointegration, in which stability is achieved through a combination of mechanical fixation and biological bonding at the interface, rather than within the bulk of the implant.

With respect to load transfer, porous NiTi theoretically offers improved biomechanical compatibility with surrounding bone due to its reduced stiffness, thereby promoting more physiological stress distribution in accordance with Wolff's law (Huiskes et al., 1992; Pilliar et al., 1981). However, if pore architecture is suboptimal or if bone ingrowth is limited, the mechanical advantage of reduced modulus may not be fully realised. In such cases, the implant may behave more like a conventional material and fail to achieve the intended biomechanical benefits.

In the present study, despite the theoretical advantages of porous NiTi, the clinical outcomes did not demonstrate successful osseointegration. While this may initially suggest that the structural parameters were insufficient, the findings from Part B indicate that the observed failure was primarily due to external factors, particularly contamination from metallic debris from surgical instrumentation. Therefore, it is

important to distinguish between intrinsic design limitations and extrinsic procedural confounders.

Nevertheless, from a critical standpoint, the relatively small pore size and moderate porosity of the implant system may have limited its capacity to achieve robust vascularized bone ingrowth, even under ideal conditions. Future design optimisation should consider increasing pore size and enhancing interconnectivity to better align with established biological thresholds for bone regeneration without jeopardising its mechanical strength.

In summary, these findings suggest that the observed complications were more likely due to external factors, especially tribochemical debris, rather than a negative biological response to the NiTi material itself. However, it is acknowledged that fully ruling out intrinsic material effects would require further controlled studies conducted under optimal surgical conditions.

5.5 Summary and Reflection on the Research Journey

Porous nickel–titanium (NiTi) has emerged as a promising biomaterial for bone implantation owing to its unique combination of mechanical resilience, shape-memory effect, and excellent biocompatibility. Over the past 15 years, Nitium Technology Sdn. Bhd. has conducted extensive investigations on porous NiTi through both *in vitro* and *in vivo* animal studies, consistently demonstrating favourable cytocompatibility and genocompatibility (Mustafa et al., 2023). Animal experiments have further confirmed good tissue tolerance in both short- and long-term models (Table 2.7, Figures 2.13 and 2.14), with no evidence of hypersensitivity or systemic toxicity (Mustafa et al., 2024). Histological evaluation revealed minimal inflammation, limited fibrosis, and notable neovascularisation compared to control groups, indicating a well-regulated tissue response. The absence of macrophages and foreign body giant cells in the animal model strongly supports the conclusion that the porous NiTi material is inherently biocompatible (Mustafa et al., 2024). and that the clinical failure observed in this study is likely attributable to external procedural factors rather than intrinsic material-related causes. More recently, our laboratory data reaffirmed these findings, showing that porous NiTi supports osteogenic differentiation and bone matrix mineralisation *in vitro*, mirroring the developmental trajectory of other implant systems during their early refinement stages before achieving clinical success.

Despite these encouraging preclinical outcomes, the clinical translation of porous NiTi implants encountered unforeseen challenges. Importantly, the complications observed were not attributable to the material's intrinsic properties but rather to technical and procedural factors related to surgical instrumentation, which differed from that used in the animal study. Specifically, the analysis revealed that the surgical drills outsourced to a third-party manufacturer were prone to wear, generating metallic debris that served as biological contaminants during osteotomy preparation. Energy-dispersive X-ray (EDX) spectroscopy and transmission electron microscopy (TEM) confirmed the presence of drill-derived debris in peri-implant tissues, provoking a foreign-body reaction characterised by multinucleated giant cells and fibrotic encapsulation, which compromised stable osseointegration.

The contribution of drill wear and debris generation has been largely overlooked in implantology. In this study, the failure of porous NiTi implants was primarily attributed to contaminants originating from drill degradation, which served as biological confounders, masking the material's inherent osteoconductive potential. This finding underscores the critical importance of employing system-specific surgical instruments developed and tested in tandem with the implant system itself. If outsourcing is unavoidable, rigorous preclinical validation, including animal studies, is essential to ensure compatibility and prevent such unforeseen complications.

Compounding these challenges, the study was conducted during the height of the COVID-19 pandemic. The clinical trial, initially scheduled for commencement in 2020, was delayed by a year due to nationwide movement control orders (MCOs) imposed by the Malaysian government. Furthermore, the pandemic imposed substantial financial and logistical constraints on both the research team and the manufacturer. As a result, the manufacturer was only able to produce the implants, while the surgical drills had to be sourced externally to allow the trial to proceed. These unavoidable circumstances inadvertently introduced variability that influenced the clinical outcomes.

Developing a reliable implant system is inherently complex and must align with stringent requirements set by international regulatory bodies such as ISO, FDA, and MDA. The extensive research conducted on the porous NiTi system demonstrates the manufacturer’s commitment to meeting these standards. Indeed, the developmental journey mirrors that of other implant systems, which often undergo years, if not

decades, of optimisation involving refinements in surface modification, surgical instrumentation, and clinical protocols before achieving predictable success.

Although the primary clinical outcomes of this study were confounded by drill-related variables, the evidence strongly supports the biological potential and safety of porous NiTi as an implant material. With improved system integration, particularly the redesign of drilling instruments, application of protective coatings, and refinement of surgical protocols, the technology holds substantial promise for clinical use.

In conclusion, the early clinical setbacks observed in this study should not be viewed as shortcomings of the porous NiTi material itself, but rather as outcomes of suboptimal surgical instrumentation and the unprecedented constraints imposed by the COVID-19 pandemic. These findings highlight a vital lesson for future implant development: successful osseointegration depends not only on biomaterial innovation but also on the precision and compatibility of the surgical tools employed. With continued collaboration between researchers, manufacturers, and clinicians, porous NiTi implants remain strong candidates for next-generation dental implant technology.

Among cases that did not yield successful outcomes, early implant failure in the porous NiTi group necessitated careful clinical and regulatory management to ensure patient safety and adherence to ethical standards. The study protocol incorporated predefined criteria for implant failure, allowing for timely identification and intervention.

Upon detection of implant failure, the affected implants were removed, and the sites were managed in accordance with standard clinical procedures, including debridement and monitoring of healing. All affected patients were placed under close follow-up to ensure symptom resolution and adequate tissue recovery.

Subsequent treatment was individualised based on clinical assessment, bone condition, and patient preference. Seven patients had received new AR implants, which have remained in place for 3 years without any signs or symptoms of complications. In contrast, the remaining five patients presented with distinct situations: one opted for a bridge, while the other four declined further treatment.

From a regulatory standpoint, the adverse outcomes were reported in accordance with Good Clinical Practice (GCP) guidelines and institutional ethical requirements. The study was discontinued prematurely to mitigate further risk to participants, reflecting adherence to the principle that patient safety supersedes research objectives.

Overall, despite implant failure, all patients received appropriate management and definitive rehabilitation, ensuring that no participant was adversely affected without subsequent treatment.

5.6 Conclusion

Within the limitations of these clinical and laboratory studies, the following conclusions may be drawn:

i. The control implant system (AnyRidge®, MegaGen) exhibited stable clinical performance and served as a procedural reference for evaluating the porous NiTi implant system.
ii. The early clinical failures observed in the porous NiTi implants were not attributable to the intrinsic properties of the material. However, they were primarily associated with contamination from metallic debris resulting from wear on outsourced surgical drills. This contamination provoked a foreign-body reaction and compromised osseointegration.
iii. *In vitro* studies confirmed the bioactive potential of porous NiTi, with human mesenchymal stem cells (hMSCs) demonstrating strong adhesion, proliferation, and osteogenic differentiation on its surface.
iv. The findings underscore the importance of system-specific surgical instrumentation to ensure implant success. Surgical drills should be designed, fabricated, and validated in conjunction with the implant system to prevent contamination and ensure compatibility.
v. Despite confounding challenges arising from drill-related factors and the logistical constraints imposed during the COVID-19 pandemic, porous NiTi remains a promising next-generation biomaterial. With refinements in instrumentation and surgical protocols, it holds significant potential for achieving predictable and long-term clinical success comparable to established titanium implant systems.

5.7 Limitations

The present study was limited by a small sample size and a shortened follow-up period because the clinical trial had to be discontinued prematurely. These constraints reduced the statistical power of the findings and limited the ability to evaluate long-term outcomes such as late implant survival and marginal bone stability. Additionally, the unforeseen technical complications arising from the use of outsourced surgical drills introduced a confounding variable that affected the assessment of the actual clinical performance of the porous NiTi implants.

5.8 Future Studies and Recommendations

Future investigations should prioritise the development and validation of a fully integrated surgical system specifically designed for porous NiTi implants. It is strongly recommended that Nitium Technology Sdn. Bhd. **U**ndertake the in-house fabrication of surgical drills tailored to the mechanical and surface characteristics of the NiTi implant system. These drills should undergo rigorous comparative evaluation against commercial counterparts to ensure optimal cutting efficiency, durability, and biocompatibility.

Following ISO certification and regulatory compliance, preclinical validation through controlled animal studies should be conducted using the newly developed drilling system to confirm safety and biological compatibility. Only after satisfactory preclinical outcomes should further clinical trials in humans be initiated. Such a structured, stepwise approach will ensure that future studies accurately reflect the intrinsic potential of porous NiTi as a next-generation biomaterial, free of procedural confounders associated with surgical instrumentation.

5.9 Acknowledgement

This study was funded by a Research Grant from the Ministry of Science, Technology, and Innovation, Malaysia, for a Clinical Trial of Porous Nickel Titanium Dental Implant (RD1019Q1346), MESTECC R&D Fund, e-DANA RM2,171,400.00

REFERENCES

Abduljabbar, F. H., Makhdom, A. M., Rajeh, M., Tales, A. R., Mathew, J., Ouellet, J., Weber, M., & Jarzem, P. (2017). Factors associated with clinical outcomes after lumbar interbody fusion with a porous nitinol implant. *Global Spine Journal*, *7*(8), 780–786. https://doi.org/10.1177/2192568217696693

Abdullah, Z., Razali, R., Subuki, I., Omar, M. A., & Ismail, M. H. (2015). An overview of powder Metallurgy (PM) method for porous Nickel Titanium Shape Memory Alloy (SMA). *Advanced Materials Research*, *1133*, 269–274.

Abidi, I. H., Khalid, F. A., Farooq, M. U., Hussain, M. A., & Maqbool, A. (2015). Tailoring the pore morphology of porous nitinol with suitable mechanical properties for biomedical applications. *Materials Letters*, *154*, 17–20. https://doi.org/10.1016/j.matlet.2015.04.057

Abraham, C. M. (2014). A brief historical perspective on dental implants, their surface coatings and treatments. *The Open Dentistry Journal*, *8*(1), 50–55. https://doi.org/10.2174/1874210601408010050

Abrahamsson, I., Linder, E., & Lang, N. P. (2009). Implant stability in relation to osseointegration: an experimental study in the Labrador dog. *Clinical Oral Implants Research*, *20*(3), 313–318. https://doi.org/10.1111/j.1600-0501.2008.01646.x

Abrishami, M. H., Shiezadeh, F., Samieirad, S., Mollaei, M., Mahrokh, F. M., & Khosravi, F. (2023). Analyzing the Causes and Frequency of Early Dental Implant Failure among Iranians: An Epidemiological Study. *International Journal of Dentistry*, *2023*, 1–6. https://doi.org/10.1155/2023/2107786

Abuhussein, H., Pagni, G., Rebaudi, A., & Wang, H. (2010). The effect of thread pattern upon implant osseointegration. *Clinical Oral Implants Research*, *21*(2), 129–136. https://doi.org/10.1111/j.1600-0501.2009.01800.x

Adell, R., Lekholm, U., Rockler, B., & Brånemark, P.I. (1981). A 15-year study of osseointegrated implants in the treatment of the edentulous jaw. *International Journal of Oral Surgery*, *10*(6), 387–416.

Adler, L., Buhlin, K., & Jansson, L. (2020). Survival and complications: A 9- to 15-year retrospective follow-up of dental implant therapy. *Journal of Oral Rehabilitation*, *47*(1), 67–77. https://doi.org/10.1111/joor.12866

Ahamed, A. S., Prakash, P. S. G., Crena, J., Victor, D. J., Subramanian, S., & Appukuttan, D. (2021). The influence of laser-microgrooved implant and abutment surfaces on mean crestal bone levels and peri-implant soft tissue healing: a 3-year longitudinal randomized controlled clinical trial. *International Journal of Implant Dentistry*, *7*(1), 102. https://doi.org/10.1186/s40729-021-00382-3

Ahmad, R., Lim, T.W. (2021). Clinical Trial Protocol Study of A Prospective, Open Label, Randomized, Double Arm, Multicenter Study to Evaluate the Performance of NiTiDent Tuah Porous NiTi Dental Implants in Single Tooth Gap in the Posterior Mandible [Unpublished protocol]. Nitium Technology Sdn. Bhd.

Akça, K., Kökat, A., Cömert, A., Akkocaoğlu, M., Tekdemir, I., & Çehreli, M. (2010). Torque-fitting and resonance frequency analyses of implants in conventional sockets versus controlled bone defects in vitro. *International Journal of Oral and Maxillofacial Surgery*, *39*(2), 169–173. https://doi.org/10.1016/j.ijom.2009.11.019

Akça, K., Chang, T., Tekdemir, İ., & Fanuscu, M. I. (2006). Biomechanical aspects of initial intraosseous stability and implant design: a quantitative micro-morphometric analysis. *Clinical Oral Implants Research*, *17*(4), 465–472. https://doi.org/10.1111/j.1600-0501.2006.01265.x

Akkocaoglu, M., Uysal, S., Tekdemir, I., Akca, K., & Cehreli, M. C. (2005). Implant design and intraosseous stability of immediately placed implants: a human cadaver study. *Clinical Oral Implants Research*, *16*(2), 202–209. https://doi.org/10.1111/j.1600-0501.2004.01099.x

Albrektsson, T., & Albrektsson, B. (1987). Osseointegration of bone implants: A review of an alternative mode of fixation. *Acta Orthopaedica Scandinavica*, *58*(5), 567-577. https://doi.org/10.3109/17453678709146401

Albrektsson, T., & Johansson, C. (2001). Osteoinduction, osteoconduction and osseointegration. *European Spine Journal*, *10*, S96–S101. https://doi.org/10.1007/s005860100282

Albrektsson, T., & Wennerberg, A. (2004). Oral implant surfaces: Part 1--review focusing on topographic and chemical properties of different surfaces and *in vivo* responses to them. *International Journal of Prosthodontics*, *17*(5).

Albrektsson, T., & Wennerberg, A. (2019). On osseointegration in relation to implant surfaces. *Clinical Implant Dentistry and Related Research*, *21*(S1), 4–7. https://doi.org/10.1111/cid.12742

Albrektsson, T., Brånemark, P. I., Hansson, H. A., & Lindström, J. (1981). Osseointegrated titanium implants: Requirements for ensuring a long-lasting, direct bone-to-implant anchorage in man. *Acta Orthopaedica*, *52*(2), 155–170. https://doi.org/10.3109/17453678108991776

Albrektsson, T., Chrcanovic, B., Mölne, J., & Wennerberg, A. (2018). Foreign body reactions, marginal bone loss and allergies in relation to titanium implants. *European journal of oral implantology*, *11 Suppl 1*, S37–S46.

Albrektsson, T., Chrcanovic, B., Jacobsson, M., & Wennerberg, A. (2017). Osseointegration of Implants – A Biological and Clinical Overview. *JSM Dental Surgery*, *2*(3), 1022.

Albrektsson, T., Dahlin, C., Jemt, T., Sennerby, L., Turri, A., & Wennerberg, A. (2013). Is Marginal Bone Loss around Oral Implants the Result of a Provoked Foreign Body Reaction? *Clinical Implant Dentistry and Related Research*, *16*(2), 155–165. https://doi.org/10.1111/cid.12142

Albrektsson, T., Dahlin, C., Reinedahl, D., Tengvall, P., Trindade, R., & Wennerberg, A. (2020). An imbalance of the immune system instead of a disease behind marginal bone loss around oral implants: Position paper. *The International Journal of Oral & Maxillofacial Implants*, *35*(3), 495–502. https://doi.org/10.11607/jomi.8218

Alevizakos, V., Mosch, R., Platte, A., & Von See, C. (2025). Effects of repeated use and sterilization on the wear of zirconia implant drills: a SEM-Based analysis. *Clinical and Experimental Dental Research*, *11*(1), e70088. https://doi.org/10.1002/cre2.70088

Alexander, H., & Ricci, J. (2017). Mechanical modification of dental implants to control bone retention. In *Bone Response to Dental Implant Materials*, 25–42.

Ali Al-Hashedi, A., Bai Taiyeb Ali, T., & Yunus, N. (2014). Short dental implants: An emerging concept in implant treatment. *Clinical Oral Implants Research, Journal of Clinical Periodontology*, *45*, 499–514. https://doi.org/10.3290/j.qi.a31539

Al-Juboori, H., Petronis, Z., & Razukevicius, D. (2024). The Interrelation between Cortical Bone Thickness and Primary and Secondary Dental Implant Stability:

A Systematic Review. *Journal of Oral and Maxillofacial Research*, *15*(4), e2. https://doi.org/10.5037/jomr.2024.15402

Almas, K., Smith, S., & Kutkut, A. (2019). What is the Best Micro and Macro Dental Implant Topography? *Dental Clinics of North America*, *63*(3), 447–460. https://doi.org/10.1016/j.cden.2019.02.010

Almassri, H. N., Ma, Y., Dan, Z., Ting, Z., Cheng, Y., & Wu, X. (2020). Implant stability and survival rates of a hydrophilic versus a conventional sandblasted, acid-etched implant surface. *The Journal of the American Dental Association*, *151*(6), 444–453.

AlRowis, R., Albelaihi, F., Alquraini, H., Almojel, S., Alsudais, A., & Alaqeely, R. (2025). Factors affecting dental implant Failure: A Retrospective analysis. *Healthcare*, *13*(12), 1356. https://doi.org/10.3390/healthcare13121356

AlSamman, A. A., Al-Rawee, R. Y., & ATawfeeq, B. (2022). Does primary stability is mandatory for dental implant success? A Systematic Review of Literature. *Journal of Dentistry and Oral Sciences.* https://doi.org/10.37191/Mapsci-2582-3736-4(1)-121

Al-Sanea, A., Mutlu, I., Kişioğlu, Y., & Mohamed, E. (2023). The effect of V-thread and square thread dental implants on bone stresses. *Journal of Biomimetics, Biomaterials and Biomedical Engineering*, *60*, 83-96. https://doi.org/10.4028/p-3qasy2

Amerinatanzi, A., Moghaddam, N. S., Ibrahim, H., & Elahinia, M. (2016). "Evaluating a NITI implant under realistic loads: A Simulation study." In *Proceedings of the ASME 2016 Conference on Smart Materials, Adaptive Structures and Intelligent Systems. Volume 2: Modelling, Simulation and Control; Bio-Inspired Smart Materials and Systems; Energy Harvesting, 2,* V002T03A030. https://doi.org/10.1115/SMASIS2016-9287

Anderson, J.M., Jiang, S. (2017). Implications of the Acute and Chronic Inflammatory Response and the Foreign Body Reaction to the Immune Response of Implanted Biomaterials. In: Corradetti, B. (eds) The Immune Response to Implanted Materials and Devices. Springer, Cham. https://doi.org/10.1007/978-3-319-45433-7_2

Anderson, J. M., & McNally, A. K. (2011). Biocompatibility of implants: lymphocyte/macrophage interactions. In *Seminars in immunopathology*, 33, 221–233. https://doi.org/10.1007/s00281-011-0244-1

Anderson, J. M., Rodriguez, A., & Chang, D. T. (2008). Foreign body reaction to biomaterials. *Seminars in Immunology*, *20*(2), 86–100. https://doi.org/10.1016/j.smim.2007.11.004

Anderson, J., & Cramer, S. (2015). Perspectives on the inflammatory, healing, and foreign body responses to biomaterials and medical devices. In book: Host Response to Biomaterials, 13–36. https://doi.org/10.1016/B978-0-12-800196-7.00002-5

Andreiotelli, M., & Kohal, R. (2009). Fracture Strength of Zirconia Implants after Artificial Aging. *Clinical Implant Dentistry and Related Research*, *11*(2), 158–166. https://doi.org/10.1111/j.1708-8208.2008.0005.x

Anitua, E., Murias-Freijo, A., Tierno, R., Tejero, R., & Alkhraisat, M. H. (2024). Assessing peri-implant bacterial community structure: the effect of microbiome sample collection method. *BMC Oral Health*, *24*(1), 1001. https://doi.org/10.1186/s12903-024-04675-y

Anselme, K. (2000). Osteoblast adhesion on biomaterials. *Biomaterials*, *21*(7), 667–681. https://doi.org/10.1016/s0142-9612(99)00242-2

Anselme, K., Linez, P., Bigerelle, M., Le Maguer, D., Le Maguer, A., Hardouin, P., ... & Leroy, J. M. (2000). The relative influence of the topography and chemistry of TiAl6V4 surfaces on osteoblastic cell behaviour. *Biomaterials*, *21*(15), 1567–1577. https://doi.org/10.1016/s0142-9612(00)00042-9

Antonacci, D., Bollero, P., Stocchero, M., Jinno, Y., & Canullo, L. (2023). Clinical effects of conventional and underprepared drilling preparation of the implant site based on bone density: A systematic review and meta-regression. *Journal of Prosthodontic Research*, *67*(1), 23–34.

Ao, J., Li, T., Liu, Y., Ding, Y., Wu, G., Hu, K., & Kong, L. (2010). Optimal design of thread height and width on an immediately loaded cylinder implant: A finite element analysis. *Computers in Biology and Medicine*, *40*(8), 681-686.

Araujo, M. G., & Lindhe, J. (2018). Peri-implant health. *Journal of Clinical Periodontology*, *45*(S20), S230-S236. https://doi.org/10.1111/jcpe.12952

Arnett TR. Extracellular pH regulates bone cell function (2008). *Journal of Nutrition, 138*(2):415S-418S. https://doi.org/10.1093/jn/138.2.415S

Assad, M., Jarzem, P., Leroux, M. A., Coillard, C., Chernyshov, A. V., Charette, S., & Rivard, C. (2003). Porous titanium-nickel for intervertebral fusion in a sheep model: Part 1. Histomorphometric and radiological analysis1. *Journal of*

Biomedical Materials Research Part B Applied Biomaterials, *64B*(2), 107–120. https://doi.org/10.1002/jbm.b.10530

Assad, M., Chernyshov, A. V., Jarzem, P., Leroux, M. A., Coillard, C., Charette, S., & Rivard, C. H. (2003). Porous titanium-nickel for intervertebral fusion in a sheep model: Part 2. Surface analysis and nickel release assessment. *Journal of Biomedical Materials Research Part B Applied Biomaterials*, *64B*(2), 121–129. https://doi.org/10.1002/jbm.b.10531

Assad, M., Chernyshov, A., Leroux, M. A., & Rivard, C. H. (2002). A new porous titanium–nickel alloy: part 2. Sensitization, irritation and acute systemic toxicity evaluation. *Bio-Medical Materials and Engineering*, *12*(4), 339–346.

Assad, M., Lemieux, N., Rivard, C. H., & Yahia, L. H. (1999). Comparative *in vitro* biocompatibility of nickel-titanium, pure nickel, pure titanium, and stainless steel: genotoxicity and atomic absorption evaluation. *Bio-Medical Materials and Engineering*, *9*(1), 1–12.

Assad, M., Likibi, F., Jarzem, P., Leroux, M. A., Coillard, C., & Rivard, C. (2004). Porous nitinol vs. titanium intervertebral fusion implants: computer tomography, radiological and histological study of osseointegration capacity. *Materialwissenschaft und Werkstofftechnik: 35*(4), 219–223. https://doi.org/10.1002/mawe.200400739

Asserghine, A., Medvidović-Kosanović, M., Nagy, L., & Nagy, G. (2019). In situ monitoring of the transpassivation and repassivation of the passive film on nitinol biomaterial by scanning electrochemical microscopy. *Electrochemistry Communications*, *107*, 106539. https://doi.org/10.1016/j.elecom.2019.106539

Atieh, M. A., Alsabeeha, N. H., & Payne, A. G. (2012). Can resonance frequency analysis predict failure risk of immediately loaded implants? *International Journal of Prosthodontics*, *25*(4), 326–339.

Atieh, M. A., Ibrahim, H. M., & Atieh, A. H. (2010). Platform switching for marginal bone preservation around dental implants: a systematic review and meta-analysis. *Journal of Periodontology*, *81*(10), 1350–1366. https://doi.org/10.1902/jop.2010.100232

Atsuta, I., Ayukawa, Y., Kondo, R., Oshiro, W., Matsuura, Y., Furuhashi, A., Tsukiyama, Y., & Koyano, K. (2016). Soft tissue sealing around dental implants based on histological interpretation. *Journal of Prosthodontic Research*, *60*(1), 3–11. https://doi.org/10.1016/j.jpor.2015.07.001

Aziz-Kerrzo, M., Conroy, K. G., Fenelon, A. M., Farrell, S. T., & Breslin, C. B. (2001). Electrochemical studies on the stability and corrosion resistance of titanium-based implant materials. *Biomaterials*, *22*(12), 1531–1539. https://doi.org/10.1016/s0142-9612(00)00309-4

Babensee, J. E., Anderson, J. M., McIntire, L. V., & Mikos, A. G. (1998). Host response to tissue engineered devices. *Advanced Drug Delivery Reviews*, *33*(1-2), 111–139. https://doi.org/10.1016/S0169-409X(98)00023-4

Bai, H., Zhao, Y., Wang, C., Wang, Z., Wang, J., Liu, H., Feng, Y., Lin, Q., Li, Z., & Liu, H. (2020). Enhanced osseointegration of three-dimensional supramolecular bioactive interface through osteoporotic microenvironment regulation. *Theranostics*, *10*(11), 4779–4794. https://doi.org/10.7150/thno.43736

Baldi, D., Colombo, J., Verardi, S., Rebaudi, A., Rebaudi, F., & Makary, C. (2020). Clinical osseointegration of bone level implants with conical shape and textured surface with low primary stability. *Minerva Stomatol*, *69*(1), 8–13. https://doi.org/10.23736/S0026-4970.20.04277-6

Baldi, D., Lombardi, T., Colombo, J., Cervino, G., Perinetti, G., Di Lenarda, R., & Stacchi, C. (2018). Correlation between insertion torque and implant stability quotient in tapered implants with knife-edge thread design. *BioMed Research International*, *2018*(1), 7201093. https://doi.org/10.1155/2018/7201093

Baltayan, S., Pi-Anfruns, J., Aghaloo, T., & Moy, P. K. (2016). The predictive value of resonance frequency analysis measurements in the surgical placement and loading of endosseous implants. *Journal of Oral and Maxillofacial Surgery*, *74*(6), 1145–1152.

Bansiddhi, A., Sargeant, T. D., Stupp, S. I., & Dunand, D. C. (2008). Porous NiTi for bone implants: a review. *Acta Biomaterialia*, *4*(4), 773–782. https://doi.org/10.1016/j.actbio.2008.02.009

Barberi, J., & Spriano, S. (2021). Titanium and protein adsorption: an overview of mechanisms and effects of surface features. *Materials*, *14*(7), 1590. https://doi.org/10.3390/ma14071590

Barewal, R. M., Oates, T. W., Meredith, N., & Cochran, D. L. (2003). Resonance frequency measurement of implant stability *in vivo* on implants with a sandblasted and acid-etched surface. *International Journal of Oral & Maxillofacial Implants*, *18*(5), 641.

Barras, C. D. J., & Myers, K. A. (2000). Nitinol–its use in vascular surgery and other applications. *European Journal of Vascular and Endovascular Surgery*, *19*(6), 564-569. https://doi.org/10.1053/ejvs.2000.1111

Bashutski, J. D., D'Silva, N. J., & Wang, H. L. (2009). Implant compression necrosis: Current understanding and case report. *Journal of periodontology*, *80*(4), 700–704. https://doi.org/10.1902/jop.2009.080581.

Behr, B., Sorkin, M., Lehnhardt, M., Renda, A., Longaker, M. T., & Quarto, N. (2012). A comparative analysis of the osteogenic effects of BMP-2, FGF-2, and VEGFA in a calvarial defect model. *Tissue Engineering Part A*, *18*(9-10), 1079–1086. https://doi.org/10.1089/ten.tea.2011.0537.

Bencharit, S., Byrd, W. C., Altarawneh, S., Hosseini, B., Leong, A., Reside, G., Morelli, T., & Offenbacher, S. (2013). Development and applications of Porous tantalum trabecular Metal-Enhanced Titanium dental implants. *Clinical Implant Dentistry and Related Research*, *16*(6), 817–826. https://doi.org/10.1111/cid.12059.

Berardini, M., Trisi, P., Sinjari, B., Rutjes, A. W., & Caputi, S. (2016). The effects of high insertion torque versus low insertion torque on marginal bone resorption and implant failure rates: A systematic review with meta-analyses. *Implant Dentistry*, *25*(4), 532–540. https://doi.org/10.1097/id.0000000000000422.

Berglundh, T., & Lindhe, J. (1996). Dimension of the periimplant mucosa: biological width revisited. *Journal of Clinical Periodontology*, *23*(10), 971-973. https://doi.org/10.1111/j.1600-051X.1996.tb00520.x

Berglundh, T., Abrahamsson, I., Lang, N. P., & Lindhe, J. (2003). De novo alveolar bone formation adjacent to endosseous implants: a model study in the dog. *Clinical oral implants research*, *14*(3), 251-262. https://doi.org/10.1034/j.1600-0501.2003.00972.x

Berglundh, T., Armitage, G., Araujo, M. G., Avila-Ortiz, G., Blanco, J., Camargo, P. M., Chen, S., Cochran, D., Derks, J., Figuero, E., Hämmerle, C. H., Heitz-Mayfield, L. J., Huynh-Ba, G., Iacono, V., Koo, K., Lambert, F., McCauley, L., Quirynen, M., Renvert, S., . . . Zitzmann, N. (2018). Peri-implant diseases and conditions: Consensus report of workgroup 4 of the 2017 World Workshop on the Classification of Periodontal and Peri-Implant Diseases and Conditions. *Journal of Clinical Periodontology*, *45*(S20), S313–S318. https://doi.org/10.1111/jcpe.12957.

Berglundh, T., Lindhe, J., & Sterrett, J. D. (1991). Clinical and structural characteristics of periodontal tissues in young and old dogs. *Journal of Clinical Periodontology*, *18*(8), 616–623. https://doi.org/10.1111/j.1600-051x.1991.tb00099.x

Berglundh, T., Mombelli, A., Schwarz, F., & Derks, J. (2024). Etiology, pathogenesis and treatment of peri-implantitis: A European perspective. *Periodontology 2000*. https://doi.org/10.1111/prd.12549

Berkmann, J. C., Herrera Martin, A. X., Ellinghaus, A., Schlundt, C., Schell, H., Lippens, E., Duda, G. N., Tsitsilonis, S., & Schmidt-Bleek, K. (2020). Early pH changes in musculoskeletal tissues upon injury—Aerobic catabolic pathway activity linked to inter-individual differences in local pH. ***International Journal of Molecular Sciences***, ***21***(7), 2513. https://doi.org/10.3390/ijms21072513

Bernabeu-Mira, J. C., Pellicer-Chover, H., Peñarrocha-Diago, M., & Peñarrocha-Oltra, D. (2020). *In Vitro* Study on Bone Heating during Drilling of the Implant Site: Material, Design and Wear of the Surgical Drill. ***Materials***, ***13***(8), 1921. https://doi.org/10.3390/ma13081921

Bernabe, E., Marcenes, W., Hernandez, C., Bailey, J., Abreu, L., Alipour, V., Amini, S., Arabloo, J., Arefi, Z., Arora, A., Ayanore, M., Bärnighausen, T., Bijani, A., Cho, D., Chu, D., Crowe, C., Demoz, G., Demsie, D., Forooshani, Z. D., . . . Kassebaum, N. (2020). Global, Regional, and National Levels and Trends in Burden of Oral Conditions from 1990 to 2017: A Systematic Analysis for the Global Burden of Disease 2017 Study. *Journal of Dental Research*, *99*(4), 362–373. https://doi.org/10.1177/0022034520908533

Bertheville, B., Neudenberger, M., & Bidaux, J. (2004). Powder sintering and shape-memory behaviour of NiTi compacts synthesized from Ni and TiH2. *Materials Science and Engineering A*, *384*(1–2), 143–150. https://doi.org/10.1016/j.msea.2004.06.025

Berzaghi, A., Testori, T., Scaini, R., & Bortolini, S. (2025). Occlusion and Biomechanical Risk Factors in Implant-Supported Full-Arch Fixed Dental Prostheses-Narrative Review. *Journal of Personalised Medicine*, *15*(2), 65. https://doi.org/10.3390/jpm15020065

Biffi CA, Fiocchi J, Valenza F, et al., 2020, Selective laser melting of NiTi shape memory alloy: Processability, microstructure, and superelasticity. *Shape*

Memory and Superelasticity, 6, 342–353. https://doi.org/10.1007/s40830-020-00298-8

Blanco, J., Pico, A., Caneiro, L., Nóvoa, L., Batalla, P., & Martín-Lancharro, P. (2017). Effect of abutment height on interproximal implant bone level in the early healing: A randomized clinical trial. *Clinical Oral Implants Research*, *29*(1), 108–117. https://doi.org/10.1111/clr.13108

Bobyn, J. D., Pilliar, R. M., Cameron, H. U., & Weatherly, G. C. (1980). The optimum pore size for the fixation of porous-surfaced metal implants by the ingrowth of bone. *Clinical Orthopaedics and Related Research*, *150*, 263–270.

Bonfante, E. A., Granato, R., Marin, C., Jimbo, R., Giro, G., Suzuki, M., Coelho, P.G. (2013). Biomechanical testing of microblasted, acid-etched/microblasted, anodized, and discrete crystalline deposition surfaces: An experimental study in Beagle dogs. *International Journal of Oral & Maxillofacial Implants 28*(1), 136–142. https://doi.org/10.11607/jomi.2331

Bornstein, M., Scarfe, W., Vaughn, V., & Jacobs, R. (2014). Cone Beam Computed Tomography in Implant Dentistry: A Systematic review focusing on guidelines, indications, and radiation dose risks. *The International Journal of Oral & Maxillofacial Implants*, *29*(Supplement), 55–77. https://doi.org/10.11607/jomi.2014suppl.g1.4

Bosshardt, D. D., Chappuis, V., & Buser, D. (2016). Osseointegration of titanium, titanium alloy and zirconia dental implants: current knowledge and open questions. *Periodontology 2000*, *73*(1), 22–40. https://doi.org/10.1111/prd.12179

Bosshardt, D. D., Salvi, G. E., Huynh-Ba, G., Ivanovski, S., Donos, N., & Lang, N. P. (2011). The role of bone debris in early healing adjacent to hydrophilic and hydrophobic implant surfaces in man. *Clinical Oral Implants Research*, *22*(4), 357–364. https://doi.org/10.1111/j.1600-0501.2010.02107.x

Boven, G. C., Raghoebar, G. M., Vissink, A., & Meijer, H. J. A. (2015). Improving masticatory performance, bite force, nutritional state and patient's satisfaction with implant overdentures: a systematic review of the literature. *Journal of Oral Rehabilitation*, *42*(3), 220–233. https://doi.org/10.1111/joor.12241

Boyce, B. F., & Xing, L. (2008). Functions of RANKL/RANK/OPG in bone modeling and remodeling. *Archives of Biochemistry and Biophysics*, *473*(2), 139–146. https://doi.org/10.1016/j.abb.2008.03.018

Brägger, U., Gerber, C., Joss, A., Haenni, S., Meier, A., Hashorva, E., & Lang, N. P. (2004). Patterns of tissue remodeling after placement of ITI® dental implants using an osteotome technique: A longitudinal radiographic case cohort study. *Clinical Oral Implants Research*, *15*(2), 158–166. https://doi.org/10.1111/j.1600-0501.2004.00988.x

Bram, M., Ahmad-Khanlou, A., Heckmann, A., Fuchs, B., Buchkremer, H. P., & Stöver, D. (2002). Powder metallurgical fabrication processes for NiTi shape memory alloy parts. *Materials Science and Engineering: A*, *337*(1-2), 254–263. https://doi.org/10.1016/S0921-5093(02)00028-X

Brånemark, P. I. (1983). Osseointegration and its experimental background. *Journal of Prosthetic Dentistry*, *50*(3), 399–410. https://doi.org/10.1016/S0022-3913(83)80101-2

Brånemark, P. I., Adell, R., Albrektsson, T., Lekholm, U., Lundkvist, S., & Rockler, B. (1983). Osseointegrated titanium fixtures in the treatment of edentulousness. *Biomaterials*, *4*(1), 25–28. https://doi.org/10.1016/0142-9612(83)90065-0

Brånemark, P. I., Breine, U., Adell, R., Hansson, B. O., Lindström, J., & Ohlsson, A. (1969). Intra-osseous anchorage of dental prostheses: I. Experimental studies. *Scandinavian Journal of Plastic and Reconstructive Surgery and Hand Surgery*, *3*(2), 81–100. https://doi.org/10.3109/02844316909036699

Brizuela, A., Herrero-Climent, M., Ríos-Carrasco, E., Ríos-Santos, J. V., Pérez, R. A., Manero, J. M., & Mur, J. G. (2019). Influence of the elastic modulus on the osseointegration of dental implants. *Materials*, *12*(6), 980. https://doi.org/10.3390/ma12060980

Brunski, J. B. (1999). *In vivo* bone response to biomechanical loading at the bone/dental-implant interface. In *Advances in Dental Research* (Vol. 13, pp. 99–119). https://doi.org/10.1177/08959374990130012301

Bryce, G., Bomfim, D. I., & Bassi, G. S. (2014). Pre- and post-operative management of dental implant placement. Part 2: Management of early-presenting complications. British Dental Journal, 217(4), 171–176. https://https://doi.org/10.1038/sj.bdj.2014.702

Buser, D., Broggini, N., Wieland, M., Schenk, R. K., Denzer, A. J., Cochran, D. L., ... & Steinemann, S. G. (2004). Enhanced bone apposition to a chemically modified SLA titanium surface. *Journal of Dental Research*, *83*(7), 529–533. https://doi.org/10.1177/154405910408300704

Buser, D., Mericske-stern, R., Bernard, J. P. P., Behneke, A., Behneke, N., Hirt, H. P., Belser, U. C., & Lang, N. P. (1997). Long-term evaluation of non-submerged ITI implants. Part 1: 8-year life table analysis of a prospective multi-center study with 2359 implants. *Clinical Oral Implants Research*, *8*(3), 161–172. https://doi.org/10.1034/j.1600-0501.1997.080302.x

Buser, D., Weber, H., & Lang, N. P. (1990). Tissue integration of non-submerged implants. l-year results of a prospective study with 100 ITI hollow-cylinder and hollow-screw implants. *Clinical Oral Implants Research*, *1*(1), 33–40. https://doi.org/10.1034/j.1600-0501.1990.010105.x

Buser, D., Schenk, R. K., Steinemann, S., Fiorellini, J. P., Fox, C. H., & Stich, H. (1991). Influence of surface characteristics on bone integration of titanium implants. A histomorphometric study in miniature pigs. *Journal of Biomedical Materials Research*, *25*(7), 889–902. https://doi.org/10.1002/jbm.820250708

Buser, D., Sennerby, L., & De Bruyn, H. (2016). Modern implant dentistry based on osseointegration: 50 years of progress, current trends and open questions. *Periodontology 2000*, *73*(1), 7–21. https://doi.org/10.1111/prd.12185

Buxton S, Garman E, Heim KE, Lyons-Darden T, Schlekat CE, Taylor MD, Oller AR. (2019). Concise review of nickel human health toxicology and ecotoxicology. *Inorganics*. *7*(7):89. https://doi.org/10.3390/inorganics7070089

Calazans Neto, J. V., Celles, C. A. S., de Andrade, C. S. A. F., Afonso, C. R. M., Nagay, B. E., & Barão, V. A. R. (2024). Recent advances and prospects in β-type titanium alloys for dental implants applications. *ACS Biomaterials Science & Engineering*, *10*(10), 6029–6060. https://doi.org/10.1021/acsbiomaterials.4c00963

Cámara, O. R., Avalle, L. B., & Oliva, F. Y. (2010). Protein adsorption on titanium dioxide: Effects on double layer and semiconductor space charge region studied by EIS. *Electrochimica Acta*, *55*(15), 4519-4528. https://doi.org/10.1016/j.electacta.2010.03.003.

Cannizzaro, G., Leone, M., Ferri, V., Viola, P., Gelpi, F., & Esposito, M. (2012). Immediate loading of single implants inserted flapless with medium or high insertion torque: a 6-month follow-up of a split-mouth randomised controlled trial. *European Journal of Oral Implantology*, *5*(4), 333–342.

Canullo, L., Caneva, M., & Tallarico, M. (2016). Ten-year hard and soft tissue results of a pilot double-blinded randomized controlled trial on immediately loaded

post-extractive implants using platform-switching concept. *Clinical Oral Implants Research*, *28*(10), 1195–1203. https://doi.org/10.1111/clr.12940.

Canullo, L., Menini, M., Santori, G., Rakic, M., Sculean, A., & Pesce, P. (2020). Titanium abutment surface modifications and peri-implant tissue behavior: A systematic review and meta-analysis. *Clinical Oral Investigations*, *24*(3), 1113–1124. https://doi.org/10.1007/s00784-020-03210-x.

Castleman, L. S., Motzkin, S. M., Alicandri, F. P., Bonawit, V. L., & Johnson, A. A. (1976). Biocompatibility of nitinol alloy as an implant material. *Journal of Biomedical Materials Research*, *10*(5), 695–731. https://doi.org/10.1002/jbm.820100505

Cempel, M., & Nikel, G. J. P. J. S. (2006). Nickel: a review of its sources and environmental toxicology. *Polish Journal of Environmental Studies*, *15*(3), 375-382.

Centers for Disease Control and Prevention. Oral Health Surveillance Report: Dental Caries, Tooth Retention, and Edentulism, United States, 2017–March 2020. U.S. Dept of Health and Human Services; 2024. [Accessed Date]. https://www.cdc.gov/oral-health/php/2024-oralhealth-surveillance-report/index.html

Cesaretti, G., Botticelli, D., Renzi, A., Rossi, M., Rossi, R., & Lang, N. P. (2016). Radiographic evaluation of immediately loaded implants supporting 2–3 units fixed bridges in the posterior maxilla: A 3-year follow-up prospective randomized controlled multicenter clinical study. *Clinical Oral Implants Research*, *27*(4), 399-405. https://doi.org/10.1111/clr.12565

Chan, W. Y., Yip, J., Yick, K. L., Ng, S. P., Lu, L., Cheung, K. M. C., ... & Tse, C. Y. (2018). Mechanical and clinical evaluation of a shape memory alloy and conventional struts in a flexible scoliotic brace. *Annals of Biomedical Engineering*, *46*, 1194–1205. https://doi.org/10.1007/s10439-018-2016-8

Chang, B. S., Hong, K. S., Youn, H. J., Ryu, H. S., Chung, S. S., & Park, K. W. (2000). Osteoconduction at porous hydroxyapatite with various pore configurations. *Biomaterials*, *21*(12), 1291–1298. https://doi.org/10.1016/S0142-9612(00)00030-2

Chawla, B. K., Cohen, R. E., Stellrecht, E. M., & Yerke, L. M. (2022). The influence of proton pump inhibitors on tissue attachment around teeth and dental implants:

A scoping review. *Clinical and Experimental Dental Research*, *8*(5), 1045–1058. https://doi.org/10.1002/cre2.616

Chen, G., Cao, P., Wen, G., Edmonds, N., & Li, Y. (2013). Using an agar-based binder to produce porous NiTi alloys by metal injection moulding. *Intermetallics*, *37*, 92–99. https://doi.org/10.1016/j.intermet.2013.02.006

Chen, L., Tong, Z., Luo, H., Qu, Y., Gu, X., & Si, M. (2023). Titanium particles in peri-implantitis: distribution, pathogenesis and prospects. *International Journal of Oral Science*, *15*(1), 49. https://doi.org/10.1038/s41368-023-00256-x

Chen, M. H., Lyons, K. M., Tawse-Smith, A., & Ma, S. (2019). Clinical significance of the use of resonance frequency analysis in assessing implant stability: A systematic review. *International Journal of Prosthodontics*, *32*(1), 51–58. https://doi.org/10.11607/ijp.6048

Cheung, J. P. Y., Samartzis, D., Yeung, K., To, M., Luk, K. D. K., & Cheung, K. M. C. (2018). A randomized double-blinded clinical trial to evaluate the safety and efficacy of a novel superelastic nickel–titanium spinal rod in adolescent idiopathic scoliosis: 5-year follow-up. *European Spine Journal*, *27*(2), 327–339. https://doi.org/10.1007/s00586-017-5245-x

Chevalier, J. (2006). What future for zirconia as a biomaterial? *Biomaterial*, *27(4)*, 535–543. https://doi.org/10.1016/j.biomaterials.2005.07.034

Chitumalla, R. K., Gopinathan, P. A., Jamjoom, F. Z., Munaga, S., Alaifi, A., & Siddeeqh, S. (2025). Success rate of dental implants in patients with autoimmune disorders: A systematic review and meta-analysis. *Journal of International Society of Preventive and Community Dentistry*, *15*(5), 402–414. https://doi.org/10.4103/jispcd.jispcd_108_25

Chiyun, W. (2024). 3-Dimensional Soft Tissue Analysis (3DSTA) of Subcrestally Placed Implants: Relating Biologic Stability with Morphologic Achievements. *Preprints.org*. https://doi.org/10.20944/preprints202404.1116.v1

Choe, S., Ma, T., Jones, D., Shiau, H. J., & Saito, H. (2024). Peri-implant mucosal tissue attachment: Narrative review. *Dentistry Review*, *4*(3), 100141. https://doi.org/10.1016/j.dentre.2024.100141

Choi, J., Lee, H., Jang, J., & Yeo, I. (2012). Comparison between bioactive fluoride modified and bioinert anodically oxidized implant surfaces in early bone response using Rabbit tibia model. *Implant Dentistry*, *21*(2), 124–128. https://doi.org/10.1097/id.0b013e318249f283

Chrcanovic, B. R., Albrektsson, T., & Wennerberg, A. (2014). Diabetes and oral implant failure: a systematic review. *Journal of Dental Research*, *93*(9), 859–867. https://doi.org/10.1177/0022034514538820

Chrcanovic, B. R., Albrektsson, T., & Wennerberg, A. (2014). Periodontally compromised vs. periodontally healthy patients and dental implants: A systematic review and meta-analysis. *Journal of Dentistry*, *42*(12), 1509–1527. https://doi.org/10.1016/j.jdent.2014.09.013

Chrcanovic, B. R., Albrektsson, T., & Wennerberg, A. (2014). Reasons for failures of oral implants. *Journal of Oral Rehabilitation*, *41*(6), 443–476. https://doi.org/10.1111/joor.12157

Chrcanovic, B. R., Albrektsson, T., & Wennerberg, A. (2015). Smoking and dental implants: A systematic review and meta-analysis. *Journal of Dentistry*, *43*(5), 487–498. https://doi.org/10.1016/j.jdent.2015.03.003

Chrcanovic, B. R., Kisch, J., Albrektsson, T., & Wennerberg, A. (2016). Factors Influencing early dental implant failures. *Journal of Dental Research*, *95*(9), 995–1002. https://doi.org/10.1177/0022034516646098

Chrcanovic, B. R., Kisch, J., Albrektsson, T., & Wennerberg, A. (2016). Factors influencing early dental implant failures. *Journal of Dental Research*, *95*(9), 995–1002. https://doi.org/10.1177/0022034516646098

Chrcanovic, B.R., Albrektsson, T. & Wennerberg, A. (2015). Platform switch and dental implants: A meta-analysis." *Journal of Dentistry, 43*(6), 629–646. https://doi.org/10.1016/j.jdent.2014.12.013

Chun Giok, K., & Menon, R. K. (2023). The microbiome of peri-implantitis: A systematic review of next-generation sequencing studies. *Antibiotics*, *12*(11), 1610. https://doi.org/10.3390/antibiotics12111610

Cimini, V., Perez, A., Lombardi, T., & Felice, R. D. (2024). Heat generated during dental implant placement: a scoping review. *Applied Sciences*, *14*(15), 6773. https://doi.org/10.3390/app14156773

Clarke, B., Carroll, W., Rochev, Y., Hynes, M., Bradley, D., & Plumley, D. (2006). Influence of Nitinol wire surface treatment on oxide thickness and composition and its subsequent effect on corrosion resistance and nickel ion release. *Journal of Biomedical Materials Research Part A*, *79A*(1), 61–70. https://doi.org/10.1002/jbm.a.30720

Clementini, M., Rossetti, P. H. O., Penarrocha, D., Micarelli, C., Bonachela, W. C., & Canullo, L. (2014). Systemic risk factors for peri-implant bone loss: A systematic review and meta-analysis. *International Journal of Oral and Maxillofacial Surgery*, *43*(3), 323–334. https://doi.org/10.1016/j.ijom.2013.11.012

Cobo-Vázquez, C., Reininger, D., Molinero-Mourelle, P., González-Serrano, J., Guisado-Moya, B., & López-Quiles, J. (2018). Effect of the lack of primary stability in the survival of dental implants. *Journal of Clinical and Experimental Dentistry*, *10*(1), 0. https://doi.org/10.4317/jced.54441

Cochran, D., Oates, T., Morton, D., Jones, A., Buser, D., & Peters, F. (2007). Clinical field trial examining an implant with a sand-blasted, acid-etched surface. *Journal of Periodontology*, *78*(6), 974–982. https://doi.org/10.1902/jop.2007.060294

Coelho, P. G., Granjeiro, J. M., Romanos, G. E., Suzuki, M., Silva, N. R., Cardaropoli, G., et al. (2008). Basic research methods and current trends of dental implant surfaces. *Journal of Biomedical Materials Research Part B, 88B*(2), 579–596. https://doi.org/10.1002/jbm.b.31264

Coelho, P. G., Jimbo, R., Tovar, N., & Bonfante, E. A. (2015). Osseointegration: hierarchical designing encompassing the macrometer, micrometer, and nanometer length scales. *Dental Material,* 37–52. https://doi.org/10.1016/j.dental.2014.10.007

Coli, P., & Sennerby, L. (2019). Is peri-implant probing causing over-diagnosis and over-treatment of dental implants? *Journal of Clinical Medicine*, *8*(8), 1123. https://doi.org/10.3390/jcm8081123

Cory E, Nazarian A, Entezari V, Vartanians V, Müller R, Snyder BD. (2010) Compressive axial mechanical properties of rat bone as functions of bone volume fraction, apparent density and micro-ct based mineral density. *Journal of Biomechanics,* *43*(5), 953-960. https://doi.org/10.1016/j.jbiomech.2009.10.047

Costa, F. O., Lages, E. J. P., Cortelli, S. C., Cortelli, J. R., Mattos-Pereira, G. H., Lima, R. P. E., & Cota, L. O. M. (2022). Association between cumulative smoking exposure, span since smoking cessation, and peri-implantitis: A cross-sectional study. *Clinical Oral Investigations*, *26*(7), 4835–4846. https://doi.org/10.1007/s00784-022-04451-8

Crespi, R., Capparè, P., Gastaldi, G., & Gherlone, E. F. (2018). Buccal-lingual bone remodeling in immediately loaded fresh socket implants: A cone beam computed tomography study. *lnternational Journal of Periodontics Restorative Dentistry*, *38*(1), 43–49. https://doi.org/10.11607/prd.3074

Daher, F. I., Abi-Aad, H. L., Dimassi, H. I., Cordioli, G., & Majzoub, Z. A. (2019). Immediate versus conventional loading of variable-thread tapered implants supporting three-to four-unit fixed partial dentures in the posterior maxilla: 3-year results of a split-mouth randomised controlled trial. *International Journal of Oral Implantology*, *12*(4), 449.

Dahlin, C., Widmark, G., Bergkvist, G., Fürst, B., Widbom, T., & Kashani, H. (2013). One-year results of a clinical and radiological prospective multicenter study on NEOSS® dental implants. *Clinical implant dentistry and related research*, *15*(2), 303-308.

Darriba, I., Seidel, A., Moreno, F., Botelho, J., Machado, V., Mendes, J. J., Leira, Y., & Blanco, J. (2022). Influence of low insertion torque values on survival rate of immediately loaded dental implants: A systematic review and meta-analysis. *Journal of Clinical Periodontology*, *50*(2), 158–169. https://doi.org/10.1111/jcpe.13733

Davies, J. E. (1998). Mechanisms of endosseous integration. *International Journal of Prosthodontics*, *11*(5), 391.

Davies, J. E. (2003). Understanding peri-implant endosseous healing. *Journal of Dental Education*, *67*(8), 932–949. https://doi.org/10.1002/j.0022-0337.2003.67.8.tb03681.x

De Oliveira, P. G. F. P., Bonfante, E. A., Bergamo, E. T., de Souza, S. L. S., Riella, L., Torroni, A., ... & Coelho, P. G. (2020). Obesity/metabolic syndrome and diabetes mellitus on peri-implantitis. *Trends in Endocrinology & Metabolism*, *31*(8), 596-610. https://doi.org/10.1016/j.tem.2020.05.005

DeAngelo, S. J., Kumar, P. S., Beck, F. M., Tatakis, D. N., & Leblebicioglu, B. (2007). Early soft tissue healing around one-stage dental implants: clinical and microbiologic parameters. *Journal of Periodontology*, *78*(10), 1878-1886. https://doi.org/10.1902/jop.2007.070122

Degidi, M., Daprile, G., & Piattelli, A. (2011). Implants inserted with low insertion torque values for intraoral welded full-arch prosthesis: 1-year follow-

up. *Clinical Implant Dentistry and Related Research*, *14*, e39-e40. https://doi.org/10.1111/j.1708-8208.2011.00345.x

Degidi, M., Piattelli, A., Gehrke, P., & Carinci, F. (2006). Clinical outcome of 802 immediately loaded 2-stage submerged implants with a new grit-blasted and acid-etched surface: 12-month follow-up. *International Journal of. Oral Maxillofacial. Implants 21*(5), 763–768.

Dehghan-Manshadi, A., Yu, P., Dargusch, M., StJohn, D., & Qian, M. (2020). Metal injection moulding of surgical tools, biomaterials and medical devices: A review. *Powder Technology*, *364*, 189–204. https://doi.org/10.1016/j.powtec.2020.01.073

Souza, J. P. D. V., De Moraes Melo Neto, C. L., Piacenza, L. T., Da Silva, E. V. F., De Melo Moreno, A. L., Penitente, P. A., Brunetto, J. L., Santos, D. M. D., & Goiato, M. C. (2021). Relation between insertion torque and implant stability quotient: a clinical study. *European Journal of Dentistry*, *15*(04), 618–623. https://doi.org/10.1055/s-0041-1725575

Dong, H., Zhou, N., Liu, H., Huang, H., Yang, G., Chen, L., … Mou, Y. (2019). Satisfaction analysis of patients with single implant treatments based on a questionnaire survey. *Patient Preference and Adherence*, *13*, 695–704. https://doi.org/10.2147/PPA.S201088

Donos, N., Hamlet, S., Lang, N. P., Salvi, G. E., Huynh-Ba, G., Bosshardt, D. D., & Ivanovski, S. (2011). Gene expression profile of osseointegration of a hydrophilic compared with a hydrophobic microrough implant surface. *Clinical Oral Implants Research*, *22*(4), 365–372. https://doi.org/10.1111/j.1600-0501.2010.02113.x

Dos Santos, M. V., Elias, C. N., & Cavalcanti Lima, J. H. (2011). The effects of superficial roughness and design on the primary stability of dental implants. *Clinical Implant Dentistry and Related Research*, *13*(3), 215–223. https://doi.org/10.1111/j.1708-8208.2009.00202.x

Jung, R.E., Zembic, A., Pjetursson, B. E., Zwahlen, M., & S. Thoma, D. (2012). Systematic review of the survival rate and the incidence of biological, technical, and aesthetic complications of single crowns on implants reported in longitudinal studies with a mean follow-up of 5 years. *Clinical Oral Implants Research*, *23*(s6), 2–21. https://doi.org/10.1111/j.1600-0501.2012.02547.x

Edelmann, A. R., Patel, D., Allen, R. K., Gibson, C. J., Best, A. M., & Bencharit, S. (2019). Retrospective analysis of porous tantalum trabecular metal–enhanced titanium dental implants. *The Journal of Prosthetic Dentistry*, *121*(3), 404–410. https://doi.org/10.1016/j.prosdent.2018.04.022

European Food Safety Authority. (2026, January 6). *Metals as contaminants in food*. https://www.efsa.europia.eu/en/topics/metals-conatminats-food

Elahinia, M. H., Hashemi, M., Tabesh, M., & Bhaduri, S. B. (2012). Manufacturing and processing of NiTi implants: A review. *Progress in Materials Science*, *57*(5), 911–946. https://doi.org/10.1016/j.pmatsci.2011.11.001

Elahinia, M., Moghaddam, N. S., Amerinatanzi, A., Saedi, S., Toker, G. P., Karaca, H., ... & Benafan, O. (2018). Additive manufacturing of NiTiHf high temperature shape memory alloy. *Scripta Materialia*, *145*, 90–94. https://doi.org/10.1016/j.scriptamat.2017.10.016

Elias, C. N., & Meirelles, L. (2010). Improving osseointegration of dental implants. *Expert Review of Medical Devices*, *7*(2), 241–256. https://doi.org/10.1586/erd.09.74

Elias, C., Oshida, Y., Lima, J., & Muller, C. (2008). Relationship between surface properties (roughness, wettability and morphology) of titanium and dental implant removal torque. *Journal of the Mechanical Behavior of Biomedical Materials/Journal of Mechanical Behavior of Biomedical Materials*, *1*(3), 234–242. https://doi.org/10.1016/j.jmbbm.2007.12.002

Ellis, E. A. (2007). [Postaining grids for transmission electron microscopy: Conventional and alternative protocols]. In J. Kuo (Ed.), Electron microscopy: Methods and protocols (2nd ed.,pp 97-106). Humana Press.

Elmahdy, M. F., Buonamici, P., Trapani, M., Valenti, R., Migliorini, A., Parodi, G., & Antoniucci, D. (2017). Long-term primary patency rate after nitinol self-expandable stents implantation in long, totally occluded femoropopliteal (TASC II C & D) lesions. *Heart, Lung and Circulation*, *26*(6), 604–611. https://doi.org/10.1016/j.hlc.2016.09.011

Elsayed, M. D. (2019). Biomechanical factors that influence the bone-implant-interface. *Research Reports in Oral and Maxillofacial Surgery*, *3*(023), 1-14. https://doi.org/10.23937/2643-3907

Emami, E., de Souza, R. F., Kabawat, M., & Feine, J. S. (2013). The impact of edentulism on oral and general health. *International Journal of Dentistry*, *2013*(1), 498305. https://doi.org/10.1155/2013/498305

Er, N., Alkan, A., Ilday, S., & Bengu, E. (2018). Improved dental implant drill durability and performance using heat and wear resistant protective coatings. *Journal of Oral Implantology*, *44*(3), 168-175. https://doi.org/10.1563/aaid-joi-D-16-00114

Eriksson, R. A., & Albrektsson, T. (1984). The effect of heat on bone regeneration: an experimental study in the rabbit using the bone growth chamber. *Journal of Oral and Maxillofacial Surgery*, *42*(11), 705-711. https://doi.org/10.1016/0278-2391(84)90417-8

Esimekara, J. F. O., Perez, A., Courvoisier, D. S., & Scolozzi, P. (2022). Dental implants in patients suffering from autoimmune diseases: A systematic critical review. *Journal of Stomatology, Oral and Maxillofacial Surgery*, *123*(5), e464-e473. https://doi.org/10.1016/j.jormas.2022.01.005

Esposito, M., Thomsen, P., Ericson, L. E., & Lekholm, U. (1999). Histopathologic observations on early oral implant failures. *The International Journal of Oral & Maxillofacial Implants*, *14*(6), 798–810.

Es-Souni, M., Es-Souni, M., & Fischer-Brandies, H. (2005). Assessing the biocompatibility of NiTi shape memory alloys used for medical applications. *Analytical and Bioanalytical Chemistry*, *381*(3), 557–567. https://doi.org/10.1007/s00216-004-2888-3

Faeda, R. S., do Nascimento, S. C. S., Santos, P. L., Boeck, R. J., Sartori, R., Margonar, R., & Marcantonio Jr, E. (2019). Human non-decalcified histology of three dental implants 45 months under function—a case report. *International Journal of Implant Dentistry*, *5*(1), 33.

Farronato, D., Manfredini, M., Farronato, M., Pasini, P. M., Orsina, A. A., & Lops, D. (2021). Behavior of soft tissue around platform-switched implants and non-platform-switched implants: A comparative three-year clinical study. *Journal of Clinical Medicine*, *10*(13), 2955. https://doi.org/10.3390/jcm10132955

Farronato, D., Pasini, P. M., Manfredini, M., Scognamiglio, C., Orsina, A. A., & Farronato, M. (2020). Influence of the implant-abutment connection on the ratio between height and thickness of tissues at the buccal zenith: a randomized

controlled trial on 188 implants placed in 104 patients. *BMC Oral Health*, *20*(1), 53. https://doi.org/10.1186/s12903-020-1037-5

Favero, V., Lang, N. P., Favero, R., Antunes, A. A., Salata, L. A., & Botticelli, D. (2016). Sequential morphometric evaluation at UnicCa® and DCD® implant surfaces. An experimental study in the dog. *Clinical Oral Implants Research*, *28*(7), 833–839. https://doi.org/10.1111/clr.12888

Fernández-Formoso, N., Rilo, B., Mora, M., Martínez-Silva, I., & Santana, U. (2011). A paralleling technique modification to determine the bone crest level around dental implants. *Dentomaxillofacial Radiology*, *40*(6), 385–389. https://doi.org/10.1259/dmfr/45365752

Figueira, N., Silva, T. M., Carmezim, M. J., & Fernandes, J. C. S. (2009). Corrosion behaviour of NiTi alloy. *Electrochimica Acta*, *54*(3), 921-926. https://doi.org/10.1016/j.electacta.2008.08.001

Fischer, E. R., Hansen, B. T., Nair, V., Hoyt, F. H., & Dorward, D. W. (2012). Scanning electron microscopy. *Current protocols in microbiology*, *Chapter 2*, Unit2B.2–2B.2. https://doi.org/10.1002/9780471729259.mc02b02s25

Franz-Odendaal, T. A., Hall, B. K., & Witten, P. E. (2005). Buried alive: how osteoblasts become osteocytes. *Developmental dynamics: an official publication of the American Association of Anatomists*, *235*(1), 176–190. https://doi.org/10.1002/dvdy.20603

French, D., Ofec, R., & Levin, L. (2021). Long term clinical performance of 10 871 dental implants with up to 22 years of follow-up: a cohort study in 4247 patients. *Clinical Implant Dentistry and Related Research*, *23*(3), 289-297. https://doi.org/10.1111/cid.12994

Fu, Q., Rahaman, M. N., Bal, B. S., & Brown, R. F. (2009). *In vitro* cellular response to hydroxyapatite scaffolds with oriented pore architectures. *Materials Science and Engineering: C*, *29*(7), 2147–2153. https://doi.org/10.1016/j.msec.2009.04.016

Fuda, S., Martins, B. G. D. S., De Castro, F. C., Heboyan, A., Gehrke, S. A., Fernandes, J. C. H., Mello-Moura, A. C. V., & Fernandes, G. V. O. (2023). Marginal Bone Level and Clinical Parameter Analysis Comparing External Hexagon and morse taper Implants: A Systematic Review and Meta-Analysis. *Diagnostics*, *13*(9), 1587. https://doi.org/10.3390/diagnostics13091587

Gahlert, M., Röhling, S., Wieland, M., Eichhorn, S., Küchenhoff, H., & Kniha, H. (2010). A comparison study of the osseointegration of zirconia and titanium dental implants. A biomechanical evaluation in the maxilla of pigs. *Clinical Implant Dentistry and Related Research*, *12*(4), 297–305. https://doi.org/10.1111/j.1708-8208.2009.00168.x

Gehrke, S. A., Frugis, V. L., Shibli, J. A., Fernandez, M. P. R., De Val, J. E. M. S., Girardo, J. L. C., Taschieri, S., & Corbella, S. (2016). Influence of implant design (Cylindrical and conical) in the load transfer surrounding long (13mm) and short (7mm) length implants: a photoelastic analysis. *The Open Dentistry Journal*, *10*(1), 522–530. https://doi.org/10.2174/1874210601610010522

Gerber, J. A., Tan, W. C., Balmer, T. E., Salvi, G. E., & Lang, N. P. (2008). Bleeding on probing and pocket probing depth in relation to probing pressure and mucosal health around oral implants. *Clinical Oral Implants Research*, *20*(1), 75–78. https://doi.org/10.1111/j.1600-0501.2008.01601.x

Gittens, R. A., Olivares-Navarrete, R., Cheng, A., Anderson, D. M., McLachlan, T., Stephan, I., Geis-Gerstorfer, J., Sandhage, K. H., Fedorov, A. G., Rupp, F., Boyan, B. D., Tannenbaum, R., & Schwartz, Z. (2013). The roles of titanium surface micro/nanotopography and wettability on the differential response of human osteoblast lineage cells. *Acta Biomaterialia*, *9*(4), 6268–6277. https://doi.org/10.1016/j.actbio.2012.12.002

Gölz, L., Knickenberg, A. C., Keilig, L., Reimann, S., Papageorgiou, S. N., Jäger, A., & Bourauel, C. (2016). Nickel ion concentrations in the saliva of patients treated with self-ligating fixed appliances: a prospective cohort study. *Journal of Orofacial Orthopedics/Fortschritte der Kieferorthopädie*, *77*(2), 85–93. https://doi.org/10.1007/s00056-016-0012-x

Gopikrishnan, S., Melath, A., Ajith, V. V., & Mathews, N. B. (2015). A comparative study of bio degradation of various orthodontic arch wires: an *in vitro* study. *Journal of International Oral Health*, *7*(1), 12–17.

Gotman, I., Ben-David, D., Unger, R. E., Böse, T., Gutmanas, E. Y., & Kirkpatrick, C. J. (2013). Mesenchymal stem cell proliferation and differentiation on load-bearing trabecular Nitinol scaffolds. *Acta biomaterialia*, *9*(9), 8440–8448. https://doi.org/10.1016/j.actbio.2013.05.030

Götz, H., Müller, M., Emmel, A., Holzwarth, U., Erben, R., & Stangl, R. (2004). Effect of surface finish on the osseointegration of laser-treated titanium alloy implants.

Biomaterials, *25*(18), 4057–4064. https://doi.org/10.1016/j.biomaterials.2003.11.002

Guabello, G., Zuffetti, F., Ravidà, A., Deflorian, M., Carta, G., Saleh, M. H., ... & Testori, T. (2023). Avoiding implant-related complications in medically compromised patients with or without unhealthy lifestyle/Elevated oxidative stress. *Periodontology 2000*, *92*(1), 329–349. https://doi.org/10.1111/prd.12503

Guo, Y., Klink, A., Fu, C., & Snyder, J. (2013). Machinability and surface integrity of Nitinol shape memory alloy. *CIRP Annals*, *62*(1), 83–86. https://doi.org/10.1016/j.cirp.2013.03.004

Hagler, H., K. (2007). [Ultramicrotomy for biological electron microscopy]. In J. Kuo (Ed.), Electron microscopy: Methods and protocols (2nd ed., pp 67–96). Humana Press.

Hamed, S., Shaaban, A. M., & El-Dibany, R. M. (2020). The effect of deep threads on the stability of dental implants in posterior maxilla. *Alexandria Dental Journal*, *45*(2), 67–73. https://doi.org/10.21608/adjalexu.2020.88440

Hämmerle, C. H., & Tarnow, D. (2018). The etiology of hard-and soft-tissue deficiencies at dental implants: A narrative review. *Journal of Clinical Periodontology*, *45*, S267-S277. https://doi.org/10.1111/jcpe.12955

Hanawa, T. (2019). Titanium–tissue interface reaction and its control with surface treatment. *Frontiers in Bioengineering and Biotechnology*, *7*, 170. https://doi.org/10.3389/fbioe.2019.00170

Hashim, D., & Cionca, N. (2020). A comprehensive review of peri-implantitis risk factors. *Current Oral Health Reports*, *7*(3), 262–273. https://doi.org/10.1007/s40496-020-00274-2

Hayat, M. D., Goswami, A., Matthews, S., Li, T., Yuan, X., & Cao, P. (2017). Modification of PEG/PMMA binder by PVP for titanium metal injection moulding. *Powder Technology*, *315*, 243–249. https://doi.org/10.1016/j.powtec.2017.04.004

Heitz-Mayfield, L. J. A., & Lang, N. P. (2010). Comparative biology of chronic and aggressive periodontitis vs. peri-implantitis. *Periodontology 2000*, *53*(1), 167–181. https://doi.org/10.1111/j.1600-0757.2010.00348.x

Heitz-Mayfield, L. J., & Salvi, G. E. (2018). Peri-implant mucositis. *Journal of Clinical Periodontology*, *45*(S20), S237-S245. https://doi.org/10.1111/jcpe.12953

Hermann, J. S., Buser, D., Schenk, R. K., Higginbottom, F. L., & Cochran, D. L. (2000). Biologic width around titanium implants. A physiologically formed and stable dimension over time. *Clinical oral implants research*, *11*(1), 1–11. https://doi.org/10.1034/j.1600-0501.2000.011001001.x

Hofmann, A. A., Bloebaum, R. D., & Bachus, K. N. (1997). Progression of human bone ingrowth into porous-coated implants: Rate of bone ingrowth in humans. *Acta Orthopaedica Scandinavica*, *68*(2), 161–166. https://doi.org/10.3109/17453679709004000

Hotchkiss, K. M., Clark, N. M., & Olivares-Navarrete, R. (2018). Macrophage response to hydrophilic biomaterials regulates MSC recruitment and T-helper cell populations. *Biomaterials*, *182*, 202–215. https://doi.org/10.1016/j.biomaterials.2018.08.029

https://www.efsa.europa.eu/en/topics/topic/metals-contaminants-food#).

Hyldahl, E., Gotfredsen, K., Pedersen, A. M. L., & Jensen, S. S. (2024). Survival and success of dental implants in patients with autoimmune diseases: a systematic review. *Journal of Oral & Maxillofacial Research*, *15*(1), e1. https://doi.org/10.5037/jomr.2024.15101

Iezzi, G., Zavan, B., Petrini, M., Ferroni, L., Pierfelice, T. V., D'Amora, U., Ronca, A., D'Amico, E., & Mangano, C. (2024). 3D printed dental implants with a porous structure: The *in vitro* response of osteoblasts, fibroblasts, mesenchymal stem cells, and monocytes. *Journal of Dentistry*, *140*, 104778. https://doi.org/10.1016/j.jdent.2023.104778

İleri, S. A., Güntekin, N., & Mohammadi, R. (2025). The Effect of Cantilever Planning on Stress Distribution in Implant-Supported Prostheses. *Journal of Oral Implantology*, *51*(4), 361–369. https://doi.org/10.1563/aaid-joi-d-25-00019

Insua, A., Galindo-Moreno, P., Miron, R. J., Wang, H. L., & Monje, A. (2023). Emerging factors affecting peri-implant bone metabolism. *Periodontology 2000*, *94*(1), 27–78. https://doi.org/10.1111/prd.12532

Ionescu, M., Glodeanu, A. D., Popescu, S. M., Marinescu, I. R., Ionescu, A. G., & Mercut, V. (2022). A brief history of dental implants. *Analele Universitatii Din Craiova - Seria Istorie*, *27*(2), 149–160. https://doi.org/10.52846/AUCSI.2022.2.11

Ismail, M. H., Bram, M., Barbosa, A. C., Koehl, M., Davies, H. A., & Todd, I. (2013). Phase transformation temperatures (PPTs) and microstructure of moulded NiTi

alloy using a water soluble binder system. *Sains Malaysiana*, *42*(12), 1769-1773.

Ismail, M. H., Goodall, R., Davies, H. A., & Todd, I. (2012). Porous NiTi alloy by metal injection moulding/sintering of elemental powders: Effect of sintering temperature. *Materials Letters*, *70*, 142–145. https://doi.org/10.1016/j.matlet.2011.12.008

Ismail, M. H., Razali, R., Abdullah, Z., Subuki, I., & Muhamad, N. (2016). Shape Memory behaviour of NITI alloy produced by MIM using palm stearin based binder. *Advanced Materials Research*, *1133*, 295–299. https://doi.org/10.4028/www.scientific.net/amr.1133.295

Israelson, H., Plemons, J. M., Watkins, P., & Sory, C. (1992). Barium-coated surgical stents and computer-assisted tomography in the preoperative assessment of dental implant patients. *International Journal of Periodontics & Restorative Dentistry*, *12*(1).

Jani, J. M., Leary, M., Subic, A., & Gibson, M. A. (2014). A review of shape memory alloy research, applications and opportunities. *Materials & Design (1980-2015)*, *56*, 1078–1113. https://doi.org/10.1016/j.matdes.2013.11.084

Jansen, V. K., Conrads, G., & Richter, E. J. (1997). Microbial leakage and marginal fit of the implant-abutment interface. *International Journal of Oral & Maxillofacial Implants*, *12*(5), 709.

Januzzi, M. S., Dos Santos, D. M., Rosa, C. D. D. R. D., Turcio, K. H. L., Neto, C. L. D. M. M., da Silva Fernandes, M. E., ... & Goiato, M. C. (2024). The Influence of Genetics and Gene Polymorphism on Biological Complications for Dental Implant Survival: A Review. *European Journal of Dentistry.18*(04): 971-975 https://doi.org/10.1055/s-0044-1787820

Javed, F., & Romanos, G. E. (2010). The role of primary stability for successful immediate loading of dental implants. A literature review. *Journal of dentistry*, *38*(8), 612–620. https://doi.org/10.1016/j.jdent.2010.05.013

Javed, F., Ahmed, H. B., Crespi, R., & Romanos, G. E. (2013). Role of primary stability for successful osseointegration of dental implants: Factors of influence and evaluation. *Interventional Medicine and Applied Science*, *5*(4), 162–167. https://doi.org/10.1556/imas.5.2013.4.3

Javed, F., Almas, K., Crespi, R., & Romanos, G. E. (2011). Implant surface morphology and primary stability: is there a connection? *Implant Dentistry*, *20*(1), 40–46. https://doi.org/0.1097/ID.0b013e31820867da.

Jemt, T. (2019). Implant survival in the posterior partially edentulous arch—30 years of experience. Part IV: A Retro-Prospective Multivariable Regression Analysis on implant failures related to arch and implant surface. *The International Journal of Prosthodontics*, *32*(2), 143–152. https://doi.org/10.11607/ijp.6012

Jemt, T., Olsson, M., Renouard, F., Stenport, V., & Friberg, B. (2016). Early implant failures related to individual surgeons: an analysis covering 11,074 operations performed during 28 years. *Clinical implant dentistry and related research*, *18*(5), 861–872. https://doi.org/10.1111/cid.12379

Jeong, C. G., & Hollister, S. J. (2010). Mechanical and biochemical assessments of three-dimensional poly (1, 8-octanediol-co-citrate) scaffold pore shape and permeability effects on *in vitro* chondrogenesis using primary chondrocytes. *Tissue Engineering Part A*, *16*(12), 3759–3768. https://doi.org/10.1089/ten.TEA.2010.0103

Jian, Y. T., Yang, Y., Tian, T., Stanford, C., Zhang, X. P., & Zhao, K. (2015). Effect of pore size and porosity on the biomechanical properties and cytocompatibility of porous NiTi alloys. *PLoS One*, *10*(6), e0128138. https://doi.org/10.1371/journal.pone.0128138

John, M. T. (2021). Foundations of oral health-related quality of life. *Journal of Oral Rehabilitation*, *48*(3), 355–359.https://doi.org/10.1111/joor.13040

Kandavalli, S. R., Wang, Q., Ebrahimi, M., Gode, C., Djavanroodi, F., Attarilar, S., & Liu, S. (2021). A brief review on the evolution of metallic dental implants: history, design, and application. *Frontiers in Materials*, *8*, 646383. https://doi.org/10.3389/fmats.2021.646383

Kang, D. Y., Kim, M., Lee, S. J., Cho, I. W., Shin, H. S., Caballé-Serrano, J., & Park, J. C. (2019). Early implant failure: a retrospective analysis of contributing factors. *Journal of Periodontal & Implant Science*, *49*(5), 287–298. https://doi.org/10.5051/jpis.2019.49.5.287

Kapanen, A., Ryhänen, J., Danilov, A., & Tuukkanen, J. (2001). Effect of nickel–titanium shape memory metal alloy on bone formation. *Biomaterials*, *22*(18), 2475-2480. https://doi.org/10.1016/s0142-9612(00)00435-x

Kapat, K., Srivas, P. K., Rameshbabu, A. P., Maity, P. P., Jana, S., Dutta, J., ... & Dhara, S. (2017). Influence of porosity and pore-size distribution in Ti6Al4 V foam on physicomechanical properties, osteogenesis, and quantitative validation of bone ingrowth by micro-computed tomography. *ACS applied Materials & Interfaces*, *9*(45), 39235–39248. https://doi.org/10.1021/acsami.7b13960

Karageorgiou, V., & Kaplan, D. (2005). Porosity of 3D biomaterial scaffolds and osteogenesis. *Biomaterials*, *26*(27), 5474–5491. https://doi.org/10.1016/j.biomaterials.2005.02.002

Karazisis, D., Ballo, A. M., Petronis, S., Agheli, H., Emanuelsson, L., Thomsen, P., & Omar, O. (2016). The role of well-defined nanotopography of titanium implants on osseointegration: cellular and molecular events *in vivo*. *International Journal of Nanomedicine*, 1367–1382. https://doi.org/10.2147/IJN.S101294

Karimi, S., & Alfantazi, A. M. (2014). Ion release and surface oxide composition of AISI 316L, Co–28Cr–6Mo, and Ti–6Al–4V alloys immersed in human serum albumin solutions. *Materials Science and Engineering: C*, *40*, 435–444. https://doi.org/10.1016/j.msec.2014.04.007

Karoussis, I. K., Salvi, G. E., Heitz-Mayfield, L. J., Brägger, U., Hämmerle, C. H., & Lang, N. P. (2003). Long-term implant prognosis in patients with and without a history of chronic periodontitis: a 10-year prospective cohort study of the ITI® Dental Implant System. *Clinical Oral Implants Research*, *14*(3), 329–339. https://doi.org/10.1034/j.1600-0501.000.00934.x

Katsoulis, J., Nikitovic, S. G., Spreng, S., Neuhaus, K., & Mericske-Stern, R. (2011). Prosthetic rehabilitation and treatment outcome of partially edentulous patients with severe tooth wear: 3-years results. *Journal of dentistry*, *39*(10), 662–671. https://doi.org/10.1016/j.jdent.2011.07.008

Khushaini, M.A.A., Ahmad, R., (2021). *Investigator's Brochure (NTSB/MD/01-01-IB-01): Porous NiTi Bone Level Dental Implants*, [Unpublished brochure], Nitium Technology Sdn. Bhd.

Kim, D., Kim, K., Ohe, J. Y., Song, S. J., & Paek, J. (2025). Correlation between implant angulation and crestal bone changes: A 5-year retrospective study. *The Journal of Prosthetic Dentistry*, *133*(1), 162.e1-162.e7. https://doi.org/10.1016/j.prosdent.2024.09.015

Kim, J. H., Noh, G., Hong, S. J., & Lee, H. (2020). Biomechanical stress and microgap analysis of bone-level and tissue-level implant abutment structure according to

the five different directions of occlusal loads. *The Journal of Advanced Prosthodontics*, *12*(5), 316–321. https://doi.org/10.4047/jap.2020.12.5.316

Kim, K. S., & Lim, Y. J. (2020). Axial displacements and removal torque changes of five different implant-abutment connections under static vertical loading. *Materials*, *13*(3), 699. https://doi.org/10.3390/ma13030699

Kim, A., Downer, M. A., Berry, C. E., Valencia, C., Fazilat, A. Z., & Griffin, M. (2023). Investigating immunomodulatory biomaterials for preventing the foreign body response. *Bioengineering*, *10*(12), 1411. https://doi.org/10.3390/bioengineering10121411

King, S., Klineberg, I., Levinger, I., & Brennan-Speranza, T. C. (2016). The effect of hyperglycaemia on osseointegration: a review of animal models of diabetes mellitus and titanium implant placement. *Archives of Osteoporosis*, *11*(1), 29. https://doi.org/10.1007/s11657-016-0284-1

Klinge, B., Klinge, A., Bertl, K., & Stavropoulos, A. (2018). Peri-implant diseases. *European Journal of Oral Sciences*, *126*(1), 88–94. https://doi.org/10.1111/eos.12529

Knychala, J., Bouropoulos, N., Catt, C. J., Katsamenis, O. L., Please, C. P., & Sengers, B. G. (2013). Pore geometry regulates early stage human bone marrow cell tissue formation and organisation. *Annals of Biomedical Engineering*, *41*(5), 917–930. https://doi.org/10.1007/s10439-013-0748-z

Koch, F. P., Weng, D., Krämer, S., Biesterfeld, S., Jahn-Eimermacher, A., & Wagner, W. (2010). Osseointegration of one-piece zirconia implants compared with a titanium implant of identical design: a histomorphometric study in the dog. *Clinical Oral Implants Research*, *21*(3), 350–356.

Köhl, M., Habijan, T., Bram, M., Buchkremer, H. P., Stöver, D., & Köller, M. (2009). Powder metallurgical near-net-shape fabrication of porous NiTi shape memory alloys for use as long-term implants by the combination of the metal injection moulding process with the space-holder technique. *Advanced Engineering Materials*, *11*(12), 959–968. https://doi.org/10.1002/adem.200900168

Koo, K. T., Kim, M. H., Kim, H. Y., Wikesjö, U. M., Yang, J. H., & Yeo, I. S. (2015). Effects of implant drill wear, irrigation, and drill materials on heat generation in osteotomy sites. *The Journal of Oral Implantology*, *41*(2), e19–e23. https://doi.org/10.1563/AAID-JOI-D-13-00151

Kotsailidi, E. A., Gagnon, C., Johnson, L., Basir, A. B., & Tsigarida, A. (2023). Association of selective serotonin reuptake inhibitor use with marginal bone level changes around osseointegrated dental implants: A retrospective study. *Journal of Periodontology*, *94*(8), 1008–1017. https://doi.org/10.1002/JPER.22-0690

Kotsakis, G. A., & Romanos, G. E. (2022). Biological mechanisms underlying complications related to implant site preparation. *Periodontology 2000*, *88*(1), 52-63. https://doi.org/10.1111/prd.12410

Koutouzis, T., Koutouzis, G., Tomasi, C., & Lundgren, T. (2011). Immediate loading of implants placed with the osteotome technique: one-year prospective case series. *Journal of Periodontology*, *82*(11), 1556–1562. https://doi.org/10.1902/jop.2011.100751

Krämer, M., Müller, C. W., Hermann, M., Decker, S., Springer, A., Overmeyer, L., Hurschler, C., & Pfeifer, R. (2017). Design considerations for a novel shape-memory-plate osteosynthesis allowing for non-invasive alteration of bending stiffness. *Journal of the mechanical behavior of biomedical materials*, *75*, 558–566. https://doi.org/10.1016/j.jmbbm.2017.08.024

Kreve, S., Ferreira, I., da Costa Valente, M. L., & Dos Reis, A. C. (2024). Relationship between dental implant macro-design and osseointegration: A systematic review. *Oral and Maxillofacial Surgery*, *28*(1), 1–14. https://doi.org/10.1007/s10006-022-01116-4

Kubášová, K., Drátovská, V., Losertová, M., Salvetr, P., Kopelent, M., Kořínek, F., ... & Daniel, M. (2024). A review on additive manufacturing methods for NiTi shape memory alloy production. *Materials*, *17*(6), 1248. https://doi.org/10.3390/ma17061248

Kühne, J. H., Bartl, R., Frisch, B., Hammer, C., Jansson, V., & Zimmer, M. (1994). Bone formation in coralline hydroxyapatite: effects of pore size studied in rabbits. *Acta Orthopaedica Scandinavica*, *65*(3), 246–252. https://doi.org/10.3109/17453679408995448

Kumar, V., Abbas, A. K., & Aster, J. C. Inflammation and repair. In Kumar, V., Abbas, A. K., Aster, J. C., & Deyrup, A. T. (Eds.). (2022). *Robbins & Kumar basic pathology, e-book: Robbins & Kumar Basic Pathology, e-book* (pp. 25–58). Elsevier Health Sciences.

Kurgan, N., & Varol, R. (2010). Mechanical properties of P/M 316L stainless steel materials. *Powder Technology*, *201*(3), 242–247. https://doi.org/10.1016/j.powtec.2010.03.041

Kurtz, S. M., & Devine, J. N. (2007). PEEK biomaterials in trauma, orthopedic, and spinal implants. *Biomaterials*, *28*(32), 4845–4869. https://doi.org/10.1016/j.biomaterials.2007.07.013

Lago, L., Da Silva, L., Martínez-Silva, I., & Rilo, B. (2018). Crestal Bone Level Around Tissue-Level Implants Restored with Platform Matching and Bone-Level Implants Restored with Platform Switching: A 5-Year Randomized Controlled Trial. *The International Journal of Oral & Maxillofacial Implants*, *33*(2), 448–456. https://doi.org/10.11607/jomi.6149

Lammer, J., Bosiers, M., Zeller, T., Schillinger, M., Boone, E., Zaugg, M. J., ... & Schwartz, L. B. (2011). First clinical trial of nitinol self-expanding everolimus-eluting stent implantation for peripheral arterial occlusive disease. *Journal of Vascular Surgery*, *54*(2), 394–401. https://doi.org/10.1016/j.jvs.2011.01.047

Lang, N. P., & Berglundh, T. (2011). Periimplant diseases: where are we now? – Consensus of the Seventh European Workshop on Periodontology. *Journal of Clinical Periodontology*, *38*(s11), 178–181. https://doi.org/10.1111/j.1600-051x.2010.01674.x

Lang, N. P., Salvi, G. E., Huynh-Ba, G., Ivanovski, S., Donos, N., & Bosshardt, D. D. (2011). Early osseointegration to hydrophilic and hydrophobic implant surfaces in humans. *Clinical Oral Implants Research*, *22*(4), 349–356. https://doi.org/10.1111/j.1600-0501.2011.02172.x

Lang, N. P., & Zitzmann, N. U. (2012). Clinical research in implant dentistry: evaluation of implant-supported restorations, aesthetic and patient-reported outcomes. *Journal of Clinical Periodontology*, *39*(s12), 133–138. https://doi.org/10.1111/j.1600-051x.2011.01842.x

Layton, D., & Walton, T. (2011). Patient-evaluated dentistry: development and validation of a patient satisfaction questionnaire for fixed prosthodontic treatment. *International Journal of Prosthodontics*, *24*(4), 332–341.

Lazzara, R. J., & Porter, S. S. (2006). Platform switching: a new concept in implant dentistry for controlling postrestorative crestal bone levels. *International Journal of Periodontics & Restorative Dentistry*, *26*(1), 9–17.

Lee, K. J., Cha, J. K., Sanz-Martin, I., Sanz, M., & Jung, U. W. (2019). A retrospective case series evaluating the outcome of implants with low primary stability. *Clinical Oral Implants Research*, *30*(9), 861–871. https://doi.org/10.1111/clr.13491

Lisowski (n.d). ***Fundamentals of H&E staining***. Knowledge Pathway. Leica Biosystems.

Lemos, C. A., Verri, F. R., de Oliveira Neto, O. B., Cruz, R. S., Gomes, J. M. L., da Silva Casado, B. G., & Pellizzer, E. P. (2021). Clinical effect of the high insertion torque on dental implants: A systematic review and meta-analysis. *The Journal of Prosthetic Dentistry*, *126*(4), 490–496. https://doi.org/10.1016/j.prosdent.2020.06.012

Levin, B. P. (2016). The correlation between immediate implant insertion torque and implant stability quotient. *International Journal of Periodontics & Restorative Dentistry*, *36*(6), 833-840. https://doi.org/10.11607/prd.2865

Li, F., Li, J., Xu, G., Liu, G., Kou, H., & Zhou, L. (2015). Fabrication, pore structure and compressive behavior of anisotropic porous titanium for human trabecular bone implant applications. *Journal of the Mechanical Behavior of Biomedical Materials/Journal of Mechanical Behavior of Biomedical Materials*, *46*, 104–114. https://doi.org/10.1016/j.jmbbm.2015.02.023

Li, D., Ferguson, S. J., Beutler, T., Cochran, D. L., Sittig, C., Hirt, H. P., & Buser, D. (2002). Biomechanical comparison of the sandblasted and acid-etched and the machined and acid-etched titanium surface for dental implants. *Journal of Biomedical Materials Research*, *60*(2), 325–332. https://doi.org/10.1002/jbm.10063

Li, J., Zhang, K., Hu, R., & Yang, J. (2024). Design and microstructure-mechanical properties of a novel metastable β titanium alloy with excellent strength-plasticity matching. *Journal of Materials Research and Technology*, *28*, 4177–4185. https://doi.org/10.1016/j.jmrt.2024.01.041

Li, J., Zhao, J., Xu, Y., Xu, A., & He, F. (2023). Titanium surface interacting with blood clot enhanced migration and osteogenic differentiation of bone marrow mesenchymal stem cells. *Frontiers in Bioengineering and Biotechnology*, *11*, 1136406. https://doi.org/10.3389/fbioe.2023.1136406

Li, Z., Wang, Q., & Liu, G. (2022). A review of 3D printed bone implants. *Micromachines*, *13*(4), 528. https://doi.org/10.3390/mi13040528

Lian, J. B., & Stein, G. S. (1992). Concepts of Osteoblast growth and differentiation: basis for modulation of bone cell development and tissue formation. *Critical Reviews in Oral Biology & Medicine*, *3*(3), 269–305. https://doi.org/10.1177/10454411920030030501

Lim, T. W., & Ariff, T. F. T. M. (2020). Single tooth implant versus resin-bonded bridge: A study of patient's satisfaction. *European Journal of General Dentistry*, *9*(02), 90-95.

Lin, C. Y., Chen, Z., Pan, W. L., & Wang, H. L. (2019). The effect of supportive care in preventing peri-implant diseases and implant loss: A systematic review and meta-analysis. *Clinical oral implants research*, *30*(8), 714–724. https://doi.org/10.1111/clr.13496

Lin, G. H., & Madi, I. M. (2019). Soft-tissue conditions around dental implants: A literature review. *Implant Dentistry*, *28*(2), 138-143.

Lindahl, C., Borchardt, P., Lausmaa, J., Xia, W., & Engqvist, H. (2010). Studies of early growth mechanisms of hydroxyapatite on single crystalline rutile: a model system for bioactive surfaces. *Journal of Materials Science: Materials in Medicine*, *21*(10), 2743–2749. https://doi.org/10.1007/s10856-010-4137-y

Lindhe, J., Meyle, J., & Group D of the European Workshop on Periodontology. (2008). Peri-implant diseases: consensus report of the sixth European workshop on periodontology. *Journal of Clinical Periodontology*, *35*, 282–285. https://doi.org/10.1111/j.1600-051X.2008.01283.x

Linkevicius, T., Apse, P., Grybauskas, S., & Puisys, A. (2010). Influence of thin mucosal tissues on crestal bone stability around implants with platform switching: a 1-year pilot study. *Journal of Oral and Maxillofacial Surgery*, *68*(9), 2272–2277. https://doi.org/10.1016/j.joms.2009.08.018

Linkevicius, T., Puisys, A., Linkeviciene, L., Peciuliene, V., & Schlee, M. (2015). Crestal bone stability around implants with horizontally matching connection after soft tissue thickening: A prospective clinical trial. *Clinical Implant Dentistry and Related Research*, *17*(3), 497–508. https://doi.org/10.1111/cid.12155

Linsley, C. S., Chesnot, P., Shah, K. C., Wu, B. M., Park, J., & Seo, Y. R. (2020). Evaluation of the wear and retention performance of a shape-memory alloy abutment system after 6 months of clinical use. *Journal of Prosthetic Dentistry*, *124*(2), 189–194. https://doi.org/10.1016/j.prosdent.2019.08.025

Liu, K. Y., Yin, L. X., Lin, X., & Liang, S. X. (2022). Development of low elastic modulus titanium alloys as implant biomaterials. *Recent Progress in Materials*, *4*(2), 1-14. https://doi.org/10.21926/rpm.2202008

Liu, S., Tang, C., Yu, J., Dai, W., Bao, Y., & Hu, D. (2014). The effect of platform switching on stress distribution in implants and periimplant bone studied by nonlinear finite element analysis. *Journal of Prosthetic Dentistry*, *112*(5), 1111–1118. https://doi.org/10.1016/j.prosdent.2014.04.017

Liu, T., Chen, Y., Apicella, A., Mu, Z., Yu, T., Huang, Y., & Wang, C. (2020). Effect of porous microstructures on the biomechanical characteristics of a root analogue implant: an animal study and a finite element analysis. *ACS biomaterials science & engineering*, *6*(11), 6356–6367. https://doi.org/10.1021/acsbiomaterials.0c01096

Liu, Y., & Wang, J. (2017). Influences of microgap and micromotion of implant–abutment interface on marginal bone loss around implant neck. *Archives of oral biology*, *83*, 153–160. https://doi.org/10.1016/j.archoralbio.2017.07.022

Locker, D., & Allen, F. (2007). What do measures of 'oral health-related quality of life'measure?. *Community dentistry and oral epidemiology*, *35*(6), 401–411. https://doi.org/10.1111/j.1600-0528.2007.00418.x

Lojen, G., Stambolić, A., Šetina Batič, B., & Rudolf, R. (2020). Experimental continuous casting of nitinol. *Metals*, *10*(4), 505. https://doi.org/10.3390/met10040505

Lossdörfer, S., Schwartz, Z., Wang, L., Lohmann, C. H., Turner, J. D., Wieland, M., Cochran, D. L., & Boyan, B. D. (2004). Microrough implant surface topographies increase osteogenesis by reducing osteoclast formation and activity. *Journal of Biomedical Materials Research. Part A*, *70*(3), 361–369. https://doi.org/10.1002/jbm.a.30025

Lumbikananda, S., Srithanyarat, S. S., Mattheos, N., & Osathanon, T. (2024). Oral fluid biomarkers for peri-implantitis: A scoping review. *International Dental Journal*, *74*(3), 387–402. https://doi.org/10.1016/j.identj.2023.11.005

M EL-Zawahry, M., I EL-Anwar, M., S EL-Mofty, M., F EL-Ragi, A., R Moussa, A., S ElGabry, H., & M Shebaita, A. (2016). Implant angulations effect on bone stresses: Clinical and FEA study. *Research Journal of Pharmaceutical, Biological and Chemical Sciences, 7*(3), 2448-2454

Macedo, J. P., Pereira, J., Faria, J., Souza, J. C., Alves, J. L., López-López, J., & Henriques, B. (2018). Finite element analysis of peri-implant bone volume affected by stresses around Morse taper implants: effects of implant positioning to the bone crest. *Computer Methods in Biomechanics and Biomedical Engineering*, *21*(12), 655–662. https://doi.org/10.1080/10255842.2018.1507025

Maceiras, L., Liñares, A., Nóvoa, L., Batalla, P., Mareque, S., Pérez, J., & Blanco, J. (2024). Marginal changes at bone-level implants supporting dental prostheses with or without intermediate standardised abutments after 36 months: Randomised controlled clinical trial. *Clinical Oral Implants Research*, *35*(9), 1072-1080. https://doi.org/10.1111/clr.14297

Mahtabi, M. J., Shamsaei, N., & Rutherford, B. (2015). Mean strain effects on the fatigue behavior of superelastic nitinol alloys: An experimental investigation. *Procedia Engineering*, *133*, 646–654. https://doi.org/10.1016/j.proeng.2015.12.645

Makary, C., Menhall, A., Zammarie, C., Lombardi, T., Lee, S. Y., Stacchi, C., & Park, K. B. (2019). Primary stability optimization by using fixtures with different thread depth according to bone density: A clinical prospective study on early loaded implants. *Materials*, *12*(15), 2398. https://doi.org/10.3390/ma12152398

Malm, M. O., Jemt, T., & Stenport, V. (2018). Early implant failures in edentulous patients: a multivariable regression analysis of 4615 consecutively treated jaws. A retrospective study. *Journal of Prosthodontics*, *27*(9), 803–812. https://doi.org/10.1111/jopr.12985

Manfredini, M., Pellegrini, M., Rigoni, M., Veronesi, V., Beretta, M., Maiorana, C., & Poli, P. P. (2024). Oral health-related quality of life in implant-supported rehabilitations: a prospective single-center observational cohort study. *BMC Oral Health*, *24*(1), 531. https://doi.org/10.1186/s12903-024-04265-y

Mangano, C., Mangano, F. G., Shibli, J. A., Roth, L. A., d'Addazio, G., Piattelli, A., & Iezzi, G. (2018). Immunohistochemical evaluation of peri-implant soft tissues around machined and direct metal laser sintered (DMLS) healing abutments in humans. *International Journal of Environmental Research and Public Health*, *15*(8), 1611. https://doi.org/10.3390/ijerph15081611

Mangano, C., Mangano, F., Gobbi, L., Admakin, O., Iketani, S., & Giuliani, A. (2019). Comparative study between laser light stereo-lithography 3D-printed and

traditionally sintered biphasic calcium phosphate scaffolds by an integrated morphological, morphometric and mechanical analysis. *International Journal of Molecular Sciences*, *20*(13), 3118. https://doi.org/10.3390/ijms20133118

Mangano, F., Raspanti, M., Maghaireh, H., & Mangano, C. (2017). Scanning electron microscope (SEM) evaluation of the interface between a nanostructured calcium-incorporated dental implant surface and the human bone. *Materials*, *10*(12), 1438. https://doi.org/10.3390/ma10121438

Mangano, F. G., Iezzi, G., Shibli, J. A., Pires, J. T., Luongo, G., Piattelli, A., & Mangano, C. (2017). Early bone formation around immediately loaded implants with nanostructured calcium-incorporated and machined surface: a randomized, controlled histologic and histomorphometric study in the human posterior maxilla. *Clinical oral investigations*, *21*(8), 2603–2611. https://doi.org/10.1007/s00784-017-2061-y

Manzano-Moreno, F. J., Herrera-Briones, F. J., Bassam, T., Vallecillo-Capilla, M. F., & Reyes-Botella, C. (2015). Factors affecting dental implant stability measured using the ostell mentor device: A systematic review. *Implant Dentistry*, *24*(5), 565–577. https://doi.org/10.1097/ID.0000000000000308

Marconcini, S., Giammarinaro, E., Toti, P., Alfonsi, F., Covani, U., & Barone, A. (2018). Longitudinal analysis on the effect of insertion torque on delayed single implants: A 3-year randomized clinical study. *Clinical Implant Dentistry and Related Research*, *20*(3), 322–332. https://doi.org/10.1111/cid.12586

Marković, A., Ćalasan, D., Čolić, S., Stojčev-Stajčić, L., Janjić, B., & Mišić, T. (2011). Implant stability in posterior maxilla: bone-condensing versus bone-drilling: a clinical study. *Oral Surgery, Oral Medicine, Oral Pathology, Oral Radiology, and Endodontology*, *112*(5), 557-563. https://doi.org/10.1016/j.tripleo.2010.11.010

Marquezan, M., Osório, A., Sant'Anna, E., Souza, M. M., & Maia, L. (2012). Does bone mineral density influence the primary stability of dental implants? A systematic review. *Clinical Oral Implants Research*, *23*(7), 767–774. https://doi.org/10.1111/j.1600-0501.2011.02228.x

Marshall, G., Canullo, L., Logan, R. M., & Rossi-Fedele, G. (2019). Histopathological and microbiological findings associated with retrograde peri-implantitis of extra-radicular endodontic origin: a systematic and critical review. *International*

Journal of Oral and Maxillofacial Surgery, *48*(11), 1475-1484. https://doi.org/10.1016/j.ijom.2019.04.012

Masccorro, J. A., Bozzolo, J. J. (2007). [Proessing biological tissues for ultrastrutural study] In J. Kuo (Ed.), Electron microscopy: Methods and protocols (2nd ed.,pp 35–46). Humana Press.

Maso'od, M., Ismail, M. H., Razali, R., & Subuki, I. (2018). Effect of sintering temperatures on microstructural changes and phase transformation of nearly equiatomic microporous NiTi alloy produced by metal injection moulding. *Journal of Mechanical Engineering (JMechE)*, (6), 115-126.

Mavrogenis, A. F., Dimitriou, R., Parvizi, J., & Babis, G. C. (2009). Biology of implant osseointegration. *Journal of Musculoskeletal Neuronal Interaction*, *9*(2), 61–71.

McNeese, M. D., Lagoudas, D. C., & Pollock, T. C. (2000). Processing of TiNi from elemental powders by hot isostatic pressing. *Materials Science and Engineering: A*, *280*(2), 334–348. https://doi.org/10.1016/S0921-5093(99)00550-X

Mediaswanti, K., Wen, C. E., Ivanova, E. P., Malherbe, F., Berndt, C. C., Pham, V. T. H., & Wang, J. (2014). Biomimetic creation of surfaces on porous titanium for biomedical applications. *Advanced Materials Research*, *896*, 259–262. https://doi.org/10.4028/www.scientific.net/AMR.896.259

Menini, M., Bagnasco, F., Calimodio, I., Di Tullio, N., Delucchi, F., Baldi, D., & Pera, F. (2020). Influence of implant thread morphology on primary stability: A prospective clinical study. *BioMed Research International*, *2020*(1), 6974050. https://doi.org/10.1155/2020/6974050

Meredith, N. (1998). Assessment of implant stability as a prognostic determinant. *International Journal of Prosthodontics*, *11*(5), 491–501.

Milošev, I., & Kapun, B. (2012). The corrosion resistance of Nitinol alloy in simulated physiological solutions: Part 1: The effect of surface preparation. *Materials Science and Engineering: C*, *32*(5), 1087–1096. https://doi.org/10.1016/j.msec.2011.11.007

Ministry of Health. Oral Health Programme. National Oral Health Plan for Malaysia 2022-2030.

Misch, C. (2008). Implant body size: A biomechanical and esthetic rationale. *Contemporary Implant Dentistry*, *3*, 160–177.

Mishra, S. K., Gaddale, R., Sonnahalli, N. K., & Chowdhary, R. (2021). Platform-Switching Concept in Dental Implants: A Systematic Review and Meta-analysis of Randomized Controlled Trials with a Minimum Follow-up of 3 Years. *International Journal of Oral & Maxillofacial Implants*, *36*(5), e97-e109. https://doi.org/10.11607/jomi.8911

Mohajerani, H., Roozbayani, R., Taherian, S., & Tabrizi, R. (2017). The risk factors in early failure of dental implants: a retrospective study. *Journal of Dentistry*, *18*(4), 298.

Mohseni, P., Soufi, A., & Chrcanovic, B. R. (2024). Clinical outcomes of zirconia implants: a systematic review and meta-analysis. In *Clinical Oral Investigations* (Vol. 28, Issue 1). Springer Science and Business Media Deutschland GmbH. https://doi.org/10.1007/s00784-023-05401-8

Mombelli, A., & Lang, N. P. (1998). The diagnosis and treatment of peri-implantitis. *Periodontology 2000*, *17*(1), 63–76. https://doi.org/10.1111/j.1600-0757.1998.tb00124.x

Mombelli, A., Hashim, D., & Cionca, N. (2018). What is the impact of titanium particles and biocorrosion on implant survival and complications? A critical review. *Clinical Oral Implants Research*, *29*, 37–53. https://doi.org/10.1111/clr.13305

Monje, A., & Salvi, G. E. (2024). Diagnostic methods/parameters to monitor peri-implant conditions. *Periodontology 2000*, *95*(1), 20–39. https://doi.org/10.1111/prd.12584

Monje, A., Amerio, E., Farina, R., Nart, J., Ramanauskaite, A., Renvert, S., Roccuzzo, A., Salvi, G. E., Schwarz, F., Trombelli, L., & Wang, H. L. (2021). Significance of probing for monitoring peri-implant diseases. *International journal of oral implantology (Berlin, Germany)*, *14*(4), 385–399..

Monje, A., Catena, A., & Borgnakke, W. S. (2017). Association between diabetes mellitus/hyperglycaemia and peri-implant diseases: systematic review and meta-analysis. *Journal of Clinical Periodontology*, *44*(6), 636–648. https://doi.org/10.1111/jcpe.12724

Monje, A., Insua, A., & Wang, H. L. (2019). Understanding peri-implantitis as a plaque-associated and site-specific entity: on the local predisposing factors. *Journal of Clinical Medicine*, *8*(2), 279. https://doi.org/10.1111/jcpe.12724

Monje, A., Kan, J. Y., & Borgnakke, W. (2023). Impact of local predisposing/precipitating factors and systemic drivers on peri-implant diseases. *Clinical Implant Dentistry and Related Research*, *25*(4), 640–660. https://doi.org/10.1111/cid.13155

Morgan, N. B. (2004). Medical shape memory alloy applications—the market and its products. *Materials Science and Engineering: A*, *378*(1-2), 16–23.

Morris, H. F., Ochi, S., & Winkler, S. (2000). Implant survival in patients with type 2 diabetes: placement to 36 months. *Annals of Periodontology*, *5*(1), 157–165. https://doi.org/10.1902/annals.2000.5.1.157

Mour, M., Das, D., Winkler, T., Hoenig, E., Mielke, G., Morlock, M. M., & Schilling, A. F. (2010). Advances in porous biomaterials for dental and orthopaedic applications. *Materials*, *3*(5), 2947–2974.

Mudjari, S., Achmad, H., Erwansyah, E., Sabir, A., & Riuwpassa, I. E. (2019). Analysis of nickel and chromium levels in the gingival crevicular fluid and hair of patients treated with fixed orthodontic appliances: a longitudinal study. *Journal of International Dental and Medical Research*, *12*(1), 151-155.

Murray, J. L. Ni-Ti (Nickel-Titanium), in Massalski TB, Okamoto H, Subramanian PR, Kacprzak, L. Binary alloy phase diagrams. ASM International Materials Park, Ohio, pp.2874.

Mustafa, N. W. N. A., Ahmad, R., Ahmad Khushaini, M. A., Kamar Affendi, N. H., Ab Ghani, S. M., Tan, S. K., Ismail, M. H., Goo, C. L., Kassim, M. Z., Lim, T. W., & Teh, L. K. (2024). Porous NiTi Dental Implant Fabricated by a Metal Injection Molding: An *in Vivo* Biocompatibility Evaluation in an Animal Model. *ACS Biomaterials Science and Engineering*, *10*(1), 405–419. https://doi.org/10.1021/acsbiomaterials.3c01551

National Center for Biotechnology Information (2025). PubChem Compound Summary for CID 23963, Titanium. Retrieved November 23, 2025, from https://pubchem.ncbi.nlm.nih.gov/compound/Titanium.

Mustafa, N. W. N. A., Ahmad, R., Kamar Affendi, N. H., Sulaiman, E., Khushaini, M. A. A., Ismail, M. H., Teh, L. K., & Salleh, M. Z. (2024). *In vitro* evaluation of cytotoxicity and genotoxicity of porous nickel titanium dental implants produced by metal injection molding technique. *Journal of Biomedical Materials Research Part B: Applied Biomaterials*, *112*(1). https://doi.org/10.1002/jbm.b.35306

Nagaraja, S., Sullivan, S. J., Stafford, P. R., Lucas, A. D., & Malkin, E. (2018). Impact of nitinol stent surface processing on in-vivo nickel release and biological response. *Acta Biomaterialia*, *72*, 424–433. https://doi.org/10.1016/j.actbio.2018.03.036

Nakaş, G. İ., Dericioglu, A. F., & Bor, Ş. (2011). Fatigue behavior of TiNi foams processed by the magnesium space holder technique. *Journal of the Mechanical Behavior of Biomedical Materials*, *4*(8), 2017-2023. https://doi.org/10.1016/j.jmbbm.2011.06.021

Navratilova P, Vejvodova M, Vaculovic T, Slaninova I, Emmer J, Tomas T, Ryba L, Burda J, Pavkova Goldbergova M. (2024). Cytotoxic effects and comparative analysis of Ni ion uptake by osteoarthritic and physiological osteoblasts. *Scientific Reports, 14*(1):16133. https://doi.org/10.1038/s41598-024-67157-9

Neto, F. C., Giaretton, M. V., Neves, G. O., Aguilar, C., Tramontin Souza, M., Binder, C., & Klein, A. N. (2022). An Overview of Highly Porous Titanium Processed via Metal Injection Molding in Combination with the Space Holder Method. Metals, 12(5), 783. https://doi.org/10.3390/met12050783

Neugebauer, J., Traini, T., Thams, U., Piattelli, A., & Zöller, J. E. (2006). Peri-implant bone organization under immediate loading state. Circularly polarized light analyses: A minipig study. *Journal of Periodontology*. 77, 152–160. https://doi.org/10.1902/jop.2006.040360

Niinomi, M., & Nakai, M. (2011). Titanium-based biomaterials for preventing stress shielding between implant devices and bone. *International Journal of Biomaterials*, *2011*, 836587. https://doi.org/10.1155/2011/836587

Norton, M. R. (2017). The Influence of Low Insertion Torque on Primary Stability, Implant Survival, and Maintenance of Marginal Bone Levels: A Closed-Cohort Prospective Study. *International Journal of Oral & Maxillofacial Implants*, *32*(4).

Noskovicova, N., Hinz, B., & Pakshir, P. (2021). Implant fibrosis and the underappreciated role of myofibroblasts in the foreign body reaction. *Cells*, *10*(7), 1794. https://doi.org/10.3390/cells10071794

Olivares-Navarrete, R., Hyzy, S. L., Pan, Q., Dunn, G., Williams, J. K., Schwartz, Z., & Boyan, B. D. (2015). Osteoblast maturation on microtextured titanium involves paracrine regulation of bone morphogenetic protein signaling. *Journal*

of Biomedical Materials Research Part A, *103*(5), 1721-1731. https://doi.org/10.1002/jbm.a.35308

Olivé, J., & Aparicio, C. (1990). The periotest method as a measure of osseointegrated oral implant stability. *International Journal of Oral & Maxillofacial Implants*, *5*(4).

Oliveira, J. A., de Oliveira Alves, R., Nascimento, I. M., Hidalgo, M. A. R., Scarel-Caminaga, R. M., & Cristina Pigossi, S. (2023). Pro-and anti-inflammatory cytokines and osteoclastogenesis-related factors in peri-implant diseases: systematic review and meta-analysis. *BMC Oral Health*, *23*(1), 420. https://doi.org/10.1186/s12903-023-03072-1

Olmedo-Gaya, M. V., Romero-Olid, M. N., Ocaña-Peinado, F. M., Vallecillo-Rivas, M., Vallecillo, C., & Reyes-Botella, C. (2023). Influence of different surgical techniques on primary implant stability in the posterior maxilla: A randomized controlled clinical trial. *Clinical Oral Investigations*, *27*(7), 3499–3508. https://doi.org/10.1007/s00784-023-04962-y

Orlandi, M., Pranno, N., Patel, V., Papi, P., Di Murro, B., Pompa, G., Polimeni, A., Letizia, C., Suvan, J., & D'Aiuto, F. (2024). Peri-implant diseases and systemic inflammation: A preliminary analysis from a cross-sectional survey of patients with hypertension. *Journal of Periodontology*, *95*(6), 525–534. https://doi.org/10.1002/JPER.21-0338

United States Government. Centers for Disease Control and Prevention. (2024, October). Oral Health Surveillance Report: Selected Findings. https://www.cdc.gov/oral-health/php/2024-oral-health-surveillance-report/selected-findings.html

Oskouei, A. B., Golkar, M., Badkoobeh, A., Jahri, M., Sadeghi, H. M. M., Mohammadikhah, M., ... & Alam, M. (2023). Investigating the effect of insertion torque on marginal bone loss around dental implants. *Journal of Stomatology, Oral and Maxillofacial Surgery*, *124*(6), 101523. https://doi.org/10.1016/j.jormas.2023.101523

Osman, R. B., & Swain, M. V. (2015). A Critical Review of Dental Implant Materials with an Emphasis on Titanium *versus* Zirconia. *Materials (Basel, Switzerland)*, *8*(3), 932–958. https://doi.org/10.3390/ma8030932

Östman, P. O., Wennerberg, A., Ekestubbe, A., and Albrektsson, T. (2013). Immediate occlusal loading of NanoTite^{TM} tapered implants: a prospective 1-year clinical

and radiographic study. *Clinical implant dentistry and related research* 15, 809–818. https://doi.org/10.1111/j.1708-8208.2011.00437.x

O'Sullivan, D., Sennerby, L., & Meredith, N. (2000). Measurements comparing the initial stability of five designs of dental implants: a human cadaver study. *Clinical Implant Dentistry and Related Research*, *2*(2), 85–92. https://doi.org/10.1111/j.1708-8208.2000.tb00110.x

Otomo-Corgel, J. (2012). Osteoporosis and osteopenia: implications for periodontal and implant therapy. *Periodontology 2000*, *59*(1), 111–139. https://doi.org/10.1111/j.1600-0757.2011.00435.x

Otsuki, B., Takemoto, M., Fujibayashi, S., Neo, M., Kokubo, T., & Nakamura, T. (2006). Pore throat size and connectivity determine bone and tissue ingrowth into porous implants: three-dimensional micro-CT based structural analyses of porous bioactive titanium implants. *Biomaterials*, *27*(35), 5892–5900. https://doi.org/10.1016/j.biomaterials.2006.08.013

Ottoni, J. M. P., Oliveira, Z. F. L., Mansini, R., & Cabral, A. M. (2005). Correlation between placement torque and survival of single-tooth implants. *International Journal of Oral & Maxillofacial Implants*, *20*(5), 769-776

Padhye, N. M., Bhange, P. D., Mehta, L. K., & Khimani, S. M. (2019). Patient awareness and perceived cost of dental implants for replacement of missing teeth: A survey in an Indian metropolitan population. *Journal of Dental Implants*, *9*(1), 30–36.

Palmquist, A., Omar, O. M., Esposito, M., Lausmaa, J., & Thomsen, P. (2010). Titanium oral implants: surface characteristics, interface biology and clinical outcome. *Journal of the Royal Society Interface*, *7*(suppl_5), S515-S527. https://doi.org/10.1098/rsif.2010.0118.focus

Papaspyridakos, P., Chen, C. J., Singh, M., Weber, H. P., & Gallucci, G. (2012). Success criteria in implant dentistry: a systematic review. *Journal of Dental Research*, *91*(3), 242–248. https://doi.org/10.1177/0022034511431252

Payo-Ollero, J., Casajús-Ortega, A., Llombart-Blanco, R., Villas, C., & Alfonso, M. (2019). The efficacy of an intramedullary nitinol implant in the correction of claw toe or hammertoe deformities. *Archives of orthopaedic and trauma surgery*, *139*(12), 1681–1690. https://doi.org/10.1007/s00402-019-03203-w

Pellicer-Chover, H., Peñarrocha-Diago, M., Aloy-Prosper, A., Canullo, L., Peñarrocha-Diago, M., & Peñarrocha-Oltra, D. (2019). Does apico-coronal implant position

influence peri-implant marginal bone loss? A 36-month follow-up randomized clinical trial. *Journal of Oral and Maxillofacial Surgery*, *77*(3), 515–527. https://doi.org/10.1016/j.joms.2018.11.002

Piattelli, A., Scarano, A., & Piattelli, M. (1998). Histologic observations on 230 retrieved dental implants: 8 years' experience (1989–1996). *Journal of periodontology*, *69*(2), 178-184.

Piatnitskaia, S., Rafikova, G., Bilyalov, A., Chugunov, S., Akhatov, I., Pavlov, V., & Kzhyshkowska, J. (2024). Modelling of macrophage responses to biomaterials in vitro: state-of-the-art and the need for the improvement. *Frontiers in Immunology*, *15*, 1349461. https://doi.org/10.3389/fimmu.2024.1349461

Piattelli, A., Piattelli, M., Mangano, C., & Scarano, A. (1998). A histologic evaluation of eight cases of failed dental implants: Is bone overheating the most probable cause?. *Biomaterials*, *19*(7-9), 683–690. https://doi.org/10.1016/S0142-9612(97)00172-5

Pilliar. (2009). *Biomedical Materials* (R. Narayan, Ed.). Springer US. https://doi.org/10.1007/978-0-387-84872-3

Pjetursson, B. E., Brägger, U., Lang, N. P., & Zwahlen, M. (2007). Comparison of survival and complication rates of tooth-supported fixed dental prostheses (FDPs) and implant-supported FDPs and single crowns (SCs). *Clinical Oral Implants Research*, *18*(SUPPL. 3), 97–113. https://doi.org/10.1111/j.1600-0501.2007.01439.x

Pjetursson, B. E., Zwahlen, M., & Lang, N. P. (2012). Quality of reporting of clinical studies to assess and compare performance of implant-supported restorations. *Journal of Clinical Periodontology*, *39*, 139–159. https://doi.org/10.1111/j.1600-051X.2011.01828.x

Pokrowiecki, R., Mielczarek, A., Zaręba, T., & Tyski, S. (2017). Oral microbiome and peri-implant diseases: where are we now?. *Therapeutics and clinical risk management*, 1529-1542. https://doi.org/10.2147/TCRM.S139795

Prasad, S., Ehrensberger, M., Gibson, M. P., Kim, H., & Monaco, E. A. (2015). Biomaterial properties of titanium in dentistry. *Journal of Oral Biosciences 57*(4), 192–199). https://doi.org/10.1016/j.job.2015.08.001

Puisys, A., Janda, M., Auzbikaviciute, V., Gallucci, G. O., & Mattheos, N. (2023). Contour angle and peri-implant tissue height: Two interrelated features of the

implant supracrestal complex. *Clinical and Experimental Dental Research*, *9*(3), 418–424. https://doi.org/10.1002/cre2.731

Puleo, D. A., & Nanci, A. (1999). Understanding and controlling the bone–implant interface. *Biomaterials*, *20*(23-24), 2311-2321. https://doi.org/10.1016/s0142-9612(99)00160-x

Qian, J., Wennerberg, A., & Albrektsson, T. (2012). Reasons for marginal bone loss around oral implants. *Clinical Implant Dentistry and Related Research*, *14*(6), 792–807. https://doi.org/10.1111/cid.12014

Quirynen, M., & Van Assche, N. (2012). RCT comparing minimally with moderately rough implants. Part 2: microbial observations. *Clinical Oral Implants Research. 23*(5), 625–634. http://doi.org/10.1111/j.1600-0501.2011.02255.x

Radi, I. A. W., Ibrahim, W., Iskandar, S. M., & AbdelNabi, N. (2018). Prognosis of dental implants in patients with low bone density: A systematic review and meta-analysis. *The Journal of prosthetic dentistry*, *120*(5), 668–677.

Raes, F., Cosyn, J., & De Bruyn, H. (2013). Clinical, aesthetic, and patient-related outcome of immediately loaded single implants in the anterior maxilla: a prospective study in extraction sockets, healed ridges, and grafted sites. *Clinical Implant Dentistry and Related Research*, *15*(6), 819–835. https://doi.org/10.1111/j.1708-8208.2011.00438.x

Rahimi, S. N. (2023). Three-dimensional radiographic and histologic assessment of bone ingrowth into porous nickel-titanium dental implant. [Unpublished PhD thesis]. Universiti Teknologi MARA.

Raines, A. L., Berger, M. B., Patel, N., Hyzy, S. L., Boyan, B. D., & Schwartz, Z. (2019). VEGF-A regulates angiogenesis during osseointegration of Ti implants via paracrine/autocrine regulation of osteoblast response to hierarchical microstructure of the surface. *Journal of Biomedical Materials Research Part A*, *107*(2), 423–433. https://doi.org/10.1002/jbm.a.36559

Rakic, M., Struillou, X., Petkovic-Curcin, A., Matic, S., Canullo, L., Sanz, M., & Vojvodic, D. (2014). Estimation of bone loss biomarkers as a diagnostic tool for peri-implantitis. *Journal of Periodontology*, *85*(11), 1566–1574. https://doi.org/10.1902/jop.2014.140069

Ramanauskaite, A., Becker, K., & Schwarz, F. (2018). Clinical characteristics of peri-implant mucositis and peri-implantitis. *Clinical Oral Implants Research*, *29*(6), 551–556. https://doi.org/10.1111/clr.13152

Ran, Q., Yang, W., Hu, Y., Shen, X., Yu, Y., Xiang, Y., & Cai, K. (2018). Osteogenesis of 3D printed porous Ti6Al4V implants with different pore sizes. *Journal of the Mechanical Behavior of Biomedical Materials*, *84*, 1–11. https://doi.org/10.1016/j.jmbbm.2018.04.010

Ravidà, A., Arena, C., Tattan, M., Caponio, V. C. A., Saleh, M. H., Wang, H. L., & Troiano, G. (2022). The role of keratinized mucosa width as a risk factor for peri-implant disease: A systematic review, meta-analysis, and trial sequential analysis. *Clinical Implant Dentistry and Related Research*, *24*(3), 287–300. https://doi.org/10.1111/cid.13080

Révész, P., Szanyi, I., Ráth, G., Bocskai, T., Lujber, L., Piski, Z., ... & Gerlinger, I. (2016). Comparison of hearing results following the use of NiTiBOND versus Nitinol prostheses in stapes surgery: a retrospective controlled study reporting short-term postoperative results. *European Archives of Oto-Rhino-Laryngology*, *273*(5), 1131-1136.

Rhalmi, S., Odin, M., Assad, M., Tabrizian, M., Rivard, C. H., & Yahia, L. H. (1999). Hard, soft tissue and *in vitro* cell response to porous nickel-titanium: A biocompatibility evaluation. *Bio-medical Materials and Engineering*, *9*(3), 151–162.

Ríos-Osorio, N., Ladino, L. G., & Guerrero-Torres, M. (2025). Structure, biology, and function of peri-implant soft tissues in health and disease: a comprehensive review of the literature. *Journal of Periodontal & Implant Science*, *55*.

Rocci, A., Rocci, M., Rocci, C., Scoccia, A., Gargari, M., Martignoni, M., et al. (2013). Immediate loading of Brånemark system TiUnite and machined-surface implants in the posterior mandible, part II: A randomized open-ended 9-year follow-up clinical trial. *International Journal of Oral Maxillofacial. Implants* 28, 891–895. http://doi.org/10.11607/jomi.2397

Rocha-Singh, K. J., Jaff, M., Joye, J., Laird, J., Ansel, G., Schneider, P., & VIVA Physicians. (2012). Major adverse limb events and wound healing following infrapopliteal artery stent implantation in patients with critical limb ischemia: the XCELL trial. *Catheterization and Cardiovascular Interventions*, *80*(6), 1042–1051. https://doi.org/10.1002/ccd.24485

Rodrigo, D., Aracil, L., Martin, C., & Sanz, M. (2010). Diagnosis of implant stability and its impact on implant survival: a prospective case series study. *Clinical oral*

implants research, *21*(3), 255–261. https://doi.org/10.1111/j.1600-0501.2009.01820.x

Romeo, E., Lops, D., Margutti, E., Ghisolfi, M., Chiapasco, M., & Vogel, G. (2004). Long-term survival and success of oral implants in the treatment of full and partial arches: a 7-year prospective study with the ITI dental implant system. *International Journal of Oral & Maxillofacial Implants*, *19*(2), 247–259.

Rompen, E. (2012). The impact of the type and configuration of abutments and their (repeated) removal on the attachment level and marginal bone. *European Journal of Oral Implantology*, *5 Suppl*, S83–S90.

Roosli, C., Schmid, P., & Huber, A. M. (2011). Biocompatibility of nitinol stapes prosthesis. *Otology & Neurotology*, *32*(2), 265–270.

Rossi, A. L., Moscone, S., Arcari, M., & Tagliatesta, L. (2021). The role of the implant-prosthetic connection in peri-implant tissue stability: AnyRidge BLUEDIAMOND® (Megagen, South Korea). *International Journal of Future Dentistry.1*(2), 28-36

Rossi, F., Lang, N. P., De Santis, E., Morelli, F., Favero, G., & Botticelli, D. (2014). Bone-healing pattern at the surface of titanium implants: An experimental study in the dog. *Clinical Oral Implants Research*, *25*(1), 124–131.

Rupp, F., Liang, L., Geis-Gerstorfer, J., Scheideler, L., & Hüttig, F. (2018). Surface characteristics of dental implants: A review. *Dental materials*, *34*(1), 40-57.

Rupp, F., Scheideler, L., Olshanska, N., de Wild, M., Wieland, M., & Geis-Gerstorfer, J. (2006). Enhancing surface free energy and hydrophilicity through chemical modification of microstructured titanium implant surfaces. *Journal of Biomedical Materials Research Part A*, *76*(2), 323–334. https://doi.org/10.1002/jbm.a.30518

Ryu, H. S., Namgung, C., Lee, J. H., & Lim, Y. J. (2014). The influence of thread geometry on implant osseointegration under immediate loading: a literature review. *Journal of Advanced Prosthodontics*, *6*(6), 547–554. https://doi.org/10.4047/jap.2014.6.6.547

Saad, N. A., Omar, N. I., Yaziz, Y. A., & Manab, E. E. A. (2023). Patients' satisfaction and quality of life after dental implant rehabilitation: A cross-sectional study. *IIUM Journal of Orofacial and Health Sciences*, *4*(1), 47–58.

Safranski, D., Dupont, K., & Gall, K. (2020). Pseudoelastic NiTiNOL in Orthopaedic Applications. *Shape Memory and Superelasticity*, *6*(3), 332–341.

Salvi, G. E., Bosshardt, D. D., Lang, N. P., Abrahamsson, I., Berglundh, T., Lindhe, J., ... & Donos, N. (2015). Temporal sequence of hard and soft tissue healing around titanium dental implants. *Periodontology 2000*, *68*(1), 135-152. https://doi.org/10.1111/prd.12054

Samara, W., Moztarzadeh, O., Hauer, L., & Babuska, V. (2024). Dental implant placement in medically compromised patients: a literature review. *Cureus*, *16*(2), e54199. https://doi.org/10.7759/cureus.54199

Sanichem Resources Sdn. Bhd. (2022). Certificate of analysis (SCR0456/22) for Nitium Technology Sdn. Bhd.

Sarfaraz, H., Johri, S., Sucheta, P., & Rao, S. (2018). Study to assess the relationship between insertion torque value and implant stability quotient and its influence on timing of functional implant loading. *Journal of Indian Prosthodontic Society*, *18*(2), 139–146. https://doi.org/10.4103/jips.jips_203_17

Sartoretto, S. C., Alves, A. T. N. N., Resende, R. F. B., Calasans-Maia, J., Granjeiro, J. M., & Calasans-Maia, M. D. (2015). Early osseointegration driven by the surface chemistry and wettability of dental implants. *Journal of Applied Oral Science*, *23*, 279–287. https://doi.org/10.1590/1678-775720140483

Saub, R., Locker, D., & Allison, P. (2005). Derivation and validation of the short version of the Malaysian Oral Health Impact Profile. *Community dentistry and oral epidemiology*, *33*(5), 378–383. https://doi.org/10.1111/j.1600-0528.2005.00242.x

Scarano, A., Carinci, F., Quaranta, A., Iezzi, G., Piattelli, M., & Piattelli, A. (2007). Correlation between implant stability quotient (ISQ) with clinical and histological aspects of dental implants removed for mobility. *International Journal of Immunopathology and Pharmacology*, *20*(1 Suppl 1), 33–36. https://doi.org/10.1177/039463200702001s08

Schell, H., Duda, G. N., Peters, A., Tsitsilonis, S., Johnson, K. A., & Schmidt-Bleek, K. (2017). The haematoma and its role in bone healing. *Journal of Experimental Orthopaedics*, *4*(1), 5. https://doi.org/10.1186/s40634-017-0079-3

Schincaglia, G. P., Rubin, S., Thacker, S., Dhingra, A., Trombelli, L., & Ioannidou, E. (2016). Marginal bone response around immediate-and delayed-loading implants supporting a locator-retained mandibular overdenture: A randomized

controlled study. *International Journal of Oral & Maxillofacial Implants*, *31*(2), 448–458. https://doi.org/10.11607/jomi.4118

Schlee, M., van der Schoor, W. P., & van der Schoor, A. R. (2015). Immediate loading of Trabecular Metal-enhanced titanium dental implants: interim results from an international proof-of-principle study. *Clinical Implant Dentistry and Related Research*, *17*(1), e308-e320. https://doi.org/10.1111/cid.12127

Schliephake, H., Sewing, A., & Aref, A. (2006). Resonance frequency measurements of implant stability in the dog mandible: experimental comparison with histomorphometric data. *International Journal of Oral and Maxillofacial Surgery*, *35*(10), 941–946. https://doi.org/10.1016/j.ijom.2006.05.002

Schmitt, C. M., Nogueira-Filho, G., Tenenbaum, H. C., Lai, J. Y., Brito, C., Doering, H., & Nonhoff, J. (2014). Performance of conical abutment (Morse Taper) connection implants: a systematic review. *Journal of Biomedical Materials Research Part A, 102*(2), 552–574. https://doi.org/10.1002/jbm.a.34709

Schwartz, Z., Lohmann, C. H., Oefinger, J., Bonewald, L. F., Dean, D. D., & Boyan, B. D. (1999). Implant surface characteristics modulate differentiation behavior of cells in the osteoblastic lineage. *Advances in Dental Research*, *13*(1), 38–48. https://doi.org/10.1177/08959374990130011301

Schwarz, F., & Ramanauskaite, A. (2022). It is all about peri-implant tissue health. *Periodontology 2000*, *88*(1), 9–12. https://doi.org/10.1111/prd.12407

Schwarz, F., Derks, J., Monje, A., & Wang, H. L. (2018). Peri-implantitis. *Journal of Clinical Periodontology*, *45*(20), S246-S266. https://doi.org/10.1111/jcpe.12954

Schwarz, F., Ferrari, D., Herten, M., Mihatovic, I., Wieland, M., Sager, M., & Becker, J. (2007). Effects of surface hydrophilicity and microtopography on early stages of soft and hard tissue integration at non-submerged titanium implants: An immunohistochemical study in dogs. *Journal of Periodontology*, *78*(11), 2171–2184. https://doi.org/10.1902/jop.2007.070157

Schwarz, F., Wieland, M., Schwartz, Z., Zhao, G., Rupp, F., Geis-Gerstorfer, J., Schedle, A., Broggini, N., Bornstein, M. M., Buser, D., Ferguson, S. J., Becker, J., Boyan, B. D., & Cochran, D. L. (2009). Potential of chemically modified hydrophilic surface characteristics to support tissue integration of titanium dental implants. *Journal of Biomedical Materials Research. Part B, Applied biomaterials*, *88*(2), 544–557. https://doi.org/10.1002/jbm.b.31233

Sculean, A., Gruber, R., & Bosshardt, D. D. (2014). Soft tissue wound healing around teeth and dental implants. *Journal of Clinical Periodontology*, *41*(15), S6–S22. https://doi.org/10.1111/jcpe.12206

Sennerby, L., & Meredith, N. (2008). Implant stability measurements using resonance frequency analysis: biological and biomechanical aspects and clinical implications. *Periodontology 2000*, *47*, 51–66. https://doi.org/10.1111/j.1600-0757.2008.00267.x

Shabalovskaya S. A. (1996). On the nature of the biocompatibility and on medical applications of NiTi shape memory and superelastic alloys. *Bio-medical Materials and Engineering*, *6*(4), 267–289.

Shabalovskaya, S., Anderegg, J., & Van Humbeeck, J. (2008). Critical overview of Nitinol surfaces and their modifications for medical applications. *Acta Biomaterialia*, *4*(3), 447–467. https://doi.org/10.1016/j.actbio.2008.01.013

Shah, F. A., Thomsen, P., & Palmquist, A. (2018). A review of the impact of implant biomaterials on osteocytes. *Journal of Dental Research*, *97*(9), 977–986. https://doi.org/10.1177/0022034518778033

Shah, F. A., Thomsen, P., & Palmquist, A. (2019). Osseointegration and current interpretations of the bone-implant interface. *Acta Biomaterialia*, *84*, 1–15. https://doi.org/10.1016/j.actbio.2018.11.018

Shah, K. C., Linsley, C. S., & Wu, B. M. (2020). Evaluation of a shape memory implant abutment system: An up to 6-month pilot clinical study. *Journal of Prosthetic Dentistry*, *123*(2), 257–263. https://doi.org/10.1016/j.prosdent.2018.11.012

Sharma, N., Jangra, K. K., & Raj, T. (2018). Fabrication of NiTi alloy: A review. *Proceedings of the Institution of Mechanical Engineers, Part L: Journal of Materials: Design and Applications*, *232*(3), 250–269. https://doi.org/10.1177/1464420715622494

Shibli, J. A., Naddeo, V., Cotrim, K. C., Kalil, E. C., de Avila, E. D., Faot, F., Faverani, L.P., Souza, J. G. S., Fernandes, J. C. H., & Fernandes, G. V. O. (2025). Osteoporosis' effects on dental implants osseointegration and survival rate: A systematic review of clinical studies. *Quintessence Int*, *56*(3), 206-16.

Siqueira, R., Ferreira, J. A., Rizzante, F. A. P., Moura, G. F., Mendonça, D. B. S., de Magalhães, D., Cimões, R., & Mendonça, G. (2021). Hydrophilic titanium surface modulates early stages of osseointegration in osteoporosis. *Journal of periodontal research*, *56*(2), 351–362. https://doi.org/10.1111/jre.12827

Simske SJ, Ayers RA, Bateman TA (1997). Porous Materials for Bone Engineering. Porous Mater Tissue Eng, 250:151–82

Slade, G. D. (1997). Derivation and validation of a short-form oral health impact profile. *Community Dentistry and Oral Epidemiology*, *25*(4), 284–290.

Slade, G. D., & Spencer, A. J. (1994). Development and evaluation of the oral health impact profile. *Community Dental Health*, *11*(1), 3-11.

Smeets, R., Stadlinger, B., Schwarz, F., Beck-Broichsitter, B., Jung, O., Precht, C., Kloss, F., Gröbe, A., Heiland, M., & Ebker, T. (2016). Impact of Dental Implant Surface Modifications on Osseointegration. *BioMed Research International*, *2016*, 6285620. https://doi.org/10.1155/2016/6285620

Sodor, A., Ogodescu, A. S., Petreuş, T., Şişu, A. M., & Zetu, I. N. (2015). Assessment of orthodontic biomaterials' cytotoxicity: an *in vitro* study on cell culture. *Romanian Journal of Morphology and Embryology = Revue roumaine de morphologie et embryologie*, *56*(3), 1119–1125.

Stavropoulos, A., Bertl, K., Pietschmann, P., Pandis, N., Schiødt, M., & Klinge, B. (2018). The effect of antiresorptive drugs on implant therapy: Systematic review and meta-analysis. *Clinical Oral Implants Research*, *29*, 54–92. https://doi.org/10.1111/clr.13282

Stević, M., Tatić, Z., Biočanin, V., Đurić, D., & Đukić, I. (2021). History of implantology from the aspect of osseointegration and mucointegration. *Journal of Regional Section of Serbian Medical Association in Zajecar*, *46*(1).

Straumann Group. History. https://www.straumann.com/group/en/home/about/our-history.html

Streckbein, P., Kleis, W., Buch, R. S., Hansen, T., & Weibrich, G. (2014). Bone healing with or without platelet-rich plasma around four different dental implant surfaces in beagle dogs. *Clinical Implant Dentistry and Related Research*, *16*(4), 479–486. https://doi.org/10.1111/cid.12026

Su, N., van Wijk, A., & Visscher, C. M. (2021). Psychosocial oral health-related quality of life impact: A systematic review. *Journal of oral rehabilitation*, *48*(3), 282-292. https://doi.org/10.1111/joor.13064

Suárez-López del Amo, F., Garaicoa-Pazmiño, C., Fretwurst, T., Castilho, R. M., & Squarize, C. H. (2018). Dental implants-associated release of titanium particles: A systematic review. *Clinical Oral Implants Research*, *29*(11), 1085–1100. https://doi.org/10.1111/clr.13372

Sun, Y., Wang, Y., Dong, B., Yang, P., Ji, C., Li, Y., ... & Ma, X. (2025). Understanding the relationship between pore structure and properties of triply periodic minimal surface bone scaffolds. *Journal of Materials Science: Materials in Medicine*, *36*(1), 6. https://doi.org/10.1007/s10856-024-06856-1

Sundelacruz, S., & Kaplan, D. L. (2009). Stem cell-and scaffold-based tissue engineering approaches to osteochondral regenerative medicine. *Seminars in Cell & Developmental Biology, 20* (6), 646–655. https://doi.org/10.1016/j.semcdb.2009.03.017

Takeuchi, O., & Akira, S. (2010). Pattern recognition receptors and inflammation. *Cell*, *140*(6), 805–820. https://doi.org/10.1016/j.cell.2010.01.022

Taniguchi, N., Fujibayashi, S., Takemoto, M., Sasaki, K., Otsuki, B., Nakamura, T., ... & Matsuda, S. (2016). Effect of pore size on bone ingrowth into porous titanium implants fabricated by additive manufacturing: An *in vivo* experiment. *Materials Science and Engineering: C*, *59*, 690–701. https://doi.org/10.1016/j.msec.2015.10.069

Tarnow, D., Cho, S. C., & Wallace, S. S. (2000). The effect of inter-implant distance on the height of inter-implant bone crest. *Journal of periodontology*, *71*(4), 546–549. https://doi.org/10.1902/jop.2000.71.4.546

Teo, A. J. T., Mishra, A., Park, I., Kim, Y. J., Park, W. T., & Yoon, Y. J. (2016). Polymeric Biomaterials for Medical Implants and Devices. *ACS Biomaterials Science and Engineering, 2*(4), 454–472. https://doi.org/10.1021/acsbiomaterials.5b00429

Terheyden, H., Lang, N. P., Bierbaum, S., & Stadlinger, B. (2012). Osseointegration–communication of cells. *Clinical Oral Implants Research*, *23*(10), 1127–1135.

Thoma, D. S., Mühlemann, S., & Jung, R. E. (2014). Critical soft-tissue dimensions with dental implants and treatment concepts. *Periodontology 2000*, *66*(1). https://doi.org/10.1111/prd.12045

Thoma, D. S., Naenni, N., Figuero, E., Hämmerle, C. H., Schwarz, F., Jung, R. E., & Sanz-Sánchez, I. (2018). Effects of soft tissue augmentation procedures on peri-implant health or disease: a systematic review and meta-analysis. *Clinical oral implants research*, *29*, 32–49. https://doi.org/10.1111/clr.13114

Tian, H., Schryvers, D., Liu, D., Jiang, Q., & Van Humbeeck, J. (2011). Stability of Ni in nitinol oxide surfaces. *Acta Biomaterialia*, *7*(2), 892–899.

Tobias, G., Chackartchi, T., Haim, D., Mann, J., & Findler, M. (2025). Dental Implant Survival Rates: Comprehensive Insights from a Large-Scale Electronic Dental Registry. *Journal of Functional Biomaterials*, *16*(2), 60. https://doi.org/10.3390/jfb16020060

Toledano-Serrabona, J., Bosch, B. M., Díez-Tercero, L., Gil, F. J., Camps-Font, O., Valmaseda-Castellón, E., Gay-Escoda, C., & Sánchez-Garcés, M. Á. (2022). Evaluation of the inflammatory and osteogenic response induced by titanium particles released during implantoplasty of dental implants. *Scientific Reports*, *12*(1), 15790. https://doi.org/10.1038/s41598-022-20100-2

Tomar, S., Saxena, D., & Kaur, N. (2025). Marginal bone loss around implants with platform switching and platform matched connection: A systematic review. *Journal of Prosthetic Dentistry*, *134*(1), 109–113. https://doi.org/10.1016/j.prosdent.2023.09.009

Tomasi, C., & Derks, J. (2022). Etiology, occurrence, and consequences of implant loss. *Periodontology 2000*, *88*(1), 13–35. https://doi.org/10.1111/prd.12408

Torres, Y., Trueba, P., Pavón, J. J., Chicardi, E., Kamm, P., García-Moreno, F., & Rodríguez-Ortiz, J. A. (2016). Design, processing and characterization of titanium with radial graded porosity for bone implants. *Materials & Design*, *110*, 179–187.

Tosun, G., Özler, E. Ü. L., Orhan, N., Durmus, A. S., & Eröksüz, H. (2013). Biocompatibility of NiTi alloy implants *in vivo*. *World Academy of Science, Engineering and Technology International Journal of Biomedical and Biological Engineering,* *7*(6), 271-274. https://doi.org/10.1016/j.copbio.2013.05.105

Trindade, R., Albrektsson, T., Galli, S., Prgomet, Z., Tengvall, P., & Wennerberg, A. (2018). Bone immune response to materials, part I: Titanium, PEEK and copper in comparison to sham at 10 days in rabbit tibia. *Journal of Clinical Medicine*, *7*(12), 526. https://doi.org/10.3390/jcm7120526

Trisi, P., Perfetti, G., Baldoni, E., Berardi, D., Colagiovanni, M., & Scogna, G. (2009). Implant micromotion is related to peak insertion torque and bone density. *Clinical Oral Implants Research*, *20*(5), 467–471. https://doi.org/10.1111/j.1600-0501.2008.01679.x.

Trisi, P., Berardi, D., Paolantonio, M., Spoto, G., D'Addona, A., & Perfetti, G. (2013). Primary stability, insertion torque, and bone density of conical implants with

internal hexagon: is there a relationship?. *Journal of Craniofacial surgery*, *24*(3), 841–844. https://doi.org/10.1097/SCS.0b013e31827c9e01

Truhlar, R. S., Orenstein, I. H., Morris, H. F., & Ochi, S. (1997). Distribution of bone quality in patients receiving endosseous dental implants. *Journal of Oral and Maxillofacial Surgery*, *55*(12), 38–45. https://doi.org/10.1016/s0278-2391(16)31196-x

Tsuchiya, A., Sotome, S., Asou, Y., Kikuchi, M., Koyama, Y., Ogawa, T., Tanaka, J., & Shinomiya, K. (2008). Effects of pore size and implant volume of porous hydroxyapatite/collagen (HAp/Col) on bone formation in a rabbit bone defect model. *Journal of Medical and Dental Sciences*, *55*(1), 91–99.

Tsujioka, Y., Mameno, T., Akema, S., Hasegawa, D., Okada, Y., Seto, E., Gonda, T., Yang, T. C., Wada, M., & Ikebe, K. (2024). Survival time analysis of remaining teeth following replacement of unilateral free-end missing teeth: A comparison between fixed implant-supported prostheses and removable partial dentures. *Clinical Oral Implants Research*, *35*(5), 526–533. https://doi.org/10.1111/clr.14248

Ude, C. C., Esdaille, C. J., Ogueri, K. S., Kan, H. M., Laurencin, S. J., Nair, L. S., & Laurencin, C. T. (2021). The mechanism of metallosis after total hip arthroplasty. *Regenerative Engineering and Translational Medicine*, *7*(3), 247–261. https://doi.org/10.1007/s40883-021-00222-1

Ueda, M., Matsuki, M., Jacobsson, M., & Tjellström, A. (1991). The Relationship Between Insertion Torque and Removal Torque Analyzed in Fresh Temporal Bone. *International Journal of Oral & Maxillofacial Implants*, *6*(4).

U.S. Food and Drug Administration. (2019, September). Biological responses to metal implants. https://www.fda.gov/medical-devices/products-and-medical-procedures/cdrhs-research-biological-responses-metal-containing-devices

Ustaoğlu, G., & Erdal, E. (2020). Relationship between risk markers for cardiovascular disease and peri-implant diseases. *International Journal of Implant Dentistry*, *6*(1), 73. https://doi.org/10.1186/s40729-020-00273-z

Valles, C., Rodríguez-Ciurana, X., Clementini, M., Baglivo, M., Paniagua, B., & Nart, J. (2018). Influence of subcrestal implant placement compared with equicrestal position on the peri-implant hard and soft tissues around platform-switched implants: a systematic review and meta-analysis. *Clinical Oral Investigations*, *22*(2), 555–570. https://doi.org/10.1007/s00784-017-2301-1

Van Bael, S., Chai, Y. C., Truscello, S., Moesen, M., Kerckhofs, G., Van Oosterwyck, H., Kruth, J. P., & Schrooten, J. (2012). The effect of pore geometry on the *in vitro* biological behavior of human periosteum-derived cells seeded on selective laser-melted Ti6Al4V bone scaffolds. *Acta biomaterialia*, *8*(7), 2824–2834. https://doi.org/10.1016/j.actbio.2012.04.001

Oers, van, R. F. M. (2010). ***Simulations of bone remodeling at the cellular scale***. [PhD Thesis 1 (Research TU/e / Graduation TU/e), Biomedical Engineering]. Technische Universiteit Eindhoven. https://doi.org/10.6100/IR675320

Vasconcelos, D. P., Águas, A. P., Barbosa, M. A., Pelegrín, P., & Barbosa, J. N. (2019). The inflammasome in host response to biomaterials: Bridging inflammation and tissue regeneration. *Acta Biomaterialia*, *83*, 1–12. https://doi.org/10.1016/j.actbio.2018.09.056

Velasco-Ortega, E., Pato-Mourelo, J., López-López, B., Monsalve-Guil, L., Moreno-Muñoz, J., López-López, J., Núñez-Márquez, E., Matos Garrido, N., Rondón-Romero, J. L., Jiménez-Guerra, Á., & Ortiz-García, I. (2025). Long-Term Clinical Study on Sandblasted–Acid-Etched Surface Dental Implants: 12-Year Follow-Up. ***Materials***, ***18***(1), 183. https://doi.org/10.3390/ma18010183

Vishwakarma, V., Kaliaraj, G. S., & Amirtharaj Mosas, K. K. (2023). Multifunctional Coatings on Implant Materials—A Systematic Review of the Current Scenario. ***Coatings***, ***13***(1), 69. https://doi.org/10.3390/coatings13010069

Vjaters, E., Nitsan, D., Mullerad, M., Engelstein, D., Leibovitch, I., & Feld, Y. (2020). First-in-man safety and efficacy of the ClearRing implant for the treatment of benign prostatic hyperplasia. *European Urology Focus*, *6*(1), 131-136. https://doi.org/10.1016/j.euf.2018.09.013

Vollmer, A., Saravi, B., Lang, G., Adolphs, N., Hazard, D., Giers, V., & Stoll, P. (2020). Factors Influencing Primary and Secondary Implant Stability—A Retrospective Cohort Study with 582 Implants in 272 Patients. ***Applied Sciences***, ***10***(22), 8084. https://doi.org/10.3390/app10228084

W. Nicholson, J. (2020). Titanium Alloys for Dental Implants: A Review. *Prosthesis*, *2*(2), 100–116. https://doi.org/10.3390/prosthesis2020011

Wåhlberg, R. D., Stenport, V. F., Wennerberg, A., & Hjalmarsson, L. (2025). A Multicenter Study of Factors Related to Early Implant Failures—Part 2: Patient Factors. *Clinical Implant Dentistry and Related Research*, *27*(4), e70081. https://doi.org/10.1111/cid.70081

Wälivaara, B., Aronsson, B. O., Rodahl, M., Lausmaa, J., & Tengvall, P. (1994). Titanium with different oxides: *in vitro* studies of protein adsorption and contact activation. *Biomaterials*, *15*(10), 827–834. https://doi.org/10.1016/0142-9612(94)90038-8

Wally, Z. J., Van Grunsven, W., Claeyssens, F., Goodall, R., & Reilly, G. C. (2015). Porous Titanium for Dental Implant Applications. ***Metals***, ***5***(4), 1902-1920. https://doi.org/10.3390/met5041902

Wang, L., Xie, L., Zhang, L.C., Chen, L., Ding, Z., Lv, Y., Zhang, W., Lu, W. and Zhang, D., (2018). Microstructure Evolution and Superelasticity of Layer-Like NiTiNb Porous Metal Prepared by Eutectic Reaction. Acta Materialia, 143:214–26. https://doi.org/10.1016/j.actamat.2017.10.021

Wang, P., Li, X., Jiang, Y., Nai, M. L. S., Ding, J., & Wei, J. (2020). Electron beam melted heterogeneously porous microlattices for metallic bone applications: Design and investigations of boundary and edge effects. *Additive Manufacturing*, *36*, 101566. https://doi.org/10.1016/j.addma.2020.101566.

Wang X, Liu F, Song Y, Sun Q. (2019). Enhanced corrosion resistance and bio-performance of Al2O3 coated NiTi alloy improved by polydopamine-induced hydroxyapatite mineralization. *Surface and Coatings Technology 364*, 81–88. https://doi.org/10.1016/j.surfcoat.2019.01.109

Wang, Q., Zhou, P., Liu, S., Attarilar, S., Ma, R. L. W., Zhong, Y., & Wang, L. (2020). Multi-scale surface treatments of titanium implants for rapid osseointegration: A review. *Nanomaterials, 10*(6), 1244. https://doi.org/10.3390/nano10061244

Wang, Y., Bäumer, D., Ozga, A. K., Körner, G., & Bäumer, A. (2021). Patient satisfaction and oral health-related quality of life 10 years after implant placement. *BMC Oral Health*, *21*(1), 30. https://doi.org/10.1186/s12903-020-01381-3

Webster, P. (2007). [Microwave-assisted processing and embedding for transmission electron microscopy]. In J. Kuo (Ed.), Electron microscopy: Methods and protocols (2nd ed., pp 47-66). Humana Press.

Wen, C. E., Mabuchi, M., Yamada, Y., Shimojima, K., Chino, Y., & Asahina, T. (2001). Processing of biocompatible porous Ti and Mg. *Scripta Materialia*, *45*(10), 1147–1153.

Wennerberg, A., & Albrektsson, T. (2009). Effects of titanium surface topography on bone integration: A systematic review. *Clinical Oral Implants Research 20*(4), 172–184. https://doi.org/10.1111/j.1600-0501.2009.01775.x

Wennerberg, A., & Albrektsson, T. (2010). On implant surfaces: a review of current knowledge and opinions. *International Journal of Oral & Maxillofacial Implants*, *25*(1).

Wennerberg, A., & Albrektsson, T. (2006). Implant surfaces beyond micron roughness. Experimental and clinical knowledge of surface topography and surface chemistry. *International Dentistry SA*, *8*(6).

Wennström, J. L., & Derks, J. (2012). Is there a need for keratinized mucosa around implants to maintain health and tissue stability?. *Clinical Oral Implants Research*, *23*, 136–146. https://doi.org/10.1111/j.1600-0501.2012.02540.x

Wever, D. J., Veldhuizen, A. G., Sanders, M. M., Schakenraad, J. M., & Van Horn, J. R. (1997). Cytotoxic, allergic and genotoxic activity of a nickel-titanium alloy. *Biomaterials*, *18*(16), 1115-1120. https://doi.org/10.1016/s0142-9612(97)00041-0

Winkler, S., Ring, K., Ring, J. D., & Boberick, K. G. (2003). Implant screw mechanics and the settling effect: an overview. *Journal of Oral Implantology*, *29*(5), 242–245. https://doi.org/10.1563/1548-1336(2003)029<0242:ISMATS>2.3.CO;2

Wu, J. C., Mills, A., Grant, K. D., & Wiater, P. J. (2019). Fracture Fixation Using Shape-Memory (Nitinol) Staples. *The Orthopedic Clinics of North America*, *50*(3), 367–374. https://doi.org/10.1016/j.ocl.2019.02.002

Wu, J., Mao, Z., Tan, H., Han, L., Ren, T., & Gao, C. (2012). Gradient biomaterials and their influences on cell migration. *Interface focus*, *2*(3), 337-355. https://doi.org/10.1098/rsfs.2011.0124

Wu, X., Chen, S., Ji, W., & Shi, B. (2021). The risk factors of early implant failure: a retrospective study of 6113 implants. *Clinical implant dentistry and related research*, *23*(3), 280–288. https://doi.org/10.1111/cid.12992

Xia, W., Lindahl, C., Lausmaa, J., & Engqvist, H. (2011). Biomimetic hydroxyapatite deposition on titanium oxide surfaces for biomedical application. *Advances in Biomimetics*, *20*, 429–452.

Xu, J. L., Bao, L. Z., Liu, A. H., Jin, X. J., Tong, Y. X., Luo, J. M., ... & Zheng, Y. F. (2015). Microstructure, mechanical properties and superelasticity of biomedical porous NiTi alloy prepared by microwave sintering. *Materials Science and*

Engineering. C, Materials for biological applications, *46*, 387–393. https://doi.org/10.1016/j.msec.2014.10.053

Xu, L. C., & Siedlecki, C. A. (2007). Effects of surface wettability and contact time on protein adhesion to biomaterial surfaces. *Biomaterials*, *28*(22), 3273-3283. https://doi.org/10.1016/j.biomaterials.2007.03.032

Yadav, T. C., & Bachhuka, A. (2023). Tuning foreign body response with tailor-engineered nanoscale surface modifications: fundamentals to clinical applications. *Journal of Materials Chemistry B*, *11*(33), 7834–7854.

Ylä-Soininmäki, A., Moritz, N., Lassila, L. V., Peltola, M., Aro, H. T., & Vallittu, P. K. (2013). Characterization of porous glass fiber-reinforced composite (FRC) implant structures: porosity and mechanical properties. *Journal of Materials Science: Materials in Medicine*, *24*(12), 2683-2693. https://doi.org/10.1007/s10856-013-5023-1

Young, F. A., & Keller, J. C. (1984). Porous titanium dental implants in primates and humans. *Engineering in medicine*, *13*(4), 203-206.

Yu BQ, Yuan WH, Qiang Xu, Yun-fang-zi GU, Xiao MM, Xu GF, Zhou LI, Zhu XI, Xiao ZA. (2021). Comparison of nickle release and cytocompatibility between porous and dense NiTi alloy. *Transactions of Nonferrous Metals Society of China, 31*(12), 3814-3820. https://doi.org/10.1016/S1003-6326(21)65766-7

Yunus, N., Masood, M., Saub, R., Al-Hashedi, A. A., Taiyeb Ali, T. B., & Thomason, J. M. (2016). Impact of mandibular implant prostheses on the oral health-related quality of life in partially and completely edentulous patients. *Clinical Oral Implants Research*, *27*(7), 904–909. https://doi.org/10.1111/clr.12657

Zaccheo, F., Petroni, G., Tallarico, M., Gioga, C., Carletti, R., Di Gioia, C. R. T., Petrozza, V., Meloni, S. M., Melodia, D., Pisano, M., & Cicconetti, A. (2025). Histological Analysis of Biological Width and Collagen Fibers Orientation Around Screw-Less, Morse Taper, Hemispherical Base Abutments 8 and 16 Weeks After Implant Uncovering: An Observational Clinical Trial. ***Dentistry Journal***, ***13***(4), 154. https://doi.org/10.3390/dj13040154

Zaharin, H. A., Abdul Rani, A. M., Azam, F. I., Ginta, T. L., Sallih, N., Ahmad, A., Yunus, N. A., & Zulkifli, T. Z. A. (2018). Effect of Unit Cell Type and Pore Size on Porosity and Mechanical Behavior of Additively Manufactured Ti6Al4V Scaffolds. ***Materials***, ***11***(12), 2402. https://doi.org/10.3390/ma11122402

Zarb, G. A., & Albrektsson, T. (1998). Towards optimized treatment outcomes for dental implants. *Journal of Prosthetic Dentistry*, *80*(6), 639-640.

Zavanelli, A. C., SÔnego, M. V., Zavanelli, R. A., Mazaro, J. V. Q., & FalcÓn-antenucci, R. M. (2017). Perception and expectation. What do patients really want from the dental treatment?. *RGO-Revista Gaúcha de Odontologia*, *65*(03), 243-248. https://doi.org/10.1590/1981-86372017000200093257

Zhang, L., Zhang, Y. Q., Jiang, Y. H., & Zhou, R. (2015). Superelastic behaviors of biomedical porous NiTi alloy with high porosity and large pore size prepared by spark plasma sintering. *Journal of Alloys and Compounds*, *644*, 513–522. https://doi.org/10.1016/j.jallcom.2015.05.063

Zhang, Q., Guo, S., Li, Y., Li, Z., Wang, D., & Zhang, K. (2024). Analysis of risk indicators for implant failure in patients with chronic periodontitis. *BMC Oral Health*, *24*(1), 1051. https://doi.org/10.1186/s12903-024-04806-5

Zhang, Y., Attarilar, S., Wang, L., Lu, W., Yang, J., & Fu, Y. (2021). A review on design and mechanical properties of additively manufactured NiTi implants for orthopedic applications. *International Journal of Bioprinting*, *7*(2), 340. http://doi.org/10.18063/ijb.v7i2.340

Zhao, Y., Taya, M., Kang, Y., & Kawasaki, A. (2005). Compression behavior of porous NiTi shape memory alloy. *Acta Materialia*, *53*(2), 337–343. https://doi.org/10.1016/j.actamat.2004.09.029

Zheng, J. P., Chen, L. J., Chen, D. Y., Shao, C. S., Yi, M. F., & Zhang, B. (2019). Effects of pore size and porosity of surface-modified porous titanium implants on bone tissue ingrowth. *Transactions of Nonferrous Metals Society of China*, *29*(12), 2534–2545. https://doi.org/10.1016/S1003-6326(19)65161-7

Zhou, W., Gallucci, G. O., Chen, S., Buser, D., & Hamilton, A. (2021). Placement and Loading Protocols for Single Implants in Different Locations: A Systematic Review. *International Journal of Oral & Maxillofacial Implants*, *36*(4), e72-e89. https://doi.org/10.11607/jomi.8750

Zoumot, Z., Kemp, S. V., Singh, S., Bicknell, S. R., McNulty, W. H., Hopkinson, N. S., Ross, E. T., & Shah, P. L. (2015). Endobronchial coils for severe emphysema are effective up to 12 months following treatment: medium term and cross-over results from a randomised controlled trial. *PloS one*, *10*(4), e0122656. https://doi.org/10.1371/journal.pone.0122656

Zuhr, O., Bäumer, D., & Hürzeler, M. (2014). The addition of soft tissue replacement grafts in plastic periodontal and implant surgery: critical elements in design and execution. *Journal of Clinical Periodontology*, *41*, S123-S142. https://doi.org/10.1111/jcpe.12185

APPENDICES

APPENDIX A

Published Article on Cytotoxicity and Genotoxicity of Porous NiTi Following ISO 10993 (Part 3, 5 & 33)

Received: 31 January 2023 | Revised: 26 May 2023 | Accepted: 12 July 2023

DOI: 10.1002/jbm.b.35306

RESEARCH ARTICLE

WILEY

In vitro evaluation of cytotoxicity and genotoxicity of porous nickel titanium dental implants produced by metal injection molding technique

Mustafa N. W. N. A.[1] | Ahmad R.[1,2] | Kamar Affendi N. H.[1] | Sulaiman E.[3] | Khushaini M. A. A.[4] | Ismail M. H.[5] | Teh L. K.[2,6] | Salleh M. Z.[2,6]

[1]Faculty of Dentistry, Unit of Prosthodontics, Centre of Restorative Dentistry Studies, Universiti Teknologi MARA (UiTM), Sungai Buloh, Malaysia

[2]Integrative Pharmacogenomics Institute (iPROMISE), Universiti Teknologi MARA Puncak Alam Campus, Puncak Alam, Malaysia

[3]Faculty of Dentistry, Department of Restorative Dentistry, University of Malaya, Kuala Lumpur, Malaysia

[4]Nitium Technology Sdn. Bhd, Kajang, Malaysia

[5]Smart Manufacturing Research Institute, College of Engineering, Universiti Teknologi MARA (UiTM), Shah Alam, Malaysia

[6]Faculty of Pharmacy, Universiti Teknologi MARA Puncak Alam Campus, Puncak Alam, Malaysia

Correspondence
Ahmad R., Unit of Prosthodontics, Faculty of Dentistry, Centre of Restorative Dentistry Studies, Universiti Teknologi MARA (UiTM), Sungai Buloh Campus, Jalan Hospital, 47000 Sungai Buloh, Selangor, Malaysia.
Email: drrohana@uitm.edu.my

Funding information
Kementerian Sains, Teknologi dan Inovasi

Abstract

Porous NiTi (pNiTi) is a promising biomaterial for functional long-term implantation that has been produced using various manufacturing techniques and tested for biocompatibility. pNiTi produced using a more recent technology of Metal Injection Molding (MIM) has shown better physical and mechanical properties than those produced by earlier manufacturing methods, but its biocompatibility has yet to be determined. Hence, extracts from pNiTi dental implants produced by MIM were tested for cytotoxicity and genotoxicity in this work. Its toxicity was evaluated at the cellular and in vitro levels using elution and 3-(4,5-dimethylthiazol-2-yl)-2,5-diphenyl-2H-tetrazolium bromide (MTT) assays. Short-term testing revealed that pNiTi extract was cytocompatible with L-929 fibroblast and V79-4 lung cells, with no cell lysis or reactivity observed, respectively (USP grade 0). Following exposure to varied extract concentrations, good cell viability was observed where the lowest concentration showed the highest optical density (OD) and cell viability (2.968 ± 0.117 and 94%, respectively), and the highest concentration had the least OD and cell viability (2.251 ± 0.054 and 71%, respectively). pNiTi extracts demonstrated genocompatibility in two independent assays: mutagenic potential using a bacterial reverse mutation test and a clastogenic effect on chromosomes using the micronucleus test. Similar to the negative control reactions, there was no significant increase in revertant colonies following exposure to 100% pNiTi extract with and without metabolic activation ($p = .00$). No DNA clastogenic activity was caused by pNiTi at varied extract concentrations as compared to the negative control when tested with and without metabolic activation ($p = .00$). As a result, both cytotoxic and genotoxic investigations have confirmed that pNiTi dental implants utilizing the MIM process are cytocompatible and genocompatible in the short term, according to the International Standard, ISO 10993 – Parts 3, 5, and 33.

KEYWORDS
biocompatibility, international standard (ISO), metal injection molding, porous nickel titanium

APPENDIX B

Published Article on Biocompatibility of Porous NiTi Fabricated through MIM Technique Following ISO 10993

ACS Biomaterials SCIENCE & ENGINEERING

pubs.acs.org/journal/abseba

Article

Porous NiTi Dental Implant Fabricated by a Metal Injection Molding: An in Vivo Biocompatibility Evaluation in an Animal Model

Nor Wati Nur Atikah Mustafa, Rohana Ahmad,* Muhammad Asif Ahmad Khushaini, Nur Hafizah Kamar Affendi, Siti Mariam Ab Ghani, Su Keng Tan, Muhammad Hussain Ismail, Chui Ling Goo, Mohd Zulkifli Kassim, Tong Wah Lim, and Lay Kek Teh

Cite This: https://doi.org/10.1021/acsbiomaterials.3c01551

Read Online

ACCESS | Metrics & More | Article Recommendations

ABSTRACT: This study assessed the corrosion resistance, intracutaneous reactivity, acute systemic toxicity, and in situ tissue effect of the implantation of porous NiTi fabricated by metal injection molding in animal models. For the intracutaneous reactivity study, five intracutaneous injections were administered per site with and without the tested extract in polar and nonpolar solutions. The extract was also delivered via intravenous and intraperitoneal routes for acute systemic toxicity. TiAl6 V4 (control) and porous NiTi were implanted in rabbit femora for a period of 13 weeks to evaluate the in situ tissue response. Corrosion was evaluated through open and cyclic polarization in PBS, while biocompatibility was investigated by assessing the general conditions, skin irritation score (edema and erythema), and histopathology. No active dissolution or hysteresis loop was observed in the corrosion study. None of the animals exhibited death, moribundity, impending death, severe pain, self-mutilation, or overgrooming. No edema was observed at injection sites. Only the positive control showed an erythematous reaction at 24, 48, and 72 h observations ($p < 0.001$). Porous NiTi showed a low in situ biological response for inflammation, neovascularization, and fibrosis in comparison to the control implant ($p = 0.247$, 0.005, and 0.011, respectively). Porous NiTi also demonstrated high pitting corrosion resistance while causing no acute hypersensitivity or acute systemic toxicity. The study concludes that porous NiTi implants were unlikely to cause local sensitization, acute systemic toxicity, or chronic inflammatory reactions in an animal model. Porous NiTi also exhibited osseointegration equivalent to Ti6Al4 V of known biocompatibility.

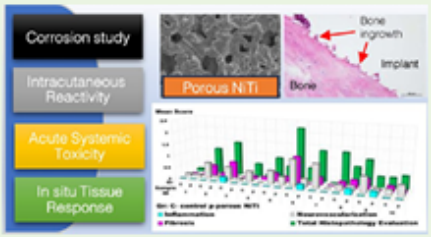

KEYWORDS: *porous nickel−titanium (NiTi), metal injection molding, corrosion, intracutaneous reactivity, acute systemic toxicity*

INTRODUCTION

Titanium dental implants have been a reliable treatment option for replacing missing teeth in oral rehabilitation for the last several decades. Even though it has a high survival rate, there are still reports of extensive bone loss around the implant.[1] Nickel−titanium alloy has shown good biocompatibility, unique shape memory properties, excellent corrosion resistance, and wear resistance.[2−7] It has been used widely in orthopedic,[4] cardiovascular,[5] urology,[6] and orthodontics.[7] Porous NiTi alloy has recently attracted a significant number of scientific interests as desirable biomedical implants.[2] Their open porosity increases the mechanical retention of fixation and reduces the elasticity mismatch between the bone and implant, increasing bonding and minimizing stress-shielding effects.[8] With an elastic modulus closer to that of human bone and a porous surface for bone ingrowth, this could be a promising candidate for dental implants.

Insertion of an endosseous implant associated with local injury due to osteotomy triggers cascades of inflammatory and wound healing reactions. The degree and extension of the host response to the implantable material are closely related to their structural and surface compatibility, which ends up with direct bone-implant contact (acceptance) or fibrous encapsulation (rejection).[9] Porous NiTi has been shown to have osteoconductive potential through bone ingrowth attributed to implant stabilization.[10] Successful soft tissue attachment in muscle further confirms its safety in living tissue.[11] However, various

Received: October 26, 2023
Revised: November 18, 2023
Accepted: November 20, 2023

APPENDIX C

Ethical approval letter (Universiti Teknologi MARA)

www.uitm.edu.my

UNIVERSITI TEKNOLOGI MARA

Pejabat
Timbalan Naib Canselor
(Penyelidikan dan Inovasi)

Reference : 600-TNCPI(5/1/6)
Our reference : REC/11/2020 (FB/365)
Date : 21st May 2021

Assoc. Prof. Dr Lim Tong Wah
Faculty of Dentistry
Universiti Teknologi MARA
Sungai Buloh Campus
Jalan Hospital
47000 Sungai Buloh
SELANGOR

Dear Assoc. Prof. Dr Lim Tong Wah,

APPROVAL LETTER - UiTM RESEARCH ETHICS COMMITTEE

Thank you for submitting your research proposal to Research Ethics Committee (REC). After reviewing the list of documents as attached the Committee approved your proposal entitled "A Prospective, Open Label, Randomized, Double arm, Multicenter Study to Evaluate the Performance of NiTi Dent Tuah Porous NiTi Dental Implants in Single Tooth Gaps in the Posterior Mandible" at Faculty of Dentistry, Universiti Teknologi MARA, Faculty of Dentistry, University of Malaya and Faculty of Dentistry, Universiti Kebangsaan Malaysia.

Details of the approval are as follows:

Ref. number:	REC/11/2020 (FB/365)
Approval Period:	22nd May 2021 until 1st June 2022
Authorised personnel:	1. Assoc. Prof. Dr Lim Tong Wah 2. Dr Nor Wati @ Nur Atikah Mustafa 3. Dr Nur Hafizah Kamar Affendi 4. Assoc. Prof. Dr Siti Mariam Ab Ghani 5. Dr Tan Su Keng

The UiTM Research Ethics Committee operates in accordance to the-ICH Good Clinical Practice Guidelines, Malaysia Good Clinical Practice Guidelines and the Declaration of Helsinki. The approval of this project is conditional upon your continuing compliance with these guidelines and declaration.

Failure to submit reports will result in withdrawal of consent for the project to proceed. Amendments, if any, to the study documents are to be submitted to REC for approval.

If you require further information, please contact REC Secretariat at 03-55448069/03-55442794 or email at recsecretariat@uitm.edu.my.

Yours sincerely,

PROFESSOR DATO' DR. ABU BAKAR ABDUL MAJEED
Chairman
UiTM Research Ethics Committee

c.c.: Dean, Faculty of Dentistry, UiTM

Universiti Teknologi MARA
Aras 3, Bangunan Wawasan
40450 Shah Alam, Selangor, MALAYSIA
Tel: (+603) 5544 2004/2255
Faks: (+603) 5544 2070

ISO 9001:2015 No. Sijil: 1020336

UiTM di hatiku

APPENDIX D

Ethique Approval letter

UNIVERSITI KEBANGSAAN MALAYSIA
The National University of Malaysia

PUSAT PENGURUSAN PENYELIDIKAN DAN INSTRUMENTASI • *CENTRE FOR RESEARCH AND INSTRUMENTATION MANAGEMENT*

Rujukan : UKM PPI/111/8/JEP-2021-018
Tarikh : 21 Mei 2021

Dr. Ho Ting Khee
Jabatan Pergigian Restoratif
Fakulti Pergigian
Universiti Kebangsaan Malaysia

Y.Bhg. Profesor/Datuk/Dato'/Datin/Tuan/Puan,

KELULUSAN ETIKA MENJALANKAN PENYELIDIKAN DI UKM

Tajuk : *A Prospective, Open Label, Randomised, Double Arm, Multicenter Study to Evaluate the performance of NiTiDent Tuah Porous NiTi Dental Implants in Single Tooth Gap in the Posterior Mandible.*

Perkara yang tersebut di atas adalah dirujuk.

Sukacita dimaklumkan, Jawatankuasa Etika Penyelidikan UKM meluluskan permohonan penyelidikan Y.Bhg. Profesor/Datuk/Dato'/Datin/Tuan/Puan bagi tajuk diatas. Tempoh kelulusan penyelidikan adalah daripada **12 Mei 2021 - 11 Mei 2024**. Sila kemukakan sebarang Laporan **Kesan Sampingan, Laporan Kemajuan Setiap 6 Bulan** dan **Laporan Akhir** sebaik sahaja penyelidikan tamat kepada Jawatankuasa Etika Penyelidikan UKM.

Sukacita dilngatkan projek penyelidikan ini hanya boleh dijalankan setelah mendapat **surat kelulusan menjalankan penyelidikan** dari Timbalan Dekan Penyelidikan Fakulti.

Sekian, terima kasih.

Yang benar,

PROFESOR DR. MOHD SHAHRIR MOHAMED SAID
Pengerusi
Jawatankuasa Etika Penyelidikan
Universiti Kebangsaan Malaysia

s.k. - **Pengarah**
Pusat Pengurusan Penyelidikan dan Instrumentasi (CRIM)
Universiti Kebangsaan Malaysia

- **Timbalan Dekan (Penyelidikan & Inovasi)**
Fakulti Pergigian
Universiti Kebangsaan Malaysia

Sekretariat Etika Penyelidikan Universiti Kebangsaan Malaysia
Tingkat 1, Blok Klinikal, Hospital Canselor Tuanku Muhriz, Pusat Perubatan UKM, Jalan Yaacob Latif, Bandar Tun Razak, 56000 Cheras Kuala Lumpur.
Telefon: +603-9145 5046 / 5048
Email: sepukm@ukm.edu.my Web: http://research.ukm.my/sepukm/

APPENDIX E

Case Report Form (CRF) Used for This Study

Appendix D

Case Report Form

Table of Content

Screening 1

- Subject Information & Demographic Data
- Inclusion Criteria
- Exclusion Criteria
- Clinical Examination
- Intra-oral Examination

Screening 1.2

- Radiographic Report
- Conclusion the eligibility

Visit 1

- Implant Placement

Visit 2

- Post-operative Review

Visit 3

- Implant Surgical Exposure

Visit 3.1

- Impression Making

Visit 4

- Crown Placement
- Peri-implant Tissue Assessment
- Crestal Bone Assessment

Visit 5

- Peri-implant Tissue Assessment
- Crestal Bone Assessment

Visit 6

- Peri-implant Tissue Assessment
- Crestal Bone Assessment
- Implant Success Criteria

Site ID _____ Subject ID _____ Subject initial _____

Screening 1

Visit: _____

Subject Information & Demographic Data

Gender : Male ☐ Female ☐

Date of birth : _____ / _____ / _____
Day Month Year

Ethnicity : Malay ☐ Chinese ☐ Indian ☐ Others ☐

Occupation :
- Manager ☐
- Professionals, Manager, Executive & Technician ☐
- Clerical & Service Wokers ☐
- Skilled Agricultural, Forestry, Livestock & Fishery Workers ☐
- Artisan ☐
- Cleaner, Janitor, Hawker etc ☐
- Armed Forces ☐
- Others (please specify) _____

Highest education level :
- No Formal Education ☐
- Primary Education ☐
- Secondary Education ☐
- Tertiary Education ☐
- Others (specify) _____

Monthly household income :
- <RM 4850 ☐
- RM 4850 – RM 10959 ☐
- RM 10959 – 15040 ☐
- >RM 15040 ☐

Body Weight : _____ kg Height: _____ m

Site ID _____ Subject ID _____ Subject initial _____

Screening 1.2 (Continued)

Inclusion Criteria	No	Yes
A. General		
At least 18 years of age	☐	☐
Ability to understand and provide informed consent	☐	☐
Ability and willingness to comply with all study requirements to be evaluated for each study visit.	☐	☐
Adequate oral hygiene to allow for implant therapy consistent with standards of care.	☐	☐
Patients must be physically able to tolerate conventional surgical and restorative procedures	☐	☐
Healthy or having mild or controlled systemic disease	☐	☐
B. Specific		
One tooth in the posterior mandible (first or second molar) planned to be restored with a dental implant as determined by the patient's dental provider	☐	☐

* **To exclude subject with ONE or more "No" in the criteria above**

Exclusion Criteria		
A. Medical history		
ASA 3 and above (Uncontrolled DM, HTN)	☐	☐
History of HIV infection, Hepatitis B or C	☐	☐
Current hematological disorder or warfarin (or similar) therapy	☐	☐

History of disease that affects bone metabolism, congenital connective tissue disorders (e.g., osteogenesis imperfecta), or Paget's disease	☐	☐
On medications / treatment known to have an effect on bone turnover, including thiazide diuretics, calcitonin, systemic steroids, bisphosphonates, vitamin D (>800 IU/day), estrogen or progesterone therapy.	☐	☐
History of steroid treatment of duration of 2 weeks or longer in the past 2 years	☐	☐
History of radiation treatment to the head or neck	☐	☐
Current chemotherapy	☐	☐
Physical or mental handicaps that would interfere with patient's ability to exercise good oral hygiene on a regular basis	☐	☐
History of usage of any investigational drug/device within the 30 days prior to implant surgery.	☐	☐
Currently pregnant or lactating (for female subject)	☐	☐
B. Social history		
History of tobacco use in the past 5 years of more than 10 cigarettes per day/ tobacco chewing	☐	☐
History of alcoholism or drug abuse in the past 5 years	☐	☐
C. Dental history		
History of previously failed implants at the site surgical site	☐	☐
D. Examination		
Inadequate oral hygiene to allow for implant therapy consistent with standards of care.	☐	☐
Severe tooth wear	☐	☐
Surgical site is less than 3 months after extraction	☐	☐
The site to be treated is not surrounded by two natural teeth	☐	☐

Inadequate bone volume to accommodate the planned endosseous dental implant placement of 4.5 mm in diameter and 10 mm in length	☐	☐
Insufficient alveolar bone at surgical site needing allogenous/ xenogenic/ alloplastic bone graft with or without membrane	☐	☐
Inadequate interocclusal distance (crown height space) of at least 6 mm measured from the alveolar crest to the occlusal table	☐	☐
Absence of opposing dentition with a functional occlusion.	☐	☐
Other treatment/ surgery is needed at a site adjacent to the intended implantation site.	☐	☐
Active infection or severe inflammation in the areas intended for implant placement.	☐	☐
Significant untreated periodontal disease, severe recession, caries, clinical or radiographic signs of infection within two adjacent tooth positions of implant area.	☐	☐
Presence of local inflammation or mucosal diseases such as lichen planus	☐	☐
E. Radiographic finding		
Non-intact buccal table as verified by Cone Beam Computed Tomography (CBCT).	☐	☐

*** To exclude subject with ONE or more "yes" in the criteria above**

Site ID _____ Subject ID _____ Subject initial _____

Screening 1 (Continued)

Clinical Examination

BP : _____ / _____ mm/hg

Random Blood sugar : _____ mmol/l

Urine test (child bearing age female subjects only): positive ☐ negative ☐

Intraoral Examination

Oral Hygiene	Good	☐	Fair	☐	Poor	☐
Limitation of mouth opening	yes	☐	no	☐	Specify:	_____
TMJ Disorder	yes	☐	no	☐		

PREPOSITION IMPLANT SITE (Examination of adjacent teeth)

Missing tooth _____

	Mesial tooth ( )		Distal tooth ( )
Gingiva biotype	☐ Thick		☐ Thick
	☐ Thin		☐ Thin
Probing Depth > 3 mm	No ☐		Yes ☐
Caries	No ☐		Yes ☐
Endodontic Disease	No ☐		Yes ☐
Tooth mobility	No ☐		Yes ☐
(If yes, please tick of any)	☐ Grade I		☐ Grade I
	☐ Grade II		☐ Grade II
	☐ Grade III		☐ Grade III

Occlusion:

Tooth contact during excursive movement

(Rt) ws nws

(Lt) ws nws

Protrusive

Restorative Space (Implant Area):

Restorative space: _____ mm  Vertical height at least 6 mm

Mesio-distal width: _____ mm 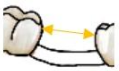 8-12 mm

Horizontal Width: Adequate Inadequate *please tick any

Radiographic Report

Visit Date: _____

OPG:	No	Yes
Absence of bony pathology at the site to be treated	☐	☐

Other comment:

_____

_____

_____

_____

_____

_____

CBCT:	No	Yes
Adequate bone volume to accommodate the planned endosseous dental implant placement of 4.8 mm in diameter and 10 mm in length	☐	☐
Intact buccal table as verified by Cone Beam Computed Tomography (CBCT). If absent, patient should be excluded from enrolment in the study.	☐	☐

Other comment:

_____

_____

_____

_____

Conclusion of The Eligibility This patient complies with all inclusion and exclusion criteria: *Proceed to Visit 1 Day 0*	No ☐	Yes ☐

Principal Investigator's Signature:

Principal Investigator's Name:_____

Date:_____

Site ID _____ Subject ID _____ Subject initial _____

Visit 1

Implant Placement

Visit Date: _____

Vital Sign

BP : _____ / _____ mm/hg

Pulse rate : _____ beats/min

SpO2 : _____ %

Respiratory rate : _____ breaths/min

Random Blood sugar : _____ mmol/l

Insertion Torque: _____

Implant Stability (ISQ): _____

Crestal Bone Level: _____

_____

Medication prescribed: _____

_____

_____

_____

_____

_____

_____

_____

Post-surgical exclusion criteria	No	Yes
Lack of implant primary stability	☐	☐
Inappropriate implant position for prosthetic requirements.	☐	☐
Major simultaneous augmentation procedures at surgery.	☐	☐

*** To exclude subject with ONE or more "yes" in the criteria above**

Visit 1 (Continued)

Implant Placement

Adverse Event (if present)

Finding:

_____

_____

_____

_____

_____

Management:

_____

_____

_____

_____

_____

_____

Discontinuation/ Withdrawal No ☐ Yes ☐

Principal Investigator's Signature:

Principal Investigator's Name:_____

Date:_____

Site ID _____ Subject ID _____ Subject initial _____

Visit 2

Post-operative review

Visit Date: _____

Chief Complaint:

Finding:

Procedure:

Site ID _____ Subject ID _____ Subject initial _____

Visit 2 (Continued)

Adverse Event (if present)

Finding:

_____

_____

_____

_____

_____

_____

_____

Management:

_____

_____

_____

_____

_____

_____

_____

_____

_____

_____

Discontinuation/ Withdrawal No ☐ Yes ☐

Principal Investigator's Signature:

Principal Investigator's Name:_____

Date:_____

Site ID _____ Subject ID _____ Subject initial _____

Visit 3

Implant Surgical Exposure

Visit Date: _____

Chief Complaint:

Implant Stability (ISQ): _____

Finding:

Lack of primary implant stability at time of abutment connection (i.e, spinning or laterally moving implant) No ☐ Yes ☐

*** To exclude subject with ONE or more "yes" in the criteria above**

Other comment/ procedure

Site ID _____ Subject ID _____ Subject Initial _____

Visit 3 (Continued)

Adverse Event (if present)

Finding:

_____

_____

_____

_____

_____

_____

_____

Management:

_____

_____

_____

_____

_____

_____

_____

_____

_____

_____

Discontinuation/ Withdrawal No ☐ Yes ☐

Principal Investigator's Signature:

Principal Investigator's Name:_____

Date:_____

Site ID _____ Subject ID _____ Subject Initial _____

Visit 3.1

Impression Procedure

Visit Date: _____

Chief Complaint:

Finding:

Procedure:

Site ID _____ Subject ID _____ Subject Initial _____

Visit 3.1 (Continued)

Adverse Event (if present)

Finding:

_____

_____

_____

_____

_____

_____

_____

Management:

_____

_____

_____

_____

_____

_____

_____

_____

_____

_____

Discontinuation/ Withdrawal No ☐ Yes ☐

Principal Investigator's Signature:

Principal Investigator's Name:_____

Date:_____

Site ID _____ Subject ID _____ Subject Initial _____

Visit 4

Crown Placement & Post-operative Assessment

Visit Date: _____

Chief Complaint:

Finding:

Procedure:

Site ID _____ Subject ID _____ Subject Initial _____

Visit 4 (Continued)

Peri-implant Tissue Condition:

General Peri-mucosal condition ☐ Normal ☐ Erythematous ☐ Swelling

Inflammation level (use gingival index)
☐ No
☐ Yes Please indicate:
☐ Mild (pink coloured) ☐ Moderate (purple pink) ☐ Severe (magenta red)

Bleeding on Probing: ☐ No ☐ Yes

If yes, please specify the area _____

Probing Depth:

Suppuration: ☐ No ☐ Yes Specify _____

Dehiscence: ☐ No ☐ Yes Specify _____

Others (Please specify): _____

_____

Crestal Bone Level: _____

X-ray not showing the implant from the first bone contact to apical tip ☐ No ☐ Yes

*** To exclude subject with "yes" in the criteria above**

Principal Investigator's Signature:

Principal Investigator's Name:_____

Date:_____

Site ID _____ Subject ID _____ Subject Initial _____

Visit 4 (Continued)

Adverse Event (if present)

Finding:

Management:

Discontinuation/ Withdrawal No ☐ Yes ☐

Site ID _____ Subject ID _____ Subject Initial _____

Visit 5

Visit Date: _____

Chief complaint: _____

_____

_____

_____

Oral hygiene ☐ Good ☐ Fair ☐ Poor

Plaque around peri-implant site ☐ No ☐ Yes Specify _____

Peri-implant Soft Tissue Condition:

General Peri-mucosal condition ☐ Normal ☐ Erythematous ☐ Swelling

Inflammation level (use gingival index) ☐ No ☐ Yes Please indicate: ☐ Mild (pink coloured) ☐ Moderate (purple pink) ☐ Severe (magenta red)

Bleeding on Probing: ☐ No ☐ Yes

If yes, please specify the area _____

Probing Depth:

Suppuration: ☐ No ☐ Yes Specify _____

Dehiscence: ☐ No ☐ Yes Specify _____

Others (Please specify): _____

Implant Stability (ISQ): _____

Crestal Bone Level: _____

_____

_____

_____

Technical Complications: _____

Abutment Screw Loosening: ☐ No ☐ Yes

Loss of Retention (Crown): ☐ No ☐ Yes

Specify _____

Fracture of Crown: ☐ No ☐ Yes

Specify _____

Fracture of Abutment: ☐ No ☐ Yes

Specify _____

Fracture of Screw: ☐ No ☐ Yes

Specify _____

Implant Fracture: ☐ No ☐ Yes

Specify _____

Others (Please Specify) _____

_____

_____

_____

_____

_____

_____

Site ID _____ Subject ID _____ Subject Initial _____

Visit 5 (Continued)

Adverse Event (if present)

Finding:

Management:

Discontinuation/ Withdrawal No ☐ Yes ☐

Principal Investigator's Signature:

Principal Investigator's Name:_____

Date:_____

Site ID _____ Subject ID _____ Subject initial _____

Visit 6

Visit Date: _____

Chief complaint: _____

_____

_____

_____

Oral hygiene ☐ Good ☐ Fair ☐ Poor

Plaque around peri-implant site ☐ Yes ☐ No Specify _____

Peri-implant Tissue Condition:

General Peri-mucosal condition ☐ Normal ☐ Erythematous ☐ Swelling

Inflammation level (use gingival index)
☐ No
☐ Yes Please indicate:
☐ Mild (pink coloured) ☐ Moderate (purple pink) ☐ Severe (magenta red)

Bleeding on Probing: ☐ No ☐ Yes

If yes, please specify the area _____

Probing Depth:

Suppuration: ☐ No ☐ Yes Specify _____

Dehiscence: ☐ No ☐ Yes Specify _____

Others (Please specify): _____

Implant Stability (ISQ): _____

Crestal Bone Level: _____

_____

_____

_____

Technical Complications: _____

Abutment Screw Loosening: ☐ No ☐ Yes

Specify _____

Loss of Retention (Crown): ☐ No ☐ Yes

Specify _____

Fracture of Crown: ☐ No ☐ Yes

Specify _____

Fracture of Abutment: ☐ No ☐ Yes

Specify _____

Fracture of Screw: ☐ No ☐ Yes

Specify _____

Implant Fracture: ☐ No ☐ Yes

Specify _____

Others (Please Specify) _____

_____

_____

_____

Principal Investigator's Signature:

Principal Investigator's Name:_____

Date:_____

Site ID _____ Subject ID _____ Subject initial _____

Visit 6 (Continued)

Adverse Event (if present)

Finding:

Management:

Discontinuation/ Withdrawal No ☐ Yes ☐

Site ID _____ Subject ID _____ Subject initial _____

Visit 6 (Continued)

Implant Success Criteria	No	Yes
Absence of persisting subjective discomfort such as pain, foreign body perception and or dysaesthesia (painful sensation)	☐	☐
Absence of a recurrent peri-implant infection with suppuration (where an infection is termed recurrent if it is observed at two or more follow-up visits after treatment with systemic antibiotics)	☐	☐
Absence of implant mobility on manual palpation	☐	☐
Absence of any continuous peri-implant radiolucency	☐	☐

Principal Investigator's Signature:

Principal Investigator's Name:_____

Date:_____

APPENDIX F

Inter-examiner calibration: A raw statistic data of peri-implant pocket depth

Reliability Statistics

Cronbach's Alpha	Cronbach's Alpha Based on Standardized Items	N of Items
.894	.894	2

Item Statistics

	Mean	Std. Deviation	N
PDvsRater1	1.4333	1.11030	60
PDvsRater2	1.3000	1.11310	60

Inter-Item Correlation Matrix

	PDvsRater1	PDvsRater2
PDvsRater1	1.000	.808
PDvsRater2	.808	1.000

Item-Total Statistics

	Scale Mean if Item Deleted	Scale Variance if Item Deleted	Corrected Item-Total Correlation	Squared Multiple Correlation	Cronbach's Alpha if Item Deleted
PDvsRater1	1.3000	1.239	.808	.654	.
PDvsRater2	1.4333	1.233	.808	.654	.

Intraclass Correlation Coefficient

	Intraclass Correlation[b]	95% Confidence Interval		F Test with True Value 0			
		Lower Bound	Upper Bound	Value	df1	df2	Sig
Single Measures	.808[a]	.699	.881	9.442	59	59	<.001
Average Measures	.894[c]	.823	.937	9.442	59	59	<.001

Two-way mixed effects model where people effects are random and measures effects are fixed.

a. The estimator is the same, whether the interaction effect is present or not.

b. Type C intraclass correlation coefficients using a consistency definition. The between-measure variance is excluded from the denominator variance.

c. This estimate is computed assuming the interaction effect is absent, because it is not estimable otherwise.

APPENDIX G

Intra-examiner calibration: A raw statistic data of peri-implant pocket depth

Reliability Statistics

Cronbach's Alpha	Cronbach's Alpha Based on Standardized Items	N of Items
.931	.931	2

Item Statistics

	Mean	Std. Deviation	N
PDRater1T1	1.4333	1.11030	60
PDRater1T2	1.3333	1.14857	60

Inter-Item Correlation Matrix

	PDRater1T1	PDRater1T2
PDRater1T1	1.000	.872
PDRater1T2	.872	1.000

Item-Total Statistics

	Scale Mean if Item Deleted	Scale Variance if Item Deleted	Corrected Item-Total Correlation	Squared Multiple Correlation	Cronbach's Alpha if Item Deleted
PDRater1T1	1.3333	1.319	.872	.760	.
PDRater1T2	1.4333	1.233	.872	.760	.

Intraclass Correlation Coefficient

	Intraclass Correlation[b]	95% Confidence Interval		F Test with True Value 0			
		Lower Bound	Upper Bound	Value	df1	df2	Sig
Single Measures	.871[a]	.793	.921	14.522	59	59	<.001
Average Measures	.931[c]	.885	.959	14.522	59	59	<.001

Two-way mixed effects model where people effects are random and measures effects are fixed.

a. The estimator is the same, whether the interaction effect is present or not.

b. Type C intraclass correlation coefficients using a consistency definition. The between-measure variance is excluded from the denominator variance.

c. This estimate is computed assuming the interaction effect is absent, because it is not estimable otherwise.

APPENDIX H

Inter-examiner calibration: A raw statistic data of the crestal bone level

Reliability Statistics

Cronbach's Alpha	Cronbach's Alpha Based on Standardized Items	N of Items
.996	.997	2

Item Statistics

	Mean	Std. Deviation	N
BoneRater1	-.7000	.60350	20
BoneRater2	-.6925	.56528	20

Inter-Item Correlation Matrix

	BoneRater1	BoneRater2
BoneRater1	1.000	.994
BoneRater2	.994	1.000

Item-Total Statistics

	Scale Mean if Item Deleted	Scale Variance if Item Deleted	Corrected Item-Total Correlation	Squared Multiple Correlation	Cronbach's Alpha if Item Deleted
BoneRater1	-.6925	.320	.994	.987	.
BoneRater2	-.7000	.364	.994	.987	.

Intraclass Correlation Coefficient

	Intraclass Correlation[b]	95% Confidence Interval		F Test with True Value 0			
		Lower Bound	Upper Bound	Value	df1	df2	Sig
Single Measures	.991[a]	.978	.997	232.291	19	19	<.001
Average Measures	.996[c]	.989	.998	232.291	19	19	<.001

Two-way mixed effects model where people effects are random and measures effects are fixed.

a. The estimator is the same, whether the interaction effect is present or not.

b. Type C intraclass correlation coefficients using a consistency definition. The between-measure variance is excluded from the denominator variance.

c. This estimate is computed assuming the interaction effect is absent, because it is not estimable otherwise.

APPENDIX I

Inter-examiner calibration: A raw statistic data of the crestal bone level

Reliability Statistics

Cronbach's Alpha	Cronbach's Alpha Based on Standardized Items	N of Items
.997	.998	2

Item Statistics

	Mean	Std. Deviation	N
BoneT1	-.7000	.60350	20
BoneT2	-.7050	.57900	20

Inter-Item Correlation Matrix

	BoneT1	BoneT2
BoneT1	1.000	.996
BoneT2	.996	1.000

Item-Total Statistics

	Scale Mean if Item Deleted	Scale Variance if Item Deleted	Corrected Item-Total Correlation	Squared Multiple Correlation	Cronbach's Alpha if Item Deleted
BoneT1	-.7050	.335	.996	.991	.
BoneT2	-.7000	.364	.996	.991	.

Intraclass Correlation Coefficient

	Intraclass Correlation[b]	95% Confidence Interval		F Test with True Value 0			
		Lower Bound	Upper Bound	Value	df1	df2	Sig
Single Measures	.995[a]	.987	.998	381.432	19	19	<.001
Average Measures	.997[c]	.993	.999	381.432	19	19	<.001

Two-way mixed effects model where people effects are random and measures effects are fixed.

a. The estimator is the same, whether the interaction effect is present or not.

b. Type C intraclass correlation coefficients using a consistency definition. The between-measure variance is excluded from the denominator variance.

c. This estimate is computed assuming the interaction effect is absent, because it is not estimable otherwise.

AUTHOR'S PROFILE

Nor Wati @ Nur Atikah Binti Mustafa is often referred to as Nur Atikah. A journey through the field of dentistry culminated in the recent completion of a PhD in Implant Prosthodontics at the Faculty of Dentistry, Universiti Teknologi MARA. Prior to this milestone, a Master's in Clinical Dentistry (MClinDent) specialising in Restorative in Prosthetic Dentistry was earned at the University of Malaya in 2014. An academic path was embarked upon in 2009 as a trainee lecturer, during which a deep passion for teaching and learning was developed. Prior to this academic pursuit, she gained valuable practical experience while working with the Ministry of Health. There, she completed first-year dental officer training in Periodontics, Orthodontics, Paediatric Dentistry, and Oral Maxillofacial Surgery at Klinik Pergigian in Wilayah Persekutuan Kuala Lumpur and Hospital Kuala Lumpur. Subsequently, she moved to Hospital Selayang as a dental officer, then and lastly to Klinik Pergigian Shah Alam, Selangor. A strong belief in the importance of education and service, and a commitment to making meaningful contributions to dentistry, are maintained. She hopes this journey inspires others to pursue their goals with determination and dedication.

LIST OF PUBLICATIONS

Indexed Journal

Nor Wati Nur Atikah Mustafa, Rohana Ahmad, Muhammad Asif Ahmad Khushaini, Nur Hafizah Kamar Affendi, Siti Mariam Ab Ghani, Su Keng Tan, Muhammad Hussain Ismail, Chui Ling Goo, Mohd Zulkifli Kassim, Tong Wah Lim, and

Lay Kek Teh. Porous NiTi Dental Implant Fabricated by a Metal Injection Molding: An *In Vivo* Biocompatibility Evaluation in an Animal Model. *ACS Biomaterials Science & Engineering* 2024 *10* (1), 405-419. DOI: 0.1021/acsbiomaterials.3c01551

Mustafa N. W. N. A., Ahmad R. Kamar Affendi N. H., Sulaiman E. Khushaini M. A. A., Ismail M. H. Teh L. K., Salleh M. Z. (2023). *In vitro* evaluation of cytotoxicity and genotoxicity of porous nickel titanium dental implants produced by metal injection molding technique. *J Biomed Mater Res B Appl Biomater. 112*(1): e35306. https://doi.org/10.1002/jbm.b.35306. PMID: 37522375

Mustafa, N. W. N. A., Ab Ghani, S. M., Amin, I. M., Khushaini, M. A. A., Affendi, N. H. K., Tan, S. K., Sulaiman, E., & Ahmad, R. (2024). Interactions of Cell-Porous NiTi Biomaterial and Nickel Ion Release. *International Dental Journal*, *74*, S303.

Muhammad Amal Abd Wahab, Rohana Ahmad, Eleena Mohd Yusof, Nor Wati Nur Atikah Mustafa, Teh Lay Kek. (2023). Differential protein expressions associated with dental implant healing. *International Dental Journal*. https://doi.org/10.1016/j.identj.2024.07.1127

Kassim MZ, Mustafa NWNA, Ahmad R, Baba NZ (2024). The effect of brand, thickness, and abutment substrate on the masking ability of monolithic zirconia ceramics. (2024). *Arch Orofac Sci, 19*(1): 19–30. https://doi.org/10.21315/aos2024.1901.OA02

Nor Wati Nur Atikah Mustafa, Nur Humaira Ishak, Nur Athira Rosli, Nik Rahayyu Nik Zulkifeli, Aiemeeza Rajali. (2021). Self-preference music for gagging patient: Effect on physiology and oral health-related quality of life during dental impression. *Complementary Therapies in Clinical Practice 43* 10139. https://doi.org/10.1016/j.ctcp.2021.101392

Others

Nor Wati Nur Atikah Mustafa, Aiemeeza Rajali, Muhammad Asif Ahmad Khushaini, Rohana Ahmad. (2024). Easy Diagnostic Implant Stability Measurement with A Novel Vibrating Fiber Optic (VFO) System. Chapter in Research Book, *Fostering Collaborative Health Clusters: Pioneering Innovation in Health & Wellness,* 71-74

Presentations

1. **Nor Wati Nur Atikah Mustafa,** Aiemeeza Rajali, Muhammad Asif Ahmad Khushaini, Rohana Ahmad. A Novel Vibrating Fiber Optic (VFO) System for Implant Stability Measurement. Presented at the International Invention & Innovation in Dentistry Exhibition 2024, Melaka (19th October 2024). **(Bronze Award).**
2. **Mustafa, N. W. N. A.,** Ab Ghani, S. M., Amin, I. M., Khushaini, M. A. A., Affendi, N. H. K., Tan, S. K., Sulaiman, E., & Ahmad, R. Interactions of Cell-Porous NiTi Biomaterial and Nickel Ion Release. Presented at FDI World Dental Congress –İstanbul 2024 between September 12-15, 2024
3. **Nor Wati Nur Atikah Mustafa,** Nurhafizah Kamar Affendi, Eshamsul Sulaiman, Rohana Ahmad. The Osteogenic Potential of Porous NiTi Dental Implant Fabricated by MIM Technique. Presented at 1st UiTM Dental Postgraduate Scientific Symposium (16 – 17 July 2024).
4. 3-Minute Thesis: Porous Nickel-Titanium: Its Potential for Long-Term Implant Survival – UiTM Level, Presented on 21st May 2024
5. 3-Minute Thesis: Porous Nickel-Titanium: Its Potential for Long-Term Implant Survival – UiTM Level, Presented on 3rd March 2024, Faculty Level **(3rd place)**
6. Nur Hafizah Kamar Affendi, Ammar Yaseer Bin Abdul Hakim @ Abdul Khakin[2], **Nor Wati @ Nur Atikah Mustafa**, Melati Mahmud, Rohana Ahmad, Muhammad Asif bin Ahmad Khushaini. Versy-T 2.0 Implant Abutment: Retentive and Effective. Presented at the International Invention & Innovation in Dentistry Exhibition 2022, Bangi, Selangor. **(Gold Award)**
7. Nur Hafizah Kamar Affendi, Ammar Yaseer Bin Abdul Hakim @ Abdul Khakin[2], **Nor Wati @ Nur Atikah Mustafa**, Melati Mahmud, Rohana Ahmad, Muhammad Asif bin Ahmad Khushaini. Versy-T Implant Abutment: Retentive and Effective. Presented at the International Invention & Innovation in Dentistry Exhibition 2023, Pulau Pinang. **(Gold Award)**

Copyright

1. Vibrating Fiber Optic (VBO) System for Implant Stability Measurement (CRD2024W06304)